TARGET STRENGTH VARIABILITY IN ATLANTIC HERRING (*CLUPEA HARENGUS*) AND ITS EFFECT ON ACOUSTIC ABUNDANCE ESTIMATES

Sascha Mario Michel Fässler

A Thesis Submitted for the Degree of PhD
at the
University of St. Andrews

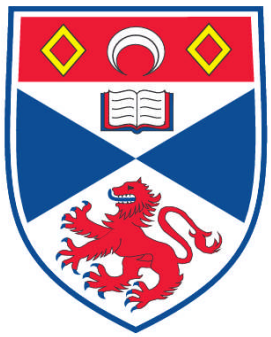

2010

Target strength variability in Atlantic herring (*Clupea harengus*) and its effect on acoustic abundance estimates

Sascha Mario Michel Fässler

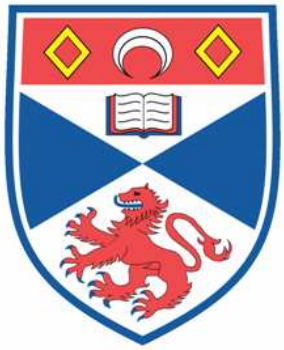

Submitted in partial fulfilment of the requirements
for the degree of Doctor of Philosophy

University of St Andrews

September 2010

Target strength variability in Atlantic herring (*Clupea harengus*) and its effect on acoustic abundance estimates

Sascha Mario Michel Fässler

Declarations

I, Sascha Mario Michel Fässler, hereby certify that this thesis, which is approximately 39’000 words in length, has been written by me, that it is the record of work carried out by me and that it has not been submitted in any previous application for a higher degree.

I was admitted as a research student in October 2006 and as a candidate for the degree of PhD in October 2007; the higher study for which this is a record was carried out in the University of St Andrews between 2006 and 2009.

date ……...…signature of candidate ……..

I hereby certify that the candidate has fulfilled the conditions of the Resolution and Regulations appropriate for the degree of PhD in the University of St Andrews and that the candidate is qualified to submit this thesis in application for that degree.

date ……...…signature of supervisor ……..

In submitting this thesis to the University of St Andrews we understand that we are giving permission for it to be made available for use in accordance with the regulations of the University Library for the time being in force, subject to any copyright vested in the work not being affected thereby. We also understand that the title and the abstract will be published, and that a copy of the work may be made and supplied to any bona fide library or research worker, that my thesis will be electronically accessible for personal or research use unless exempt by award of an embargo as requested below, and that the library has the right to migrate my thesis into new electronic forms as required to ensure continued access to the thesis. We have obtained any third-party copyright permissions that may be required in order to allow such access and migration, or have requested the appropriate embargo below.

The following is an agreed request by candidate and supervisor regarding the electronic publication of this thesis:

Access to printed copy and electronic publication of thesis through the University of St Andrews.

date ……...…signature of candidate ……..

date ……...…signature of supervisor ……..

Acknowledgements

I would like to express my sincere gratitude to my supervisors, Prof Andrew Brierley of the University of St Andrews and Dr Paul Fernandes of the Marine Scotland Marine Laboratory, Aberdeen, for providing me with continued support, advice and guidance. I very much appreciated their knowledge, encouragement and suggestions which kept me on the right tracks during this work and contributed to the ideas and understanding gained. Special thanks to Paul for initially introducing me to the subject of fisheries acoustics during a work placement and for being a very encouraging mentor throughout the years.

Many thanks to the Marine Laboratory in Aberdeen for accommodating me during my studies and providing me with acoustic herring survey data. Members of the 'Sonar Section' - Eric Armstrong, Phil Copland and Mike Stewart - are thanked for their technical support and their relaxed but thorough approach. I am grateful to Brian Ritchie, Colin Stewart and David Lee from the Engineering Services for doing a sheer marvellous job in constructing the pressure chamber. Dr David Borchers (CREEM, St Andrews University), Dr Elizabeth Clarke (Marine Laboratory), and Colin Millar (CREEM and Marine Laboratory) are thanked for providing me with expert advice and help with Bayesian statistical methods. I acknowledge the crew and Captain of FRV *Scotia* and colleagues of the Marine Laboratory who assisted in collecting data on acoustic surveys for herring in the North Sea.

During my studies I had the honour and great pleasure to meet and get to know better many fellow fisheries acousticians from all over the world. Colleagues of the ICES Working Group on Fisheries Acoustic Science and Technology (WGFAST) are thanked for providing such an encouraging and friendly community that is a great source of inspiration. I am deeply indebted to Prof Egil Ona (IMR, Norway) and Prof Natalia Gorska (University of Gdańsk, Poland) for their collaboration that encouraged me to pursue the investigation into Baltic herring TS. Dr Dezhang Chu (NWFSC, USA) and Dr Gareth Lawson (WHOI, USA) kindly provided assistance with the DWBA model. Many thanks to Prof John Horne (University of Washington, USA) and Dr Michael Jech (NEFSC, USA) for the invitation to attend the Acoustic

Backscatter Modelling workshop at Friday Harbor in January 2008. Additional thanks to Michael for his help with the KRM model. Together with Dr Héctor Peña (IMR, Norway) I had much joy looking at herring under pressure in an MRI scanner at the hospital in Bergen!

This thesis would not have been possible without the funding I received through the Overseas Research Student Award Scheme (ORSAS) and the University of St Andrews. Throughout my studies I have additionally received financial support from the Dr. Max Husmann-Stiftung, the Jubiläumsstiftung of the Basellandschaftliche Kantonalbank and an Ausbildungsbeitrag of the Kanton Basel-Landschaft.

Finally, a big thank you to the friends I made in the Aberdeen Oilers Floorball Club, especially Neil, Linda, Osku and Kimmo, who made my whole stay in Aberdeen very enjoyable and allowed me to have a sporty and social alternative to fisheries acoustics research! Most importantly, I am grateful to my wife, Lorna, for her love, support and company.

Au e grosses Dangschön an mini Fründe und Familie deheim, mini Eltere und Brüedere, dr Ron und dr Chris, womi bi jedr Ruckkehr immr widr willkomme gheisse hän, für euri Aarüef, chats, e-mails und Bsüech. Merci vylmol!

„Im Hering isch manchs einerlei
Är weiss nur öppis ganz genau
Dr Mensch mit sin'rä Fischerei
Isch schlimmr als dr Kabeljau"

(source by Ingo Baumgartner)

Abstract

Acoustic survey techniques are widely used to quantify abundance and distribution of a variety of pelagic fish such as herring (*Clupea harengus*). The information provided is becoming increasingly important for stock assessment and ecosystem studies, however, the data collected are used as relative indices rather than absolute measures, due to the uncertainty of target strength (TS) estimates. A fish's TS is a measure of its capacity to reflect sound and, therefore, the TS value will directly influence the estimate of abundance from an acoustic survey. The TS is a stochastic variable, dependent on a range of factors such as fish size, orientation, shape, physiology, and acoustic frequency. However, estimates of mean TS, used to convert echo energy data from acoustic surveys into numbers of fish, are conveniently derived from a single metric - the fish length (L). The TS used for herring is based on TS-L relationships derived from a variety of experiments on dead and caged fish, conducted 25-30 years ago. Recently, theoretical models for fish backscatter have been proposed to provide an alternative basis for exploring fish TS. Another problem encountered during acoustic surveys is the identification of insonified organisms. Trawl samples are commonly collected for identification purposes, however, there are several selectivity issues associated with this method that may translate directly into biased acoustic abundance estimates. The use of different acoustic frequencies has been recognised as a useful tool to distinguish between different species, based on their sound reflection properties at low and high frequencies.

In this study I developed theoretical models to describe the backscatter of herring at multiple frequencies. Data collected at four frequencies (18, 38, 120 and 200 kHz) during standard acoustic surveys for herring in the North Sea were examined and compared to model results. Multifrequency backscattering characteristics of herring were described and compared to those of Norway pout, a species also present in the survey area. Species discrimination was attempted based on differences in backscatter at the different frequencies. I examined swimbladder morphology data of Baltic and Atlantic herring and sprat from the Baltic Sea. Based on these data, I modelled the acoustic backscatter of both herring stocks and

attempted to explain differences previously observed in empirical data. I investigated the change in swimbladder shape of herring, when exposed to increased water pressures at deeper depths, by producing true shapes of swimbladders from MRI scans of herring under pressure. The swimbladder morphology representations in 3-D were used to model the acoustic backscatter at a range of frequencies and water pressures. I developed a probabilistic TS model of herring in a Bayesian framework to account for uncertainty associated with TS. Most likely distributions of model parameters were determined by fitting the model to *in situ* data. The resulting probabilistic TS was used to produce distributions of absolute abundance and biomass estimates, which were compared to official results from ICES North Sea herring stock assessment.

Modelled backscatter levels of herring from the Baltic Sea were on average 2.3 dB higher than those from herring living in northeast Atlantic waters. This was attributed to differences in swimbladder sizes between the two herring stocks due to the lower salinity Baltic Sea compared to Atlantic waters. Swimbladders of Baltic herring need to be bigger to achieve a certain degree of buoyancy. Morphological swimbladder dimensions of Baltic herring and sprat were found to be different. Herring had a significantly larger swimbladder height at a given length compared to sprat, resulting in a modelled TS that was on average 1.2 dB stronger. Water depth, and therefore the increase in ambient pressure, was found to have a considerable effect on the size and shape of the herring swimbladder. Modelled TS values were found to be around 3 dB weaker at a depth of 50 m compared to surface waters. At 200 m, this difference was estimated to be about 5 dB. The Bayesian model predicted mean abundances and biomass were 23 and 55% higher, respectively, than the ICES estimates. The discrepancy was linked to the depth-dependency of the TS model and the particular size-dependent bathymetric distribution of herring in the survey area.

Contents

Chapter 1

General introduction

This thesis addresses issues related to the acoustic assessment of abundance and biomass of herring (*Clupea harengus*). Herring and other small pelagic clupeoid fish (Clupeiformes: Clupeoidei), such as sardines (e.g. *Sardina pilchardus*), shads (e.g. *Alosa fallax*), menhaden (e.g. *Brevoortia tyrannus*) and anchovies (e.g. *Engraulis ringens*), form a vital part of many of the world's pelagic ecosystems. These plankton-feeding fish represent an important link between planktic secondary production (Blaxter and Hunter 1982; Frederiksen et al. 2006; Hunt and McKinnell 2006) and piscivorous predators such as large pelagic fish, demersal fish, marine birds and mammals (Thompson et al. 1991; Northridge et al. 1995; Greenstreet et al. 2006). Many of the commercially important predatory species can only be supported by large numbers of small pelagic forage fish. In cases where their crucial position at the mid-trophic level is dominated by a low number of species, which therefore exert 'wasp-waist control', the whole system can become increasingly susceptible to changes (Rice 1995; Cury et al. 2000; Bakun 2006). Fluctuations in the abundance of the predatory species has often been found to follow closely that of their small pelagic fish prey (Crawford et al. 1987; Lluch-Belda et al. 1989; Greenstreet et al. 1998; Frederiksen et al. 2006), which in turn is strongly influenced by the variability of local environmental conditions (Cury et al. 2000; Edwards et al. 2002; Beaugrand

2004; Edwards and Richardson 2004). Food availability and physical processes control larval success and subsequent recruitment (Cushing 1996), and predators may also influence the size of the stock (Griffiths 2002). Moreover, plankton abundance is generally thought to influence the distribution and abundance of small pelagic fish (Verheye and Richardson 1998; Corten 2000; Kaartvedt 2000; Prokopchuk and Sentyabov 2006). The central role of these fish as a link between lower and higher trophic levels makes clupeoids important to anyone interested in research or management of species directly or indirectly linked to the pelagic ecosystem.

In addition to their ecological significance, clupeoids are of increasing socio-economic importance. Despite the low biodiversity exhibited by these species (Cury et al. 2000), global marine catches are dominated by small pelagic fish. They represent half of the ten highest landing biomass species (anchovy, Atlantic herring, chub mackerel, Chilean jack mackerel, and Japanese anchovy) and in 2007 accounted for 30% of the total reported global marine fish catch by weight (FAO 2008a). The contribution of pelagic fisheries to marine fish catches has risen from 54% in 1950 to a present level of 65% (FAO 2008b). Nonetheless, many stocks of clupeoids have gone through major series of collapse and recovery (Hempel 1978; Kondo 1980; Pauly et al. 1989; Beverton 1990; Schwartzlose et al. 1999; Hutchings 2000), and their increasing contribution to global catches is thought to reflect a gradual transition in landings towards species at lower trophic levels (Pauly et al. 1998). Although the impact of fishing on fluctuations and abundances of pelagic fish remains controversial (Lluch-Belda et al. 1989; Beverton 1990; Gjøsæter 1995), their schooling behaviour makes small pelagic fish particularly vulnerable to modern fishing techniques. Fish schools can easily be detected by acoustic devices such as sonar and echosounders, and effectively caught by large pelagic trawls or purse seines (Parish 2004). This is especially problematic since the clustering and number of small pelagic fish schools was found to be density independent and hence not to be related to their abundance (Petitgas et al. 2001). Even at a low stock size, herring were found to aggregate in large schools and could therefore still be detected and potentially fished towards extinction (Beare et al. 2002). While fishing was identified as an

obvious cause of the collapse of some stocks of clupeoids (Saville and Bailey 1980; Beverton 1990), environmental factors have also been recognised to play a major role in recruitment success (Lasker 1985). Nevertheless, fishing may be expected to influence the natural cycle of abundance of small pelagic species by shortening periods of high abundance and extending periods of scarcity (Cury et al. 2000). Because of the influence environmental factors have on clupeoids in addition to fishing pressure, it is hard to predict their stock size (Lasker 1985; Beverton 1990). In order to fulfil the current demand for a shift from classical single-species management to a multi-species ecosystem-based fisheries management (EBFM) approach (Gislason et al. 2000; Hall and Mainprize 2004; Pikitch et al. 2004; Cury and Christensen 2005; Garcia and Cochrane 2005; Greenstreet and Rogers 2006; Frid et al. 2006), it is, however, vital to have detailed knowledge about the respective roles different species play in the ecosystem. Consequently, it is of particular importance to have reliable estimates of absolute abundance and distribution of an ecologically and economically important species such as the herring.

1.1. Assessment of North Sea herring

By the middle of the 20th century the North Sea herring fisheries had gone through periods of enhanced technological development, which resulted in high levels of fishing mortality (Saville and Bailey 1980). After lack of management action and the consequential collapse of the North Sea herring stock in 1977 the fishery was closed for four years to allow for a recovery of the spawning stock biomass, whose abundance was at about 1.25% of the post-war levels (Bailey and Simmonds 1990). Previously, the size of the stock had been estimated annually based on a regression between indices of larval abundance and estimates of spawning stock biomass from virtual population analysis (VPA, Pope and Shepherd 1982). The problem however was that at those low levels of spawning stock biomass, the regression would have had to be extrapolated beyond the data points available. In order to monitor the stock size in the absence of any fisheries data and at low numbers of spawning herring, an acoustic survey for North Sea herring was started in 1979 (ICES 1980). Since the

initial stage, when the survey duration, timing, and methodology were determined, acoustic surveys have been carried out annually until the present time. These surveys have contributed towards improving scientific knowledge about the stock size and allowed to justify and implement appropriate management action when the stock was going towards low levels in 1996 for a second time after its collapse in 1977 (Simmonds 2007). Similarly to estimates from larval and recruitment surveys, abundance estimates from acoustic surveys for North Sea herring are treated as relative numbers and are used as an index to 'tune' the presently used integrated catch-at-age population model (Patterson and Melvin 1996; Woillez et al. 2009). This is due to the fact that the stock estimate from acoustic surveys is strongly dependent on the assumed echo value produced by one fish - the target strength (TS).

The total error in the abundance estimate from an acoustic survey generally consists of two components: the random and the systematic error (Table 1.1). Random error is largely influenced by the chosen sampling strategy or survey design and can be reduced by collecting more samples. The systematic error in contrast affects all observations equally irrespective of sample size and may therefore bias the abundance estimate. Most of the large systematic error sources (air bubbles, migration or vessel avoidance; see Table 1.1) can be minimised or ignored if a modern research vessel is used and the survey designed in a robust way (Simmonds and MacLennan 2005). Since the abundance estimate is inversely proportional to the error prone TS (see Equation 1.9), any error in the assumed TS value will bias the abundance estimate to a large extent. Due to the high uncertainty associated with the TS (Table 1.1), absolute estimates from acoustic survey tend to have a low accuracy (Simmonds et al. 1992).

Table 1.1 Sources of error in acoustic surveys (estimated by Simmonds et al. 1992). Negligible error estimates are given in brackets.

Source	Error		Comments
	Random (precision)	Systematic (accuracy)	
Species identification	0 - 50 %		Dependent on species mix and TS differences between species
Random sampling	5 - 20 %		Dependent on spatial distribution
Equipment calibration		± 3 - 10 %	
Bubble attenuation		(0 - -90 %)	Negligible with modern research vessels
Hydrographic conditions	± 2 - 25 %	± 2 - 25 %	Uncertainties in sound absorption
Migration		0 - 30 %	
Diurnal behaviour	0 - 50 %		Affects TS
Vessel avoidance		(0 - 50 %)	Negligible with quiet research vessel in open deep water
Target strength	**± 5 - 25 %**	**0 - 50 %**	

Of all the different indices used in the assessment of the North Sea herring stock, the acoustic survey has been assigned the highest weighing for most ages, including all adults, due to its superior precision (ICES 2002; Simmonds 2003). Improving the knowledge about the uncertainty of the TS may increase the accuracy of acoustic surveys and therefore enhance their potential to produce absolute abundance and biomass estimates. In order to achieve an EBFM approach, absolute biomass estimates of predators, prey and exploited species need to be fed into dynamic ecological models at suitable temporal and spatial scales (Koslow 2009). Acoustic methods are among the most promising to meet these demands as they can provide increased data richness and spatial coverage by offering continuous and high-resolution observations throughout the water column (Mackinson et al. 2004). Future ecosystem based stock assessment for species like the North Sea herring will

therefore benefit from knowledge of appropriate TS values and its associated variability.

The following sections give an outline about acoustic survey methods and review approaches to determine the TS of herring and to investigate its variability by means of empirical measurements and, more recently, theoretical modelling.

1.2. Acoustic surveys

1.2.1. Principles

Fishery-independent data provide a different perspective to sometimes questionable commercial catch data (Pauly et al. 2002; Agnew et al. 2009). Since herring have a pelagic lifestyle and spend at least part of their time in dense schools in mid-water, they are an appropriate target for acoustic surveys (MacLennan 1990). Acoustic methods have a distinct advantage in that sound propagates over long distances at high speeds in water (typically 1500 m s^{-1}), resulting in a high-resolution coverage of extensive water bodies within short time periods. During an acoustic survey the vessel usually steams along predefined parallel transect lines, covering the survey area in such a way that the data collected can be used to provide a statistically robust abundance estimate of the stock of interest (Simmonds and MacLennan 2005). The acoustic survey usually involves an echosounder system, which contains a transmitter that generates bursts of electrical energy. A vertically downward pointing transducer mounted on the hull of the vessel converts the electrical energy from the transmitter to ‘mechanical’ sound energy at discrete frequencies (typically 18, 38, 120 and 200 kHz for surveys of North Sea herring) (Figure 1.1). The transducer serves both to propagate the sound and receive resulting echoes. The sound is projected in a directional beam similar to a beam of light generated by a torch. Any objects that have a different density or sound speed contrast from that of water (e.g. fish schools or the seabed) will reflect the transmitted sound waves and generate backscattering waves (echoes), which are eventually detected by the transducer. The acoustic signals are then amplified and converted back into electrical energy as the received signal. The time that the echo is received enables the distance to the encountered object to be

determined, while the intensity of the signal reveals information about its size/density (Simmonds and MacLennan 2005). A two-dimensional picture (known as an echogram, Figure 1.2) of the scanned water body is built up as the vessel is steaming along survey transect lines. Encountered objects, usually referred to as targets, are displayed on the echogram as so-called ‘marks’ or ‘echo traces’ and colour scales are used to indicate their echo intensity.

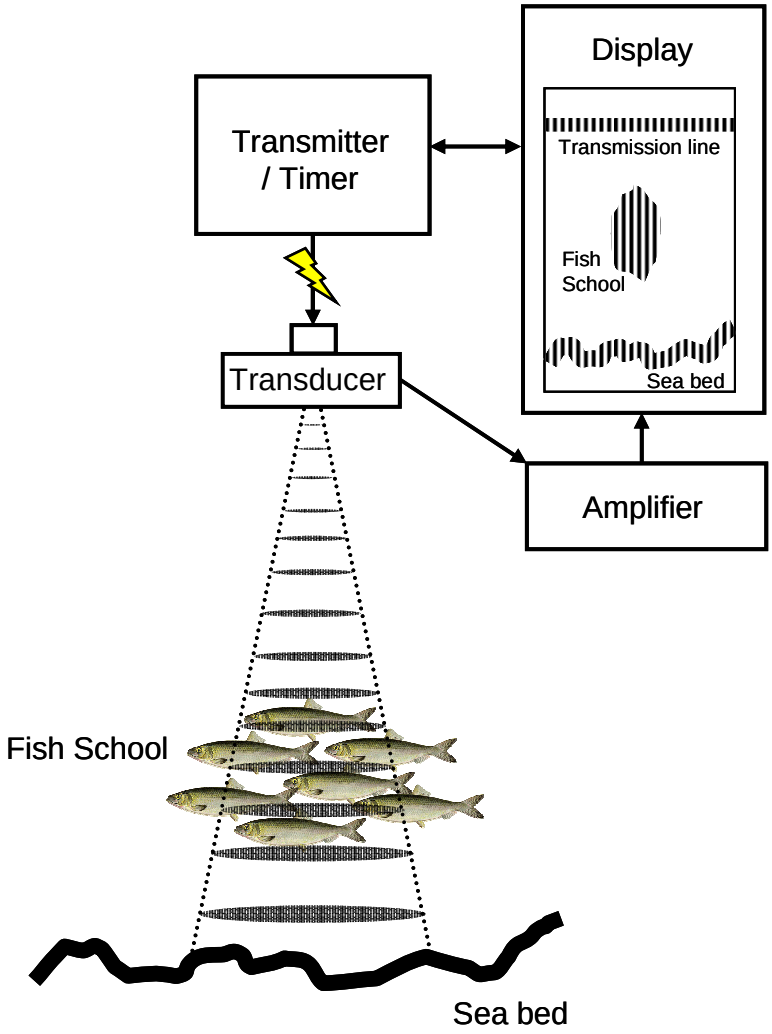

Figure 1.1 Schematic representation of an echosounder system. The pulse of sound generated by the transducer is reflected by targets in the water column (fish school and sea bed), received, amplified and subsequently displayed on an echogram (adapted from Simmonds and MacLennan 2005).

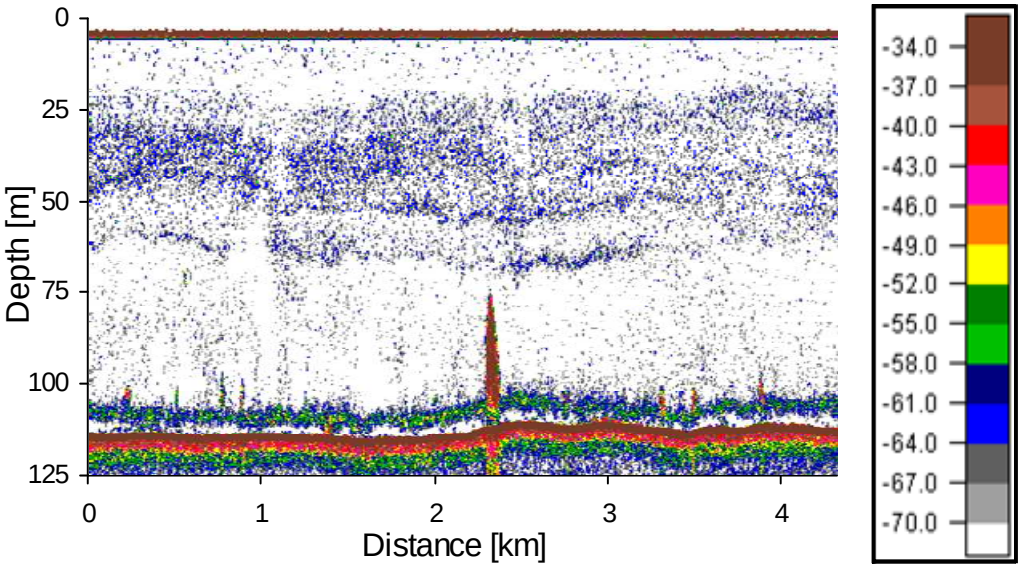

Figure 1.2 A school of North Sea herring (*Clupea harengus*) shown as a red-brown 'mark' at a depth of about 100 m in the middle of the echogram. Plankton appears as a blue layer at depths between 25 and 60 m. The seabed is given as a dark continuous line at about 115 m. Colours represent echo intensities in volume backscattering strength (S_v; units: dB, see Equation 1.7) according to the scale on the right side.

1.2.2. Quantification of echo strength

Backscattered acoustic energy from detected targets is quantified as a proportion of the transmitted incident energy. Assuming that I_i represents the intensity at the midpoint of the pulse of the incident sound wave at the target, and I_{bs} the respective intensity of the backscattering pulse, then:

$$\sigma_{bs} = R^2 \frac{I_{bs}}{I_i} \tag{1.1}$$

where R is the distance from the target at which the intensity is measured (1 m is used by convention). σ_{bs} is the resulting quantification of backscatter, the backscattering cross-section, which is measured in units of area (m^2). The TS is a logarithmic

representation of the backscattering cross-section and is expressed in decibels (dB) according to:

$$TS = 10 \log_{10}(\sigma_{bs}) \quad (1.2)$$

Both the backscattering cross-section (σ_{bs}) and TS are representations of the same physical properties of the detected target, i.e. the strength or intensity of the backscattered energy (Simmonds and MacLennan 2005). The logarithmic TS measure has the advantage that only a relatively short span on the decibel scale is needed to express backscatter intensities of different organisms that can vary greatly, over several orders of magnitude. For example, the TS of a 20 cm herring (about -45 dB) is the same order of magnitude as the TS of a 35 mm krill (*Euphausia superba*, about -85 dB). However, if the same echo strengths were presented as σ_{bs}, they would range over four orders of magnitude (3.16×10^{-5} and 3.16×10^{-9} m^2, respectively): this large range is difficult to converse in.

The short burst of sound, called the 'pulse' or the 'ping', which is transmitted by an echosounder, consists of several waves of length λ, at the respective operating frequency. Depending on the number of waves (*n*) and the frequency (*f*), the pulse has a specific duration $\tau = n/f$. The length of the pulse (L_p, in m) is then dependent on its duration (τ, in s) and the speed of sound (c, in m s^{-1}) in water according to:

$$L_p = c\tau \quad (1.3)$$

In order to resolve two discrete targets (e.g. two single fish) at ranges (distance between transducer face and target) R_1 and R_2, their range difference (R_2 - R_1) must be large enough to preclude the two resulting echoes from overlapping (Simmonds and MacLennan 2005). To achieve this, the targets must differ in range by at least half the pulse length, so that:

$$R_2 - R_1 > \frac{L_p}{2} \tag{1.4}$$

If individual targets are so close together that it is not possible to resolve their echoes singly, their echoes combine to form a common backscattered signal. The echo intensity then still provides a proportional measure of biomass in the water column, but it represents a sum of echoes from all individual targets contributing to the whole echo. Such a situation would typically occur if a shoal of fish, rather than a single fish, were insonified. The measurement of backscatter from multiple targets is the volume backscattering coefficient (s_v):

$$s_v = \sum \sigma_{bs} / V_0 \tag{1.5}$$

where the sum represents all targets contributing to a combined echo from the sampled volume of water (V_0). To calculate the sampled volume, the cross-sectional area of the beam (angle of the sound beam (ψ) times the square of the range (R^2)) has to be multiplied by half the pulse length (L_p):

$$V_0 = \psi R^2 L_p / 2 \tag{1.6}$$

Similar to the TS measure for single targets, there is also a logarithmic measure for multiple target backscatter, namely the volume backscattering strength (S_v):

$$S_v = 10 \log_{10} (s_v) \tag{1.7}$$

If S_v is averaged over a larger volume than V_0, covering several pings and a large range interval, the equivalent backscatter is expressed in the logarithmic domain and called mean volume backscattering strength ($\hat{S}_v$). An important measure generally used in acoustic surveys is the area backscattering coefficient (s_a). It is the integral of

the backscattered energy (s_v) in a layer between two depths in the water column. A version of s_a in common use is the nautical area scattering coefficient (s_A), which is for historical reasons based on the spherical scattering coefficient ($\sigma_{sp} = 4\pi\sigma_{bs}$) and the nautical mile (= 1852 m) (MacLennan et al. 2002):

$$s_A = 4\pi (1852)^2 s_a \tag{1.8}$$

Once a number of echoes from a given area have been integrated over a wider survey distance (Ehrenberg 1973), the density of fish (ρ) can be calculated by dividing the acoustic density (s_A) by the expected mean backscattering cross-section of one fish ($\langle\sigma_{bs}\rangle$) according to:

$$\rho = \frac{s_A}{4\pi\langle\sigma_{bs}\rangle} \tag{1.9}$$

In order to infer quantitative information such as numbers per unit volume accurately, it is important to first identify the insonified targets (to allocate s_A to species) and then to know their appropriate TS (or σ_{bs}, see Equation 1.2).

1.3. Empirical target strength measurements

There are essentially three different experimental methods that have been used by a number of investigators to measure the TS of fish and its variability with parameters such as size, angle of orientation or water depth. As the TS is not a point function but a probability density function (PDF), it is important to understand the full scale of variability if survey data are to be interpreted correctly. Hence, the pursuit of TS has attracted a considerable effort. Empirical TS measurement methods are described and summarised in reviews by Love (1971a), Midttun (1984) and MacLennan (1990), and are generally based on insonification of either: (1) immobilised or unconscious fish,

(2) active fish confined within a cage, or (3) wild fish, which are free to behave normally.

1.3.1. Immobile fish

Early investigations were based on dead or stunned fish held by wires at a certain orientation in the acoustic beam. Nakken and Olsen (1977) made measurements of dead herring, which were fixed in space and situated in the beams of a 38 and a 120 kHz transducer (Figure 1.3). The experimental set-up allowed the fish to be tilted between -45º (i.e. head down) and +45º (i.e. head up). Measured maximum dorsal aspect TS at both frequencies was plotted against fish length (L), resulting in a positive linear relationship. Linear representation of TS to L relationships led to the use of a standard equation:

$$TS = m \log_{10} L + b \tag{1.10}$$

Coefficients m and b are determined by a least-mean-squares regression analysis. Love (1977) later concluded that σ_{bs} was approximately proportional to L^2 and consequently adjusted Equation 1.10 to the presently recognised form, which has since been used in echo integrator surveys to convert fish length to TS (e.g. see ICES 2008b):

$$TS = 20 \log_{10} (L) + b_{20} \tag{1.11}$$

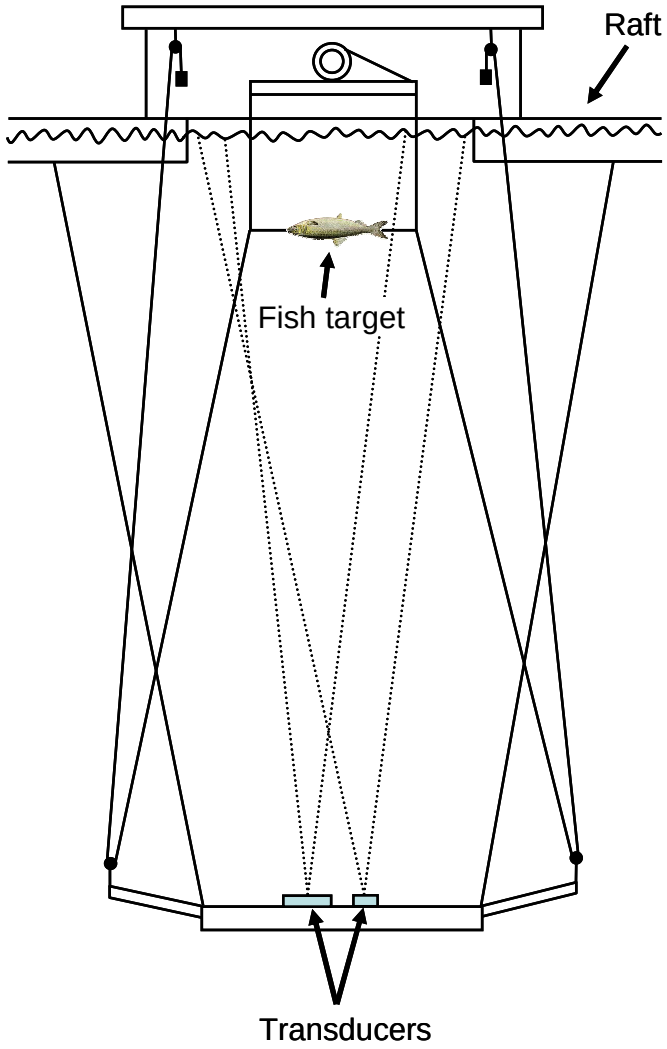

Figure 1.3 Apparatus for target strength measurements on immobile fish. The fish were suspended on wires that allowed tilting of the platform where the 38 and 120 kHz transducers were mounted (redrawn and adapted from Nakken and Olsen 1977).

Demer and Martin (1995) argue that a linear regression of TS versus length can be inappropriate. This is especially true for zooplankton, which exhibit highly non-linear, behaviour-dependent scattering responses at frequencies where the wavelength (λ) is much smaller than the size of the animal (Chu et al. 1992). Nakken and Olsen (1977) found that TS was also strongly dependent on the tilt of the fish. Higher TS values were generally observed for tilt angles around 0º (i.e. broadside dorsal aspect).

Consequently, any observations of maximum dorsal aspect TS would be of limited practical use since free-swimming fish would adopt a range of tilt angles (Foote 1980b). Although based on limited amounts of data, mean TS values (for tilt angles within ±3º of angle of maximum value) for herring were found to be 6 dB lower than corresponding maximum values (Nakken and Olsen 1977). Waves scattered by different parts of the body appeared to magnify the change of TS as the fish tilted. Love (1971b) performed similar experiments by determining dorsal-aspect TS of anaesthetised small fish, including anchovies and menhaden, as a function of size and incident acoustic frequency. He observed a marked dip in length-based backscatter (σ_{bs}/L^2) for both anchovy and menhaden at a fish length to wavelength relationship (L/λ) of about 10. These results provide further evidence for possible interactions between different parts of the fish (swimbladder, bone, and flesh), resulting in a complex backscattering response over a range of frequencies. In a variety of previous experiments investigators have dissected fish to determine the importance of different body parts as acoustic reflectors. Jones and Pearce (1958) showed that the dorsal and side-aspect TS of a perch (*Perca fluviatilis*), at frequencies where $L/\lambda \approx 4$, was reduced by approximately 50% when the swimbladder was removed. Foote (1980a) provided further evidence for the importance of the gas-filled swimbladder when he compared differences in acoustic backscatter between the swimbladdered cod (*Gadus morhua*) and the non-swimbladdered Atlantic mackerel (*Scomber scombrus*). The relative swimbladder contribution to both maximum and averaged dorsal aspect backscattering cross-section (σ_{bs}) was found to be approximately 90% to 95% (Foote 1980a).

1.3.2. Caged fish

Cage experiment techniques were developed and applied by Edwards and Armstrong (1981, 1983, 1984) and Edwards et al. (1984), who moored a raft with acoustic equipment and a suspended cage (diameter: 2 m) in a sea loch on the west coast of Scotland (Figure 1.4). They collected TS data at 38 and 120 kHz from herring that were swimming inside the cage. At the start of the experiment the cage was lowered

to a depth of 17.5 m and the recorded 24-hour average TS for herring showed a gradual decrease over 5 days. An explanation for this phenomenon is the diffusion of gas out of the swimbladder over time and a resulting steady decrease in swimbladder volume (Blaxter et al. 1979). When the cage was lowered from a depth of 17.5 m to 47.5 m, a rapid drop in TS was observed. More recently, Ona (2003) lowered herring in a large cage to a depth of about 100 m while making continuous measurements at 38 kHz with an echosounder mounted at the top of the cage (Figure 1.5). In agreement with previous investigators he observed a consistent reduction in herring TS with depth. These results can most likely be explained by the fact that herring are physostomes and, hence, they do not have a gas gland that allows them to alter the amount of gas in the swimbladder. The effect is a decrease in swimbladder volume with depth, according to Boyle's law, and a consequent reduction in backscatter from this organ compared to other potentially important body components (e.g. the flesh and the bone) (Ona 1990; Blaxter and Batty 1990; Mukai and Iida 1996). Ona (2003) applied Boyle's volume contraction model to *in situ* TS data of caged and free swimming herring at depths down to 500 m to estimate the contraction-rate factor (γ):

$$\sigma_{bs} \propto (1 + z/10)^{\gamma} \tag{1.12}$$

He found that γ = -0.23 gave the best fit to the data. At the frequency of 38 kHz, used by Ona (2003), backscatter from herring is proportional to the dorsal cross-sectional surface area of its swimbladder (Horne and Clay 1998). If the volume of a spherical balloon changes with depth according to Boyle's Law, its γ value would be equal to -2/3. Ona's (2003) findings therefore suggest that the horizontal cross-section of the herring swimbladder contracts to a smaller extent than its volume. Pedersen et al. (2009) further confirmed this suggestion. Their *in situ* TS measurements showed that the lateral-aspect TS of herring decreased to a higher degree with depth than dorsal-aspect TS, suggesting an enhanced reduction in the lateral dimension. Following the methods of Edwards and Amrstrong (1981, 1983, 1984), Thomas et al. (2002) made measurements of caged Pacific herring (*Clupea pallasi*) at depths down to 43 m at

120 kHz. They also found a decline in TS with depth in accordance with that expected from the effects of Boyle's law. Nonetheless, it is difficult to estimate the effect of depth-dependent swimbladder volumes on TS directly. Herring can release gas from the swimbladder through an anal duct that connects the swimbladder to the exterior (Blaxter and Batty 1984; Wahlberg and Westerberg 2003; Wilson et al. 2003). Gas release has been observed in herring schools ascending towards the sea surface (Thorne and Thomas 1990) and in herring schools under predator attack (Nøttestad 1998).

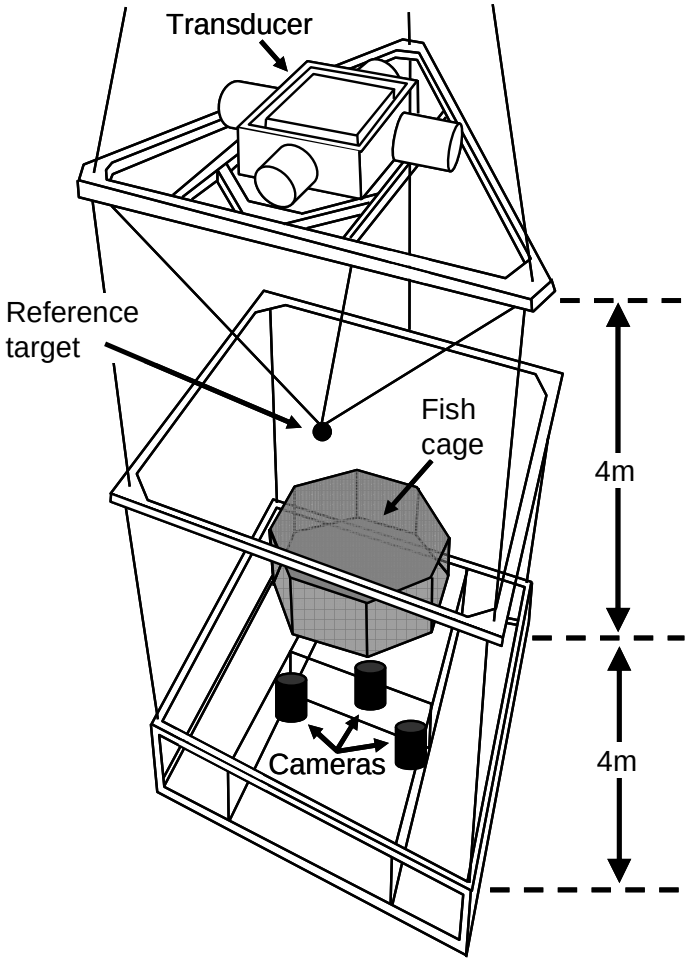

Figure 1.4 Frame for target strength measurements on live fish in a cage. The cage is about 2 m in diameter and 1 m deep. A reference target provides continuous calibration of the fish echoes (redrawn and adapted from Edwards et al. 1984).

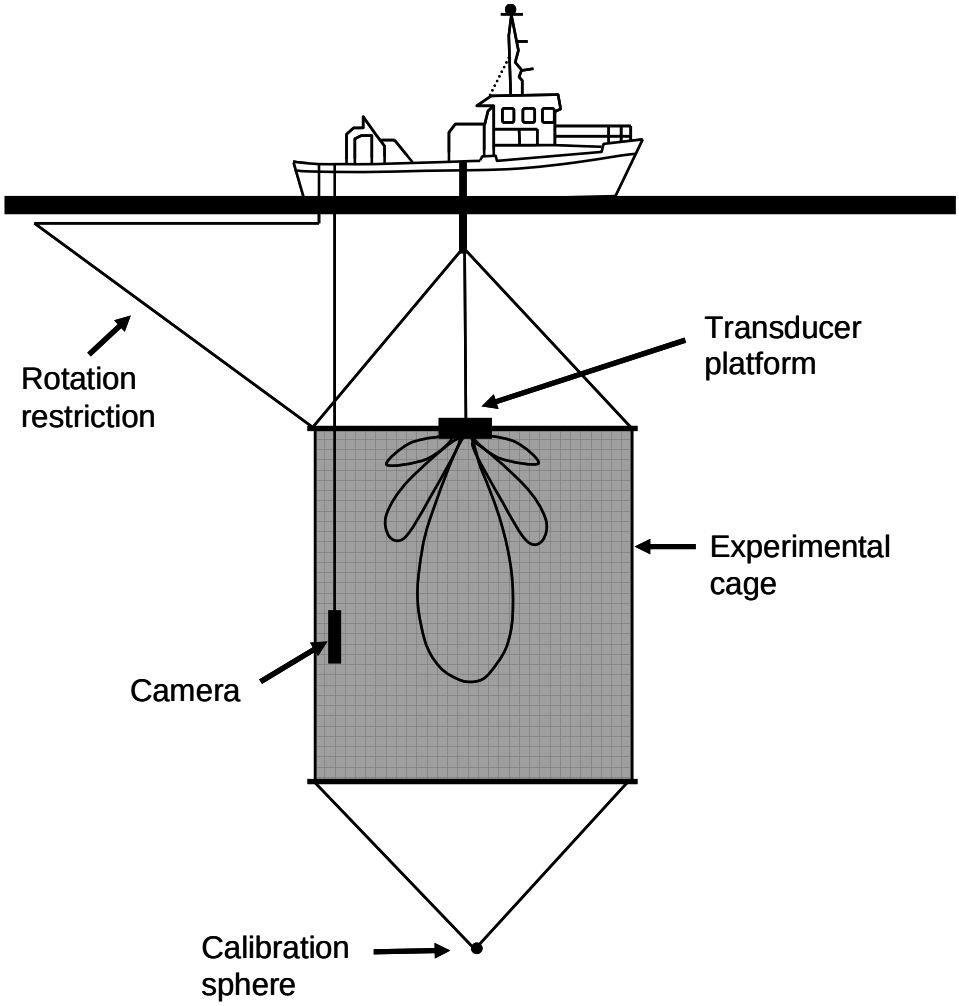

Figure 1.5 Experimental setup for target strength measurements and video analysis of herring swimming behaviour. Dimensions of the cage are 12.5 × 12.5 × 21 m (redrawn and adapted from Ona 2001).

Ona et al. (2001) investigated potential changes in herring TS over two full reproductive seasons. They insonified herring at 38 and 120 kHz in a large net pen (4500 m^3) and found that, at the same depth, herring exhibited increased TS values at times when their gonadosomatic indices (GSI) were high. Gonads can be expected to influence the TS directly by changing fish density, and indirectly by deforming the swimbladder (Machias and Tsimenides 1995; Ona 1990, 2003; Ona et al. 2001).

Consequently the following equation was suggested to include both the depth (z) dependence and the GSI in the length based TS relationship for herring:

$$TS = 20\log_{10}(L) - 2.3\log_{10}(1+z/10) - 65.4 + 0.24\,(GSI) \qquad (1.13)$$

However, independent effects of pressure and gonads are difficult to separate and it is likely that they interact with each other (Ona 2003). Nevertheless, if abundances of Norwegian spring-spawning herring were to be calculated using a modification of Equation 1.13 (i.e. excluding the GSI factor), instead of the presently used TS-L relationship (TS = 20 $\log_{10}$(L) - 71.9), estimates of biomass would be reduced by 50% (Ona 2003).

1.3.3. Wild fish

Results from cage experiments have emphasised the importance of physical and physiological factors on TS. However, since fish are confined within cages and therefore in an unnatural environment, it is plausible to assume that the stress of captivity might influence the measurements (MacLennan 1990). To be applicable to acoustic abundance estimation, TS measurements should preferably be obtained from fish free to behave unconstrained in their natural environment.

1.3.3.1. Direct method

Direction-sensitive apparatuses, such as dual-beam and split-beam transducers, are required to collect 'direct' *in situ* data (Ehrenberg 1974; Foote et al. 1984). These transducer systems can determine the position of a single target in the acoustic beam and measure the TS directly (Ehrenberg and Torkelson 1996). If the same target is detected over a certain period of time, its speed and track direction can be calculated by combining single detections (Ehrenberg and Torkelson 1996; McQuinn and Winger 2003). Foote et al. (1986) made *in situ* measurements of herring around the Shetland Isles using the direct method. After collection of TS data, insonified fish aggregations were sampled by trawls. Mean values for TS were then plotted against mean fish length to determine the b_{20} coefficient in Equation 1.11 (see Table 1.2). In

1983, the Planning Group on ICES-coordinated Herring and Sprat Acoustic Surveys (ICES 1983) recommended that for herring, the b_{20} coefficient in Equation 1.11 should be set at -71.2, based on two sets of data published by Nakken and Olsen (1977) and Edwards and Armstrong (1983). These values are still used on surveys for various herring and sprat stocks today (e.g. ICES 2008a) and compare reasonably well with other *in situ* measurements (Table 1.2), including those of Foote et al. (1986) for herring and those of Foote (1987) for clupeoids (i.e.: $TS = 20 \log_{10}(L) - 71.9$). Warner et al. (2002) used a split-beam echosounder at 70 kHz to determine relationships between *in situ* TS and both length and mass of alewives (*Alosa pseudoharengus*), another clupeoid, in freshwater. They observed a similar slope (20.53 ± 0.78 s.e.) but a considerably higher intercept for Equation 1.11 (-64.25 ± 0.80 s.e.) compared to previous publications for marine clupeids of similar size. A higher mean TS for a freshwater clupeoid may be the result of lower specific gravity of freshwater or lower lipid content of alewives (Warner et al. 2002). Using similar methods, Didrikas and Hansson (2004) found that herring from the brackish Baltic Sea had a mean TS that was 3.4 dB higher than the one suggested using the currently accepted herring TS-length equation used for their assessment. In a subsequent publication, Peltonen and Balk (2005) estimated TS-length equations (Equation 1.11) for herring from the northern Baltic Sea using split-beam recordings and trawl catches. When Equation 11 was fitted to their data, the resulting intercept was -63.9, suggesting a TS value for northern Baltic herring that is 7.3 dB higher than derived from the equation used by ICES to assess herring within the North and Baltic Sea (e.g. ICES 2006, 2008b). The discrepancy between abundance estimates derived from those two alternative equations would result in a more than five-fold difference.

1.3.3.1.1. Target tracking

Huse and Ona (1996) made use of split-beam tracking methods combined with photographs to study the swimming behaviour of overwintering Norwegian spring-spawning herring. In the winter months, these herring form dense schools in deep water during the day (down to 400 m). At night, part of the population migrates to the

upper water layers. Lacking the ability to refill their swimbladder, herring become increasingly negatively buoyant with depth (Brawn 1969; Ona 1990). Huse and Ona (1996) found that herring had a positive tilt angle (up to 40º) at deeper depths (300 - 400 m), which might be a response to compensate for the negative buoyancy. In shallow waters (0 - 62 m) and intermediate waters by day (100 - 200 m), herring were found to swim approximately horizontally. Since TS is strongly dependent on tilt angle (Nakken and Olsen 1977; Edwards et al. 1984; Blaxter and Batty 1990; Hazen and Horne 2003), such findings have huge implications for acoustic abundance estimation, suggesting behaviour induced systematic changes in TS with time of the day. This was confirmed when Huse and Korneliussen (2000) examined survey data for Norwegian spring-spawning herring and found higher s_A values during the day compared to low values during the night. They attributed these observations to diel variation in tilt angle distributions. The same phenomenon, with much more dramatic consequences, has also been observed in Antarctic krill (Everson 1982). In a further study, Ona (2001) used a split-beam echosounder and a video camera to simultaneously measure both the swimming angle and the tilt angle of a single herring in a large net pen (4500 m^3). He concluded that the difference between actual mean tilt angle and mean swimming angle (-0.06º, S.E. = 0.10º) is small and comparable to the accuracy in photographically determined tilt angles.

1.3.3.2. Indirect method

At times before direction-sensitive techniques were not commonly available, *in situ* data were collected with conventional single beam transducers by the so-called indirect method (Craig and Forbes 1969). Such measurements are less reliable, because the position of a detected target in the beam is not known and therefore the effect of the directivity pattern of the transducer cannot be compensated for. Algorithms which assume a certain density and random distribution of targets within the beam, and incorporate the transducer beam pattern, have been developed to determine the TS frequency distribution of detected targets (Craig and Forbes 1969; Clay 1983). A variety of TS measurements of herring were made using the indirect

method and mean TS values converted to fish length using Equations 1.10 and 1.11 (see Table 1.2, Halldorsson and Reynisson 1983; Lassen and Stæhr 1985; Degnbol et al. 1985; Rudstam et al. 1988).

1.3.3.3. Comparison method

Another method to determine TS *in situ* is the comparison method: a well-defined fish school has to be insonified to determine its total geometric volume and its nautical area scattering coefficient (s_A). Subsequently, the whole school has to be caught by use of, for example, a purse seine (Hamre and Dommasnes 1994). The number of fish divided by school volume gives the density, which is required to calculate the mean TS using Equation 1.8 and echo-integrator data (s_A) from the school. Misund and Beltestad (1996) have applied this method to determine TS-length relationships for herring (Table 1.2).

Table 1.2 Results from target strength estimates of various clupeoids. The function of fish length (L) to target strength (TS) is $TS = m \log_{10}(L) + b$, or the standard formula $TS = 20 \log_{10}(L) + b_{20}$. Methods are as follows: IF = immobile fish, CF = caged fish, Ind = indirect *in situ* observation, Comp = comparison method, SB = direct *in situ* observation using a split-beam echosounder.

Species	Location	Length	Frequency	m	b	b_{20}	Method	Reference
Herring (*Clupea harengus*)	Norwegian Fjord	8 – 39 cm	38	13.6	-56.8		IF	Nakken and Olsen (1977)
	Norwegian Fjord	8 – 39 cm	120	18.8	-62.4		IF	Nakken and Olsen (1977)
	Iceland	9 – 33 cm	38	21.9	-71.2	-69.4	Ind	Halldorsson and Reynisson (1983)
	N.E. Atlantic	7 – 27 cm	38	20.1	-71.5	-71.3	CF	Edwards et al. (1984)
	North Sea	24 – 34 cm	38			-72.1	SB	Foote et al. (1986)
	Baltic	6 – 24 cm	70	21.7	-75.5	-69.9	Ind	Rudstam et al. (1988)
	Iceland	6.5 – 34.0 cm	38	20.5	-67.7	-67.1	SB	Reynisson (1993)
	Norwegian Fjord	mean = 32.8 cm	38			-71.1	Comp	Misund and Beltestad (1996)
	Norwegian Fjord	mean = 31.2 cm	38			-64.6	CF	Ona et al. (2001)
	N.E. Pacific	11.3 – 26.8 cm	120	26.2	-72.5	-66.0	CF	Thomas et al. (2002)
	Norwegian Fjord	mean = 31.8 cm	38			-67.3	SB	Ona (2003)
	Baltic	4.5 – 28.5 cm	38	25.5	-73.6	-67.8	SB	Didrikas and Hansson (2004)
	N. Baltic	10 – 26.5 cm	38	16.8	-60	-63.9	SB	Peltonen and Balk (2005)
Herring & Sprat	N.E. Atlantic/ Norway	9 – 30 cm	38			-71.2	IF / CF	ICES (1983)
	Kattegat/Skagerrak	19 – 26 cm	38			-72.6	Ind	Degnbol et al. (1985)
	Baltic	mean = 14.6 cm	38			-70.8	Ind	Lassen and Stæhr (1985)
	Baltic	mean = 14.6 cm	120			-73.4	Ind	Lassen and Stæhr (1985)
Clupeoids	Various	6 – 34 cm	38			-71.9	All	Foote (1987)

1.4. Theoretical target strength modelling

Since the TS is a stochastic measure dependent on a variety of parameters (Blaxter and Batty 1990; MacLennan 1990; Ona 1990, 2001, 2003; Hazen and Horne 2003), the presently used Equation 1.11 is a convenient if not accurate description to derive mean TS from a single metric - the fish length. McClatchie et al. (1996) used an analysis of variance (ANOVA) to combine data from different studies and attempted to analyse discrepancies in results between TS estimation methods. They found significant effects of species, freshwater vs. marine, swimbladdered vs. non-swimbladdered and dead vs. alive fish on the relationship between maximum dorsal aspect TS and fish length. Additionally, quadratic dependence of TS on fish length (i.e. equation 1.10, where m = 20) was found to be the exception rather than the rule (McClatchie et al. 1996; McClatchie et al. 2003), with data usually widely scattered around the slope (Simmonds and MacLennan 2005). Considerable variation in TS estimates based on empirical measurements, as observed in herring (c.f. Table 1.2), led to an increased interest in developing theoretical scattering models of fish to aid the interpretation of experimental results (Horne and Clay 1998). These models are generally based on representing different body components of the fish (most importantly the swimbladder) as a function of their shape, orientation and acoustic properties.

Early models dealt with the representation of the swimbladder as a gas-filled simple geometric shape such as a sphere (Andreeva 1964; Haslett 1965; Love 1978) or a finite cylinder (Do and Surti 1990; Clay 1992). Nero et al. (2004) used Love's (1978) model to estimate the swimbladder volume of herring from low frequency acoustic measurements near the resonance region (1.5 - 5 kHz). More recently, Gorska and Ona (2003a, 2003b) have attempted to approximate the herring swimbladder using a prolate spheroid to more realistically represent its true shape. The scattering theory of such simple geometric shapes is well known and acoustic equations can be solved to give exact results for the backscattering strength (Horne and Clay 1998). More sophisticated models can make use of the true arbitrary shape of scattering objects such as the swimbladder. Such approaches usually involve

mapping of the object surface from physical replica reconstructions (Foote 1985) or radiographic imaging techniques like computer tomography (CT, Horne et al. 2000) or magnetic resonance imaging (MRI) scanners (Peña and Foote 2008).

1.4.1. Approximation solutions

1.4.1.1. Deformed cylinder model

Several approximation solutions have been applied to calculate backscatter for prolate spheroids and more realistic morphological shapes of various fish body components. Stanton (1988, 1989) described a method where the target is modelled as a cylinder whose radius varies along the axis. Total backscatter is then derived as the combined contributions from a modal series of single narrow sections of the cylinder along the axis. This so-called modal series-based deformed cylinder model (MSB-DCM) has been applied by Gorska and Ona (2003a, 2003b) to calculate herring backscatter by representing both the swimbladder and the fish body as respective gas-filled and fluid-filled prolate spheroids. They attempted to determine the depth and frequency dependence of the herring swimbladder by fitting different swimbladder contraction factors and compared the results to Ona's (2003) empirical *in situ* TS data set. They found that the decrease in mean backscatter with increasing depth could be explained by the compression of the herring swimbladder. Also, the model fitted the empirical data best if the swimbladder length-contraction was less than the width (or height)-contraction.

1.4.1.2. Kirchhoff ray-mode approximation

A different model, the Kirchhoff ray-mode approximation (KRM), calculates backscatter of objects by approximating them as a set of short cylinders along the main axis (Clay and Horne 1994; Horne and Jech 1999). The model uses the Helmholtz-Kirchhoff integral (Foote and Traynor 1988), which assumes that the reflection at every point of the surface is the same as the reflection of an infinite plane wave from an infinitive tangential interface (Medwin and Clay 1998). The total backscatter is determined by summation of the combined contributions of each

cylinder element. Morphological dimensions of fish components (height and width), such as the swimbladder, are usually determined by radiological imaging using X-ray techniques (Clay and Horne 1994; Horne et al. 2000; Hazen and Horne 2004). So far, herring backscatter has not been modelled by the KRM, however, Horne and Jech (1999) used the method to calculate backscatter of a simulated population of another clupeoid, the threadfin shad at multiple frequencies. They found that theoretical backscatter amplitudes varied unpredictably among frequencies between 38 and 420 kHz. Hazen and Horne (2003) and Horne (2003) used the KRM method to evaluate the effects of factors affecting fish TS, such as length, frequency, tilt angle, ontogeny, physiology and behaviour. Even though the KRM is relatively simple to compute it has a distinct disadvantage in that it is inaccurate at low frequencies and high tilt angles (Simmonds and MacLennan 2005).

1.4.1.3. Boundary element method

Similar to the KRM model, the boundary element method (BEM) can calculate backscatter from arbitrarily shaped surfaces (Francis 1993). It takes account of energy diffracted into the shadow zone within the scattering body, which is not true for the KRM (Simmonds and MacLennan 2005). It also enables backscatter modelling of three-dimensional structures with discrete interior inclusions that may have different acoustic properties (Foote and Francis 2002). Like the KRM, the BEM has so far not been applied to model backscatter of herring. Nevertheless, both these models are promising since they can be applied to accurate representations of fish body parts, and therefore provide a distinct advantage over models based on simple geometric shapes. Foote and Francis (2002) used both the KRM and BEM method to model gadoid TS and found the results to be in close agreement. In a further study on gadoids, Francis and Foote (2003) attempted to quantify the depth-dependence of TS caused by increased mass density of the swimbladder gas assuming a constant volume. They modelled the swimbladder backscatter of depth-adapted pollack and saithe (*Pollachius virens*) and found that the mean TS did not change significantly

with depth. Even though the orientation dependence of TS was found to increase with depth they concluded that there were no implications for echo counting applications.

1.4.1.4. Distorted wave Born approximation

An approach that can be applied to weak scattering bodies of any shape is the distorted wave Born approximation (DWBA; Morse and Ingard 1968). Backscattering is expressed as a three-dimensional integral over the body volume. The model is valid at all acoustic frequencies and object orientations, however, secondary scattering and absorption within the body are ignored. Because of its abilities, the DWBA has so far been widely used to model backscatter of plankton (McGehee et al. 1998; Stanton et al. 1998; Lavery et al. 2002), but could equally well be applied to weak scattering components of fish, such as the fish flesh.

1.5. Conclusion

Herring play an important ecological role in many marine ecosystems by providing the critical mid-trophic link between planktic secondary producers and piscivorous predators. Additionally, they are an important commercial species and support a number of fisheries around the world. In order to maintain healthy stock levels, there is a need for accurate estimates of fish populations that provide the basis for sustainable resource and ecosystem management. Patchily distributed pelagic fish, such as herring, that occur in dense aggregations can efficiently be assessed by means of acoustic survey methods. Due to uncertainty associated with acoustic surveys, however, abundance estimates derived from them tend to have a low accuracy and are therefore usually treated as relative indices in stock assessment models (Bailey and Simmonds 1990; Simmonds et al. 1992). Apart from calibrated survey equipment and adequate geographic coverage of the fish population, it is crucial to have an improved knowledge of the fish sound scattering properties - the target strength (TS) - and its variability. The TS is the single most important source of error contributing to total accuracy in acoustic estimates of absolute abundance (Table 1.1; Simmonds et al. 1992). Of the several practical TS estimation techniques used so far, experiments on dead or stunned fish have given vital information about effects such as fish

orientation, however, unknown physiological changes are likely to occur once the animal is rendered unconscious, leading to misinterpretation (McClatchie et al. 1996). Experiments on live fish may therefore have lead to more accurate results. Cage experiments have shown in particular how TS is dependent on fish physiology, their behaviour and environmental influences. In terms of the physostomous herring this is especially true for pressure effects and resulting depth-dependent changes in TS. The method has the advantage in that the fish are alive and easily observable by cameras. Confinement may however make experimental fish not representative of those in the wild, leading to biased results. *In situ* TS measurements on live fish, free to behave in their natural environment may therefore have given answers that are most applicable to an acoustic survey situation. Nonetheless, these methods are limited due to practical difficulties such as multiple target detection or correct collection and identification of biological samples.

Theoretical backscatter models have helped to improve the understanding and interpretation of empirical data. Particular progress has been made in quantifying effects of tilt angle and frequency on TS. Backscattering models are now increasingly sophisticated to take into account actual anatomical details of the fish and its physical properties. A valuable approach may therefore entail the combination of modelling and empirical data to determine the TS of a particular fish species and improve its accuracy and precision, and consequently, that of derived abundance and biomass estimates.

In this thesis, a range of theoretical backscattering models have been adapted and applied to estimate the TS of herring at multiple frequencies commonly used for acoustic surveys (Chapter 2). Acoustic multifrequency data from the North Sea were used in an attempt to distinguish herring echoes from those of a cohabitant species, the Norway pout (*Trisopterus esmarkii*), and to discriminate different herring size classes. The models were subsequently applied to explain the observed pattern in the empirical multifrequency data. In Chapter 3, swimbladder sizes of herring from the low-salinity Baltic Sea were compared to those of herring from the northeast Atlantic. The different swimbladder morphologies then provided the input data for a

backscatter model used to estimate the likely TS variation between the two herring stocks. Another modelling investigation looked at differences in TS between herring and sprat in the Baltic Sea using swimbladder morphology data from X-ray radiographs. In Chapter 4, the change in herring swimbladder morphology with depth was examined by magnetic resonance imaging of a specimen in a pressure chamber. Resulting morphological data were used to model the depth-dependency of the herring TS. Eventually, Chapter 5 describes an attempt to determine the most likely distribution of TS model parameters by fitting the model to empirical TS data in a Bayesian framework. This allowed the development of a probabilistic herring TS that was applied to acoustic survey data from the North Sea to estimate absolute abundance and biomass. The final Chapter 6 examines how the findings from this study may improve abundance estimates from herring surveys and discusses potential further work that could be done to advance the research. Particular focus is on the combination of modelling and empirical TS estimates and how this coupled system could enhance the potential of acoustic methods as a tool for implementing EBFM.

Chapter 2

Modelling target strength of Atlantic herring (*Clupea harengus*) at multiple frequencies

Part of the work described here has been published as:
Fässler, S.M.M., Santos, R., García-Núñez, N., Fernandes P.G. (2007). Multifrequency backscattering properties of Atlantic herring (*Clupea harengus*) and Norway pout (*Trisopterus esmarkii*). Canadian Journal of Fisheries and Aquatic Sciences 64: 362-374.

2.1. Introduction

The use of more than one frequency in an acoustic survey may improve the accuracy of allocating echotraces to species (i.e. the 'scrutinizing process'), especially if the acoustic properties of individual species vary with the frequency in use (Madureira et al. 1993). Such techniques have been used to discriminate between groups of fish, micronekton and zooplankton (Fernandes et al. 2006; Everson et al. 2007; Axenrot et al. 2009) and also for discrimination between biological targets and physical phenomena such as bubbles (see Horne 2000). Korneliussen and Ona (2002) used multifrequency processing techniques to distinguish various targets such as mackerel, swimbladdered fish and zooplankton. A similar approach was used by Kloser et al. (2002) to identify and distinguish three dominant deep-sea fish groups. The

difference in mean volume backscattering strength ($\Delta\hat{S}_v$) between frequencies was described by Kang et al. (2002) as one of the most promising methods for acoustic species identification. If nothing else, the technique has been recommended because it enables objective classification, and escapes the subjectivity of traditional visual scrutiny (Watkins and Brierley 2002; Korneliussen et al. 2009a).

Despite these advances, the practice in acoustic surveys with regard to target identification is still mostly based on visual scrutiny (Reid et al. 1998; Korneliussen et al. 2009a) aided by trawling (McClatchie et al. 2000). The international North Sea herring acoustic survey is one such example (Bailey et al. 1998). The north-west component of this survey, which contains over 80% of the adult biomass (e.g. ICES 2008b), presents few major species identification problems. One problem that is encountered, however, is distinguishing echotraces of herring schools from those due to Norway pout (*Trisopterus esmarkii*). These fish have similar acoustic properties in part because their physiologies and behaviours are also quite similar. Both species occur close to the seabed in densely packed schools, which are similar in shape and size. In addition, both species possess swimbladders. Nevertheless, the nature of their swimbladders is essentially different: Norway pout are physoclists and therefore have a closed swimbladder with a gas gland to regulate its volume. Herring on the other hand are physostomes. They have a swimbladder that is connected to the exterior via the alimentary canal.

Since the early 2000's, multifrequency data have been collected during these surveys. The aim of this Chapter was to describe the empirical backscattering characteristics of herring and Norway pout at multiple frequencies. A range of numerical backscatter models were developed in an attempt to investigate whether the model data could be used to describe scattering features observed in the empirical multifrequency data. Eventually, herring echotrace data were divided according to fish size distributions in the corresponding trawl catches to compare size class specific backscattering levels.

2.2. Methods

2.2.1. Data collection

Data were obtained from the Scottish component of the International North Sea Herring Acoustic Survey (Figure 2.1), in the summers of 2000, 2001 and 2002, carried out on the Fisheries Research Vessel (FRV) *Scotia*. Scotland is responsible for surveying the north-western part of the area, which covers the western half of ICES Division IVa. Further details of survey procedures can be found in individual survey reports (e.g. ICES 2008b).

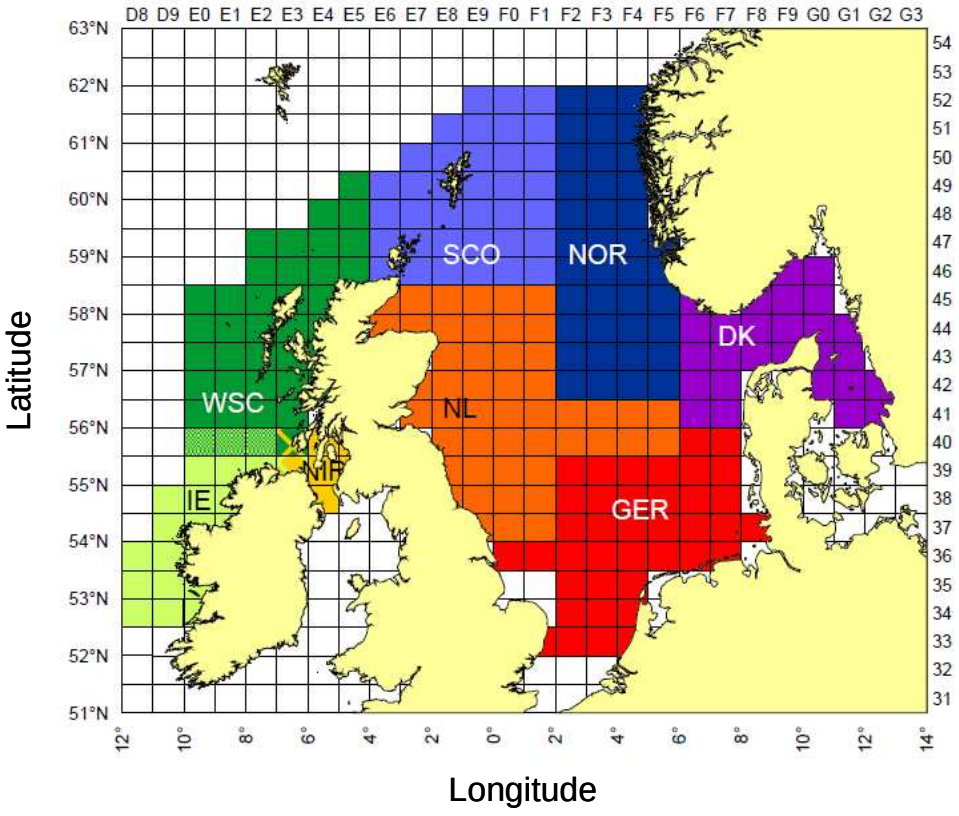

Figure 2.1 Map of the area covered by the North Sea herring acoustic survey in 2009. Coloured areas represent ICES rectangles covered by the various countries participating in the survey. (GER: Germany on FRV *Solea*; DK: Denmark on FRV *Dana*; NL: The Netherlands on FRV *Tridens*; NOR: Norway on FRV *Johan Hjort*; SCO: Scotland on FRV *Scotia*; WSC: Scotland on a charter vessel; NIR: Northern Ireland on FRV *Corystes*; IE: Republic of Ireland on FRV *Celtic Explorer*).

Acoustic data were collected using a Simrad EK500 scientific echosounder (Bodholt et al. 1989), operating three split-beam transducers at frequencies of 38, 120 and 200 kHz. A Simrad EA500 echosounder operating an 18 kHz single-beam transducer was also used. The EA500 was adapted to use EK500 software by replacing firmware on the signal and main processor boards in consultation with the manufacturer. Transducers connected to the EK500 were located adjacent to one another (within 0.5 m) on the drop-keel of the vessel and were deployed approximately 3 m below the hull. The 18 kHz transducer was hull-mounted just over 5 m directly forward of the other transducers. The echosounders were configured to ping simultaneously at each frequency every second, with pulse lengths of 1.0 ms at all frequencies, in order to have the same sampling resolution between frequencies (Korneliussen et al. 2008). Both echosounders were calibrated using standard-target calibration techniques (Foote et al. 1987; Fernandes and Simmonds 1996) with respective transducer settings given in Table 2.1. In years when due to time constraints not all transducers could be calibrated, settings of the previous or subsequent year were applied respectively. Acoustic data were collected between sunrise and sunset from 03:00 to 23:00 hours. Since herring exhibit diel vertical migration and occur in schools near the seabed when it is light, they presented better acoustic targets during that period.

Data were logged from the echosounders to a personal computer with Myriax Echolog software (Myriax Pty Ltd, GPO Box 1387, Hobart, Tasmania, Australia). The raw data were collected as echogram (Q) telegrams consisting of time and depth stamped digitised mean volume backscattering strengths ($\hat{S}_v$). Each pixel on the echogram, therefore, corresponded to a volume backscattering strength (symbol: S_v, units: dB re $1m^{-1}$). Major fish schools were sampled with a pelagic trawl with a net of 20 mm mesh in the cod end. The idea ultimately being to link acoustic data with species as identified by trawling (McClatchie et al. 2000). When trawling at a speed of approximately four knots, the trawl's vertical opening was 12 m and the horizontal opening was 20 m. Trawl data provided information on catch composition in numbers, and were indexed by latitude and longitude, time of start and end of the

haul, as well as other parameters such as trawl depth and a description of the fished echotraces. Data from a total of 124 trawl hauls were examined from the three surveys: 34 trawl hauls contained exclusively herring and 2 trawls contained exclusively Norway pout. Since these numbers for single species catches were quite small, other trawl hauls which contained a mixture of these and other species were analysed here: trawl hauls which comprised >85% of Norway pout by numbers in the catch and >90% of numbers of herring were considered indicative of that species.

Table 2.1 Transducer settings used during the North Sea herring surveys on FRV *Scotia* for 2000 - 2001.

Parameter	Year			Units
	2000	2001	2002	
Frequency: 18 kHz				
Simrad transducer type	ES18-11	ES18-11	ES18-11	-
Absorption coefficient	-	2.5	-	dB km^{-1}
Pulse duration	-	1.0	-	ms
Bandwidth	-	1.57	-	kHz
Transmitted power	-	2000	-	W
Two-way beam angle	-	-17.0	-	dB
Angle sensitivity	-	24.8	-	degrees
Transducer gain	-	21.72	-	dB
3dB beam width (along)	-	10.4	-	degrees
3dB beam width (athwart)	-	10.4	-	degrees
Sound speed	-	1497.4	-	m s^{-1}
Calibration sphere TS	-	-42.64	-	dB
Frequency: 38 kHz				
Simrad transducer type	ES38B	ES38B	ES38B	-
Absorption coefficient	10	10	10	dB km^{-1}
Pulse duration	1.0	1.0	1.0	ms
Bandwidth	2.43	2.43	2.43	kHz
Transmitted power	2000	2000	2000	W
Two-way beam angle	-20.9	-20.9	-20.9	dB
Angle sensitivity	28.4	28.4	28.4	degrees
Transducer gain	26.73	26.53	26.75	dB
3dB beam width (along)	5.56	5.56	5.56	degrees
3dB beam width (athwart)	5.43	5.43	5.43	degrees
Sound speed	1494.5	1497.6	1501.5	m s^{-1}
Calibration sphere TS	-42.40	-42.40	-42.40	dB
Frequency: 120 kHz				
Simrad transducer type	ES120-7	ES120-7	ES120-7	-
Absorption coefficient	39.3	39.3	39.3	dB km^{-1}
Pulse duration	1.0	1.0	1.0	ms
Bandwidth	3.03	3.03	3.03	kHz
Transmitted power	250	250	250	W
Two-way beam angle	-20.7	-20.7	-20.7	dB
Angle sensitivity	28.3	28.3	28.3	degrees
Transducer gain	24.33	24.72	24.29	dB
3dB beam width (along)	7.00	7.00	7.00	degrees
3dB beam width (athwart)	7.00	7.00	7.00	degrees
Sound speed	1493.2	1497.4	1498.5	m s^{-1}
Calibration sphere TS	-40.6	-40.6	-40.6	dB

Frequency: 200 kHz				
Simrad transducer type	ES38B	ES38B	ES38B	-
Absorption coefficient	-	56.4	56.4	dB km^{-1}
Pulse duration	-	1.0	1.0	ms
Bandwidth	-	3.09	3.09	kHz
Transmitted power	-	120	120	W
Two-way beam angle	-	-20.6	-20.6	dB
Angle sensitivity	-	23.0	23.0	degrees
Transducer gain	-	24.89	24.61	dB
3dB beam width (along)	-	7.10	7.10	degrees
3dB beam width (athwart)	-	7.20	7.20	degrees
Sound speed	-	1497.4	1498.7	m s^{-1}
Calibration sphere TS	-	-39.9	-39.9	dB

2.2.2. Acoustic data analysis and correction

Myriax Echoview was used for the analysis of the acoustic data. Using the positional information from the trawl haul, polygons were constructed to delimit the areas on the echograms sampled by the trawl: these sample polygons were designated as ‘sampols’. Echoview’s school module, based on Barange's (1994) SHAPES algorithm, was then used to detect schools and make measurements of school descriptors. The algorithm uses dimensions of echotraces and classifies them as fish schools based on predetermined minimum dimensions, such as school height or length. The fish schools contained inside the ‘sampols’ were detected and identified, and then divided into two categories according to the species caught: herring and Norway pout.

The characteristics of the 18 kHz transducer (specifically its 11° beam) and more importantly, its position on the hull of the vessel 5 m ahead of the other transducers, required positional corrections, so that data from the four frequencies were contemporaneously comparable. Ideally, data collected at multiple frequencies should be collected with all the transducers in close proximity to each other, so that distinctively observed echotraces can be aligned (Korneliussen et al. 2008). Similarly to the idea of having same pulse lengths (see Section 2.2.1.), and therefore the same vertical data resolution between frequencies, these positional corrections were thus

made to align isolated distinctive echotraces in the two datasets (hereafter referred to as EA data for the 18 kHz and EK data for the 38, 120 and 200 kHz).

A vertical offset of approximately 3 m was applied to the EA data in order to match the vertical position of echotraces. The seabed on the EA data was then adjusted to be equivalent in range to that detected by the 38 kHz in the EK data. In some cases, the border that defined the detected echotraces on the EK data did not match with a whole ping on the EA data. This was due to a drift in clock times between the two systems. Echoview's Match Ping Time operator was applied to accommodate this as follows: this operator selects pings from the first operand in such a way as to match the times of the pings in the second operand. The EA data echotraces had an additional horizontal displacement compared to the EK data (due to the alongship displacement and occasional major time mismatches). Echoview's Ping Time Shift operator was applied, shifting the time of each ping to either the time of the prior or subsequent ping. The procedure was repeated until the spatial position of echotraces on both the EA and EK echograms were synchronised.

To account for the differences in beam width between the EA and EK systems, two types of corrections were attempted, which resulted in two separate sets of data. Under one correction, school parameters were corrected using Echoview's Echotrace Statistics, which applies a beam angle correction algorithm according to Diner (2001). In another procedure, image analysis techniques were used to isolate the 'kernel' of the school as recommended by Korneliussen et al. (2008). This was done by applying an erosion filter (Reid and Simmonds 1993) to replace each data point with the minimum value of the data points in the cells directly surrounding it (dimensions: 3x3 cells). Specific reasons for applying the erosion process were: 1) to reduce the local pixel-by-pixel variability within detected schools caused by fish at the periphery exhibiting different target strength levels to those in the centre of the insonified school (Reid and Simmonds 1993). The resulting within-school differences in S_v may for instance be due to differences in orientation (Foote 1980a) or size distributions (DeBlois and Rose 1995) of the fish; 2) during the insonification process of a fish school, from time of the first to the last detection of the school by the

acoustic beam, there is a regular variation of echo levels from one beam to another (Korneliussen et al. 2008). This variation is partly dependent on the proportion of the beam width occupied by the fish school. When passing over a fish school, S_v levels are smaller and more variable in the first and last few pings when only part of the school is contained within the acoustic beam. Differences in beam widths between the different transducers will obviously enhance this problem. Effectively the erosion process reduced all echotrace boundaries by one pixel. Schools were then re-detected on the eroded data and the new 'eroded' borders were used to create an alternative dataset (see Figure 2.2 for details). The sample sizes of schools used in the analysis are given in Table 2.2.

Table 2.2 Number of echotraces (n) used for the analyses of eroded and non-eroded herring (*Clupea harengus*) and Norway pout (*Trisopterus esmarkii*) echotraces as indicated, with breakdown of numbers by size class (total length in cm).

Echotrace	n at length (in cm)						Σn
	5-10	10-15	15-20	20-25	25-30	30-35	
Herring	-	-	31	112	526	35	704
Herring eroded	-	-	13	47	226	13	299
Norway Pout	31	25	6	-	-	-	62
Norway Pout eroded	18	7	4	-	-	-	29

2.2.3. Backscattering levels

Energetic parameters of the detected echotraces from the herring and Norway pout categories (Table 2.2) were extracted in linear units (i.e. mean volume backscattering coefficients, symbol $\hat{s}_v$, units m^{-1}), using Echoview's export facility. A minimum threshold level of -70 dB was applied at all frequencies. $\hat{s}_v$ values were then

transformed into the log domain (i.e. mean volume backscattering strength; symbol $\hat{S}_v$ (= $10\log_{10}[\hat{s}_v]$), units dB re 1 m^{-1}). Backscattering levels at the four frequencies were examined with reference to $\hat{S}_v$ of the beam angle corrected echotraces (hereafter referred to as 'corrected $\hat{S}_v$'), and the $\hat{S}_v$ of the eroded echotraces (hereafter referred to as 'eroded $\hat{S}_v$'), of both species. Differences between the mean values of these variables at each frequency were tested for both species using a Mann-Whitney test (Zar 1984).

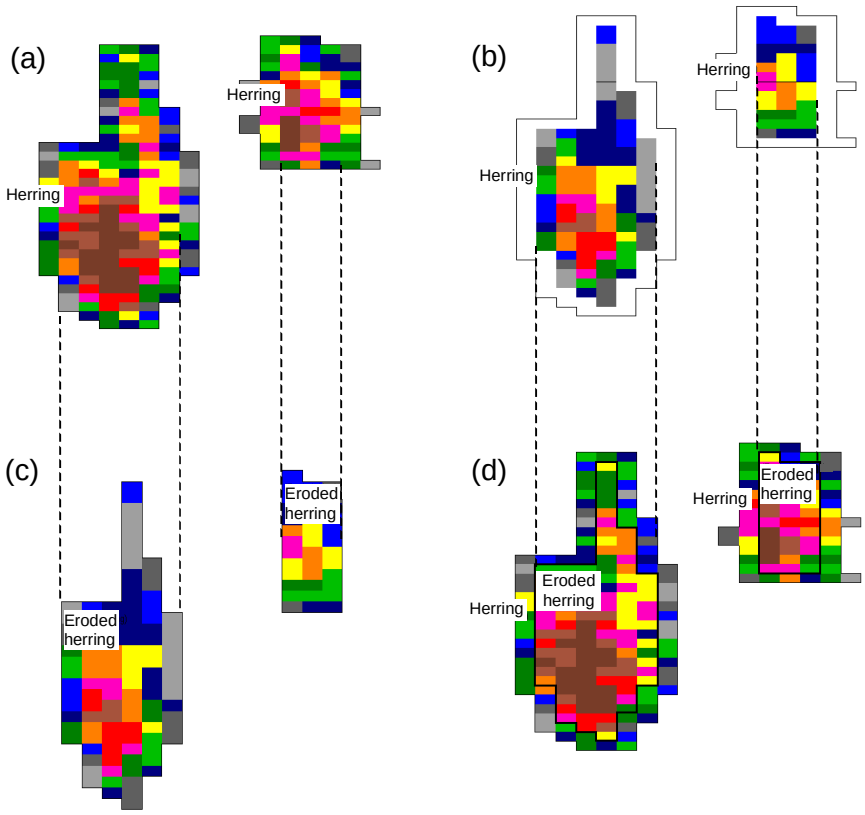

Figure 2.2 Processing steps to produce eroded echotraces which define the "kernel" of the school: (a) Original echotraces of two fish schools; (b) the same echotraces after applying an erosion filter, shown inside the borders of the original detected echotraces; (c) eroded echotraces with new detected borders; (d) original echotraces with borders of the eroded "kernel" shown. Dotted lines indicate how the borders of the echotraces line up ping to ping. Note that the erosion only redefines the borders of the schools to define a kernel: the actual Sv values used are in this inner "Eroded herring" kernel area of (d), which are the same as the equivalent pixels in (a).

The frequency specific characteristics of each echotrace were then examined using two measures: the decibel (dB) difference, ΔdB; and the frequency response, r(*f*) (Korneliussen and Ona 2003; Pedersen and Korneliussen 2009; Korneliussen et al. 2009a), where:

$$\Delta dB = \hat{S}_v(f) - \hat{S}_v(38) \quad (2.1)$$

$$r(f) = \hat{s}_v(f) / \hat{s}_v(38) \quad (2.2)$$

$\hat{S}_v(f)$ is the mean volume backscattering strength of the echotrace at a frequency (*f*) and $\hat{s}_v(f)$ is the mean volume backscattering coefficient of the echotrace at a frequency (*f*). These measures are actually equivalent, since $S_v = 10\log_{10}(s_v)$ (MacLennan et al. 2002), such that $r(f) = 10^{\Delta dB/10}$. Naturally, comparative backscattering profiles (i.e. backscattering strengths values at all frequencies), using one or the other, can look quite different according to the scales used.

2.2.4. Size classes

The frequency-specific backscattering levels of herring and Norway pout were considered for different size classes of fish. Based on the mean length of fish in each haul, echotrace data were partitioned into groups corresponding to fish in 5 cm size classes, ranging from the smallest size class of 5-10 cm to the largest of 30-35 cm. Similar to the species specific backscattering levels, both the corrected $\hat{S}_v$ and the eroded $\hat{S}_v$ data were examined for the echotraces corresponding to the different size classes of both species. Likewise, frequency specific characteristics were compared using ΔdB and r(*f*) (see Equations 2.1 and 2.2)

2.2.5. Herring backscattering models

A range of commonly used theoretical backscattering models for swimbladdered fish were considered alongside the empirical size-class data. The output of the models was the backscattering cross-section (σ_{bs} in m^2) for an individual fish, which was converted to target strength (TS, in dB) according to MacLennan et al. (2002) as:

$$TS = 10\log_{10}(\sigma_{bs}) \quad (2.3)$$

r(*f*) and ΔdB were calculated from σ_{bs} using Equations 2.1 and 2.2 (replacing $\hat{s}_v$ with σ_{bs} and $\hat{S}_v$ with TS).

Many of the early studies that have modelled backscatter from swimbladdered fish have been restricted to a models that consider only the swimbladder (Love 1978; McClatchie et al. 1996; Kloser et al. 2002). This was due primarily to the assumption that the backscatter was dominated by the swimbladder component (Foote 1980a). More recent attempts have been aimed at combining the swimbladder and fish body, such as the modal-series-based deformed-cylinder model (MSB-DCM) used by Gorska and Ona (2003a, 2003b) for herring, and the more elaborate Kirchhoff ray-mode (KRM) approach that has been used for a variety of fish species (Clay and Horne 1994; Jech et al. 2000; Gauthier and Horne 2004b). In the present Chapter, three different models using simple geometric shapes to represent fish backscattering components are described. The swimbladder was assumed to be a gas-filled prolate spheroid, and the fish body a fluid-filled ellipsoid. Results from these individual components were then combined coherently to approximate total backscatter for herring.

The first combined backscatter model for herring (model I) consisted of three separate components which were combined to give a total for the whole fish backscatter: a low frequency (LF) resonance model for the swimbladder at 18 and 38 kHz, a high frequency (HF) empirical model for the swimbladder at 120 and 200 kHz, and a distorted-wave Born approximation (DWBA) model for the fish body at all frequencies analysed. The second backscatter model (model II) also used the DWBA to model fish body backscatter, but a modal-series-based deformed-cylinder model (MSB-DCM) was chosen to calculate the swimbladder contribution. The third model (model III) applied a Kirchhoff ray-mode approximation for both the fish body and swimbladder. Details of individual models used are given in Table 2.3.

Table 2.3 Summary of backscattering model types applied to model the swimbladder as gas-filled prolate spheroid and the fish body as a fluid-filled ellipsoid at the frequencies used on the survey (18, 38, 120 and 200 kHz). Chapter sections where model details are explained are given. LF = low frequency; HF = high frequency; MSB-DCM = modal-series-based deformed-cylinder model; DWBA = distorted-wave Born approximation; KRM = Kirchhoff-ray mode approximation. References: (1) Weston 1967, (2) Love 1971b, (3) Stanton 1989, (4) Stanton et al. 1993, (5) Clay and Horne 1994.

Model	frequencies	model type	section	Ref.
model I: LF swimbladder	18 & 38	resonance	2.2.5.2	1
model I: HF swimbladder	120 & 200	empirical	2.2.5.3	2
model II: swimbladder	all	MSB-DCM	2.2.5.4	3
model I & II: fish body	all	DWBA	2.2.5.5	4
model III: whole fish	all	KRM	2.2.5.6	5

The total backscattering cross-section was expressed according to Gorska and Ona (2003b) by:

$$\sigma_{bs}^{f} = \sigma_{bs}^{sb}(z) + \sigma_{bs}^{fb} \tag{2.4}$$

where σ_{bs}^{f} is the backscatter of the whole fish. $\sigma_{bs}^{sb}(z)$ and σ_{bs}^{fb} denote the backscattering cross-section of the swimbladder at a water depth z, and of the fish body, respectively. Backscatter of the herring swimbladder was assumed to be depth dependent. In herring and most other physostomes, the swimbladder is connected to the digestive tract by a pneumatic duct (Bone et al. 1995). There is no interior gas gland which allows the fish to inflate the swimbladder once its volume has decreased after the fish has descended (Nero et al. 2004). It is assumed, as discussed or suggested previously by various authors (Brawn 1962; Blaxter et al. 1979; Ona

1990), that herring are only able to inflate their swimbladder by 'gulping' atmospheric air at the surface. This means that a herring could not increase the gas content of its swimbladder without access to the surface. The result is a decrease in swimbladder volume with depth, and, therefore, a reduction in backscatter from this organ, compared to other potentially important components (e.g. the body itself and the bone; Gorska and Ona 2003, Gorska et al. 2007). The following sections describe the model components in more detail.

2.2.5.1. List of symbols

σ_{bs}	backscattering cross-section [m^2]	c	sound speed [$m\ s^{-1}$]
a_{es}	radius of equivalent sphere [m]	L	fish length [m]
f_{ps}	prolate spheroid resonance frequency [Hz]	λ	acoustic wave length [m]
f	echosounder frequency [Hz]	f_{bs}	backscattering length [m]
Q	resonant quality factor [no units]	b_m	m^{th} modal series coefficient [no units]
z	depth [m]	ϕ	azimuthal angle [°]
V	volume [m^3]	ε_m	Neumann factor [no units]
P	pressure [Pa]	C_m	mode coefficient [no units]
w	fish weight [kg]	g	density contrast [no units]
e	prolate spheroid roundness [no units]	h	sound speed contrast [no units]
a_{ps}	prolate spheroid semi minor-axis [m]	p_{inc}	incident sound pressure [Pa]
b_{ps}	prolate spheroid semi major-axis [m]	r	distance from sound source [m]
α	semi minor-axis contraction factor [no units]	a_e	ellipsoid semi minor-axis (height) [m]
β	semi major-axis contraction factor [no units]	b_e	ellipsoid semi minor-axis (width) [m]

γ	ratio of specific heats [no units]	c_e	ellipsoid semi major-axis (length) [m]
μ_1	real part of complex shear modulus [Pa]	W	fish maximum body width [m]
ρ	density [kg m^{-3}]	H	fish maximum body height [m]
θ	tilt angle [º]	R	reflection coefficient [no units]
D	directivity [no units]	A	empirical amplitude adjustment [no units]
k	acoustic wave number [m^{-1}]	ψ	empirical phase adjustment [no units]

2.2.5.2. Resonance swimbladder model

The low frequency swimbladder component of backscatter model I was based on a prolate spheroid model, modified from Kloser et al. (2002). This model was first developed for spheres by Andreeva (1964) and was later adapted for prolate spheroids by Weston (1967), before being applied by Holliday (1972) for swimbladders in schooling pelagic fish. It was then used, with slight changes in notations, by Ye (1997) and then by Kloser et al. (2002) to model backscatter from deepwater fish species. Backscattering by the swimbladder, where normal dorsal incidence was assumed, was:

$$\sigma_{bs}^{sb}(z) = a_{es}^{2}(z)\left(\left(\left(\frac{f_{ps}}{f}\right)^{2} - 1\right)^{2} + \frac{1}{Q^{2}}\right)^{-1} \tag{2.5}$$

where, f_{ps} represents the prolate resonant frequency and f describes the incident acoustic frequency. Q is the resonant quality factor. $a_{es}(z)$ is the radius of an equivalent sphere at a depth z, whose volume is the same as that of the swimbladder. This volume is depth-dependent, as it was assumed that the swimbladder volume

decreases with increasing ambient pressure (Ona 1990; Nero et al. 2004). $a_{es}(z)$ was defined by:

$$a_{es}(z) = \sqrt{\frac{3}{4\pi} V(z)} \quad .6)$$

where:

$$V(z) = \frac{P(0)V(0)}{P(z)} \quad (2.7)$$

The gas filled swimbladder was, therefore, assumed to compress below the sea surface according to Boyle's Law where $P(0)\times V(0) = P(z)\times V(z)$ (Boyle 1662). Ambient pressure was calculated according to Kloser et al. (2002):

$$P = (1 + 0.103z)\times 10^5 \quad (2.8)$$

The volume of the swimbladder at the surface, V(0), was assumed to be a function of fish weight and ultimately fish size. The conversion from herring length to weight is given by $w = 0.0033\times L^{3.3078}$, where w is the weight (in g) and L is the total fish length (in cm). This was based on the lengths and weights of 3290 herring caught during the 2002 North Sea acoustic survey. According to Brawn (1969), fish density for herring at the surface was assumed to be 1026 kg m^{-3}. The herring swimbladder volume was assumed to be 5% of the total fish volume at the surface. This represents the upper limit as suggested by Ona (1990), and is considered a general value for marine fish according to Simmonds and MacLennan (2005). However, according to Nero et al. (2004), herring are naturally positively buoyant at the sea surface and, therefore, contain up to three times greater a volume of gas than neutrally buoyant fish. Consequently, $V(0) = 0.15\times w/1026$.

f_{ps} is a function of the spherical resonant frequency f_0 and the prolate spheroid roundness e at an ambient hydrostatic pressure P:

$$f_{ps} = f_0 2^{\frac{1}{2}} e^{-\frac{1}{3}} \left(1 - e^2\right)^{\frac{1}{4}} \left\{ \ln \left[\frac{1 + \left(1 - e^2\right)^{\frac{1}{2}}}{1 - \left(1 - e^2\right)^{\frac{1}{2}}} \right] \right\}^{-\frac{1}{2}} \tag{2.9}$$

The swimbladder was assumed to be 0.26 times the total length of the fish (Gorska and Ona 2003a). e describes the prolate spheroid roundness and is the ratio of the semi minor-axis a_{ps} to the semi major-axis b_{ps} of the spheroid. b_{ps} is the swimbladder length and a_{ps} can be calculated using the volume (V) equation for a prolate spheroid where: $a_{ps} = \sqrt{(3 \times V)/(4\pi \times b_{ps})}$.

The major modifications applied to the model in this paper are concerned with depth-dependent contraction rates of the swimbladder dimensions according to Gorska and Ona (2003a). The axes are assumed to contract with depth at different rates:

$$a_{ps}(z) = a_{ps}(0)\left(\frac{1+z}{10}\right)^{-\alpha} \tag{2.10}$$

$$b_{ps}(z) = b_{ps}(0)\left(\frac{1+z}{10}\right)^{-\beta} \tag{2.11}$$

Boyle's law requires that the different contraction rates behave according to $2\alpha + \beta = 1$. Gorska and Ona's (2003a) intermediate contraction rates (case ii) were used, where $\alpha = 2/5$ and $\beta = 1/5$. This results in the contraction of swimbladder length being relatively small compared to that of its width or height. Gorska and Ona (2003a)

found that for any case where $0 < \beta < \alpha$, model values were similar to empirical measurements of swimbladder contraction.

The spherical resonant frequency was calculated according to Holliday (1972) as:

$$f_0 = \frac{1}{2\pi a_{es}} \left(\frac{3\gamma P + 4\mu_1}{\rho_{fb}} \right)^{\frac{1}{2}} \tag{2.12}$$

where ρ_{fb} is the fish tissue density and γ the ratio of specific heats for the swimbladder gas. To make the model specifically applicable to herring, constants were taken from studies on herring by Brawn (1969) and other similar pelagic species such as northern anchovy (*Engraulis mordax*) (Holliday 1972). The following values were used: μ_1 = 105 Pa, γ = 1.4, ρ_{fb} = 1071 kg m^3, and Q = 5. For the depth z, the mean depth of the echotraces in each size class was used (15-20 cm = 84 m; 20-25 cm = 112 m; 25-30 cm = 131 m; 30-35 cm = 162 m).

To account for the directivity dependent tilt angle distribution, a directivity pattern $D_{sb}(\theta,z)$ (Medwin and Clay 1998) was determined and applied to the backscattering length (square root of the backscattering cross-section) of the swimbladder as:

$$\sigma_{bs}^{sb}(\theta, z) = \left(D_{sb}(\theta, z) \sqrt{\sigma_{bs}^{sb}(90^o)} \right)^2 \tag{2.13}$$

$$D_{sb}(\theta, z) = \frac{\sin^2\left\{k b_{ps}(z) \sin(\theta + \Delta\theta)\right\}}{\left\{k b_{ps}(z) \sin(\theta + \Delta\theta)\right\}^2} \cos(\theta + \Delta\theta) \tag{2.14}$$

θ refers to the fish tilt angle. $\Delta\theta$ is the offset of the swimbladder axis relative to the body axis, which was found to be 5.6°. k is the wave number ($k = 2\pi f/c$), and $b_{ps}(z)$ is the depth-dependent length of the prolate spheroid.

2.2.5.3. Empirical swimbladder model

The high frequency swimbladder component of model I was based on the simple model developed by Love (1971b) and applied more recently by Nero et al. (2004). Complex high frequency backscattering models for fish with swimbladders require detailed information on size and shape that were not available in the present study. Love (1971b) fitted a pair of regression lines to empirical TS measurements on various marine and freshwater fish. He found that backscatter decreased as the ratio L/λ (fish length to wave length) increases to about 14; for values of L/λ beyond 14, backscatter increases again:

if $L/\lambda \leq 14$, then

$$TS = 15.8\log(\frac{L}{100}) + 7.5\log(\lambda) - 22.9 \quad (2.15)$$

and if $L/\lambda > 14$, then

$$TS = 27.5\log(\frac{L}{100}) - 4.2\log(\lambda) - 36.2 \quad (2.16)$$

where the wavelength $\lambda = c/f$ (Chapter 1) and c is the sound speed in sea water (1500 m s^{-1}). The directivity was also applied to the high frequency component of the model, using the same parameters as for the low frequency model.

2.2.5.4. MSB-DCM swimbladder model

The swimbladder backscatter component of model II was calculated using the modal-series-based deformed-cylinder model (MSB-DCM). The depth-dependent backscattering length $f_{bs}^{sb}(z)$, where:

$$\sigma_{bs}^{sb}(z) = \left| f_{bs}^{sb}(z) \right|^2 \tag{2.17}$$

was obtained by assuming that the swimbladder was a gas-filled prolate spheroid. According to Stanton (1989), the solution for the normal dorsal incidence is:

$$f_{bs}^{sb}(z) = \frac{-i}{\pi} b_{ps}(z) \int_0^1 \sum_{m=0}^{\infty} b_m(z,u) \cos(m\phi) du \tag{2.18}$$

where the mode coefficient b_m is dependent on the depth (z), and hence the size of the swimbladder, at every length fraction u (= x/[b_{ps}(z)/2]) along the distance x of the major-axis of the prolate spheroid. At normal dorsal incidence, where the azimuthal angle $\phi = \pi$, $\cos(m\phi) = (-1)^m$. The coefficient b_m was defined as:

$$b_m = -\varepsilon_m / (1 + iC_m) \tag{2.19}$$

where the Neumann factor $\varepsilon_m = 1$ for m = 0, and $\varepsilon_m = 2$ for m > 0. Mode coefficient C_m is given in Clay (1991) as:

$$C_m = \frac{J'_m(k'a_{ps})N_m(ka_{ps}) - ghN'_m(ka_{ps})J_m(k'a_{ps})}{J'_m(k'a_{ps})J_m(ka_{ps}) - ghJ'_m(ka_{ps})J_m(k'a_{ps})} \tag{2.20}$$

where g and h are the density and sound speed contrasts respectively between the swimbladder and the surrounding fish body. According to Gorska and Ona (2003a) g = 0.00129 and h = 0.23. $J_m(x)$ and $N_m(x)$ are Bessel functions of the first and second

Neumann kinds of order m, and $J_m'(x)$ and $N_m'(x)$ their respective first order derivates. $k' = k/h$, where k is the wave number in the surrounding seawater.

2.2.5.5. DWBA fish body model

The fish body component of models I and II was applied over the entire frequency range. This was a distorted wave Born approximation (DWBA) for a fluid-filled ellipsoid. For a plane incident wave $p_{inc} = e^{ikr}$, where p_{inc} describes the sound pressure at a distance r from the source, backscattering by a fluid-filled ellipsoid, whose acoustic impedance (the product of sound speed and density) is close to that of the surrounding medium, can be calculated using a DWBA. The quadratic surface of the ellipsoid in the Cartesian coordinates is:

$$\frac{x^2}{a_e^2} + \frac{y^2}{b_e^2} + \frac{z^2}{c_e^2} = 1 \tag{2.21}$$

where a_e, b_e, and c_e are the lengths of the semi-axes of the ellipsoid. For the fish body the length $L = 2\ c_e$, width (dorsal view) $W = 2\ b_e$, and height (lateral view) $H = 2\ a_e$. In spherical coordinates, (21) becomes:

$$\frac{r^2 \sin^2\theta \cos^2\phi}{a_e^2} + \frac{r^2 \sin^2\theta \sin^2\phi}{b_e^2} + \frac{r^2 \cos^2\theta}{c_e^2} = 1 \tag{2.22}$$

where the azimuthal angle $\phi \in [0, 2\pi]$ and polar angle $\theta \in [0, \pi]$. A vector $\vec{\mu}$ is then defined whose x, y, and z components can be expressed by:

$$\begin{cases} \mu_x = 2\sin\theta\cos\phi \\ \mu_y = 2\sin\theta\sin\phi \\ \mu_z = 2\cos\theta \end{cases} \tag{2.23}$$

The backscattering length of the fish body component (f_{bs}^{fb}) can then be expressed as:

$$f_{bs}^{fb} = C_B k^2 a_e b_e c_e \frac{J_1(k a_e \mu_\Theta)}{k a_e \mu_\Theta} \quad (2.24)$$

where $J_1(x)$ is the spherical Bessel function of order 1, k is the wave number in the fish and

$$C_B = \frac{1 - gh^2}{gh^2} - \frac{g - 1}{g} \quad (2.25)$$

$$\mu_\Theta = \sqrt{\mu_x^2 + \left(\frac{b_e}{a_e}\right)^2 \mu_y^2 + \left(\frac{c_e}{a_e}\right)^2 \mu_z^2} \quad (2.26)$$

g and h are the density and sound speed contrasts respectively between the fish body and the surrounding water. According to Gorska and Ona (2003a) both were set to 1.04. The backscattering cross-section for the fish body is then:

$$\sigma_{bs}^{fb} = \left| f_{bs}^{fb} \right|^2 \quad (2.27)$$

For a broadside backscatter of dorsal view, $\theta = \pi/2$. The model required specific relationships between the different dimensions of the ellipsoid. The ratio of fish length (L) to half the height (a_e) was 9.42. The ratio of fish length (L) to half the width (b_e) was 22.84. Values were determined from 40 measurements of North Sea herring.

2.2.5.6. KRM whole fish model

Model III used the Kirchhoff-ray mode (KRM) approximation to model backscatter from both the swimbladder and fish body as a respective set of gas- and fluid-filled cylinders. Backscattering cross-sections from each finite cylinder component were

summed over the whole respective scattering object and added coherently. For values of the swimbladder where $ka_{ps}(z) < 0.2$, a low-mode (m = 0) finite bent cylinder solution was used (see Appendix A1 in Horne and Jech 1999). The Kirchhoff-ray approximation for the backscattering length of the swimbladder at $ka_{ps}(z) > 0.2$ from N_e swimbladder elements is:

$$f_{bs}^{sb}(z) = -i\frac{R_{fs}(1-R_{wf}^2)}{2\sqrt{\pi}}\sum_{j=0}^{N_e-1}A_{sb}\sqrt{[ka(j)+1]}\times e^{-i[2kv_U(j)+\psi_{sb}]}\Delta u(j) \quad (2.28)$$

Empirical amplitude (A_{sb}) and phase (ψ_{sb}) adjustments for small $ka(z)$ were:

$$A_{sb} = \frac{ka_{ps}(j)}{ka_{ps}(j)+0.083} \quad (2.29)$$

$$\Psi_{sb} = \frac{ka_{ps}(j)}{40+ka_{ps}(j)} - 1.05 \quad (2.30)$$

Reflection coefficients R at the swimbladder-fish body (R_{fs}) and water-fish body (R_{wf}) interface were defined as:

$$R_{fs} = \frac{gh-1}{gh+1} \quad (2.31)$$

$$R_{wf} = \frac{\rho_{fb}c_{fb}-\rho_w c_w}{\rho_{fb}c_{fb}+\rho_w c_w} \quad (2.32)$$

Here, g (=0.23) and h (=0.23) represent density and sound speed contrast between swimbladder and fish body. Subscripts for density (ρ) and sound speed (c) values refer to the fish body ('fb'; ρ = 1049 kg m^{-3}, c = 1540 m s^{-1}) and the surrounding sea water ('w'; ρ = 1027 kg m^{-3}, c = 1500 m s^{-1}). The backscattering length for the fish body (f_{bs}^{fb}) was:

$$f_{bs}^{fb} = -i\frac{R_{wf}}{2\sqrt{\pi}}\sum_{j=0}^{N_e-1}\left[k b_e(j)\right]^{1/2}\left[e^{-i2kv_U(j)+\psi_{sb}} - (1-R_{wf}^2)\right. \\ \left.\times e^{i(-2kv_U(j)+2k(v_U(j)-v_L(j)+\psi_{fb}))}\right]\Delta u(j) \tag{2.33}$$

with empirical phase adjustment:

$$\Psi_{fb} = \frac{\pi k v_U(j)}{2\left[k v_U(j) + 0.4\right]} \tag{2.34}$$

Subscripts 'U' and 'L' refer to the upper and lower surfaces in u-v coordinates, where the fish body is centred along the x-axis. Δu(j) stands for incremental distances between individual cylinders.

All model components were evaluated as a mean value of distributions of fish length and tilt. The distributions of fish length were taken from those in the trawl data size classes and the tilt was taken from a Gaussian distribution with a mean of –1° and standard deviation of 10° (Ona 2001).

2.3. Results

2.3.1. Species specific backscattering levels

The empirical observations of backscattering levels indicate that herring and Norway pout have very similar trends in backscattering levels at the four frequencies studied (Figure 2.3). Corrected $\hat{S}_v$ in both species were highest at 18 kHz and lowest at 120 kHz (Figure 2.3a). Herring had higher mean corrected $\hat{S}_v$ at all frequencies, as well as larger ranges of corrected $\hat{S}_v$, compared to Norway pout. However, this difference was only significant at 120 and 200 kHz (Mann-Whitney; $p < 0.05$) and not significant at 18 and 38 kHz (Mann-Whitney; $p_{18kHz} = 0.20$, $p_{38kHz} = 0.07$).

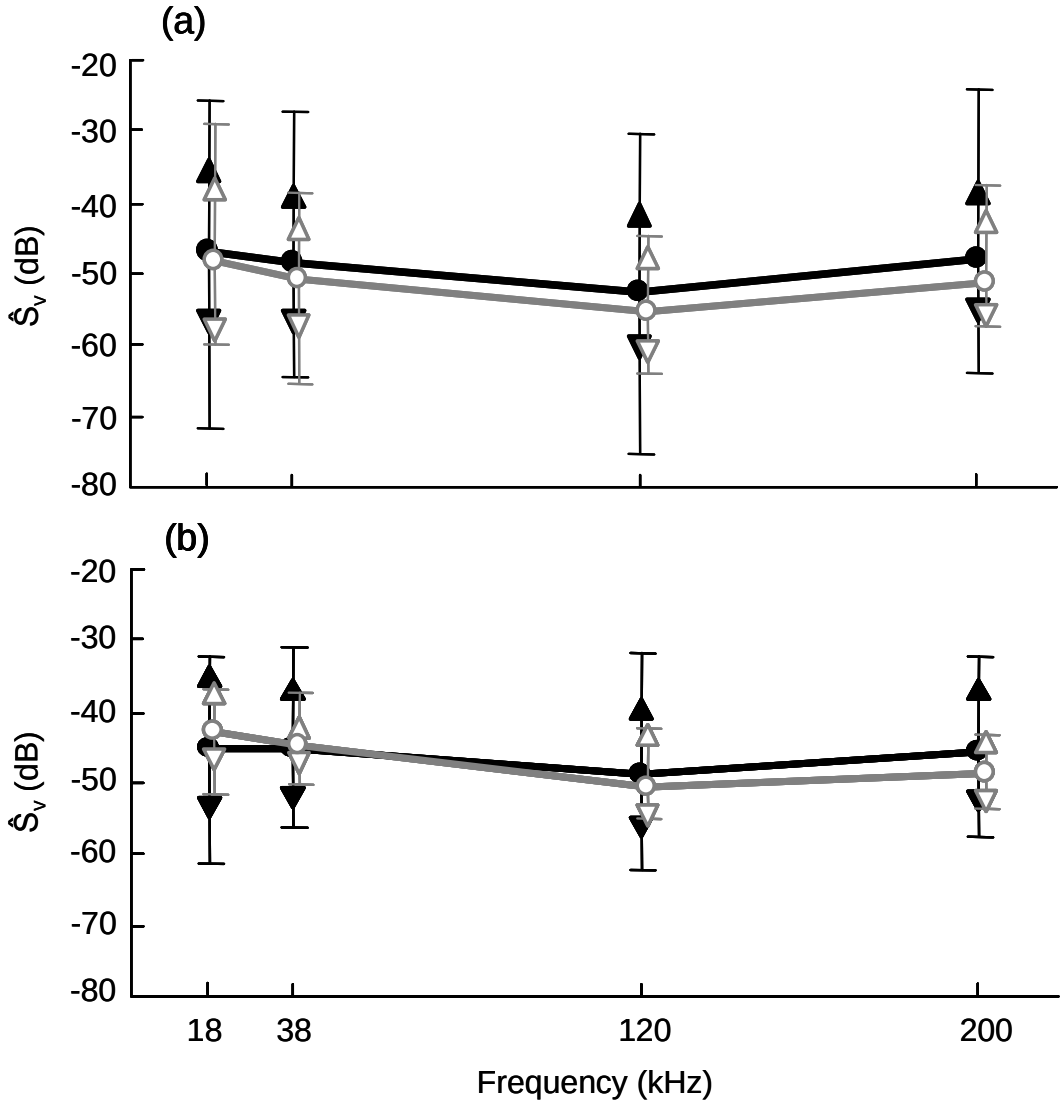

Figure 2.3 Mean values of: (a) corrected $\hat{S}_v$ and (b) eroded $\hat{S}_v$ echotraces. Closed symbols – herring; open symbols – Norway pout. Upright triangles – 95th percentile; inverted triangles – 5th percentile. Horizontal bars represent the respective maximum and minimum values. The values for Norway pout have been shifted slightly along the x axis for clarity.

With regards to the eroded echotraces, the trends according to frequency of herring and Norway pout $\hat{S}_v$ were also similar (Fig. 2.2b). However, at 18 and 200 kHz values of herring and Norway pout were significantly different (Mann-Whitney; $p<0.05$), with herring having lower mean values at 18 kHz and higher mean values at

200 kHz. Mean $\hat{S}_v$ at 38 and 120 kHz were not significantly different (Mann-Whitney; $p>0.05$) between herring and Norway pout. The eroded herring echotraces exhibited a smaller range of $\hat{S}_v$ at all frequencies compared to the range of corrected $\hat{S}_v$; those for Norway pout were similar. As the trends between corrected $\hat{S}_v$ and eroded $\hat{S}_v$ were similar regardless of subsequent analyses, further comments are restricted to the eroded data, but could equally apply to corrected $\hat{S}_v$.

The decibel difference (ΔdB, Equation 2.1) of the mean $\hat{S}_v$ values relative to 38 kHz showed similar trends according to frequency for both species (Figure 2.4a). Norway pout had positive values at 18 kHz and negative values at 120 kHz and 200 kHz, whereas herring had a mean dB difference close to 0 at 18 kHz and negative values at 120 and 200 kHz (Fig. 2.3a). The differences between the mean values at 18 and 38 kHz were +1.84 dB and -0.30 dB for Norway pout and herring respectively. Another point to note is that on average Norway pout had a ΔdB at 200 kHz that was much lower (-4.16) than that of herring (-0.78).

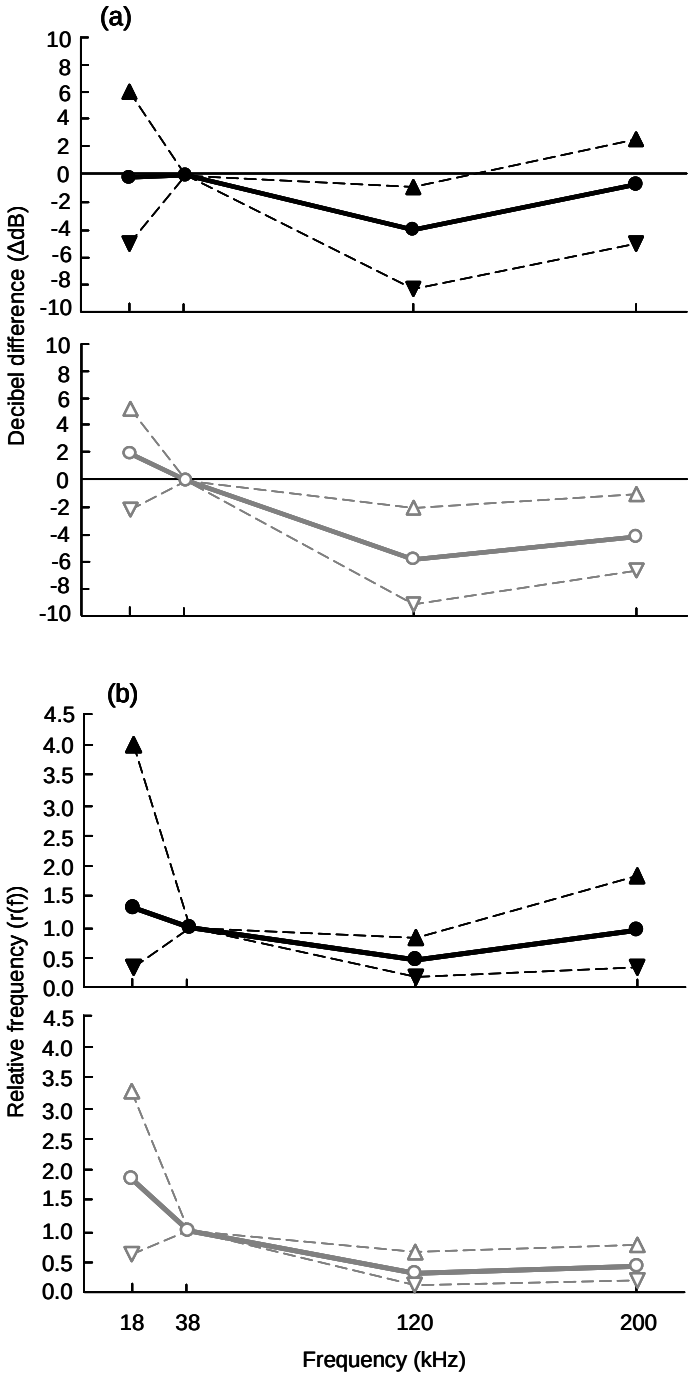

Figure 2.4 Mean values of: (a) decibel difference ΔdB and (b) relative frequency r(*f*) for herring (closed symbols) and Norway pout (open symbols). Upright and inverted triangles represent 95th and 5th percentiles, respectively. Both decibel difference and relative frequency response are expressed in relation to 38 kHz.

Examination of the frequency response (r(*f*), Equation 2.2) revealed identical patterns, as expected given that the measures are equivalent according to $r(f) = 10^{\Delta dB/10}$. However, the presentation of this parameter is different due to the differences in scale at which they are plotted (Figure 2.4b). This is particularly noticeable at low values of r(*f*) (negative ΔdB) where the scale makes it difficult to observe any significant changes. Another presentational difference concerns the variability of the mean value which looks higher at 18 kHz where the ΔdB difference is positive. The highest r(*f*) values were observed at 18 kHz compared to the three other frequencies for both species. For the other two frequencies (120 and 200 kHz) the frequency response was rather flat, close to 1, and therefore very similar to 38 kHz.

2.3.2. Size specific backscattering levels

Given the similarity between backscattering levels of the two species, and the fact that the sample sizes for Norway pout when broken down into size classes were small (Table 2.2), only results of the size specific backscattering levels for herring are reported here.

One consistent trend was apparent in the backscattering levels of the different herring size classes: the ΔdB between 18 kHz and 38 kHz changed according to size class, whereas the ΔdB at 120 and 200 kHz did not (Figures 2.5a-2.5d). Generally, the ΔdB at 18 kHz was high (and positive) for small fish, lower for progressively larger fish, and negative for the largest size class of fish (Figures 2.5a-2.5d). For every size class ΔdB values at 120 kHz were smallest. The r(*f*) values for the eroded echotrace data for different herring size classes behaved in a manner analogous to the ΔdB data (Figures 2.5e-2.5h). A decrease in r(*f*) at 18 kHz from the smallest to the biggest size class was detected, whereas r(*f*) levels at 120 kHz and 200 kHz remained similar.

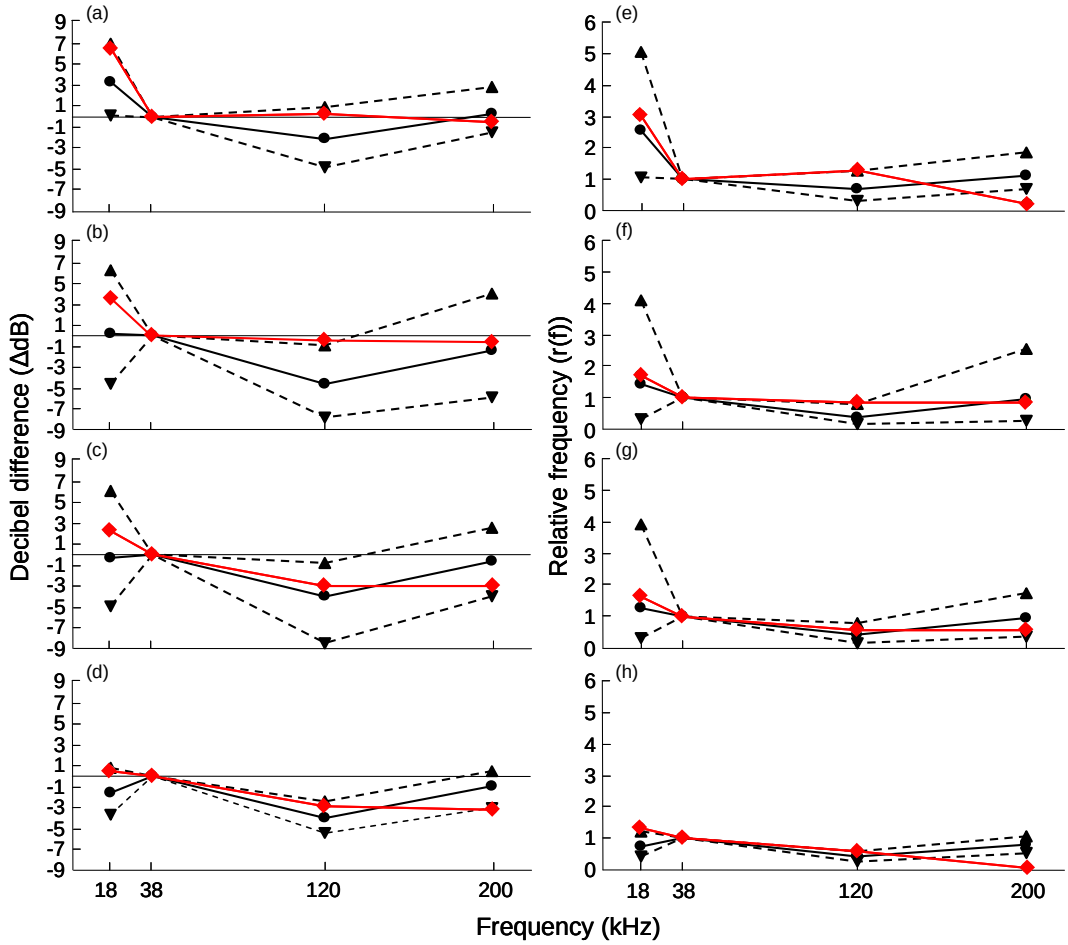

Figure 2.5 Mean values (circles) of (a) – (d) decibel difference ΔdB and (e) – (h) relative frequency r(*f*) with 95th (upright triangles) and 5th percentile (inverted triangles), for eroded herring echotraces. Figures correspond to different size classes: (a)+(e) 15-20cm; (b)+(f) 20-25cm; (c)+(g) 25-30cm; (d)+(h) 30-35cm. Both decibel difference and relative frequency response are expressed in relation to 38 kHz. Model I outputs (red diamonds) are superimposed.

.

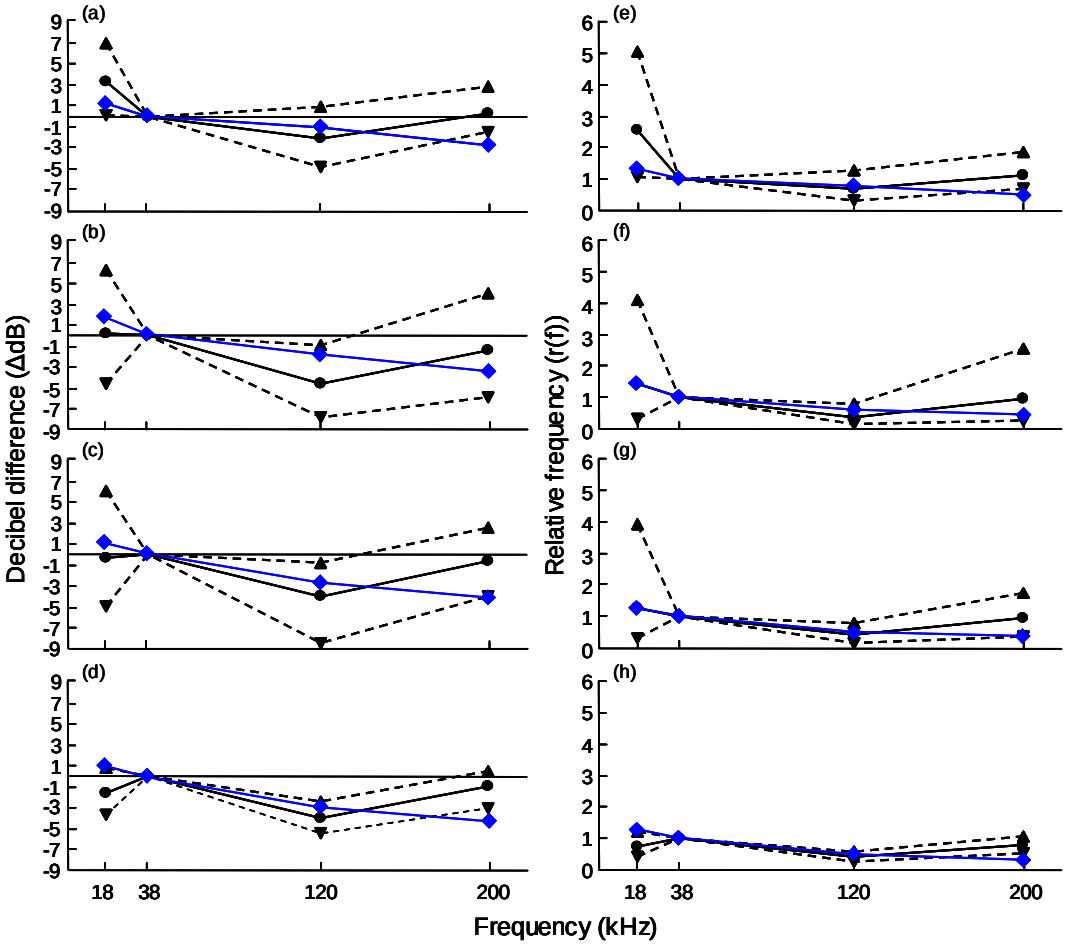

Figure 2.6 Mean values (circles) of (a) – (d) decibel difference ΔdB and (e) – (h) relative frequency r(*f*) with 95th (upright triangles) and 5th percentile (inverted triangles), for eroded herring echotraces. Figures correspond to different size classes: (a)+(e) 15-20cm; (b)+(f) 20-25cm; (c)+(g) 25-30cm; (d)+(h) 30-35cm. Both decibel difference and relative frequency response are expressed in relation to 38 kHz. Model II outputs (blue diamonds) are superimposed.

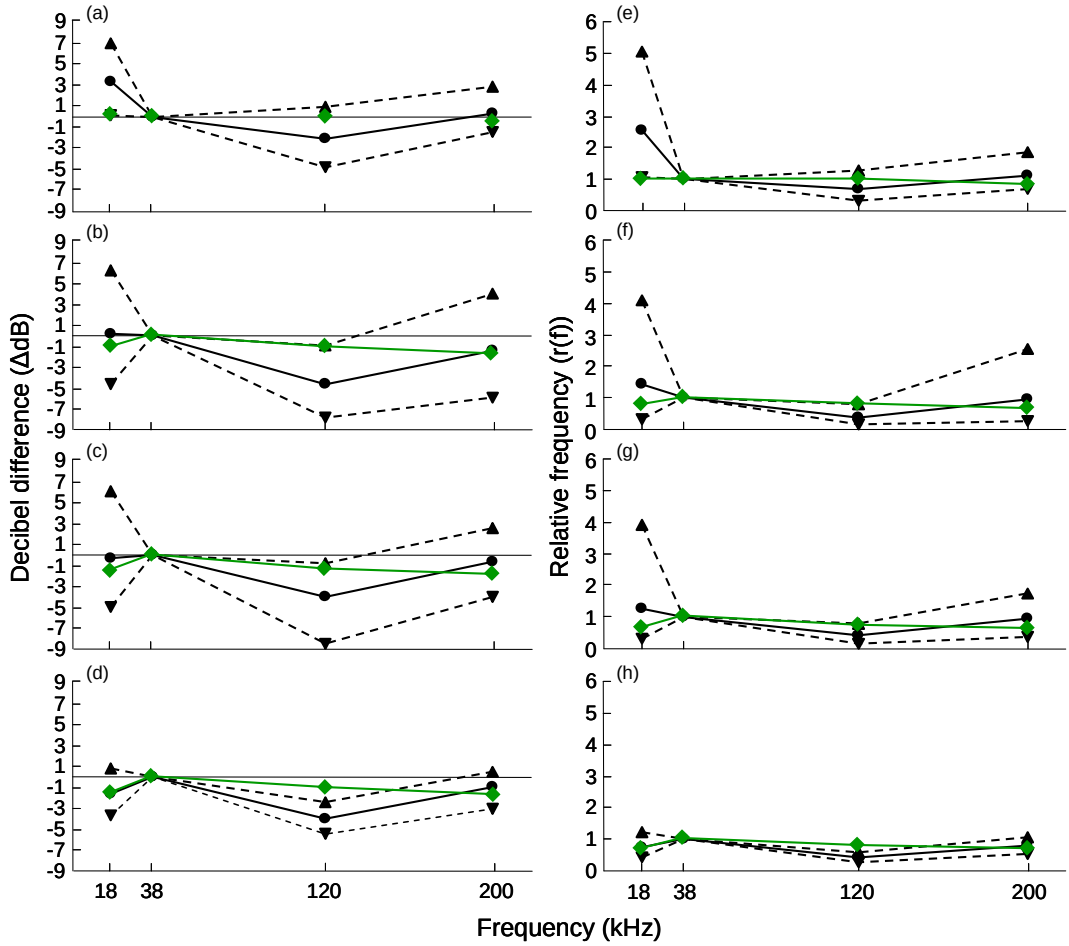

Figure 2.7 Mean values (circles) of (a) – (d) decibel difference ΔdB and (e) – (h) relative frequency r(*f*) with 95th (upright triangles) and 5th percentile (inverted triangles), for eroded herring echotraces. Figures correspond to different size classes: (a)+(e) 15-20cm; (b)+(f) 20-25cm; (c)+(g) 25-30cm; (d)+(h) 30-35cm. Both decibel difference and relative frequency response are expressed in relation to 38 kHz. Model III outputs (green diamonds) are superimposed.

2.3.3. Model predictions

In order to compare the model outputs with the empirical data, modelled backscatter values at 18, 38, 120 and 200 kHz were converted to the ΔdB and r(*f*) metrics used previously for each size class. Values derived from all three backscattering models (I, II, and III) followed similar trends to the eroded herring echotraces and were similar to the empirical values (Figures 2.5, 2.6 and 2.7). In common with the empirical data,

model outputs for ΔdB and r(*f*) at 18 kHz decreased with increasing fish size, however the degree of decrease differed between models. Model I showed the largest decrease in r(*f*) at 18 kHz with values ranging from 3.1 for the smallest size class to 1.3 for the biggest size class (Figure 2.5). Models II and III showed much smaller decreases ranging from 1.3 to 1.2 (model II, Figure 2.6) and from 1.0 to 0.7 (model III, Figure 2.7). The same was true for the ΔdB metric, with values decreasing from the smallest (model I: 5.7; model II: 1.1; model III: 0.0) to the biggest size class (model I: 0.4; model II: 0.9; model III: -1.6), with model I again showing the largest decrease. However, while model I and II predicted neither negative values for ΔdB nor values smaller than 1 for r(*f*) at 18 kHz, model III did. Outputs of all models for at 200 kHz were usually lower than the empirical data, resulting in a rather flat or decreasing response at the higher frequencies (120 and 200 kHz). Nonetheless, both models I and III showed increased variability for ΔdB and r(*f*) values at 18 kHz and consistently flat or decreasing ones at 120 and 200 kHz (Figures 2.5 and 2.7), which is in agreement with the empirical data for the different size classes. On the other hand, model II revealed very similar frequency responses for all size classes with little variability between them (Figure 2.6).

An example of predicted target strengths from the herring models are given in Figure 2.8. The combined model output was made up of the coherent addition of the fish body and swimbladder backscatter, as illustrated in Figure 2.9. The resonant peak derived from backscattering of the swimbladder component of model I occurred at approximately 1.8 kHz for herring in the 20-25 cm size class (Figure 2.9). Beyond resonance, for frequencies higher than 10 kHz, backscatter was influenced by the oscillating features of the fish body component in both models I and II. Backscattering from the body component predicted by the DWBA rose at low frequencies to a peak at about 18 kHz of approximately -42.5 dB and then exhibited dampened oscillations to a level of about -44.3 dB at 120 kHz. In models I and II, TS at 18 and 38 kHz was influenced more by the fish body component than the swimbladder, which will decrease in size at deeper water depths. Compared with model I, model II generally predicted higher values for the swimbladder component,

and therefore the combined TS was less influenced by the oscillating features of the fish body part. Model III on average gave lower TS values compared to model II, however, the predicted tilt angle induced decrease in backscatter at higher frequencies was not as extreme as observed in model I. Values of mean herring target strength modelled at the commonly used frequency of 38 kHz were -43.8, -38.3 and -40.6 dB, respectively for models I, II and III.

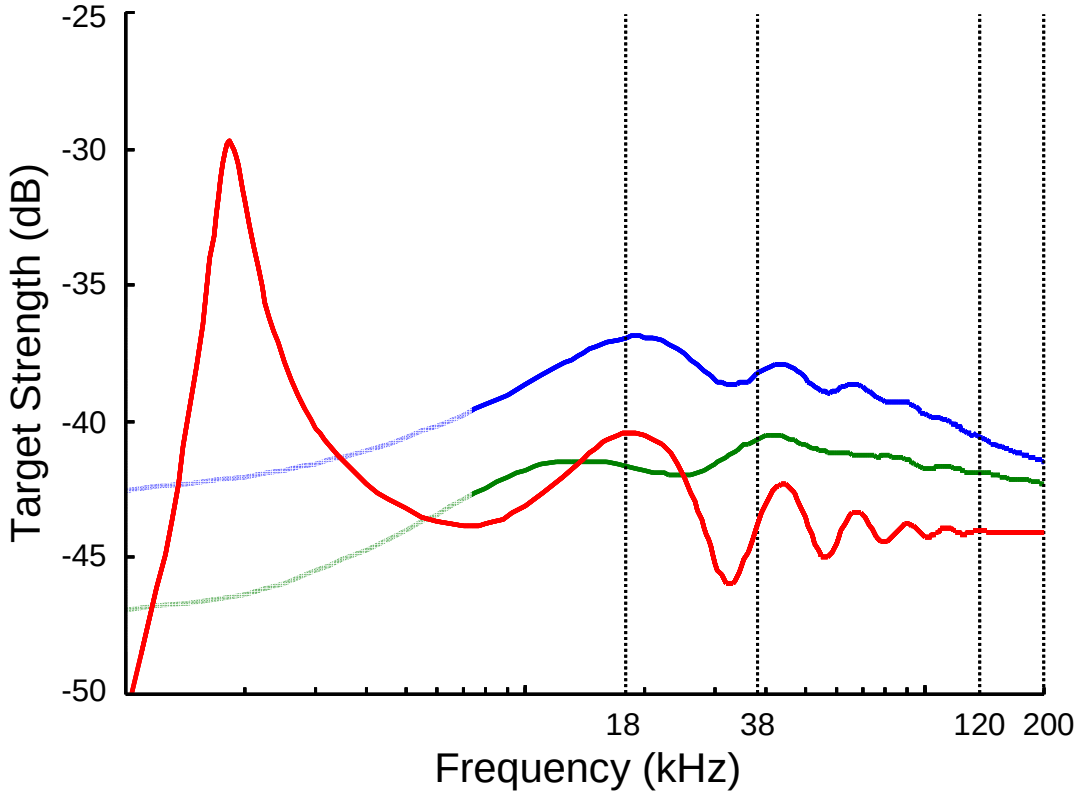

Figure 2.8 Comparison of predicted backscattering strengths from herring of the 20-25cm size class at 112 m water depth. Coloured lines represent frequency responses of the combined (fish body and swimbladder) model outputs (model I = red; model II = blue; model III = green). Computations were done at each 1 kHz step, over 10 000 realisations of fish size (within the size class) and normally distributed tilt angles (mean = -1°, standard deviation = 10°). Values of models II and III at low frequencies in the resonance scattering region are given in light colours, because the models are not valid there.

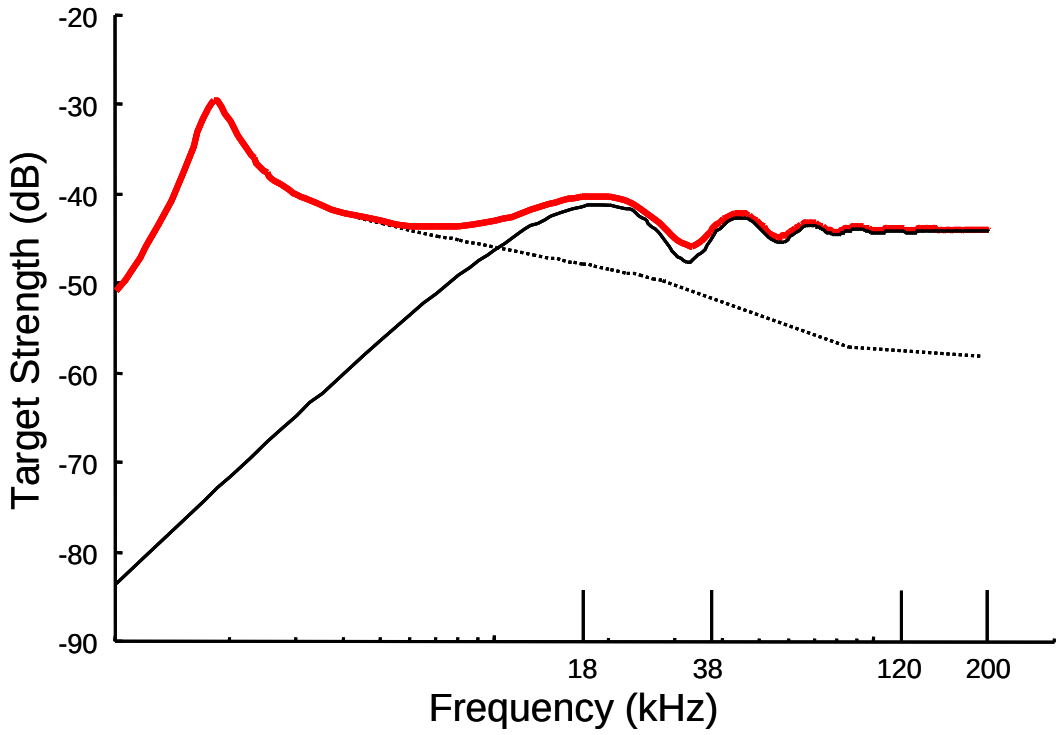

Figure 2.9 Modelled predicted backscattering strength from herring of the 20-25cm size class at 112 m depth using model I. Solid red line = combined model output. The swimbladder (dashed black line) was modelled using a prolate spheroid to represent the lower frequency range (0-40kHz), and a simple regression model based on empirical measurements to represent the higher frequencies (40-200kHz). The fish body model (solid black line) was based on a DWBA fluid filled ellipsoid backscattering model averaged over fish size distribution and tilt angle.

2.4. Discussion

Use of multiple frequencies in fisheries acoustics has long been recognised as a means to aid species identification and, therefore, improve the accuracy of abundance estimates from acoustic surveys (Horne 2000). Multifrequency species identification methods generally work well for discriminating species that have different morphologies. Korneliussen and Ona (2004) examined multifrequency backscattering properties of the non-swimbladdered Atlantic mackerel (*Scomber scombrus*). They found that backscatter increased with higher frequencies for this species (r(*f*) at 200 kHz was 4). Compared to non-swimbladdered fish, fish with swimbladders generally seem to have weaker backscatter at higher frequencies (eg. 200 kHz) relative to lower frequencies (Foote et al. 1993). Gorska et al. (2007) modelled average backscatter of mackerel schools using a combined model for the fish body and the backbone. They showed that the lack of a swimbladder and the increasingly more important backscatter of the backbone at higher frequencies may explain the high r(*f* = 200 kHz) observed for that species. Based on the same principle, Gauthier and Horne (2004a, 2004b) found frequency dependent differences in backscatter between swimbladdered and non-swimbladdered fish species in the Gulf of Alaska and the Bering Sea. Their findings were based on Kirchhoff-ray mode approximation (KRM) backscatter models. If discrimination algorithms, based on frequency specific backscatter differences, are applied, distinction between swimbladdered fish (e.g. herring) and non-swimbladdered fish (e.g. Atlantic mackerel) can be facilitated (Korneliussen and Ona 2004; Gorska et al. 2005; Gorska et al. 2007). More recently, multifrequency echosounders have been applied in conjunction with newly developed quantitative multibeam sonars to improve species classification (Berger et al. 2009; Korneliussen et al. 2009b).

Results presented in this Chapter indicate that based on energetic characteristics at multiple frequencies, herring and Norway pout have similar mean backscattering levels at frequencies of 18, 38, 120 and 200 kHz. Echotraces for analysis were chosen where, based on biological samples taken with a pelagic trawl, herring and Norway

pout were believed to be the main single source of backscattering. Although Norway pout were caught in smaller numbers, and their lengths were on average smaller than herring (Figure 2.10), the echoes derived from the Norway pout schools were of comparable strengths to those of herring. Since there was not a big overlap in the size distribution of Norway pout and herring, it might be expected that a distinction between the two species could be obtained due to the weaker reflecting properties of smaller fish (Love 1971b; Nakken and Olsen 1977; Foote 1987). Nonetheless, since comparison was made between mean volume backscattering values, differences in fish packing density within schools may have played a role as well. The smaller Norway pout might just have had higher packing densities and therefore generated similar volume backscattering values to herring. However, Nakken and Olsen (1977) examined backscatter of different swimbladdered fish and found distinct differences between differently sized fish species at 38 and 120 kHz. Similarly, Gauthier and Horne (2004b) suggested potential differences in backscatter among swimbladdered forage fish species of different sizes and emphasised the importance of the specific frequency ratios used. Especially at higher frequencies (e.g. 200 kHz), the TS response becomes more variable with increasing fish length (Gauthier and Horne 2004b). Kloser et al. (2002) managed successfully to distinguish between three swimbladder bearing fish species in deep waters using multifrequency acoustic methods. Nevertheless, the vast differences in terms of swimbladder type (e.g. one of the species studied, orange roughy (*Hoplostethus atlanticus*), has a wax ester-filled swimbladder) and size of the observed species facilitated such an attempt.

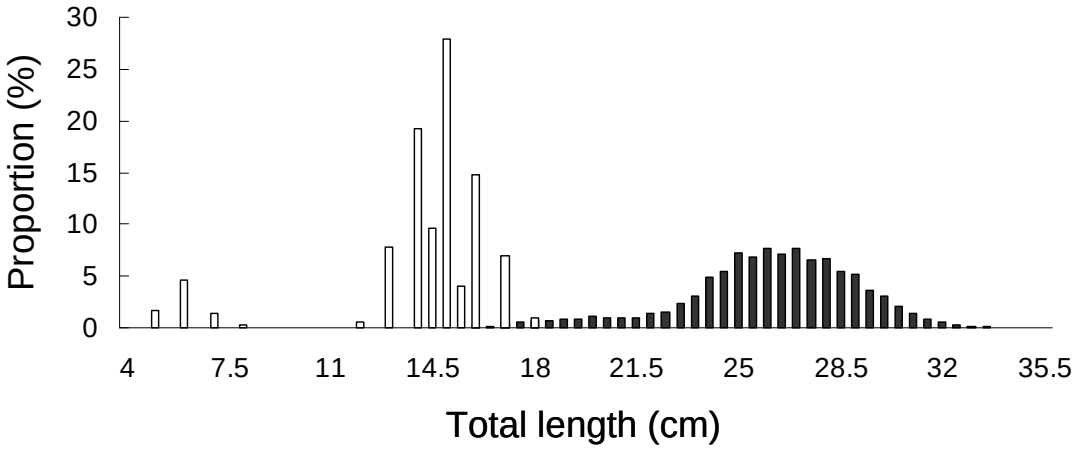

Figure 2.10 Length-frequency distributions of herring (black bars) and Norway pout (white bars) from trawl samples taken to verify species and size-composition of analysed echotraces.

Differences between $\hat{S}_v$ in herring and Norway pout may be influenced by erroneous allocation of species to the supposed ground truthed echograms (Suuronen et al. 1997; Bethke et al. 1999; McClatchie et al. 2000). For instance, in some cases, information on the echograms might not have corresponded exactly with data on the matching trawl, either by not sampling the whole school, or targeting a different school. As in every acoustic fish survey, the assumption made - that haul composition represented the echotrace composition - is uncertain. Nonetheless, during all the North Sea herring acoustic surveys from which data were used, much care was taken while sampling. Trawling processes were constantly monitored using a net sonde (net mounted echosounder displayed in real time), and echograms were compared during pre-trawl and trawl phases to make sure the correct schools were captured.

A decrease in variability of $\hat{S}_v$ between eroded and non-eroded echotraces was observed for both species, at all frequencies (Figure 2.3). This was probably an artefact of the erosion process, which removed the smaller values at the edges of the schools and resulted in a much narrower range of data. The statistically significant differences in $\hat{S}_v$ values at 18 and 200 kHz between eroded Norway pout and eroded herring schools may be explained in part by the erosion process that separates the

mean values further, and in part by the amount of data, which led to small standard deviations. However, despite these differences being statistically significant, they are unlikely to be useful as a discriminator due to the overlap that remains.

There are a number of other techniques other than multifrequency methods that could be used to distinguish herring from Norway pout echoes. For instance, algorithms that incorporate morphological (e.g. height, width, depth or size) and positional (bathymetric or geographic location) parameters of fish schools, in addition to frequency differences may have some merit (Scalabrin et al. 1996; Reid et al. 1998; Korneliussen et al. 2009a). Fernandes (2009) described a method to identify species based on "classification trees" that use acoustic multifrequency data in combination with additional features. Such an approach could provide a more sophisticated tool for objective species allocation by combining several sources of potential 'classification parameters'. The method would also give a measure of uncertainty that could be quantified as a component of total uncertainty in the abundance estimate. Also, backscatter of herring and Norway pout may be compared over a wider band of frequencies rather than at a limited number of distinct frequencies. Broadband techniques are becoming increasingly available and provide promising results in terms of species classification and data interpretation (Stanton 2009; Chapter 6).

Nero et al. (2004) compared measured backscattering levels with values from theoretical backscattering models in herring (length: 19-29 cm, mean length: 23.4 cm) at high (38-200 kHz), and low (1.5-5 kHz) frequencies. A distinct resonant peak was observed at 2.5 kHz. At higher frequencies, backscattering values decreased, reaching a minimum level at 38 kHz for measured values and 90 kHz for model values. In the study presented in this Chapter, a similar trend was observed with the empirical data in the high frequency domain. However, minimum values occurred at 120 kHz. From the output of the low frequency resonance model (model I) used here, backscatter from the swimbladder changes most dramatically around the resonant frequency domain. In the geometric scattering region, i.e. beyond ~10 kHz in the present case,

average backscatter from the swimbladder gradually flattens and decreases steadily at higher frequencies (see Horne and Clay 1998).

The MSB-DCM (model II) and KRM (model III) are not valid at typical swimbladder resonance frequencies of adult herring (Foote 1985; Stanton 1989) and therefore did not reproduce any resonant peaks in the results given here. The fish body component had negligible backscatter in the resonant frequency region (1-3 kHz) and it was generally lower than backscatter from swimbladders if they are at neutral buoyancy size (around 5% of total fish volume in marine fish) (Foote 1980a; Horne and Clay 1998). The dominant contributor in the resonant frequency range, independent of fish depth, is the swimbladder (Farquhar 1977). The relatively high amplitude of the resonant peak allows useful information to be derived from measurements of backscatter in that frequency region for the purposes of species identification (Holliday 1972; Love 1993; Nero and Huster 1996; Nero et al. 1998; Nero et al. 2004). However, low operating frequencies require specialised hardware and large transducers, so their usage is rather limited. Additionally, previous studies that examined the enhanced backscatter at low frequencies, found the resonance frequency also to differ with fish size, species and depth (in the case of physostomes) (Sand and Hawkins 1973; Love 1978; Feuillade and Nero 1998). Such implications might limit potential low frequency (less than 10 kHz) dependent species discrimination that involves swimbladder bearing fish. Furthermore, the range of frequencies used by commercial fishing vessels (12-200 kHz) is similar to those examined here and so these results will be of interest to that community.

Of the models used to date, which incorporate simple geometric shapes, the fluid-filled ellipsoid most accurately reflects the shape of the herring body. Gorska and Ona (2003a, 2003b) modelled backscatter from herring, but they used a prolate spheroid to approximate the fish body. In contrast to the sausage-shaped prolate spheroid, the ellipsoid is a better representative of the herring's body shape because the herring body width is much smaller than its height (e.g. see Knorr 1974). Since the same object shapes (swimbladder = spheroid, fish body = ellipsoid) were used for all models in the present investigation, observed differences between model outputs

were due to the specific approximation solutions. Average swimbladder backscatter as predicted by model I was lower than that of models II and III. Additionally, the DWBA used to model the fish body component in models I and II on average gave higher backscatter values than predicted from the KRM in model III. Consequently, the body backscatter had an increased effect on overall fish backscatter in model I, resulting in more oscillating features in the frequency response at frequencies > 10 kHz (Figure 2.8). Model predictions for the whole fish from model II were more influenced by the stronger swimbladder backscatter, resulting in less variable frequency responses for all size classes (Figure 2.6). Nonetheless, simple geometric shapes may be inadequate representations of fish scattering components as they are symmetrical relative to the horizontal axis, while important organs such as the swimbladder are not (Foote 1985). Arguably, model techniques that apply the Kirchhoff approximation (Foote 1985; Peña and Foote 2008) or the Boundary element method (BEM; Francis and Foote 2003) could provide more realistic outputs in terms of accuracy of fish body shapes, since they do not assume any symmetry and can, therefore, be applied to realistic fully three-dimensional arbitrary shapes of fish (Simmonds and MacLennan 2005). Such models would have required precise mapping of the swimbladder surface. Since such data were not available here and the purpose of the models used was to explain the observed empirical data and concentrate on the body-swimbladder relationship in particular, models applying geometrical shape approximations were found to be sufficient. However, more detailed investigations into the herring swimbladder morphology when exposed to increased pressures and its application in high resolution 3-D backscatter modelling is described in subsequent Chapters of this Thesis.

Including the directivity associated with the tilt angle distribution into the swimbladder model components resulted in lower average backscattering levels with increasing frequency. This can be attributed to the higher amplitudes in directivity patterns at higher frequencies, which lead to reduced average scattering if the swimbladder is not near orthogonal orientation (Horne and Clay 1998). The result was a more dominant fish body contribution to the total backscatter at progressively

higher frequencies beyond resonance. Subsequently, due to the backscattering features of the fish body component, the relative frequency and decibel difference at 18 kHz was more emphasised and variable than would be in the normal incidence case. Since no data were available, the tilt angle distribution was chosen as having a Gaussian distribution. Ona (2001) observed tilt angle distributions in herring having a mean of 88.9° and 86.9° (90° = normal incidence) with standard deviations of 10° and 14.2° respectively. The former measurement was used in the current study, and other authors have found similar results (Beltestad 1974). Gorska and Ona (2003a) did not take into account the shift of the swimbladder axis relative to the body axis in herring. However, measures of 40 herring caught in the North Sea suggested that this axis was 5.6°, and this value was implemented into the directivity calculation. Diurnal changes in tilt angle, as observed for Norwegian spring-spawning herring (Huse and Ona 1996), have profound implications on acoustic backscatter. Ideally, tilt angle distributions should be ascertained for the fish schools in question as this may be affected by species, time of year and time of day.

In addition to directivity, depth is another contributing factor that reduces expected average swimbladder backscatter of the physostomous herring and allows the fish body component to become more dominant. At a certain depth, the body may even become a stronger scatterer than the swimbladder and contribute most to the total backscatter of the fish. Gorska and Ona (2003b) modelled swimbladder contraction in a 32 cm herring, using prolate spheroids to represent swimbladder and fish body. They found the depth where the swimbladder and the fish body contributed equally to the total backscatter at 38 kHz, to be at about 180 m. An important but still largely unresolved aspect, however, is the assumption about the swimbladder volume at sea surface pressure. The volume of the swimbladder at the sea surface (= 15% of total fish volume) assumed in the present investigation was essentially based on the only currently available but limited data set of herring swimbladder volumes estimated *in situ* (Nero et al. 2004). This value is greatly different from those previously assumed for marine fish that are neutrally buoyant at the sea surface (Jones and Marshall 1953; Ona 1990). Until a reliable solution can be found,

assumptions about surface swimbladder volumes of physostomous fish will remain potentially significant but largely unknown influences on results of backscattering models.

Considering the oscillating shape of the predicted backscatter response of ellipsoid fluid-filled bodies of different sizes, responses varied considerably at certain frequencies. Compared to bigger fish, smaller fish were found to have stronger backscatter at 18 kHz relative to 38 kHz. Based on modelling results, the gradual positional change of frequency response observed at 18 kHz relative to 38 kHz for different herring size classes was due solely to the relative shape of the body backscatter. As for the two higher frequencies used (120 and 200 kHz), the models generally failed to explain the frequency specific backscatter observed in the empirical data, with lower scatter at 120 kHz compared to 200 kHz. The reason might be that backscatter at these frequencies is greatly influenced by the shape of the scattering objects and the simple geometric shapes may therefore have been too coarse and hence inadequate (Foot 1985; Horne and Clay 1998; Horne and Jech 1999). Additionally, Rayleigh scattering of the backbone will become more important at higher frequencies and may contribute to the higher backscatter observed at 200 kHz (Gorska et al. 2005; Gorska et al. 2007). The trend for a reduced frequency response at 18 kHz with increasing fish size does not support a potential discrimination between different herring size classes, since the overlap in the empirical data was still considerable. However, the trend was most clearly marked for eroded herring data, possibly due to these data being less variable. Interestingly, Johnsen et al. (2009) managed to distinguish between schools comprising of small, 1-year-old, and large, 2-year-old sandeel (*Ammodytes marinus*) based on the frequency responses at 18 and 38 kHz. Significant findings were that the statistical discriminant analysis they used to examine differences in frequency responses was facilitated by using log-transformed r(*f*) values, and classification success was markedly better for schools with higher mean s_A.

An important result from this Chapter is that for the physostomous herring, tilt angle averaged backscatter will be more affected by the fish body component at

increasing water depth. The oscillating feature of the fluid-filled body component backscatter will therefore greatly affect relative backscattering features at frequencies commonly used in fisheries science (18 and 38 kHz). The findings may be useful in species identification to distinguish physostomes at deeper depths from physoclists, which may show less variable backscattering features at these frequencies due to the nature of their swimbladder. A depth dependent TS for physostomes will in addition have implications for acoustic surveys of herring where presently simple size-dependent TS equations are used to estimate biomass abundances. Ona (2003) argues that estimates of herring abundance would be about 50% less if a depth dependent TS model was considered in the calculations. It is postulated that, if possible, precise measurements of the herring swimbladder at various depths should be incorporated into fully three-dimensional backscatter models, using techniques such as KRM or BEM, to reveal more precise depth-dependent target strength estimates.

Chapter 3

Intra- and inter-species variability in target strength: the case of the Baltic herring

Parts of the work described here have been published as:
Fässler, S.M.M., Gorska, N., Ona, E. Fernandes, P.G. (2008). Differences in swimbladder volume between Baltic and Norwegian spring-spawning herring: consequences for mean target strength. Fisheries Research 92: 314-321.

Fässler, S.M.M., Gorska, N. (2009). On the target strength of Baltic clupeids. ICES Journal of Marine Science 66: 1185-1190.

3.1. Introduction

The gas filled swimbladder, present in many species of teleost fish, makes a large contribution to the total backscattered sound energy (Jones and Pierce 1958; Foote 1980a). In some cases, the physical environment may influence the physiology and morphology of the fish and its swimbladder, resulting in increased intra- and inter-species variation in target strength (TS) throughout the distributional range as a whole (Blaxter and Batty 1990; Horne 2003). *In situ* target strength (TS) measurements suggest that Baltic herring may have an average TS which is 3-7 dB higher than herring living in the North Sea (Lassen and Stæhr 1985; Rudstam et al. 1988; Rudstam et al. 1999; Didrikas and Hansson 2004; Didrikas 2005; Peltonen and Balk

2005). Observed variations in TS between the two conspecific herring stocks was linked to the fundamentally different physical environments that fish in the different seas live in, physical differences that in turn result in different morphological adaptations (Didrikas and Hansson 2004; Peltonen and Balk 2005). The Baltic Sea has a lower salinity (approx. 7), and therefore lower density, than the waters in the northeast Atlantic and North Sea (salinity: approx. 35). Additionally, Baltic herring have been found to have a much lower fat content (~2-15%) than both Norwegian spring-spawning and North Sea herring (~15-25%) (Huse and Ona 1996; Cardinale and Arrhenius 2000; Ona et al. 2001; Aidos et al. 2002; Kiviranta et al. 2003). In order to maintain neutral buoyancy the swimbladder has to counterbalance the mass of the fish body to match the density of the surrounding sea water. Fat has a lower density than sea water and can, therefore, also contribute to positive buoyancy (Brawn 1969). Hence, swimbladder volumes of Baltic herring of a given length may be larger, leading to higher average TS values (Didrikas and Hansson 2004).

Furthermore, there is ambiguity as to whether the same TS-fish length (L) relationship can be used for both herring and sprat within the Baltic Sea (Kasatkina 2009). Presently, acoustic stock size estimation for the Baltic clupeids herring and sprat are derived using the same TS-L relationship developed for North Sea herring (i.e. $TS = 20\log_{10}(L) - 71.2$, ICES 1983). Similar to Baltic herring, recent *in situ* measurements suggest that Baltic sprat may also have higher TS values than those currently used to assess their stock (Rudstam et al. 1988; Rudstam et al. 1999; Didrikas and Hansson 2004; Didrikas 2005). However, exactly which TS-L relationship is appropriate to use in biomass estimation of clupeids in the Baltic Sea is still an open question. Strong variability in Baltic clupeid TS has been demonstrated in different regions and seasons (up to 8 dB difference, Lassen and Stæhr 1985; Rudstam et al. 1988, 1999; Didrikas and Hansson 2004; Didrikas 2005; Peltonen and Balk 2005; Kasatkina 2007; Kasatkina 2009). As potential reasons for the observed variability in TS, Peltonen and Balk (2005) suggested: (i) spatial and temporal biological differences between herring stocks occupying various parts of the Baltic Sea; and (ii) differences in data collection and analysis approaches between different

studies. Moreover, recent *in situ* TS measurements of single species aggregations of Baltic herring and sprat made by Kasatkina (2007 and 2009) provide further proof that these two species may have distinct TS-L relationships.

In this Chapter I aim to explain: firstly, why Baltic herring may have a higher TS than another particular herring stock from the northeast Atlantic, the Norwegian spring-spawning herring; and secondly, why there might be a discrepancy between TS-L relationships determined for Baltic herring and sprat. Volume and dimension of swimbladders and fish bodies of the respective species and stocks were measured. The size of herring swimbladders necessary to enable the fish to achieve neutral buoyancy was estimated theoretically assuming typical fat content and salinity conditions experienced by the two stocks. The morphological data were subsequently used to model the mean TS applying 'model II' described in Chapter 2. New TS-L relationships based on the model results are proposed for both clupeid species and stocks, and results compared to empirical TS measurements. Furthermore, sensitivity analyses were performed to examine direct (depth, frequency and fish orientation) and indirect (water salinity and fish fat content) effects on TS of Baltic clupeids.

3.2. Methods

3.2.1. Morphological measurements

3.2.1.1. Herring swimbladder volumes

Data on the volume of Baltic herring swimbladders were collected at Forsmark nuclear power plant (60º24′N 18º10′E), on the Swedish east coast north of Stockholm in 1988. In order to prevent damage to internal organs the fish were caught close to the surface by land seines and were allowed to swim freely to a 5 m^3, 1 m deep holding tank at the experimental site. Total lengths of the herring ranged from 17.2 to 32.6 cm. The fish were held in the holding tanks where they were allowed to adapt to surface pressures for 7-10 days. Immediately before taking swimbladder volume measurements, the herring (n = 104) were scooped over to a smaller tank in batches of five, where they were anaesthetised with 300‰ benzocaine. The swimbladders of the fish were then emptied by gentle ventral massage from beneath the pelvic fins

towards the anal opening. Swimbladder gas was collected with an inverted funnel suspended beneath the water with a top mounted glass burette. Swimbladders were then emptied completely by underwater dissection and their volume measured to the nearest 0.1 ml. No residual gas was found in the main chamber or the anal duct after inspection. Each fish was weighed to the nearest 1 g and its length measured to the nearest 0.1 cm. Finally, all fish samples were analysed for percentage fat content by standard methods using sodium sulphate grinding and ethyl ether extraction (see Brawn 1969). These measurements were compared to swimbladder volumes obtained from Norwegian spring-spawning herring (Ona 1990) collected in 1983 at Skogsvåg (60º15′N 5º05′E) in western Norway using the same methods.

Swimbladder volumes were also calculated assuming that herring aim to minimise energy expenditure by maintaining a state of neutral buoyancy (i.e. the density of the whole fish has to equal the sea water density). For the fish to gain neutral buoyancy, the swimbladder has to acquire a certain volume (V_{sb}, in %) relative to the whole fish volume in order to balance the density of the surrounding sea water (ρ_{sw}) and fish body (ρ_{fish}):

$$V_{sb} = \frac{\rho_{fish} - \rho_{sw}}{\rho_{fish} - \rho_{sb}} \tag{3.1}$$

The density of the swimbladder gas (ρ_{sb}) was assumed to be 0.0013 g cm^{-3} (Brawn 1969). Sea water density was calculated according to an algorithm developed by Fofonoff and Millard (1983) using an equation of the form $\rho_{sw} = \rho(T,S,z)$, where the density is a function of temperature (T), salinity (S) and depth (z). Uniform values for temperature of 10 ºC and salinity of 35 were assumed for the Norwegian Sea. Values of 10 ºC and 7 respectively were chosen for the Baltic Sea.

Density of the fish body (ρ_{fish}, i.e. whole fish excluding the swimbladder) was calculated using an adapted proportion key for the volume proportions of various body components (V_f, V_{sc}, V_b, V_r for fat, scales, bones and the 'rest' of the body, respectively) as determined by Brawn (1969) for Pacific herring (*Clupea pallasii*):

$$V_f : V_{sc} : V_b : V_r = [V_f] : [0.5] : [1.2] : [98.3 - V_f] \quad (3.2)$$

where fat contents (V_f) were based on measurements made on the collected herring samples (Norwegian spring-spawning herring: mean = 18.4%; Baltic herring: mean = 7.3%). Considering the steadily decreasing trend in fat content of herring in the Baltic proper since the early 1980s (Cardinale and Arrhenius 2000), present values were based on recent findings of Bignert et al. (2007) and were assumed to be 2.1%. Swimbladder volume estimates for Baltic herring were performed using both the 1980s and current fat content values.

The density of the fish body was calculated by dividing the sum of the weighed densities (the product of volume proportion and density) of each body component by the sum of all body volume proportions:

$$\rho_{fish} = \frac{\rho_f V_f + \rho_{sc} V_{sc} + \rho_b V_b + \rho_r V_r}{V_f + V_{sc} + V_b + V_r} \quad (3.3)$$

The following density values were used for both herring stocks according to data published by Brawn (1969): fat, ρ_f = 0.926 g cm^{-3}; scales, ρ_{sc} = 1.966 g cm^{-3}; bones, ρ_b = 1.993 g cm^{-3}; and the 'rest' (= other body tissues), ρ_r = 1.057 g cm^{-3}. Mean values of ρ_{fish} were 1.049 g cm^{-3} for Norwegian spring-spawning and 1.063 g cm^{-3} for Baltic herring. By inserting ρ_{fish} into Equation (3.1), swimbladder proportions of total fish volume could be estimated theoretically for both Norwegian spring-spawning and Baltic herring cases. Conversion to absolute volumes was achieved by calculating the volume of the fish body by dividing the weight by the density (ρ_{fish}). Predicted model and observed empirical values were then compared using correlation and linear regression analysis.

3.2.1.2. Baltic clupeid body and swimbladder dimensions

Baltic herring and sprat samples were collected in October 2002 on the Swedish component of the Baltic International Acoustic Survey (BIAS) in the Baltic Sea (ICES Subdivisions 25, 27 and 29). Live fish were selected from the catch and placed in a tank with seawater immediately after they were hauled on board. Fish that were still swimming horizontally after 2-5 minutes were carefully transferred into an anaesthetic bath (4-6‰ clove oil solution) with a small net. The fish were left in the anaesthetic bath for 5 minutes and then measured (total length, to the nearest 0.5 cm; maximum height and width, to the nearest 0.1 mm). Afterwards, the fish were frozen and X-rayed (at 20 kV and 900 mA). Maximum dimensions (length, height and width) of the swimbladder were measured using good quality X-ray images of the herring (n = 25; length: 13 - 24.5 cm) and sprat (n = 21; length: 7 - 13.5 cm). The narrow extensions at the anterior and posterior ends of the swimbladder were excluded from the measurements.

3.2.2. Target strength model

The theoretical backscattering model described as ‘model II’ in Chapter 2 was used to derive estimates of mean TS. The model consisted of two separate components that were combined to give a total backscattering cross-section that was expressed according to Equation 2.4. The term ‘fish body’ describes all parts of the body (flesh, bones, scales and organs) except the swimbladder. Assumptions about ellipsoid dimensions of the fish body model were based on X-ray images (Norwegian spring-spawning herring: E. Ona, unpublished data). Density and sound speed contrasts were assumed to be 1.04 and 1.04 for the fish body and 0.00128 and 0.23 for the swimbladder for both herring stocks and sprat, respectively. Herring swimbladder volume decreases with depth, according to Boyle’s law (Ona 1990; Fässler et al. 2009a, see Chapter 4). Swimbladder dimensions were assumed to contract with increasing pressure at depth according to Equations 2.10 and 2.11, considering that Boyle’s law requires the compression factors α and β to behave according to $2\alpha + \beta = 1$. TS values were evaluated for extreme cases of contraction

rates, i.e. maximum: $\alpha = 1/3$, $\beta = 1/3$; and minimum: $\alpha = 1/2$, $\beta = 0$ (Gorska and Ona 2003a; see Section 2.2.5.2.). Recent work (Gorska and Ona 2003a, 2003b; Fässler et al. 2009a, Chapter 4) and studies of fish morphology (Blaxter et al. 1979; Ona 1990) suggest that the latter case (minimum contraction rates) is more realistic, and therefore, this was consequently used to estimate TS-L and TS-L-depth relationships. To account for the tilt-dependent directivity pattern of the swimbladder, the simple solution for a straight cylinder was used (Medwin and Clay 1998). For simplicity, the angle between the swimbladder and snout-tail axis was ignored. Unless specifically stated otherwise, a Gaussian tilt-angle distribution with a mean of 0º and standard deviation of 5º (Gorska and Ona 2003a) and acoustic frequency of 38 kHz were used for TS estimations.

3.2.2.1. Target strength model specifications: Baltic and Norwegian spring-spawning herring

In the combined TS model for Baltic and Norwegian spring-spawning herring, the fish body was modelled as a fluid-filled ellipsoid and the swimbladder as a gas-filled elongated prolate spheroid. The modelled swimbladder length at the sea surface was assumed to be 0.26 times the total length of the fish for both Norwegian spring-spawning and Baltic Sea herring (Gorska and Ona 2003a). The remaining dimension (width) of the prolate spheroid was adjusted to give measured swimbladder volumes for a given fish weight (equation: volume = $4/3\pi \times \text{width}^2 \times \text{length}$). Fish weight (W) was then converted into length (L) using the relationship $W = 0.0033 \times L^{3.3078}$ determined for Atlantic herring (Chapter 2, Fässler et al. 2007). These parameters were not significantly different from the values Kasatkina (2009) found for Baltic herring larger than 16 cm ($a = 0.0032$ (standard error, s.e. = 0.00069); $b = 3.2$ (s.e. = 0.07)), and therefore they were assumed to be valid for that stock as well.

Backscattering characteristics averaged over fish orientation were determined and TS values could be calculated for a variety of fish lengths and depths. Standard length-dependent TS relationships were derived by fitting a linear regression to the modelled mean TS at 38 kHz estimated for a range of fish lengths. TS values were

modelled for typical fish lengths and water depths of Norwegian spring-spawning (length: 16-40 cm, depth: 0-400m; Huse and Ona 1996; ICES 2007) and Baltic herring (length: 9-25 cm, depth: 0-100 m; N. Håkansson, F. Arrhenius, B. Lundgren, T. Didrikas, pers. comm.). Additionally, length- and depth-dependent TS relationships at 38 kHz were determined for a 32 cm herring and compared to *in situ* TS data from Norwegian spring-spawning herring (Ona 2003).

3.2.2.2. Target strength model specifications: Baltic clupeids

Mean TS of Baltic herring and sprat was estimated using the combined backscatter model partly described as 'model II' in Chapter 2. Fish body and the swimbladder were both modelled as fluid-filled and gas-filled elongated prolate spheroids, respectively. Mean TS of all fish samples were estimated using actual measured dimensions of the fish body and swimbladder to represent the major and minor axes of the simplified scattering objects (prolate spheroids). For the sensitivity analysis of TS to water salinity and fish fat content, the model described in Section 3.2.1.1., approximating the swimbladder volume as a function of these parameters, was used. Salinity (S) in the Baltic Sea was assumed to be: $1 \leq S \leq 10$; and herring fat contents to range from 1.5% to 5% (Bignert et al. 2007). The same values were assumed for sprat.

3.3. Results

3.3.1. Morphological measurements

3.3.1.1. Swimbladder volumes: Baltic and Norwegian spring-spawning herring

Surface adapted Baltic herring had significantly larger swimbladder volumes for a given fish weight (differences between slopes: Student's t-test, $p<0.001$; difference between intercepts: Student's t-test, $p<0.001$) than Norwegian spring-spawning herring (Figure 3.1). For fish that weighed more than 44.25 g, swimbladder volumes of Baltic herring (slope = 0.057) were on average about three times larger than those of Norwegian spring-spawning herring (slope = 0.017; see Ona 1990). Spring-

spawning herring that were lighter than 44.25 g on average had a larger swimbladder compared to Baltic herring (see the lower intercept of the regression line fitted to the Baltic herring data; Figure 3.1). However, confidence intervals of estimated swimbladder volumes did overlap at these low weights, making potential differences insignificant. Moreover, there were no data for fish weights less than about 25 g.

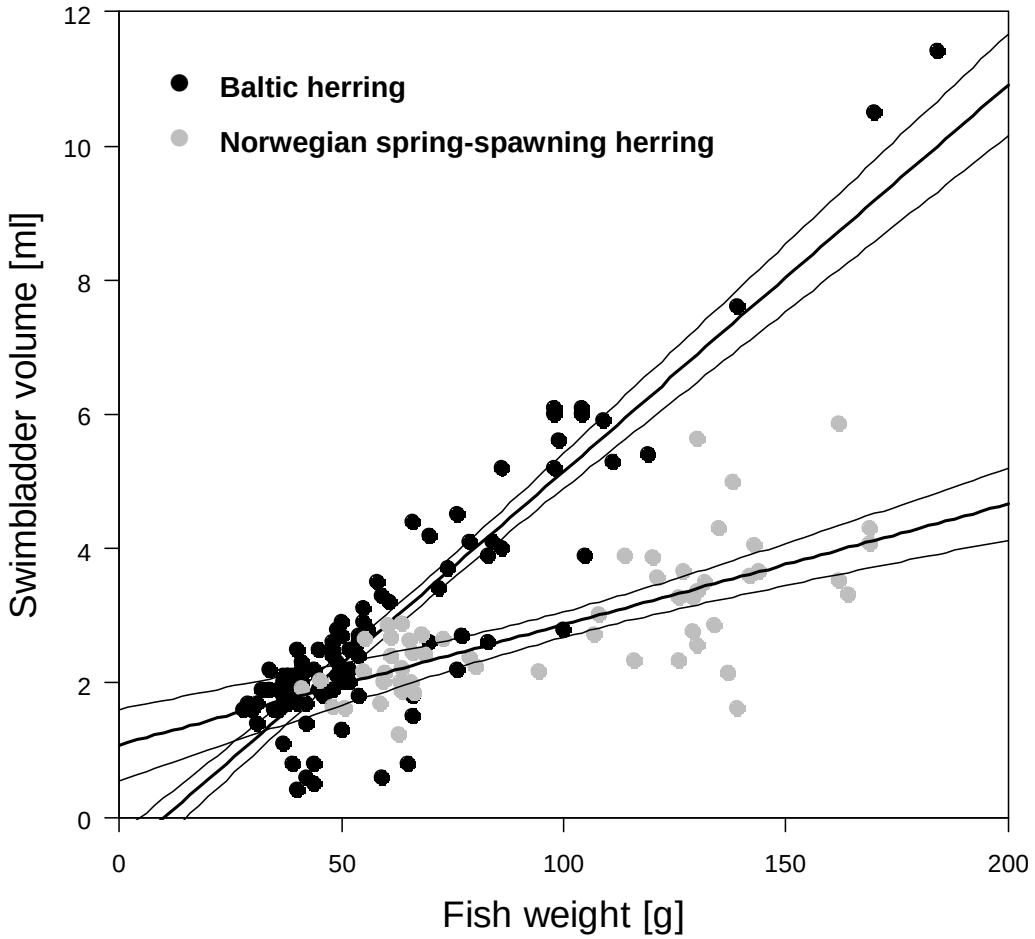

Figure 3.1 Swimbladder volume (y-axis) in relation to fish weight (x-axis) for Baltic (black circles) and Norwegian spring-spawning herring (grey circles) collected between 1983 and 1988. Regression lines with 95% confidence intervals are given. Baltic herring: $y = 0.057x - 0.59$, $n = 104$, s.e. = 0.77, $r^2 = 0.82$. Norwegian spring spawning herring: $y = 0.017x - 1.18$, $n = 60$, s.e. = 0.66, $r^2 = 0.77$ (see Ona 1990).

There were significant relationships between empirically determined swimbladder volumes and modelled values assuming neutral buoyancy of the fish (Norwegian spring-spawning herring: $r = 0.937$, $p<0.001$; Baltic herring: $r = 0.901$, $p<0.001$; Figure 3.2). The slopes of the lines fitted to the theoretically determined swimbladder volumes for a given weight (Norwegian spring-spawning herring: 0.020; Baltic herring: 0.056) were similar to the ones of the lines fitted to the empirical data (Figure 3.1). This would suggest that the input parameters of the swimbladder model (salinity and herring fat content) were appropriate to describe the empirical data. The results of the regression analysis however showed that the straight lines fitted to the observed and expected swimbladder volume data had slopes and intercepts that were almost all significantly different from respectively 1 (Baltic herring: $t = -6.79$, $p<0.001$; Norwegian spring-spawning herring: $t = 5.23$, $p < 0.001$) and 0 (Baltic herring: $t = 9.70$, $p<0.001$; Norwegian spring-spawning herring: $t = -8.00$, $p < 0.001$). These differences are mainly driven by the assumed input parameters used in the theoretical swimbladder volume model. If current fat content percentages were used, the model suggested that swimbladder volumes of Baltic herring would be 18% larger than what they were at the beginning of the 1980s. For that reason and to reflect current conditions, recently observed values of fat content were used to adjust measured swimbladder volumes for subsequent TS modelling.

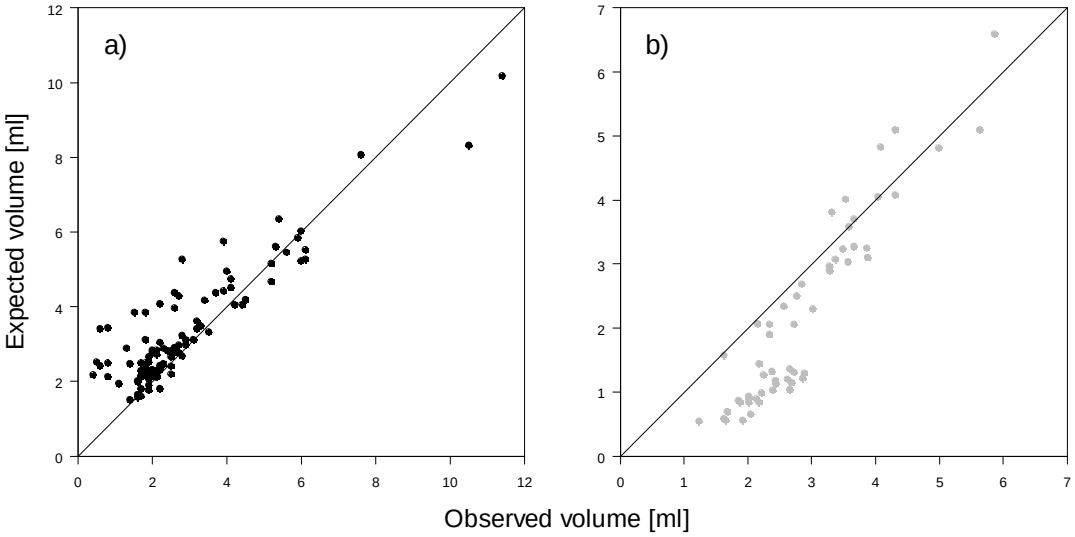

Figure 3.2 Correlation between observed and expected swimbladder volumes for (a) Baltic herring and (b) Norwegian spring-spawning herring. Expected volumes are based on observed fat contents of the fish and typical salinity values of Baltic (salinity = 7) and Northeast Atlantic waters (salinity = 35). Solid lines indicate the 1:1 relationships.

3.3.1.2. Swimbladder and fish morphology: Baltic clupeids

Swimbladder dimensions of Baltic herring and sprat differed significantly between species (Figure 3.3). While there were no differences in proportion of swimbladder length to fish total length (Student's t-test: $t = -1.39$, d.f. = 44, $p = 0.172$; Figure 3.3a), Baltic herring had significantly larger proportions of swimbladder height to length (Student's t-test: $t = 5.21$, d.f. = 44, $p < 0.001$; Figure 3.3b) and swimbladder width to length (Student's t-test: $t = 8.28$, d.f. = 44, $p < 0.001$; Figure 3.3c). Figure 3.4 shows an example of X-ray radiographs illustrating the different swimbladder growth pattern between the species, which results in a higher bladder height-to-length ratio in herring.

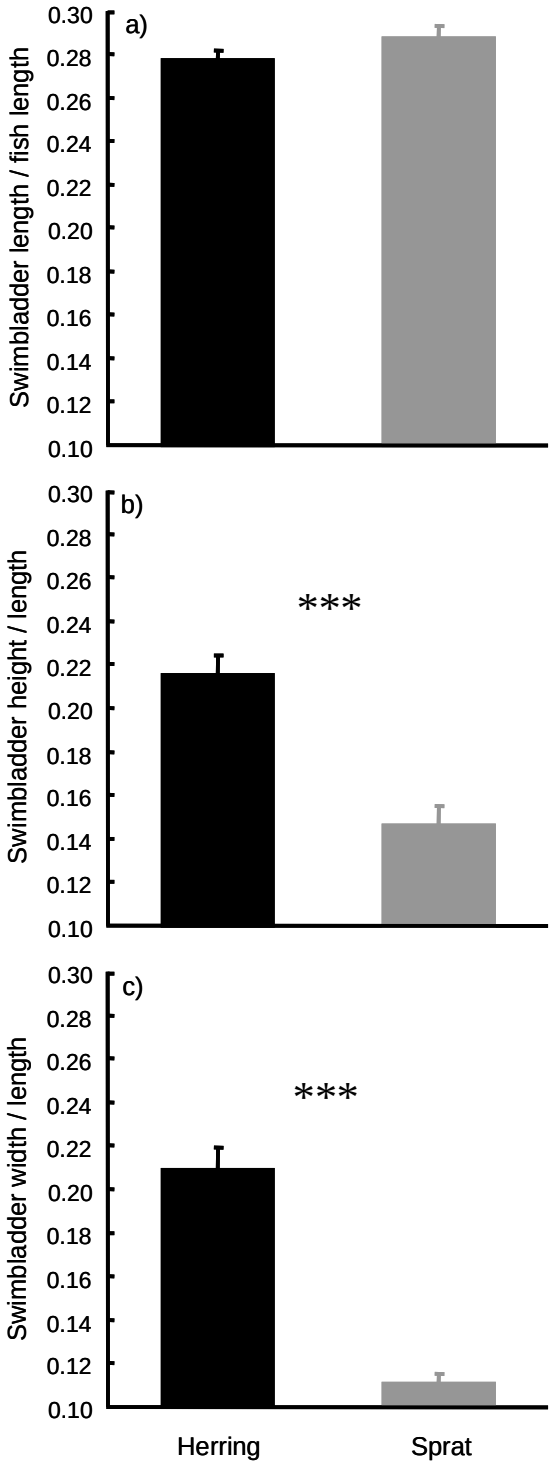

Figure 3.3 Differences in morphology of swimbladder between Baltic herring and sprat. Probability value for differences between swimbladder dimension proportions is given: *** $p < 0.001$.

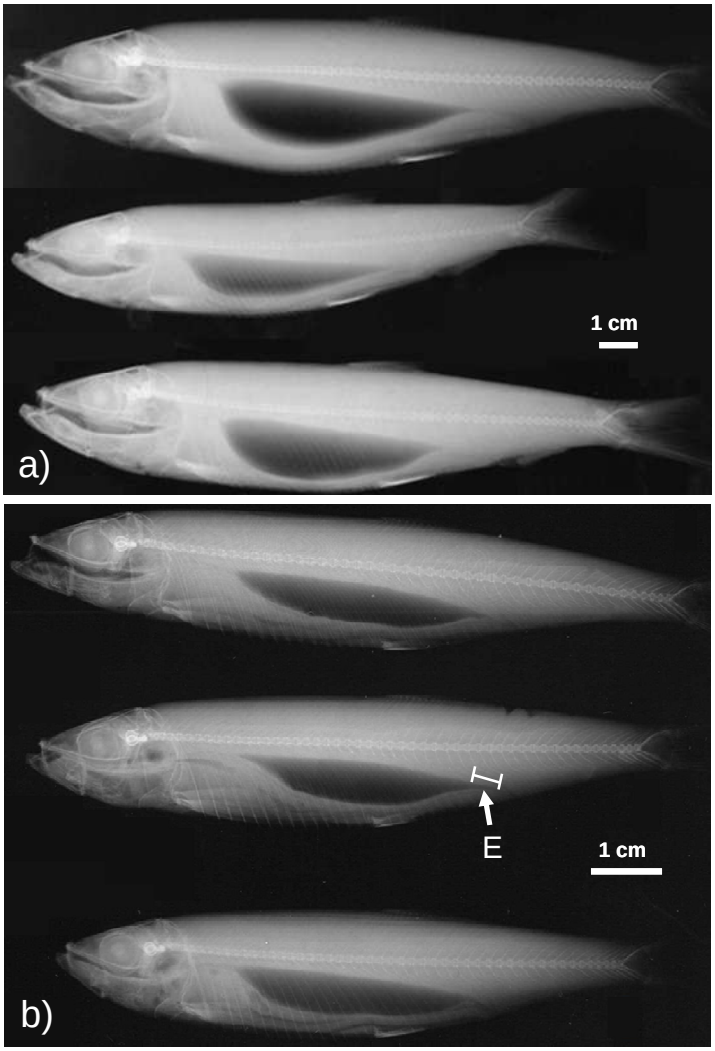

Figure 3.4 Example X-ray radiographs of Baltic herring (a) and sprat (b) showing the gas-filled swimbladder as a dark object in the centre of the fish body below the vertebral column. An example of a narrow extension (E) of the swimbladder, which was ignored for the dimension measurements, is shown.

3.3.2. Target strength modelling

3.3.2.1. Baltic and Norwegian spring-spawning herring

Incorporating swimbladder volumes from measured herring samples (Figure 3.1) into the TS model enabled for the computation of backscattering strengths for a range of depths and fish sizes for both Baltic and Norwegian spring-spawning herring. The

ratio of fish length to lateral height based on X-ray measurements was found to be 5.3 for both herring stocks. The ratio of fish length to dorsal width was 8.0 for Norwegian spring-spawning and 10.7 for Baltic herring. Figure 3.5 shows contour plots of modelled TS values assuming minimum contraction rates ($\alpha = 1/2$, $\beta = 0$; see Section 2.2.5.2.), i.e. the swimbladder length did not change with increasing water depth. The model revealed higher TS values for Baltic herring, especially so for large fish ($\geq$30 cm), where differences of about 2 dB were found.

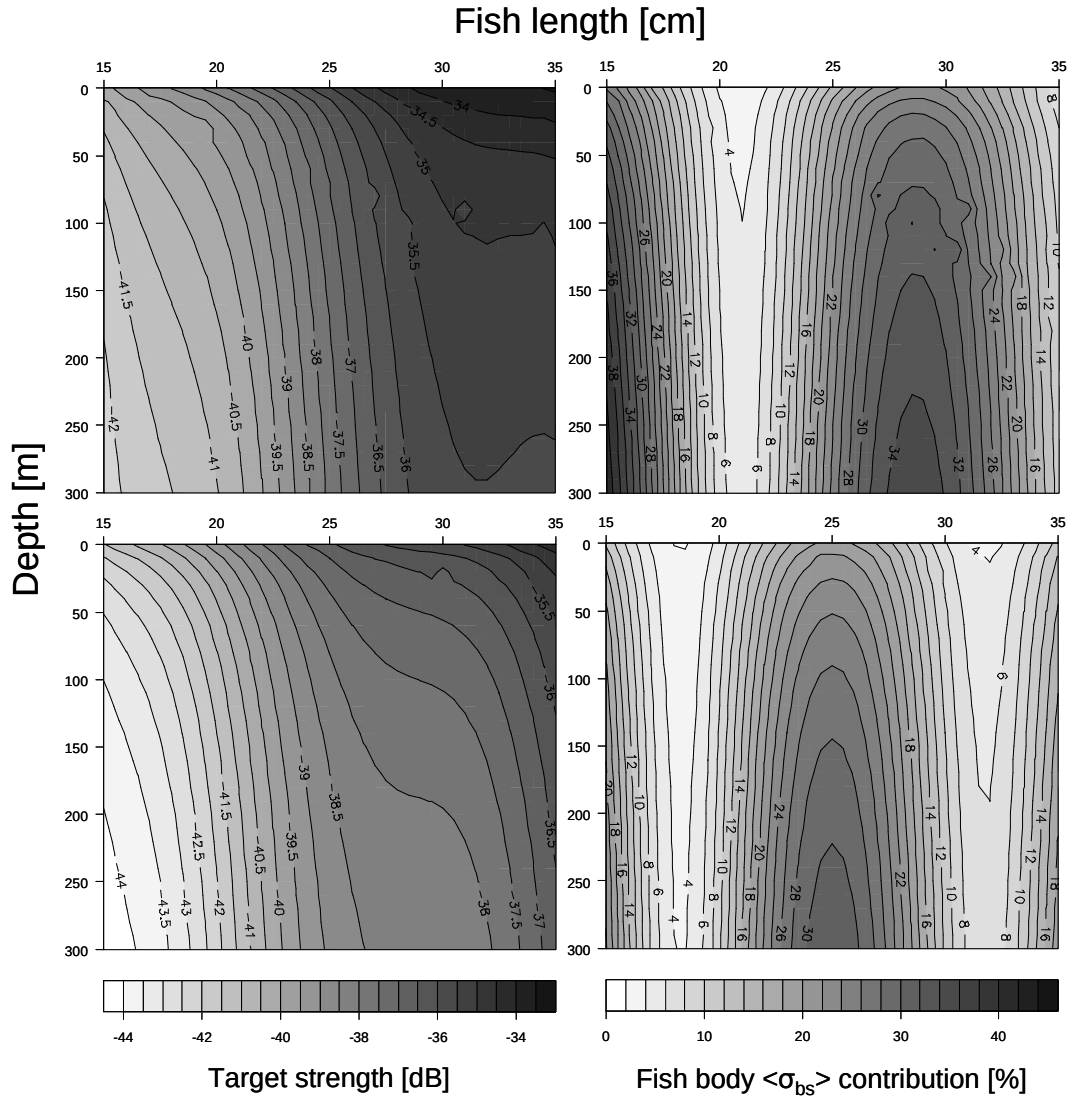

Figure 3.5 Depth dependence of the modelled mean target strength at 38 kHz (left panels) and the body contribution to the total backscatter (right panels) of Baltic (upper panels) and Norwegian spring-spawning herring (lower panels). Swimbladder dimensions were assumed to contract with depth according to compression factors $\alpha = 1/2$ and $\beta = 0$.

Changes in total TS with depth were not consistent among fish sizes between Baltic and Norwegian spring-spawning herring stocks (Figure 3.5). The oscillating nature of the averaged fish body backscatter estimated by the DWBA modelling method resulted in some fish size ranges being more influenced by the backscatter of

the fish body as opposed to the swimbladder (i.e. the fish sizes corresponding with the maxima of the oscillating fish body averaged backscattering cross-section). This was especially true for Norwegian spring-spawning herring of 22.5-27.5 cm and Baltic herring of 26.0-31.0 cm (Figure 3.5). For these fish sizes the total TS variation with depth was about 1.5-2.0 dB for both herring stocks. On the other hand, Norwegian spring spawners of 15.0-22.5 cm and >30 cm, and Baltic herring of 18-23 cm were less influenced by the fish body backscatter (i.e. the fish sizes corresponding with the minima of the oscillating fish body averaged backscattering cross-section). At these sizes the total TS variation with depth was about 2.5-3.0 dB. The variability of TS with depth depends, therefore, on the fish body contribution to the total backscatter of the fish.

To bring the modelled TS values into context, they were compared to data from *in situ* observations of Norwegian spring-spawning herring TS published by Ona (2003). The narrow length distributions of herring observed by Ona (2003) suggested the measured TS could be normalised to a common fish size of 32 cm. Consequently, models were run for fish of that size for both Norwegian spring-spawning and Baltic herring cases. Estimated mean TS values for both herring stocks were within the range of most *in situ* TS values apart from a few low values at shallow water depth (Figure 3.6). Since the empirical measurements were based on a range of different experiments performed at various times of the year, it can be assumed that the measured herring expressed differences in density, behaviour and condition. These factors can affect the measured TS (Ona 1990; Blaxter and Batty 1990; Ona et al. 2001; Ona 2003) and might therefore have resulted in the large spread observed in the empirical measurements over the depth range covered (5-500 m) by Ona (2003). Modelled mean TS at the surface (depth = 0 m) for Norwegian spring-spawning herring were around 2 dB lower than that of Baltic Sea herring. Shaded areas in Figure 3.6 represent modelled TS values that fall between the extreme cases of swimbladder dimension contraction with depth, where the length compression factor was equal to or less than that of swimbladder width. Mean TS values for Norwegian spring-spawning herring over the stated depth interval (0-300 m) ranged from -35.2

to -38.1 dB for minimum swimbladder contraction rates and from -35.2 to -44.4 dB for maximum swimbladder contraction rates. Similarly, values for Baltic herring ranged from -33.5 to -35.5 dB for minimum and from -33.5 to -39.5 dB for maximum contraction rates. Modelled mean TS values overlap in cases where high swimbladder compression factors are assumed for Baltic and low ones for Norwegian spring-spawning herring. Most model and empirical TS estimates were higher than the presently applied depth-independent length-based TS relationships used for estimates of stock size (Figure 3.6).

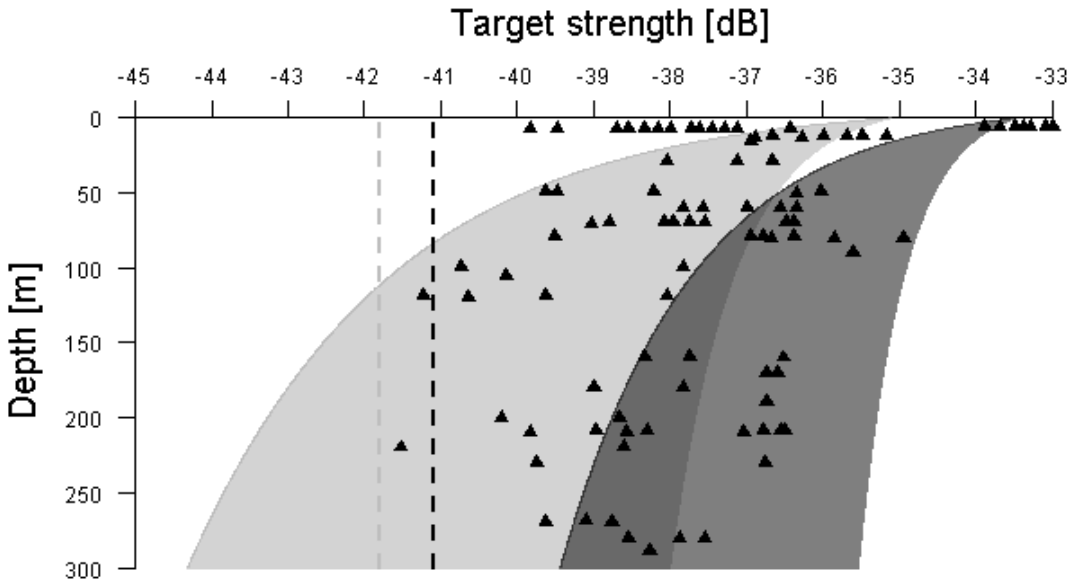

Figure 3.6 Modelled depth-dependent mean target strength values for Baltic (dark shaded area) and Norwegian spring-spawning (light shaded area) herring compared to measured *in situ* values for Norwegian spring-spawning herring (Ona 2003) standardised to a fish size of 32 cm (black triangles). Borders of the shaded areas are defined by the extreme cases of swimbladder contraction rates, i.e. assuming maximum (α = 1/3, β = 1/3) and minimum (α = 1/2, β = 0) compression factors, respectively. Length based target strength relationships currently used for stock size estimation are drawn as dashed lines for both Norwegian spring-spawning (grey) and Baltic (black) herring.

Averaging the mean TS values for the entire water column gave values for Norwegian spring-spawning herring of -37.2 and -42.0 dB for the minimum and maximum contraction cases, respectively. The equivalent values for Baltic herring were -35.0 and -38.3 dB. The standard depth-independent relationships between TS and fish length (L, in cm), of the form presented in Equation 1.11, obtained from averaged modelling results using typical lengths and depth ranges of both herring stocks and assuming minimum swimbladder compression were:

$$TS = 20 \log_{10}(L) - 67.1 \tag{3.4}$$

for Norwegian spring-spawning herring and

$$TS = 20 \log_{10}(L) - 64.8 \tag{3.5}$$

for Baltic Sea herring. Estimated intercepts in both equations were higher (Norwegian spring-spawning herring: +4.8 dB; Baltic Sea herring: +6.4 dB) than the ones presently used for estimation of the respective stock sizes (Norwegian spring-spawning herring: see e.g. ICES 1988; Baltic herring: see e.g. ICES 1997). Similarly, the length- and depth-dependent TS relationships fitted to the modelled mean TS data for a 32 cm herring, in the format proposed by Ona (2003), were:

$$TS = 20 \log_{10}(L) - 1.9 \log_{10}(1 + z/10) - 65.2 \tag{3.6}$$

for Norwegian spring-spawning herring and

$$TS = 20 \log_{10}(L) - 1.4 \log_{10}(1 + z/10) - 63.6 \tag{3.7}$$

for Baltic Sea herring.

3.3.2.2. Baltic clupeids

Figure 3.7 shows the difference in the modelled TS-L relationships between herring and sprat at 38 kHz. It was assumed that fish occupy the near-surface layer (depth z = 0 m). The different points in the figure represent modelled mean TS data calculated for each of the individual fish samples used. Regression curves of TS versus fish total length (L, in cm) using Equation 1.10 were fitted to the modelled data for Baltic herring and sprat. The results were: TS = 20.08 $\log_{10}$ (L) - 64.07 (s.e. for m = 2.77; s.e. for b = 3.52) for herring and TS = 27.50 $\log_{10}$ (L) - 73.06 (s.e. for m = 2.06; s.e. for b = 2.19) for sprat. Additionally, for each set of data the commonly applied equation TS = 20 $\log_{10}$ (L) + b_{20} was determined (Figure 3.7). The intercept b_{20} was estimated as -63.88 dB (s.e. = 0.19) and -65.08 dB (s.e. = 0.17) for herring and sprat, respectively. Figure 3.7 demonstrates that for fish smaller than about 16 cm the regression equation (Equation 1.10) gives up to 4 dB higher TS for herring than the regression equation for sprat. Including effects of fat content and salinity caused only marginal differences in modelled TS. For both herring and sprat, TS values varied by 0.2 dB over the range of analysed fat contents. TS differed by 0.4 dB for both species over the salinity range analysed.

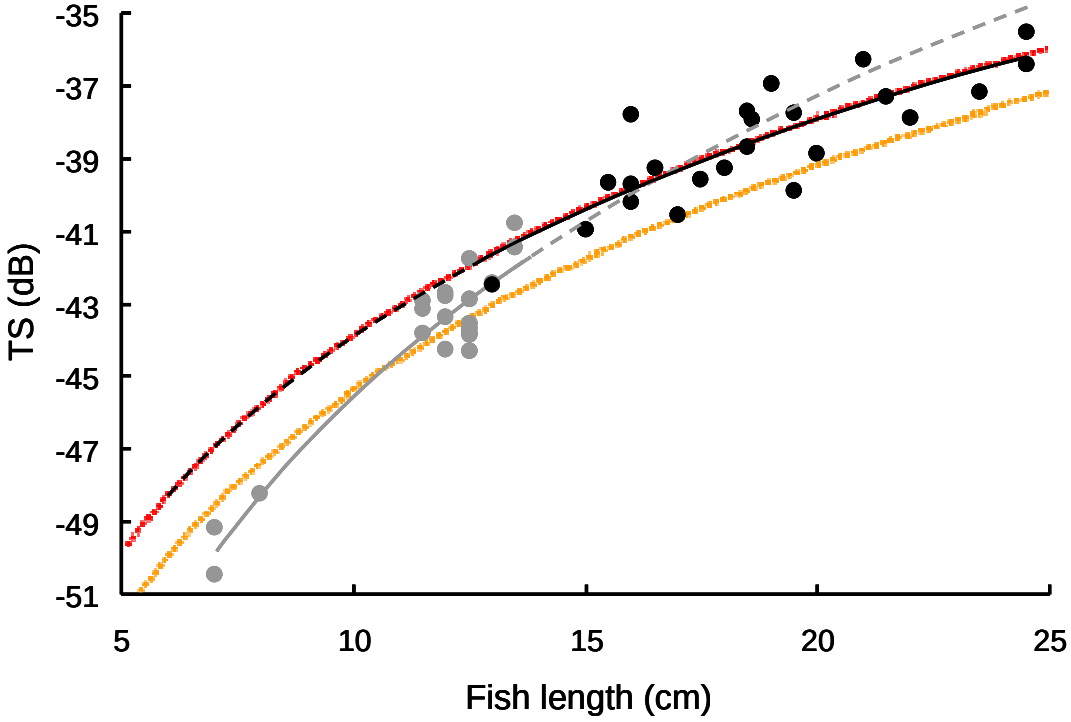

Figure 3.7 Modelled near-surface TS for Baltic herring (black) and sprat (grey) at 38 kHz, based on measured swimbladder morphology. TS-L relationships of the standard form (20 $\log_{10}$ (L) + b_{20}) are fitted to the data for herring (red dotted line) and sprat (orange dotted line).

3.3.2.2.1. Effect of depth

Previous *in situ* (Ona 1990; Ona 2003; Chapter 4, Fässler et al. 2009a) and theoretical modelling (Gorska and Ona 2003a) studies have shown that TS of Atlantic herring may decrease significantly with water depth. Correspondingly, results presented in ICES (2006) also demonstrated that Baltic herring TS decreases with depth and that the depth variability (the difference between maximum and minimum TS over the entire depth range: from 0 to 100 m) depends on fish size. Reported ranges of values were: 1.70 - 2.34 dB at 38 kHz, 1.37 - 2.23 dB at 70 kHz and 0.52 - 1.93 dB at 120 kHz. To understand how fish depth affects the TS-L relationship, two sets of TS data at 38 kHz for depth z = 0 m and z = 100 m were calculated from the herring and sprat morphology data. The regression curves (Equation 1.10) were also fitted to each

dataset. Figure 3.8 demonstrates that there is an approximately 2 dB difference in TS between fish at 0 and 100 m depth for both herring and sprat.

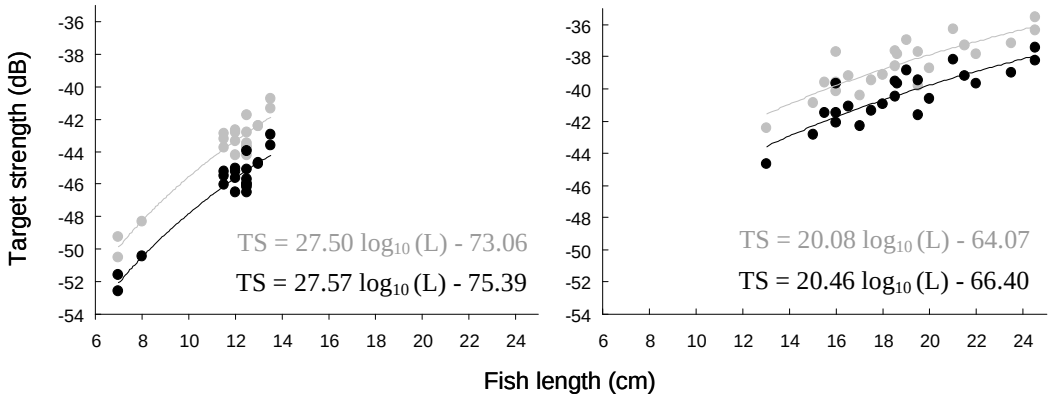

Figure 3.8 Effect of depth on modelled TS for Baltic sprat (left panel) and herring (right panel) at 38 kHz. Values were modelled at depth = 0 m (grey) and 100 m (black). Respective regression equations are given.

3.3.2.2.2. Effect of frequency

To understand the effect of acoustic frequency on herring and sprat TS, the TS-L relationship was fitted to modelled data at the three different frequencies used commonly in acoustic biomass estimation of Baltic clupeids (38, 70 and 120 kHz). Figure 3.9 shows that for both species the slope (m) and intercept (b) of the TS-L relationship (Equation 1.10) is sensitive to acoustic frequency over the considered depth range (0 - 100 m). The difference in TS at 38 and 120 kHz varies with fish length up to 5 dB and 3 dB for herring and sprat, respectively. At 38 and 70 kHz the difference in TS can be up to 2 dB for both species.

Figures 3.9a and 3.9b demonstrate only a slight sensitivity of the TS-difference to the depth of herring, while for sprat a higher depth sensitivity is observed (Figures 3.9c and 3.9d). For example, for 13.5 cm sprat the difference in TS at 38 and 70 kHz is negligible for fish near the surface, whereas this difference is about 1 dB for fish at 100 m depth. Moreover, the difference between sprat TS at 38 and 120 kHz increases from 2 to about 3 dB with increasing depth down to 100 m. These results further

suggest that *in situ* TS data collected for Baltic herring and sprat at 38 and 70 kHz and at various water depths may not be treated as equivalent. Comparing backscatter levels of the two species between frequencies following Equation 2.1 revealed a positive mean ΔdB level for sprat at 70 kHz (Figure 3.10). Herring had a negative mean ΔdB level at 70 kHz. Respective mean values of ΔdB at 200 kHz were negative at about -2.5 for herring and -1.5 for sprat. These results may suggest that there is potential merit in using differences in backscatter at 38 and 70 kHz to distinguish Baltic herring from sprat.

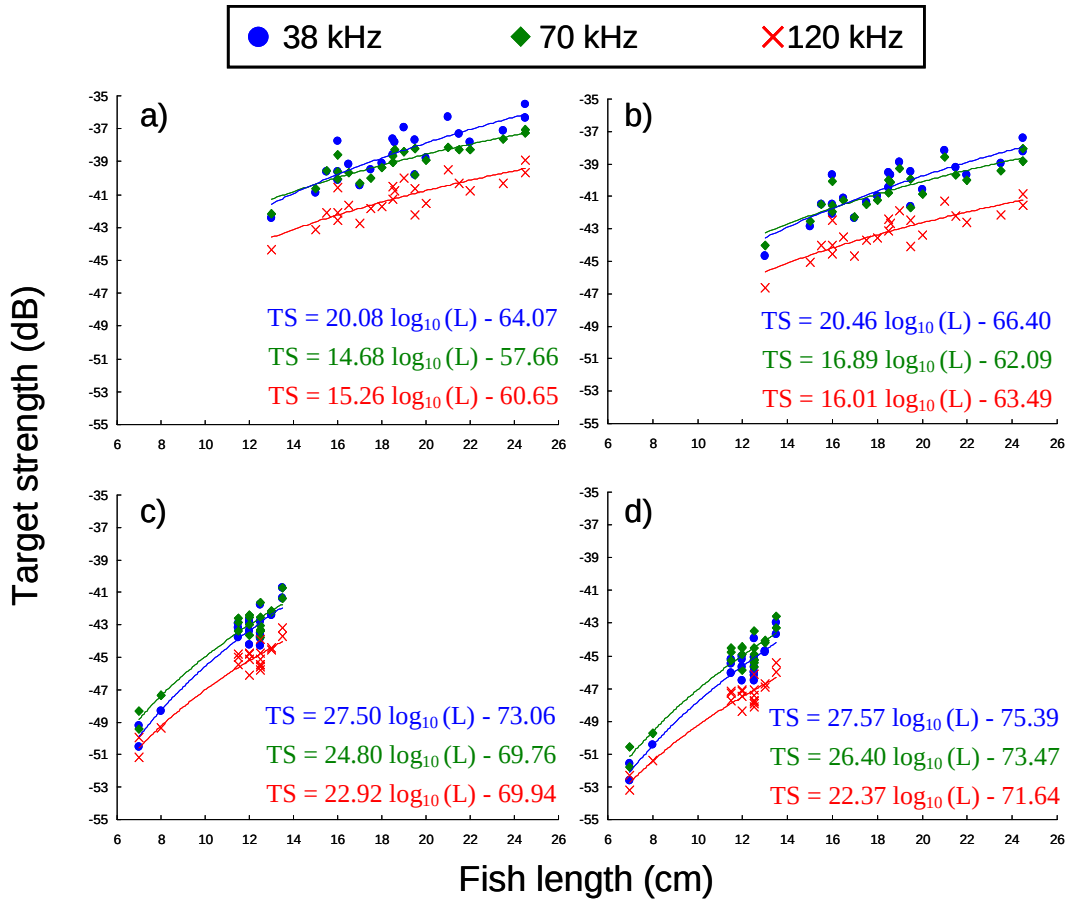

Figure 3.9 Effect of acoustic frequency on modelled TS for Baltic herring (upper panels: a and b) and sprat (lower panels: c and d). Values were calculated for depth = 0 m (left panels: a and c) and 100 m (right panels: b and d). Respective regression equations are given.

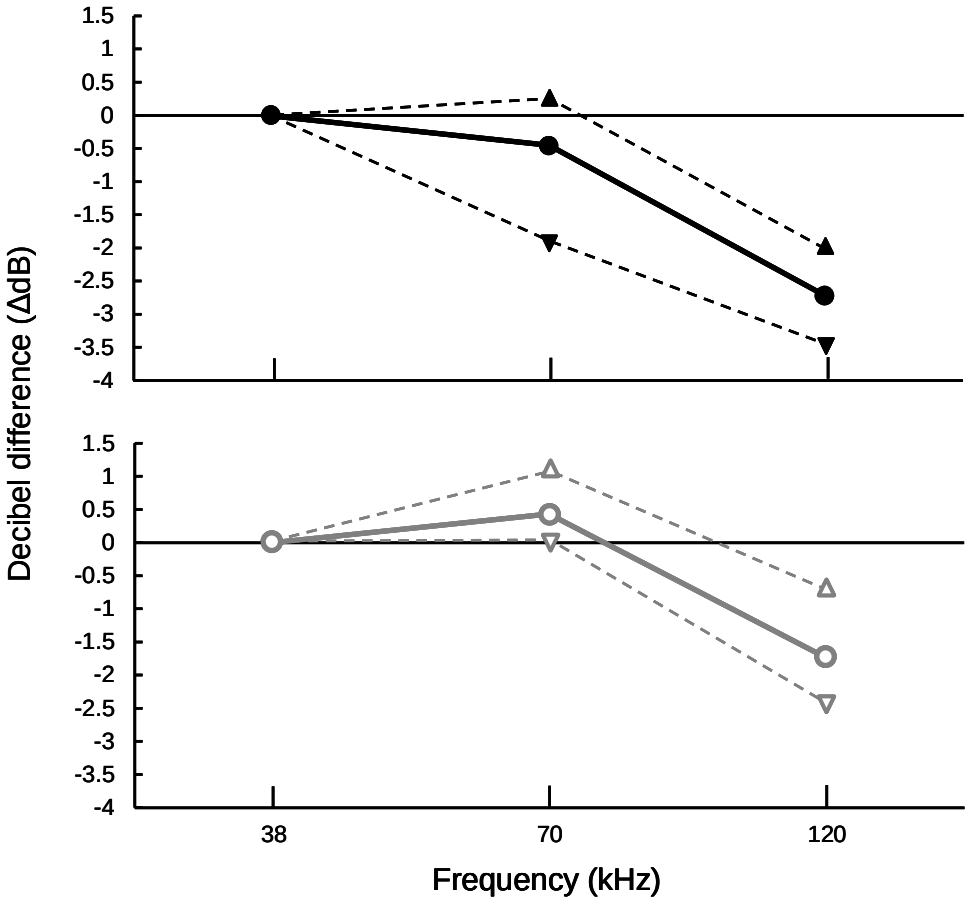

Figure 3.10 Mean (circles), minimum (inverted triangles) and maximum (upright triangles) values of decibel difference relative to 38 kHz for Baltic herring (black) and sprat (gray).

3.3.2.2.3. Effect of orientation

As in previous sections, TS-L relationships (Equation 1.10) were fitted to the modelled TS data of Baltic sprat and herring. However, to investigate the effect of fish orientation on backscatter, different standard deviations of Gaussian fish tilt angle distributions (s.d. = 5º and 10º) were used to calculate average TS values. Figure 3.11 shows the sensitivity of the TS-L relationship to fish orientation at 38 kHz. For herring the difference between average TS between 5º and 10º s.d. of tilt angle distributions increases with increasing fish length from approximately 1 to 2 dB irrespective of water depth. The same phenomenon was observed for sprat, however,

corresponding differences in TS for the smallest fish analysed ranged from 0.3 to 1 dB.

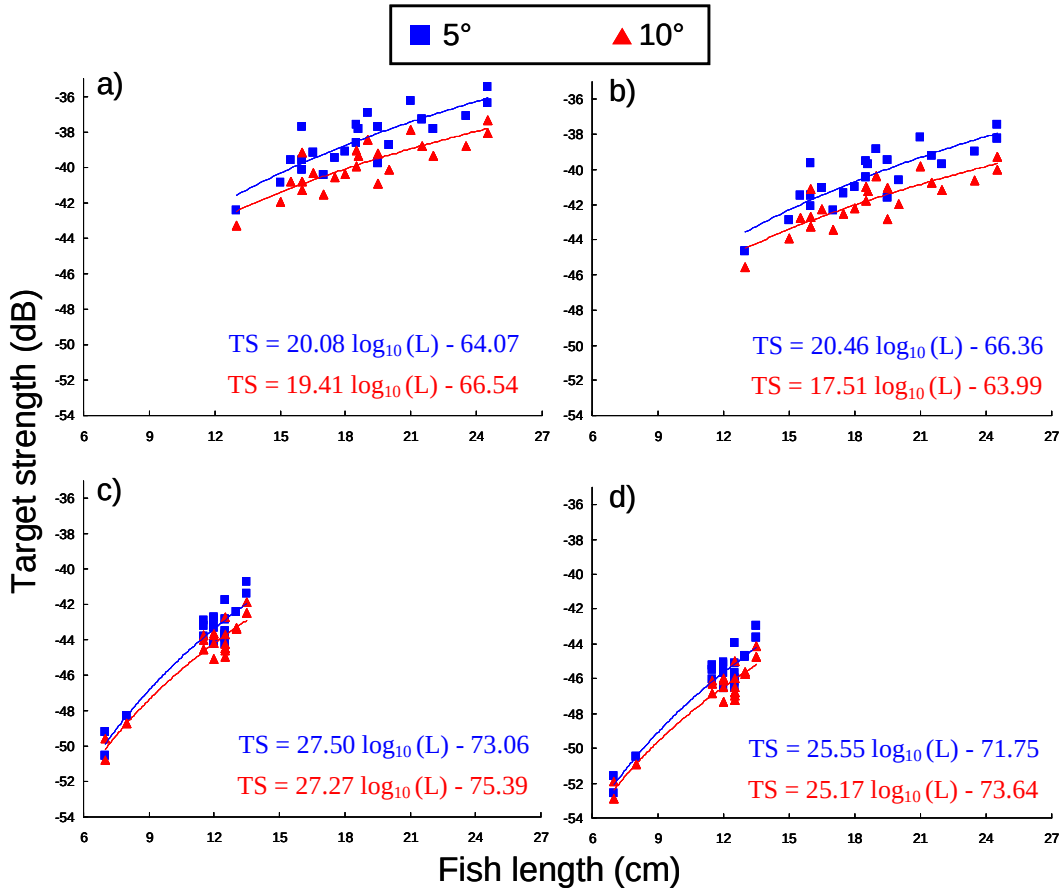

Figure 3.11 Effect of s.d. of fish tilt angle distribution on modelled TS for Baltic herring (upper panels: a and b) and sprat (lower panels: c and d). Values were calculated for depth = 0 m (left panels: a and c) and 100 m (right panels: b and d). Respective regression equations are given.

3.4. Discussion

3.4.1. Intra-species target strength variability: Baltic and Norwegian spring-spawning herring

This Chapter has provided evidence to support the existing assumption that due to the lower salinity in the Baltic Sea and the lower fat content of Baltic herring, these fish require a larger swimbladder volume for a given fish size than do fatter herring living in more saline waters. A larger swimbladder is a more efficient scatterer of acoustic energy at frequencies typically used in acoustic surveys for fish (38, 120 and 200 kHz). At these frequencies and object sizes, backscatter is in the geometric region (Simmonds and MacLennan 2005) and therefore dependent on the surface area of the swimbladder (Horne and Clay 1998). Modelling of the acoustic backscatter based on measured swimbladder volumes revealed higher mean TS for Baltic herring of a given length when compared to Norwegian spring-spawning herring (Figure 3.5). These results may explain the TS values observed in central and northern Baltic herring (Didrikas and Hansson 2004; Peltonen and Balk 2005), which are 3-7 dB higher than those currently applied for both North Sea and Baltic herring. The same principle may apply to freshwater fish (salinity = 0). Warner et al. (2002) measured *in situ* TS of alewives in freshwater and found the corresponding TS-L relationship to be 8 dB higher than the standard relationship for marine clupeids recommended by Foote (1987), based on Atlantic herring. Unfortunately, Warner et al. (2002) did not investigate whether alewife swimbladder volumes were bigger than those of similarly sized marine clupeids. However, a potential link between low salinity, low fat content (9.1% in alewives; Flath and Diana 1985) and hence a larger swimbladder causing the corresponding high TS in alewives is also likely.

Modelled TS values for both Norwegian spring-spawning and Baltic Sea herring at a range of water depths were similar to *in situ* values from Norwegian spring-spawning herring at 38 kHz measured by Ona (2003) (Figure 3.6), although variability was large. In fact, the length-dependent TS equation determined for Norwegian spring-spawning herring (Equation 3.4) is nearly identical to the

equivalent equation (Equation 4) published in Ona (2003), who based his findings on *in situ* values measured at various (5-500 m) depths. Model values determined for Baltic herring (Equation 3.5) are higher (by +3.0 dB) than those proposed by Didrikas and Hansson (2004) at 38 and 70 kHz, and lower (by -0.9 dB) than those determined by Peltonen and Balk (2005) for northern Baltic herring at 38 kHz. Both of these analyses were based on *in situ* TS measurements. Nevertheless, it is generally suggested that both Baltic and Norwegian spring-spawning herring have a higher TS than that used to assess their respective stock. If the TS relationships corresponding to the model values determined here were used to estimate stock sizes, abundance estimates would be lower than if the currently applied solely length-dependent TS relationships are used (i.e. Norwegian spring-spawning herring: $TS = 20\log_{10}(L) - 71.9$; Baltic Sea herring: $TS = 20\log_{10}(L) - 71.2$). If the higher TS values for Baltic herring were correct and applied to estimate the size of the stock, the estimates of Baltic herring biomass from acoustic surveys would be less than half as large.

3.4.2. Inter-species target strength variability: Baltic herring and sprat

The investigation into TS variability among clupeids in the Baltic Sea revealed a contradicting picture to the widespread assumption that the TS-L relationship developed for herring can be used as a 'universal clupeid TS'. If the TS-L relationship $TS = 20\log_{10}(L) - 63.88$ obtained for Baltic herring was applied to estimate sprat abundance, acoustic survey results of sprat biomass would be underestimated by about 30%. On the other hand, if the TS-L relationship $TS = 20\log_{10}(L) - 65.08$ for sprat was used in herring abundance estimation, it would cause an overestimation of herring biomass of about the same percentage. It should be noted that sprat samples used in this study covered the typically observed length range of sprat in the Baltic Sea (ca. 6 - 16 cm). However, this was not true for the herring samples, since lengths of Baltic herring normally range between about 9 and 25 cm (Section 3.2.2.1., Fässler et al. 2008). Small herring were therefore not sufficiently represented in the dataset. To verify whether Baltic herring of lengths below 16 cm may have the same TS-L relationship as sprat, as suggested by

Kasatkina (2009), more herring samples covering the same length range as sprat would have been necessary. Nonetheless, based on the results presented here, it appears as though the TS-L relationship fitted to TS data of Baltic herring of lengths >16 cm should not be used for abundance estimation of Baltic sprat and vice versa.

The b_{20} value determined for Baltic herring based on measurements of swimbladder morphology from X-rays (-63.88; Section 3.3.2.2.) was higher than the one estimated from modelled TS based on swimbladder volumes (-64.8; Section 3.3.2.1.). Nonetheless, these two estimates were essentially based on different types of input data. On the other hand, the comparison between Baltic clupeid TS was done using the same type of morphological dimension data, allowing a valid qualitative comparison between model outputs for the two species.

Observed differences in TS between herring larger than 16 cm and sprat may be explained by the different morphologies of these two species. As demonstrated in Figures 3.3 and 3.4, the width and height of the Baltic herring swimbladder are on average larger than the width and height of the sprat swimbladder for fish of the same length. This means that the insonified dorsal swimbladder area and swimbladder volume, which influence the backscatter of the fish at different ka_{ps} (k is the wave number and a_{ps} is the swimbladder radius defined in Equation 2.10), are larger for herring than for sprat. The result is a higher TS for herring than sprat of a given length. The larger slope of the regression line fitted to the modelled Baltic sprat TS data may further suggest that the quadratic dependence of TS on fish length does not hold for this species (Figure 3.7; McClatchie et al. 1996). While the curve fitted to the Baltic herring TS data was only marginally different from the one with a fixed slope of 20, there were considerable differences between the respective curves fitted to the Baltic sprat TS data (Figure 3.7). Observed differences in swimbladder growth pattern between the herring and sprat samples (Figure 3.3) would imply that either a shape correction (e.g. McClatchie et al. 2003) or a different TS-L relationship for each species is necessary.

The evaluation of the differences between the regression curves fitted to the TS data (Figure 3.7) may explain the large variability (up to 8 dB) of herring TS

measured in different parts and seasons in the Baltic Sea (Lassen and Stæhr 1985; Rudstam et al. 1988, 1999; Didrikas and Hansson 2004; Didrikas 2005; Peltonen and Balk 2005; Kasatkina 2009). As previously mentioned, *in situ* TS data of Baltic herring and sprat gathered so far were collected and analysed in different ways: some authors collected *in situ* TS data by insonifying single species aggregations of sprat and herring (Peltonen and Balk 2005; Kasatkina 2009), while others (Didrikas and Hansson 2004; Didrikas 2005) did not make a distinction between those two species and insonified mixed species aggregations. A previous investigation that evaluated the effects of treating herring and sprat in the Baltic Sea as 'acoustically identical' suggests that care should be taken when using a TS-L relationship obtained for one species in abundance estimation of other or mixed aggregations of clupeids (Kasatkina 2007; Kasatkina 2009). Parameters of TS-L relationships for these two species of fish will be dependent on the length range observed (Kasatkina 2009). The study described in this Chapter, based on morphological data, demonstrated a 1.2 dB difference between the intercept parameter (b_{20}) of the TS-L relationships for Baltic herring and sprat. These results are in accordance with empirical observations made by Kasatkina (2009), who found the mean b_{20} value of Baltic sprat to be lower (by 4.35 dB) than that of herring. Following results presented in Section 3.3.2.1., estimated intercepts (b_{20}) of modelled TS data, based on morphological dimensions of both herring (-63.88 dB) and sprat (-65.08 dB), were higher than that determined for North Sea herring (-71.2 dB; see ICES 1982), presently used to estimate stock sizes of Baltic clupeids. This is in agreement with recent *in situ* TS measurements, suggesting that both Baltic sprat and herring may have higher TS values than those presently applied to estimate their stock sizes (Didrikas and Hansson 2004; Peltonen and Balk 2005; Section 3.3.2.1., Fässler et al. 2008; Kasatkina 2009).

Results shown here have indicated that, in order to obtain accurate TS-L relationships for Baltic clupeids, it is important to conduct controlled TS measurements, and additionally collect data on environmental parameters (water temperature, salinity and depth of measured fish layer), morphology (fat content) and behaviour (orientation pattern) of the fish. The TS modelling results have shown that

there may be considerable discrepancies in TS measurements of fish at different depths. Additionally, variations in tilt angle distributions and the applied acoustic frequency were also identified as potentially interacting factors that may reveal significant discrepancies in measured TS, depending on the size of the fish studied. Unlike identified in the investigation into TS differences between Baltic and Norwegian spring-spawning herring, fat content and salinity were not identified as critical parameters affecting clupeid TS variability within the Baltic Sea. Backscatter models of Baltic herring and sprat may be improved with the help of more accurate biological data, and subsequently be used to examine backscatter characteristics of fish from various locations and at different times in the Baltic Sea.

It should be noted that the model used in the present study was based on a highly simplified approximation of fish swimbladder and body shapes. Factors such as the depth-dependence of the swimbladder shape may have considerable effects on the outcome of modelled TS values. It has been shown previously that the change in acoustic backscatter of herring with depth is dependent on the dorsal cross-section of the swimbladder rather than its volume (Ona 1990). Additionally, it is also more likely that the swimbladder diameter reduces more rapidly with depth than does the length (Gorska and Ona 2003a; Chapter 4, Fässler et al. 2009a). Given these facts, improved knowledge about the true depth-dependent morphology of the swimbladder is needed to enable the use of more sophisticated backscattering models. Therefore, precise measurements of the actual swimbladder size and dimensions (e.g. using X-ray or MRI techniques) made at a range of water pressures will provide a better understanding of the mechanics of depth-dependent swimbladder compression (see Chapter 4). Improved, fully three-dimensional backscatter modelling, using techniques such as the Kirchhoff-ray mode (KRM; Clay and Horne 1994) could then be used together with actual morphological swimbladder dimensions to approximate the expected TS (Chapter 4) and examine effects of depth-dependence on abundance estimates more accurately (Chapter 5).

Chapter 4

Depth-dependent swimbladder compression in Atlantic herring (*Clupea harengus*)

Part of the work described here has been published as:
Fässler, S.M.M., Fernandes, P.G., Semple, S.I.K., Brierley, A.S. (2009). Depth-dependent swimbladder compression in herring *Clupea harengus* observed using magnetic resonance imaging. Journal of Fish Biology 74: 296-303.

4.1. Introduction

Target strength (TS) of fish is primarily dependent on the size and morphology of the fish, the acoustic frequency used (the echosounder frequency), and the orientation of the fish in the water (Nakken and Olsen 1977; Blaxter and Batty 1990; Ona 1990). For fish with a gas-filled swimbladder, the swimbladder can be responsible for up to 90 - 95% of the backscattered sound intensity at frequencies used for surveys (Foote 1980a). Consequently, for such fish, understanding the structural morphology of the swimbladder and its variation with fish behaviour is particularly important for understanding and modelling TS and its variability.

The herring is a physostome and, as such, its swimbladder is not closed but connected to the anal opening and to the alimentary canal via a valved pneumatic duct (see Figure 4.1; Blaxter et al. 1979). Unlike physoclists, most physostomes have

no known mechanisms, such as a gas gland, with which to adjust the volume of their swimbladder actively. The present hypothesis for herring is that they are only able to inflate their swimbladders by “gulping” atmospheric air at the sea surface (Brawn 1962; Blaxter et al. 1979; Ona 1990). Thus, once a herring has left the sea surface, the volume of its swimbladder will decrease with increasing ambient pressure at greater water depths (Blaxter and Hunter 1982). Since TS at common survey frequencies is primarily a function of swimbladder size, the TS in herring and other physostomes is likely to be dependent to some extent on the depth of the fish (Edwards and Armstrong 1984; Ona 1990; Mukai and Iida 1996).

At frequencies typically used in herring surveys (18, 38, 120 and 200 kHz), the acoustic backscattering of the swimbladder is in the geometric scattering region (Simmonds and MacLennan 2005), where backscatter is expected to be proportional to the dorsal cross-sectional surface area of the scattering body (Ona 1990; Horne and Clay 1998). Consequently, it is important to know how this particular dimension of the swimbladder changes with depth in order to assess potential effects of depth on herring TS and ultimately biomass estimates.

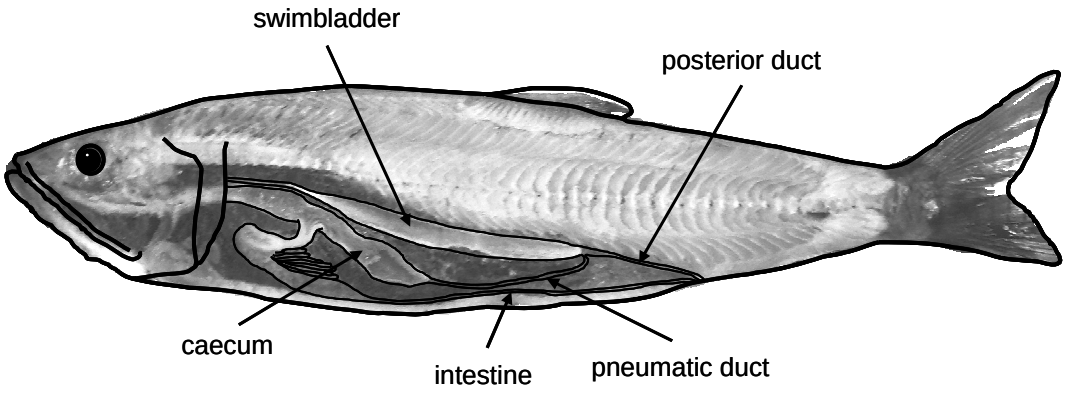

Figure 4.1 Schematic view of the swimbladder and alimentary canal superimposed on a cross-section of a herring from the North Sea. The caecum forms the posterior part of the stomach and is connected to the swimbladder via a thin pneumatic duct.

In an in vitro experiment, Blaxter et al. (1979) showed that the different dimensions of the herring swimbladder do not compress isometrically with increasing ambient pressure. They observed that the vertical axis of the swimbladder was most affected by an increase in pressure, and that the length of the swimbladder changed more slowly than its height. As a result, Blaxter et al. (1979) suggested that as pressure changed the swimbladder would not contract concentrically, but would adopt the shape of a flat ellipse. The invasive experimental technique applied by Blaxter et al. (1979) may, however, have led to misleading results: in order to observe changes in swimbladder shape with pressure, fish had to be dissected to expose the swimbladder. The results of Blaxter et al. (1979) were, therefore, effectively based on observations of partly exposed swimbladders, which may have behaved differently than if they had been fully surrounded by tissue. Gorska and Ona (2003a) compared empirical observations of herring TS at various water depths with results of models that applied different swimbladder contraction-rates. The spheroid model they used led them to conclude that the swimbladder must contract in a way where the length-contraction is less than the width-contraction, but they could not quantify the difference. Moreover, recent *in situ* work has provided further evidence that the model used by Gorska and Ona (2003a) may not have been adequate to describe the depth-dependence of herring TS (Pedersen et al. 2009)

In Chapters 2 and 3 of this thesis, I have shown that the use of simple geometric shapes to represent fish sound scattering bodies in models may be inadequate to explain certain backscattering features. More elaborate backscattering models such as the Kirchhoff-ray mode (KRM) or boundary element method (BEM) can compute the TS of arbitrarily shaped bodies such as the true shapes of the fish and its internal organs (Horne and Jech 1999; Horne et al. 2000; Francis and Foote 2003; Peña and Foote 2008). Radiographic techniques have been used extensively to extract shapes of swimbladders for use in acoustic backscattering models (Clay and Horne 1994; Horne and Jech, 1999; Macaulay 2002; Hazen and Horne 2003; Gauthier and Horne 2004b Reeder et al. 2004; Peña and Foote 2008). These techniques are non-invasive and can deliver high-resolution representations of the swimbladder and other

important scattering structures (e.g. vertebral column, bones or gas-filled organs). To date, such examinations have mostly been made on physoclists, where pressure effects are less important, since swimbladder volumes may well remain constant throughout the water column (but see Horne et al. 2009 for an exception). This Chapter aims to examine changes in true, three-dimensional swimbladder morphology of Atlantic herring with pressure. Magnetic resonance imaging (MRI) was applied to observe swimbladders of dead fish in a purpose-built pressure chamber at various simulated water pressures down to an equivalent depth of 60 m. High-resolution three-dimensional shapes of the herring swimbladders were reconstructed from the MRI data and subsequently used to compute tilt angle averaged TS by applying the KRM backscattering model ('model III', see Chapter 2).

4.2. Methods

4.2.1. Fish samples and pressure chamber

North Sea herring were caught in the northern North Sea during the 2007 herring acoustic survey using a PT160 pelagic trawl at depths between 77-165 m (ICES, 2008b). The herring were euthanized using benzocaine straight after the trawl was hauled on board and then frozen. One suitable specimen (length = 25.0 cm) was selected after X-ray examination to ensure that the swimbladder and other internal organs were intact. Norwegian spring-spawning herring were collected from the Matre facilities of the Institute of Marine Research (IMR, Matre Aquaculture Research Station, 5984 Matredal, Norway). These herring had been reared in tank facilities and were, therefore, assumed to be adapted to surface water pressures. The specimens (n = 7) were transferred individually with a small net from a circular holding tank (height = 1.5 m, radius = 2 m) to a 120 l plastic container (height = 40 cm, length = 60 cm, width = 50 cm) containing sea water and an overdose of MS222 anaesthetic (200 mg l^{-1}). After the fish were euthanized, the anal opening was sealed with Superglue and a piece of plaster to prevent any gas potentially escaping from the swimbladder. Afterwards the herring were kept chilled on ice and transported for 2 h to IMR in Bergen where they were frozen to -20ºC. All herring samples were

defrosted in a cooler box for 12 h before being subject to a range of water pressures (1 - 7 bar) using a purpose built, MRI compatible (built using only non-ferrous components) Perspex pressure chamber (Figure 4.2).

The pressure chamber essentially consisted of a Perspex cylinder with end-caps made of brass. Air could be pumped under pressure into a small compartment at one end of the chamber. This compartment was separated from the water-filled main section of the chamber by an elastic rubber membrane. Increasing air pressure hence increased the water pressure within the chamber. A perforated screw in the lid enabled the chamber to be filled with water and air to escape preventing the formation of air bubbles inside. The pressure chamber was connected to the air source via a 10 m long plastic tube and a control board that enabled air pressure to be adjusted and measured (see Figure 4.3). For safety reasons, and mainly due to the fact that they contained ferromagnetic materials that could be attracted by the force field of the MR scanner, all other components of the system had to be kept outside the scanner room while the magnet was switched on. During scans, the pressure chamber was therefore connected to the pressure source and control board via the 10 m plastic tube that was fed through a hole in the MR scanner room wall.

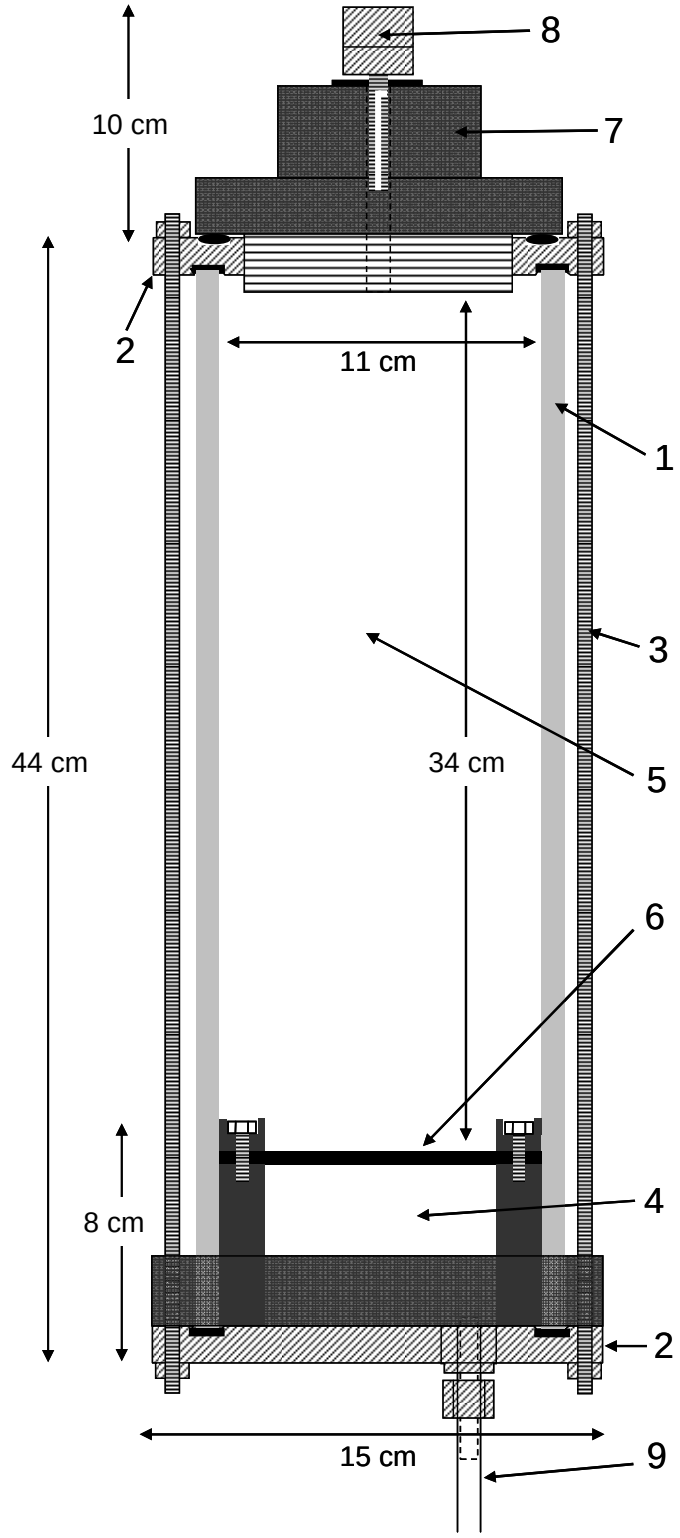

Figure 4.2 (Caption on following page)

← Figure 4.2 Diagram of the chamber used to expose herring to various water pressures (maximum total [atmospheric + water] pressure = 7 bar) inside an MRI scanner. The chamber consisted of a Perspex (thickness = 1 cm) cylinder (1) with end caps on either side (2) connected by screw rods (3). The air-filled compartment (4) was separated from the water-filled compartment (5) by an elastic rubber membrane (6). The screw-top lid (7) and perforated screw (8) enabled closure of the chamber without the retention of air bubbles. Pressurised air was supplied from an external pump via a tube (9) (length = 10 m). Plastic parts are shown in shades of dark grey, brass parts are hatched.

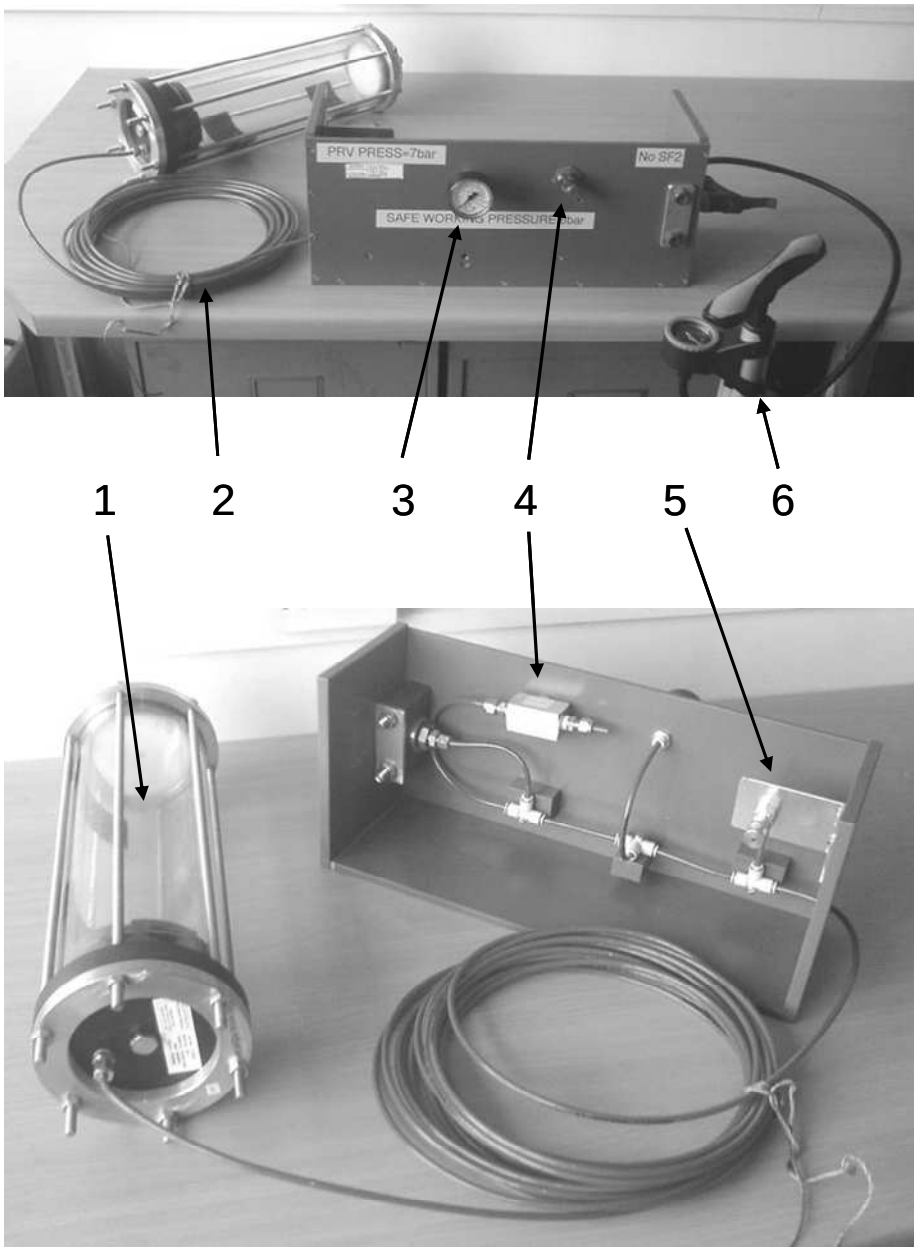

Figure 4.3 Apparatus that enabled pressure inside the chamber (1) to be varied. A 10 m plastic tube (2) ran from a pump (6) kept outside the MRI scanner room. The control board included a pressure gauge (3) and a control valve (4). A pressure release valve (PRV; 5) ensured that the air pressure inside the chamber never exceeded the maximum test pressure value of 7 bar. The air pressure was increased by use of an ordinary foot pump (6).

4.2.2. Magnetic resonance imaging

4.2.2.1. North Sea herring: Scan 1 (Aberdeen, UK)

MRI techniques work by aligning nuclear spins of protons in hydrogen atoms along the direction of a strong magnetic field. Radiofrequency pulses are then introduced into the imaging system to excite these protons, giving them enough energy to move away from their alignment with the magnetic field. Once the radiofrequency pulse is switched off, the protons relax back and align with the magnetic field again. In doing so, the protons give off energy at particular resonant frequencies, which the MR system detects. The resonant frequencies of the protons depend on the main magnetic field and vary with magnetic gradients applied. This gives spatial information of these frequencies across the imaging field of view to build up a 3D MRI dataset of images. The relaxation rate of the protons back to equilibrium is governed by various factors which reflect the local chemical environment and hydrogen concentration. Therefore, different tissues have different 'MR contrast' due to their chemical makeup and concentration.

The North Sea herring sample was scanned using a Philips 3-tesla Achieva X-Series scanner (Philips Medical, Best, Netherlands) at the Aberdeen University Department of Radiology (Lilian Sutton Building, Foresterhill, Aberdeen, Scotland, UK) in a chamber, the chamber was filled with fresh water. It was then secured with foam pads and Velcro straps in the 16 channel neurovascular array coil: the securing was to prevent movement of the chamber within the coil during image acquisition (Figure 4.4). After an initial survey scan was acquired for positioning of subsequent scans, a T2-weighted spin-echo utilising a homogeneity filter (called CLEAR, Philips Medical) was used to acquire high-resolution scans of the swimbladder in the sagittal plane. Image acquisition parameters are given in Table 4.1, and were set to maximise image resolution and obtain all required scan sequences within the available 3 hour time slot. During protocol development, spin-echo sequences were acquired using SENSE (Pruessmann et al. 1999) in an attempt to cut down the acquisition time, but it was observed that the brass components of the pressure tank interfered with the

SENSE sensitivity map, resulting in severe image artefacts. Subsequently, all spin-echo scans used in this study were acquired without SENSE, or any other speed-up factor. The herring was scanned at discrete water pressures (1 - 7 bar) corresponding to 0, 10, 20, 40, and 60 m depth. The choice of the water pressures reflects the fact that volume reduction of gas-filled elastic objects is greatest over these near-surface depths (e.g. ~85% reduction in volume from 0 - 60 m; only a further 4% reduction to 100 m). At the end of the series of increasing pressures a repeat scan was made at the lowest pressure in an attempt to determine if any gas had been lost out of the swimbladder over the course of the experiment.

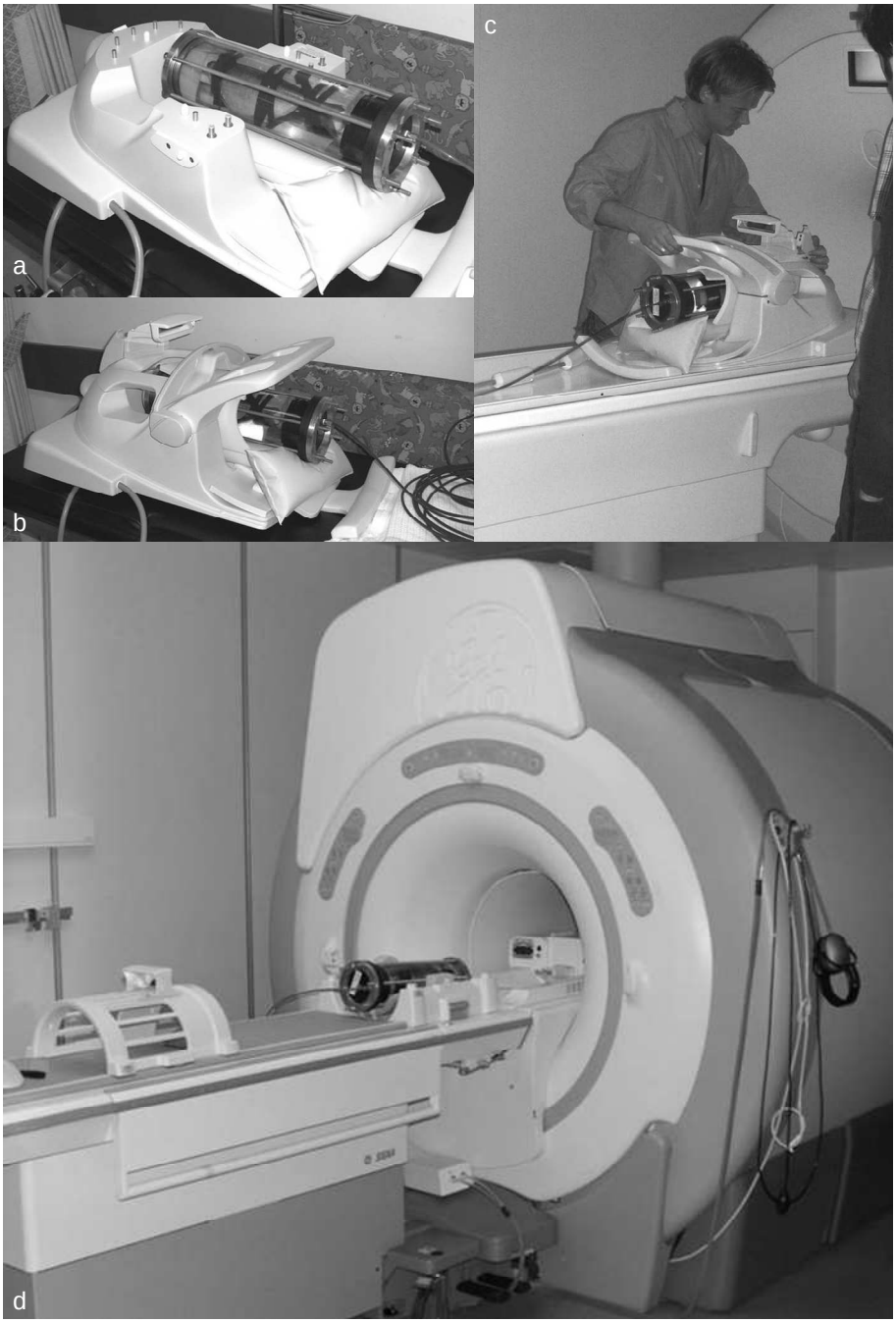

Figure 4.4 Photographs of the herring sample inside the water filled pressure chamber on the lower part of the neurovascular array MRI coil (a). The chamber was secured with foam pads inside the closed coil (b) and then placed inside the MRI scanner (c). (d) shows the pressure chamber on the lower part of the head coil used during 'Scan 2', at the entrance of the MRI scanner just before commencement of a scanning sequence.

Table 4.1 Settings used for MRI acquisition in Scan 1 (Aberdeen, UK) and Scan 2 (Bergen, Norway).

MRI attribute	Scan 1	Scan 2
Pixel size (mm)	0.5	1.0
Slice thickness (mm)	1.0	1.0
Samples per pixel	1	1
Acquisition type	2D	3D
Repetition time (ms)	1000.0	6.8
Echo time (ms)	50.000	1.936
Acquisition time (min:sec)	17:08	12:47
Space between slices (mm)	1.0	0
Number of slices	30	256
Number of averages	4	1
Percentage phase FOV	80	100
Image rows x columns	320 x 320	256 x 256

4.2.2.2. Norwegian spring-spawning herring: Scan 2 (Bergen, NO)

A second MRI scan series was performed on the Norwegian spring-spawning herring samples at the Haukeland University Hospital in Bergen, Norway on the 8th, 9th and 12th December 2007. The scanner used was a whole-body 3-tesla General Electric Signa Excite scanner (GE Medical Systems, Milwaukee, WI, USA). The water-filled pressure chamber containing the fish was stabilised with pads inside a head coil (Figure 4.4d). In order to optimise the compromise between spatial imaging resolution and size of the imaging region (see Peña and Foote 2008), while completing all scans of the 7 herring samples within the time available, scanning parameters given in Table 4.1 were chosen. In contrast to ‘Scan 1’ (Section 4.2.2.1) swimbladder scans were acquired in the axial plane. Even though more slices were needed (256 slices c.f. 30 slices in the sagittal direction; Table 4.1), scanning time per fish could still be reduced by compromising the image resolution slightly. During the

axial scanning sequences of ‘Scan 2’ no space remained between scan slices, resulting in contiguous images without need for interpolation. All herring were scanned at water pressures corresponding to 0, 20, 40, and 60 m depth, i.e. one pressure step less compared to ‘Scan 1’, resulting in a total of 28 scan series and 7168 individual slices. Digital images of each slice were generated in both ‘Scan 1’ and ‘Scan 2’ series and exported from the respective scanners in the Digital Imaging and Communications Medicine (DICOM) file format.

4.2.3. Swimbladder reconstruction

An image processing and programming routine was developed using MATLAB (version 7.0; The MathWorks Inc., MA, USA) with the Image Processing Toolbox™ to reconstruct 3-D representations of the swimbladders from the MR image slices. The high image contrast between the gas-filled swimbladder and surrounding tissue enabled accurate assessment of the swimbladder boundaries. The MATLAB routine (see Figure 4.5) allowed the boundaries of the swimbladder to be defined on every slice of each scanning series by applying a threshold value to accept all the grey scale values corresponding to the darker pixels characteristic of the gas-filled bladder. Since the threshold value was set based on a subjective evaluation of the grey scale contrast between pixels associated with the swimbladder and surrounding tissue, the routine enabled the threshold to be altered from slice to slice if necessary. In that way, an acceptable threshold was defined that resulted in the swimbladder pixels forming a continuous shape. All pixels corresponding to grey scale values equal to or lower than the selected threshold appeared on a ‘selection window’ where they were manually selected (Figure 4.6). The swimbladder was then built up from its individual cross-sections on all individual image slices of the combined sequence. Since the pixel resolution and slice thickness was known, the swimbladder volume was calculated by adding all single voxels that made up the swimbladder. Similarly, the dorsal cross-sectional surface area of the swimbladder was defined as the area covered by pixels of all dorsal aspect swimbladder slices superimposed on each other. The swimbladder trace quality was improved by applying the ‘smooth3’ 3-D object smoothing function

with a Gaussian convolution kernel in the MATLAB routine. A 3-D object corresponding to the smoothed swimbladder was then created using the ‘patch’ function, and a mesh defining the surface was reconstructed based on the x, y, and z coordinates of the object boundaries.

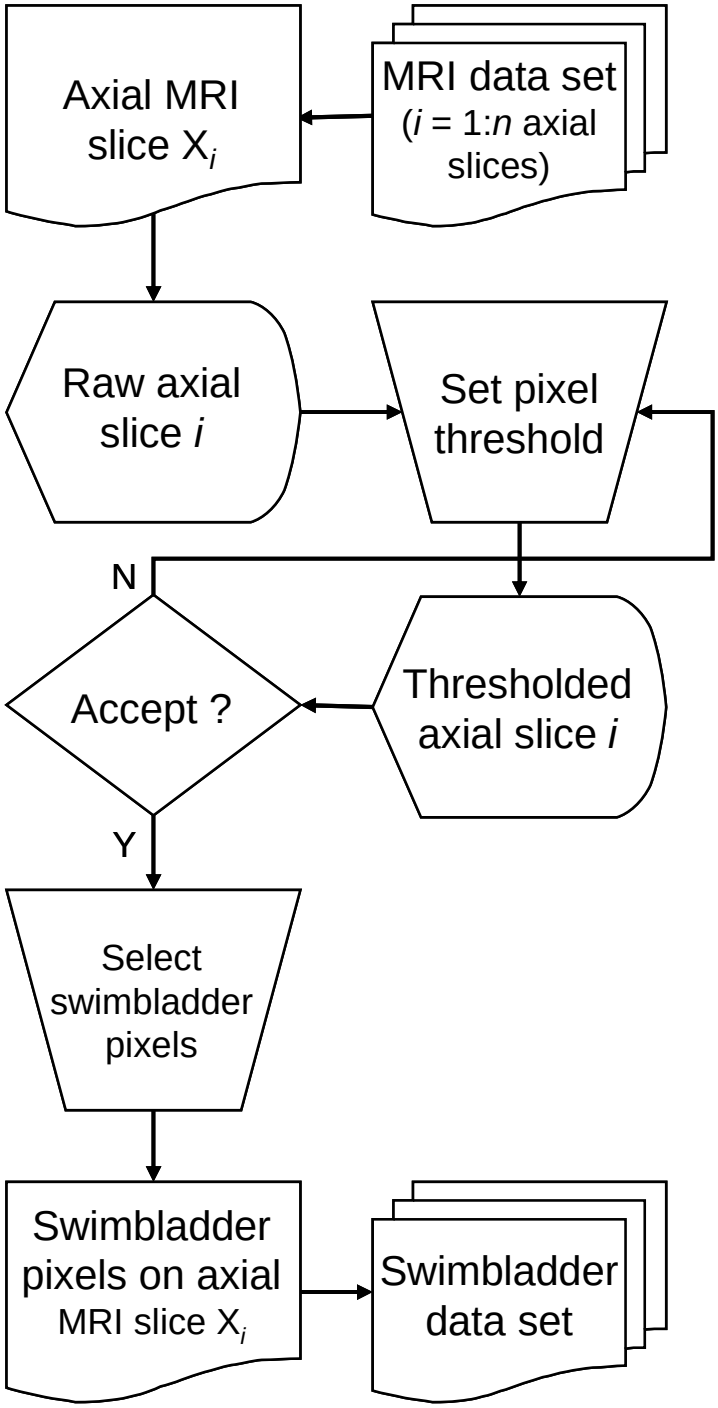

Figure 4.5 Flowchart illustrating the routine developed in MATLAB to extract swimbladder pixels from individual axial MRI slices and to eventually rebuild the swimbladder shape in 3-D.

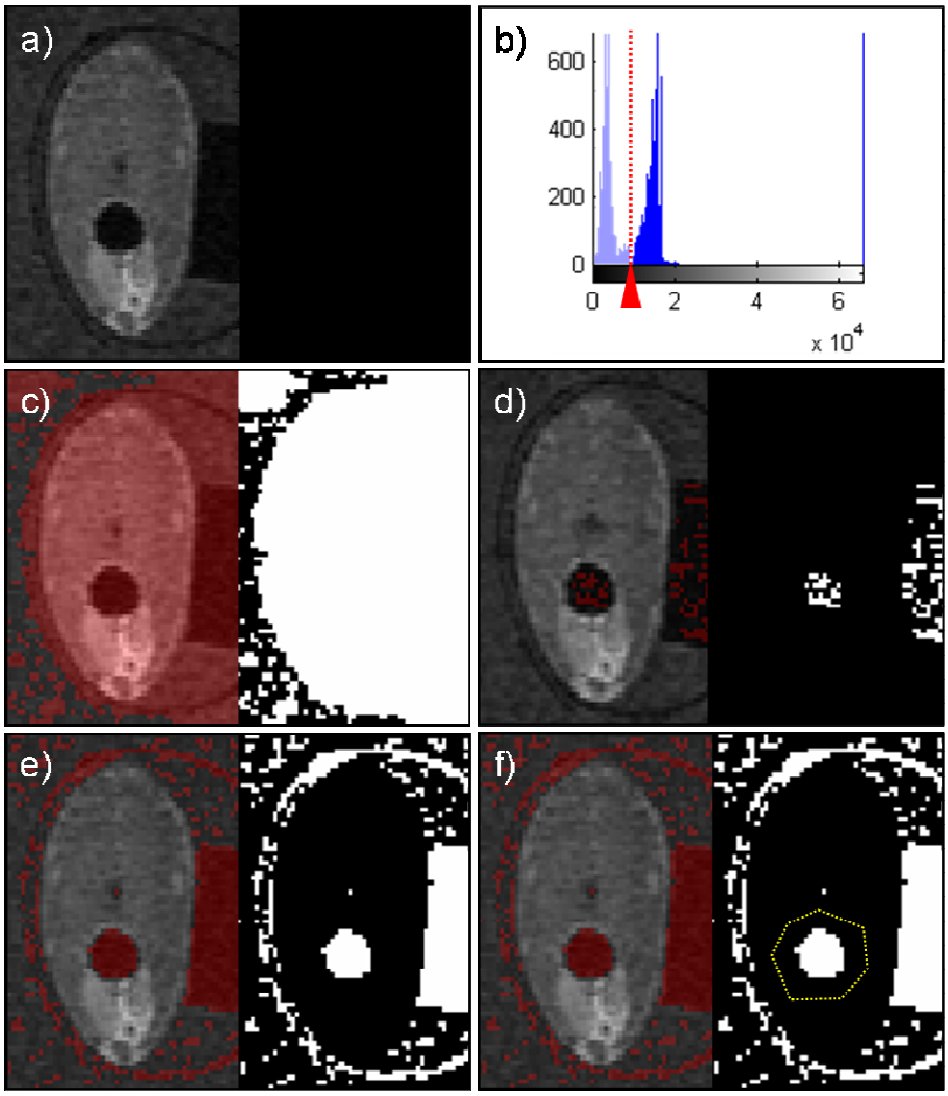

Figure 4.6 Screen shots from the routine developed in MATLAB to extract the swimbladder shape in 3-D from individual axial MRI slices. (a, left panel): Example of an axial MRI slice of herring #2 at a pressure of 1 bar. At this stage, no pixels have yet been allocated to the swimbladder, producing only black pixels in the 'selection window' (a, right panel). (b): Histogram of pixel grey scale values (0 to 65,535) from the MRI slice with the set threshold indicated by the red triangle and dotted line. (c): threshold set too high. Pixels corresponding to values below the set threshold are superimposed in red colour on the MRI slice (c, left panel) and given as white pixels in the 'selection window' (c, right panel). (d): threshold set too low. (e): acceptable threshold value resulting in the swimbladder pixels forming a homogenous object in the 'selection window' (e, right panel) that can be manually selected (f).

4.2.4. Target strength modelling

The theoretical acoustic backscattering of the herring was modelled using the 3-D swimbladder shapes by applying the Kirchhoff ray-mode approximation (KRM) described previously as 'model III' in Chapter 2 (Clay and Horne 1994; see Section 2.2.5.6. for details of the model). The model essentially approximated the scattering objects as a series of 1 mm long elliptical cylinders. The backscattering cross-section of each object was then expressed as a function of size, frequency and fish orientation relative to the transducer by summing backscattering cross-sections of all individual cylinder components. The fish body was represented as a set of fluid-filled cylinders surrounding the gas-filled cylinder sections of the swimbladder. Total fish backscatter was eventually calculated as the coherent sum of backscattering-cross sections of both swimbladder and fish body according to Equation 2.4. Since the MRI scans focused on the swimbladders, true shapes of the fish body could not be traced and reconstructed from the scanning slices. Instead, fish body dimensions were traced from the silhouettes of lateral and dorsal aspect digital images of herring #43 and linearly scaled as a function of length for use with the other individual herring. Individual cylinder components of the fish body and swimbladder were generated based on the height and width of the respective scattering bodies along the axis directions from the snout to the tip of the caudal peduncle (Horne et al. 2000). The swimbladder was assumed to be gas-filled with a density of 1.3 kg m^{-3} (Brawn 1969), while the fish body component was assumed to be fluid-filled with a slightly higher density (1049 kg m^{-3}, Section 3.2.1.1.; Fässler et al. 2008) than the surrounding sea water (1027 kg m^{-3}, Section 2.2.5.6.). Speed of sound in sea water, fish body and swimbladder were 1500, 1570, and 340 m s^{-1}, respectively.

Mean TS values were predicted for each individual herring specimen as a function of fish length and frequency by averaging 100,000 samples of modelled backscatter values applying tilt angle distributions with mean 0º (i.e. broadside dorsal aspect) and standard deviations used commonly for herring of 5º (Gorska and Ona 2003a; Fässler et al. 2008) and 10º (Ona et al.2001; Fässler et al.2007). All estimates were first averaged in the linear domain before being transformed logarithmically.

Standard length-dependent TS relationships were derived by fitting a linear regression to the modelled mean TS at 38 kHz to determine the value of the intercept. In order to compare results between the different herring used in this study to an extensive *in situ* TS data set collected by Ona (2003) for 32 cm herring, TS values for all specimens considered here were also scaled linearly to a common fish length of 32 cm. Consequently, length- and depth-dependent TS relationships were determined at 38 kHz from the model values of the size standardised herring specimens.

4.3. Results

4.3.1. Swimbladder compression with depth

Of the 19 Norwegian spring-spawning herring collected from the Matre facilities, 7 were selected for MRI scanning based on criteria such as MRI scanner time availability, length range coverage (29.5 - 36 cm, Table 4.2) and the fact that some exhibited gas venting from the anal opening during the euthanizing process. The one specimen selected out of the 96 herring collected from the North Sea was deemed to have a 'normal' swimbladder. The judgment about 'normal' swimbladder shape was based on the relative swimbladder proportion of the whole fish volume assuming a mean fish density of 1.049 g cm^{-3} (see Section 3.2.1.1.), comparison to X-ray images of Baltic herring (N. Håkansson, F. Arrhenius, B. Lundgren, pers. comm.; see Chapter 3), lateral cross-sections of 40 frozen North Sea herring (also described in Section 2.2.5.5.) and published images of herring X-rays (Gauthier and Horne 2004b). Total length of the 8 herring specimens used for MRI scans in this Chapter ranged from 25 to 36 cm and the weight from 130 to 345 g (Table 4.2).

MRI scans of the herring showed a clear reduction of swimbladder height with increasing water pressure (Figure 4.7 and 4.8). This reduction appeared to involve a collapse of the ventral region of the swimbladder while the dorsal surface did not alter considerably in position or extent (Figure 4.7). The result was a change from a near-circular cross-sectional swimbladder shape in the axial aspect at low pressure to a more half-moon shaped cross-section at progressively higher pressures, with a convex dorsal and concave ventral surface.

It appeared that there were different inclination angles along the swimbladder dorsal surface relative to the fish axis similar to those observed in Chilean jack mackerel (Peña and Foote 2008). The difference between swimbladder dorsal surface inclination angles along the swimbladder became larger with increasing water pressures, with the anterior swimbladder section having a steeper angle relative to the fish body axis compared to the posterior section (Figure 4.7 and 4.8).

Due to the larger lengths of the Norwegian spring-spawning herring (fish #2 - #11; Table 4.2) compared to the single North Sea herring specimen (fish #43), there were considerable MR image artefacts in the Norwegian spring-spawning herring at their anterior ends caused by the close proximity to the air filled compartment of the pressure chamber. Overall, pixels had lighter shades of grey towards the head region of the fish (Figure 4.7). This phenomenon was overcome by the ability of the MATLAB routine to apply a specific pixel grey scale threshold on respective MR image slices in order to define pixels belonging to the gas-filled swimbladder.

Table 4.2 Biological features of 8 herring subject to water pressures (P) ranging from 1 - 7 bar. Total lengths (L) are given in cm and fish weight in g. Swimbladder surface cross-sectional areas (in cm^2) and volumes (in cm^3) are given for respective water pressures (in bar). Estimated parameters a, b, b_{20} and γ correspond to the following equations fitted to the modelled mean TS values and swimbladder cross-sectional surface areas of each herring: $TS = 20\log_{10}(L) + a\log_{10}(1+P) + b$; $TS = 20\log_{10}(L) + b_{20}$; and $A = A_0 \times P^{\gamma}$.

fish no.	fish measurements		swimbladder measurements												
	total length	weight	area (A) at pressure (P)					volume (V) at pressure (P)					a	b	b_{20}	γ
			1	2	3	5	7	1	2	3	5	7				
2	35.5	320	7.8	-	5.7	3.9	3.2	5.0	-	2.4	1.2	0.8	-3.5	-65.50	-67.25	-0.41
4	36	315	9.7	-	6.7	4.9	4.1	7.2	-	3.1	1.7	1.2	-4.7	-64.77	-67.12	-0.42
5	29.5	130	4.9	-	4.2	3.4	2.9	2.9	-	1.4	0.8	0.6	-3.0	-65.30	-66.80	-0.24
8	32.1	190	3.3	-	2.5	2.2	1.7	1.6	-	0.6	0.4	0.3	-4.7	-68.52	-70.85	-0.29
9	34	215	7.4	-	5.7	4.8	4.3	6.0	-	2.3	1.3	0.8	-2.1	-65.21	-66.25	-0.27
10	35.1	345	7.7	-	5.2	3.7	3.1	5.1	-	2.3	1.3	0.9	-5.2	-65.43	-68.03	-0.44
11	35.8	275	7.7	-	5.2	4.4	3.7	7.3	-	2.9	1.6	1.0	-3.5	-66.00	-67.72	-0.36
43	25	230	11.0	9.3	7.8	5.3	4.6	7.7	3.9	2.4	1.2	0.7	-4.9	-63.20	-65.46	-0.42

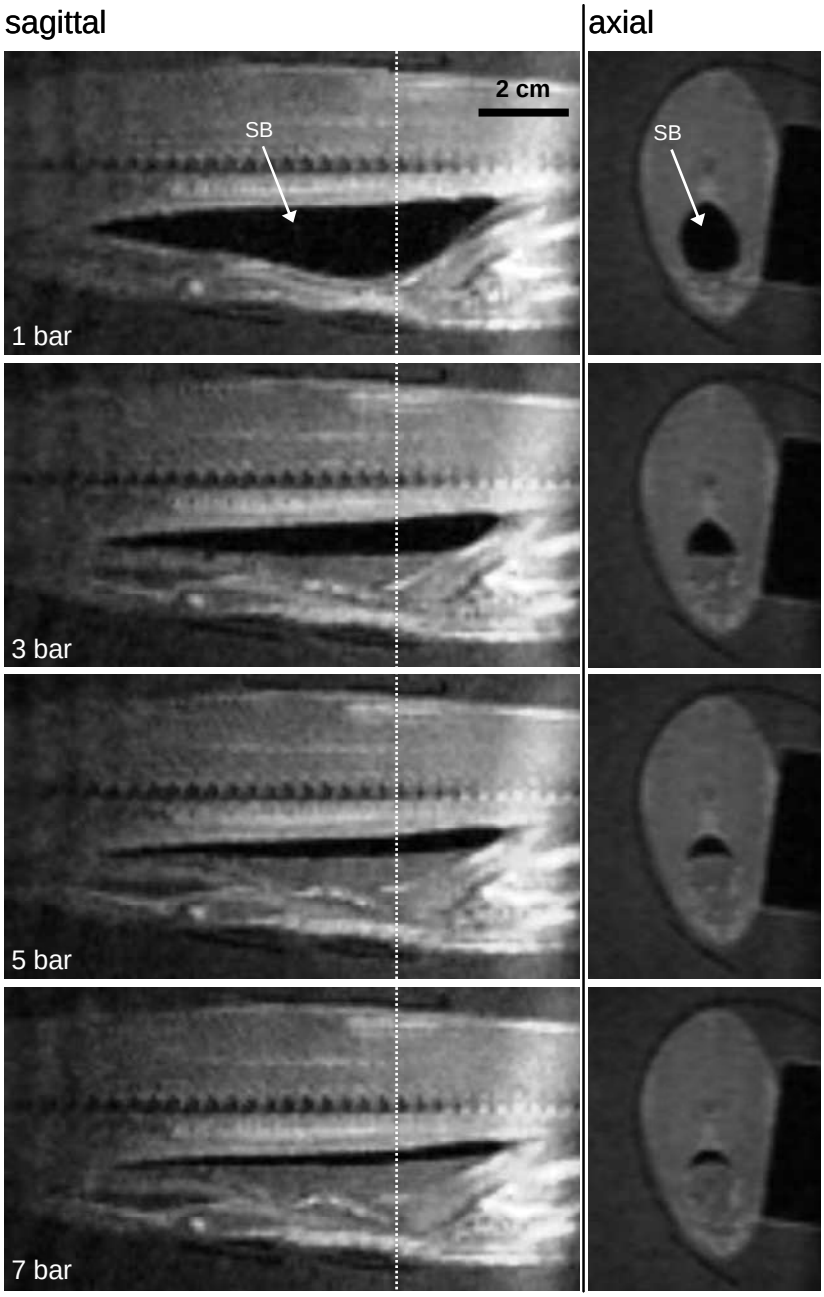

Figure 4.7 Sequence of sagittal and axial magnetic resonance (MR) images of herring #9 at a range of water pressures (1 - 7 bar), showing the swimbladder (SB) as a dark object in the centre of the fish. The position of the axial image at every pressure step is given as a dashed line in the respective sagittal image. The proximity of the herring head to the air filled pressure chamber compartment caused artefacts on the sagittal images in the form of lighter grey shades.

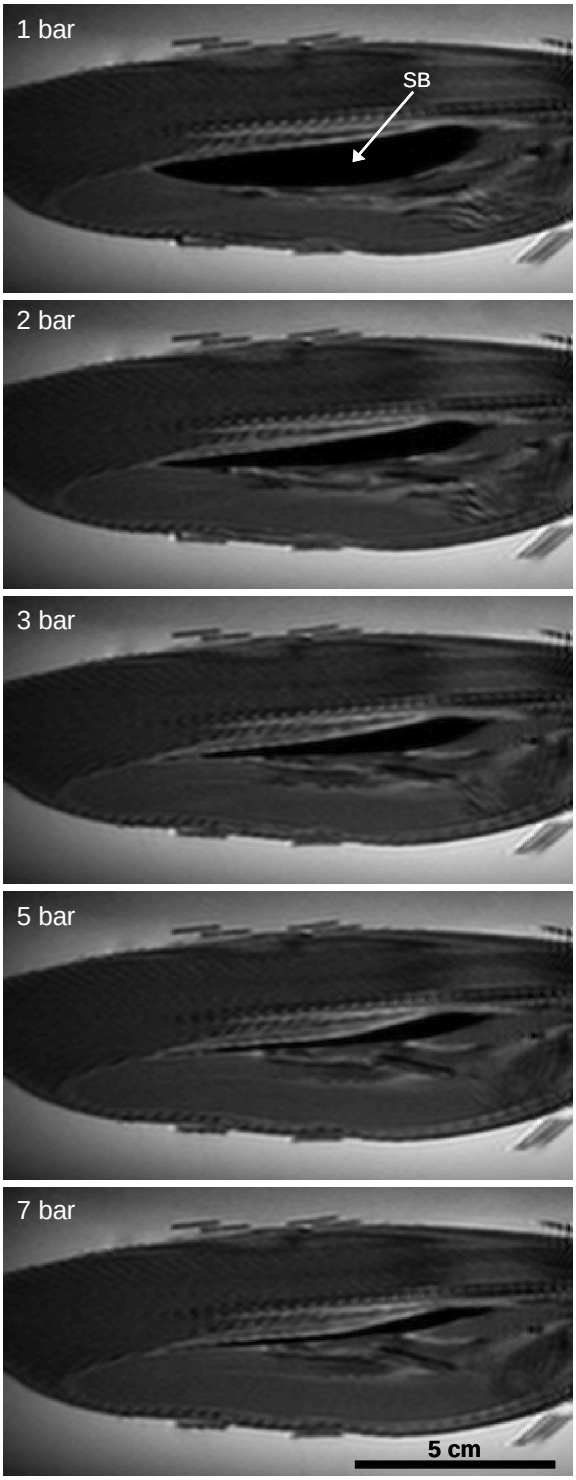

Figure 4.8 Sequence of sagittal MR images of herring #43 at a range of water pressures (1 - 7 bar), showing the swimbladder (SB) as a dark object in the centre of the fish.

Three-dimensional representations of the herring swimbladders generally showed an elongated elliptic dorsal shape at surface pressures. The lateral shape included a rounded ventral contour with a higher anterior part that becomes gradually thinner towards the tapering posterior end (Figure 4.9a). The shape of the peaky anterior end was more variable among specimens and its size depended on swimbladder fullness (Figure 4.9). At higher water pressures, the elliptic dorsal shape became more pear-shaped with the anterior section remaining the same width while there was a more pronounced decrease in width towards the thinner anterior end (Figure 4.9a). The change in swimbladder dimension was especially pronounced in the posterior part, while most of the remaining gas seemed to accumulate in the anterior part at higher pressures (Figure 4.8 and Figure 4.9a). Observed swimbladder dorsal surface areas and volumes are given for each fish at every pressure step in Table 4.2. Ranges of surface areas determined from the reconstructed swimbladder models varied between 3.3 to 11.0 cm^2 at 1 bar (equivalent to depth = 0 m) and 1.7 to 4.6 cm^2 at 7 bar water pressure (equivalent to depth = 60 m). Swimbladder volume ranges were 1.6 to 7.7 cm^3 at 1 bar and 0.3 to 1.2 cm^3 at 7 bar. According to Boyle's Law, the swimbladder volume (V) should decrease with depth (z) in accordance with $V \propto (1+z/10)^{-1}$ (Gorska and Ona 2003a; Horne et al. 2009). There was a strong correlation between observed swimbladder volumes derived from contiguous cylinders of herring standardised to a common length of 32 cm, and those volumes predicted for the observed depths using Boyle's Law ($r = 0.99$, $P < 0.001$). The nonlinear least squares regression fitted to the swimbladder volume data was significant ($P < 0.001$; 95% CI of exponent = -1.05 – -0.78; Figure 4.10). The difference between swimbladder volumes at the lowest pressure observed at the start and the end of 'Scan 1' was insignificant (2.5%), and I conclude that gas loss was therefore not an issue in the experiment. If the volume of a spherical balloon changes with depth according to Boyle's Law, its cross-sectional area (A) will change in accordance with $A \propto (1+z/10)^{\gamma}$, with the contraction-rate factor (γ) equal to -2/3 (Ona, 2003). However, the contraction-rate factor determined by a nonlinear least

squares fit to the observed length standardised dorsal cross-sectional area data determined from the cylinder swimbladder models was close to -1/3 ($P < 0.010$; 95% CI of exponent (γ) = -0.43 – -0.29; Figure 4.10). Contraction-rate factors (γ) for swimbladder dorsal area decrease with increasing water pressure (P), according to $A = A_0 \times P^{\gamma}$, ranged from -0.24 to -0.44 (Table 4.2).

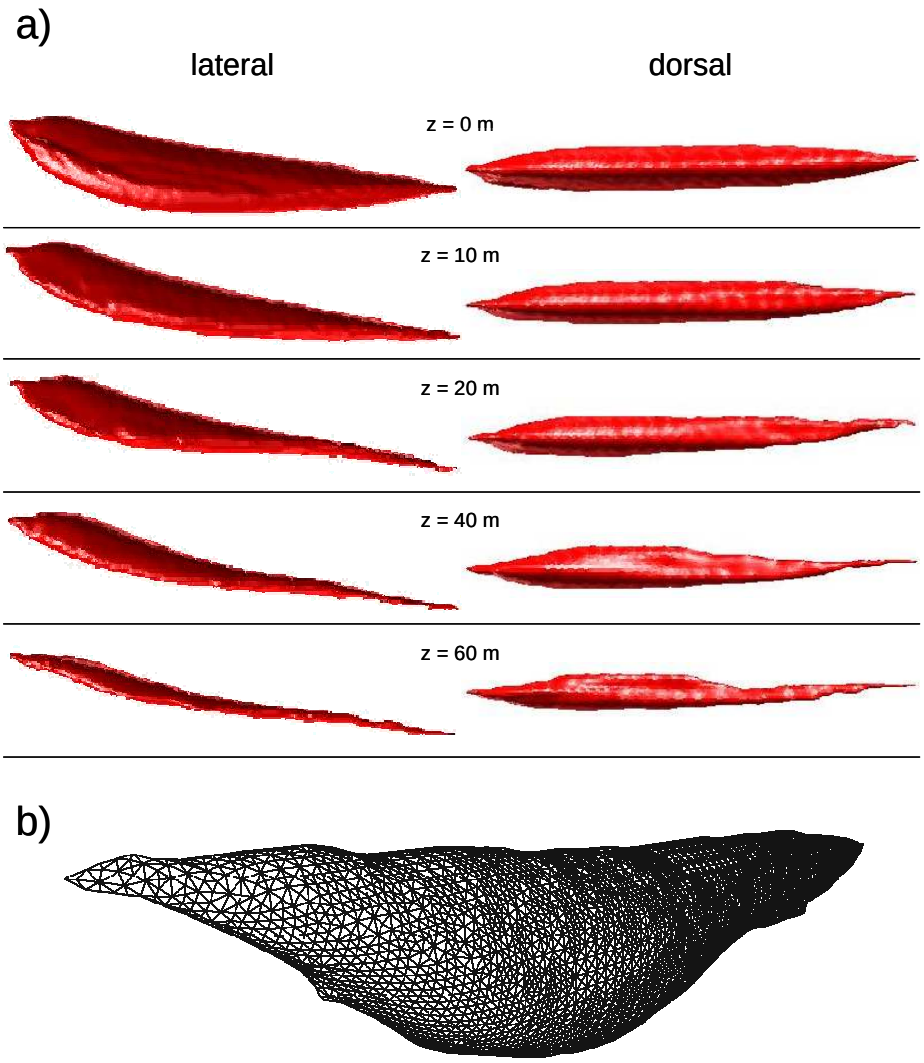

Figure 4.9 (a) Three-dimensional representations of the swimbladder of herring #43 exposed to pressures equivalent to water depths (z) from 0 to 60 m. (b) The swimbladder surface portrayed as a mesh of nodes obtained from sequences of magnetic resonance images (example is herring #9 at surface water pressure).

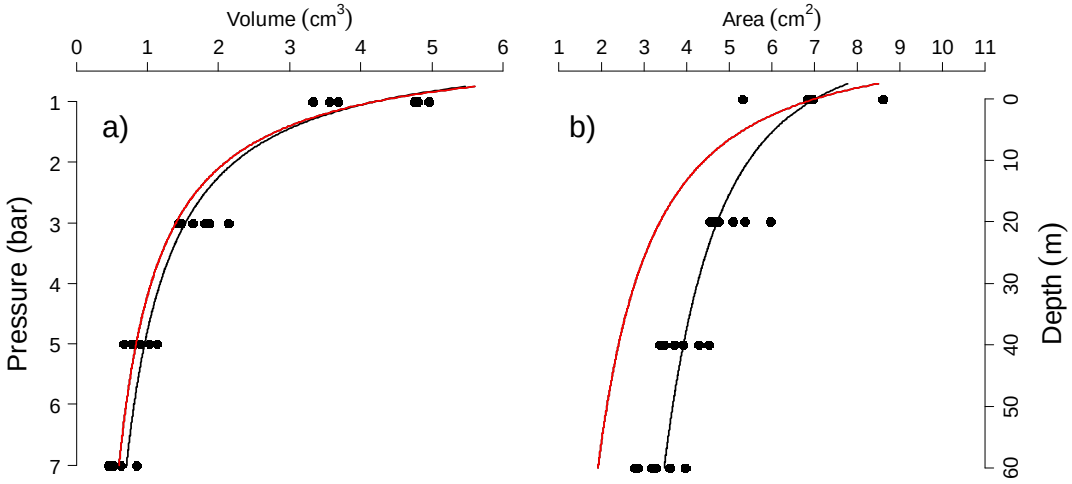

Figure 4.10 Change in volume (V; panel a) and dorsal cross-sectional area (A; panel b) of swimbladders of 8 herring subjected to pressures equivalent to a depth (z) range of 0 - 60 m (1 - 7 bar) and standardised to a common fish total length of 32 cm. Non-linear regression curves (black) were fitted: (a) $V = 4.20\ (1 + z/10)^{-0.92}$ and (b) $A = 7.01\ (1 + z/10)^{-0.36}$. The red lines represent the theoretical curves assuming isometric compression according to Boyle's Law: (a) $V = 4.20\ (1 + z/10)^{-1}$ and (b) $A = 7.01\ (1 + z/10)^{-2/3}$.

4.3.2. Depth-dependent target strength modelling

Standard depth-independent TS-fish length (L) relationships ($TS = 20 \log_{10} (L) + b_{20}$) fitted to the modelled mean TS at 38 kHz of each herring over the entire depth range analysed (0 - 60 m) revealed b_{20} values that ranged from -70.85 dB to -65.46 dB (Table 4.2). Gaussian distributions of fish tilt angles used for these calculations assumed a mean of 0º with standard deviation of 10º. At tilt angles much larger/smaller than broadside dorsal incidence, acoustic scattering levels predicted by the KRM model for different tilt angles and frequencies did not change considerably over the range of different water pressures considered (Figure 11). Generally, maximum backscatter increased with increasing frequency over the different water pressures. At lower frequencies, backscatter was less affected by fish aspect and generally declined with increasing water pressure. Periodic peaks and troughs along the ridge of maximum backscatter values along the frequency range corresponded to

areas of constructive and destructive interference between the fish body and swimbladder (Horne et al. 2000). Maximum backscatter amplitudes indicated parallel alignment of the majority of the dorsal swimbladder surface to the transducer face. At higher frequencies (~ >50 kHz), another ridge of increased backscatter was observed at tilt angles that may coincide with the inclination angle of the anterior part of the swimbladder (see Section 4.3.1.) being perpendicular to the acoustic beam (Figure 4.11). Modelled mean TS of all herring standardised to a common length of 32 cm decreased with increasing pressure (Figure 4.12a). The mean TS values ranged from -35.46 dB for a tilt angle distribution with 10º standard deviation and -34.11 dB with 5º standard deviation at surface pressures, to -38.61 dB and -37.31 dB, respectively at water pressures equivalent to a depth of 60 m (Figure 4.12a). Fitting a depth-dependent TS- relationship ($TS = 20 \log_{10} (L) + a \log_{10} (1 + z/10) + b$) to the modelled mean TS values over the range of pressures analysed gave values for 'a' that ranged from -2.1 to -5.2, and values for 'b' ranging from -63.20 to -68.52 (Table 4.2). Equivalent values for the standardised fish length data were 'a' (± 1 standard error) = -3.9 (± 0.85) and 'b' = -65.50 (± 0.497) for 10º standard deviation of tilt angle distribution, and 'a' = -4.1 (± 0.97) and 'b' = -64.16 (± 0.564) for the 5º tilt angle standard deviation case. Respective mean b_{20} values (± 1 SE) for the depth-independent relationships were -67.44 (± 0.341) and -66.19 (± 0.375) dB.

Both depth-dependent relationships fitted to the model data using either 5º or 10º standard deviation of tilt angle distributions were compared to a set of 95 *in situ* TS measurement series published in Ona (2003) between 0 and 300 m water depth (Figure 4.12b). Depth-independent TS values that would currently be applied for estimation of fish abundance and biomass from acoustic survey data for a 32 cm herring are also indicated in Figure 4.12b. Stock sizes of Norwegian spring-spawning herring are estimated using a b_{20} value of -71.9 in the relationship $TS = 20 \log_{10} (L) + b_{20}$ to convert TS into fish length and eventually weight (ICES 1988). The b_{20} value used in acoustic abundance estimation of, for instance, North Sea or Baltic Sea herring is -71.2 (ICES 1997). Corresponding depth-independent TS for a 32 cm herring would be -41.10 dB and -41.80 dB for stocks of North Sea and Norwegian

spring-spawning herring, respectively (Figure 4.12b). Most of the *in situ* data were included within the 95% confidence interval of the fitted relationships. Nonetheless, the majority of observations that fell outside the confidence interval were higher than expected by the model (Figure 4.12b).

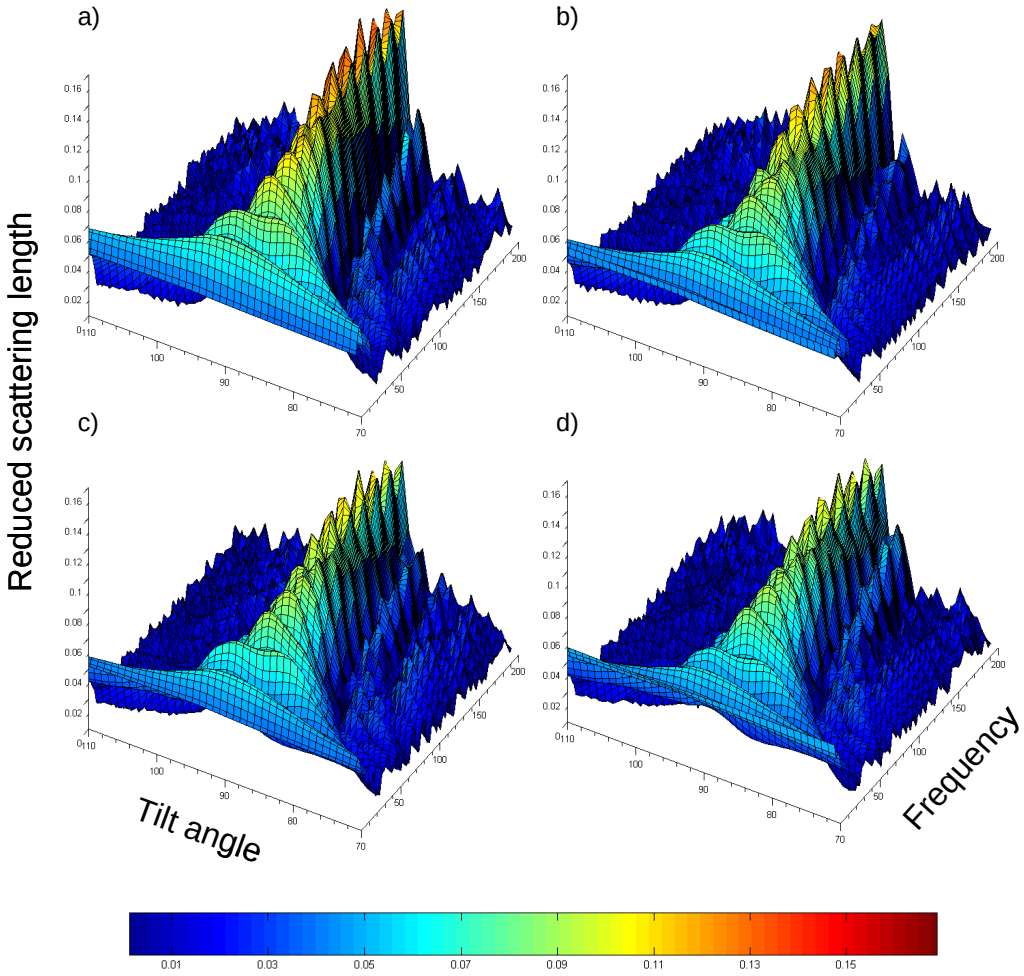

Figure 4.11 Surface plots of acoustic backscattering levels (reduced scattering length = $\sqrt{\sigma_{bs} / L^2}$, unitless) predicted by the KRM model at a range of fish tilt angles (in º) and acoustic frequencies (in kHz) for herring #9 at pressures of 1 bar (a), 3 bar (b), 5 bar (c), and 7 bar (d). Angles <90º indicate a head-down tilt orientation.

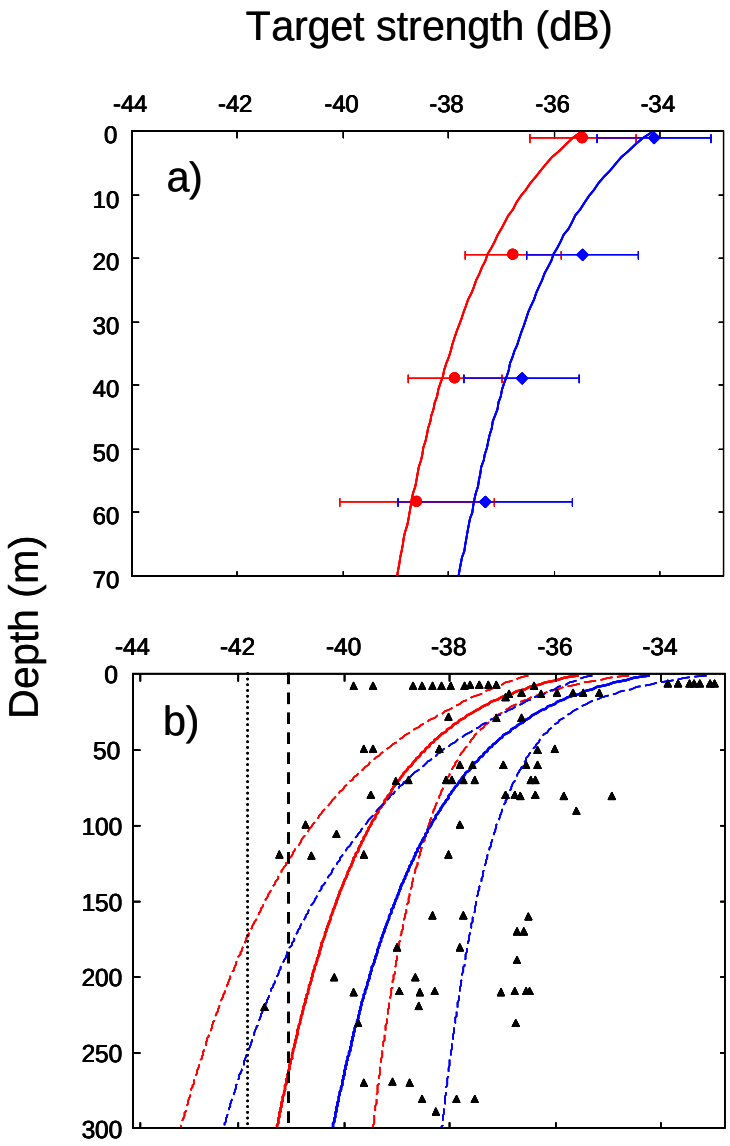

Figure 4.12 Modelled mean target strength (TS) values of herring (n = 8 standardised to a total fish length of 32 cm) exposed to various pressures and: (a) Length- and depth-dependent TS relationships fitted to the model data. X-axis error bars represent 95% confidence intervals of the mean model estimates averaged over Gaussian fish orientation distributions with mean 0º and s.d. of either 5º (diamonds, blue) or 10º (circles, red); (b) TS-depth relationships from the model data with 95% confidence limits compared to measured mean *in situ* herring TS values (black triangles, Ona 2003). Depth-independent TS values currently applied for acoustic abundance and biomass estimation for various herring stocks are shown as black dotted (e.g. Norwegian spring-spawning herring) and dashed (e.g. North Sea herring) lines.

Acoustic target strength (TS) is obtained from the backscattering cross-section (σ_{bs}) using Equation 2.3. Given the proportionality of σ_{bs} to the dorsal cross-sectional area of the swimbladder at frequencies used routinely in surveys for herring (Simmonds and MacLennan, 2005), the expected acoustic backscatter at depth (z) has previously been approximated using the general simple model $\sigma_z = \sigma_0(1+z/10)^{\gamma}$ (Ona 2003). Herring in the North Sea are found commonly at water depths down to about 200 m (see Chapter 5). The difference between modelled mean TS of 32 cm herring at the surface and 200 m using the KRM was 5.47 dB and 5.21 dB for 5º and 10º standard deviation of tilt angle distribution, respectively. If the swimbladder behaved like a spherical balloon (i.e. contraction-rate factor γ = -2/3), herring at the surface would have a TS that is stronger by 8.8 dB compared to herring at 200 m depth. Using the γ estimated from the cross-sectional dorsal swimbladder surfaces in this study (i.e. γ = -0.36; Figure 4.10) would suggest that this difference is 4.8 dB. Consequently, the difference between depth-dependent acoustic backscatter at 200 m depth, as approximated using either the spherical balloon assumption or the γ estimated in this study, would result in acoustic abundance estimates that differ by a factor of 2.49. Correspondingly, using the actual depth-dependent TS relationship fitted to the length-standardised tilt averaged (10º standard deviation) model data, extrapolated to 200 m depth, would elicit abundance estimates that differ by a factor of 2.28 from those estimated assuming isometric compression according to the spherical balloon case.

4.4. Discussion

Herring swimbladders do become smaller with increasing pressure in deeper water. Based on the results reported in this Chapter, the swimbladder volume reduction does not differ significantly from what would be predicted by Boyle's Law. Nonetheless, the swimbladder did not compress in an isometric fashion as expected according to the free spherical balloon model assuming Boyle's Law. Pressure had a lesser effect on the dorsal cross-sectional swimbladder area due to the fact that the swimbladder

length and width reduction was much less than the height reduction. This particular nature of swimbladder compression is most likely due to the swimbladders' ventral connections to spinal chord, ribs, and musculature (Blaxter et al. 1979). In some other cases, swimbladders do compress isometrically and the depth-dependence of TS can be predicted following Boyle's Law. For instance, Mukai and Iida (1996) observed that TS of anaesthetised tethered kokanee salmon (*Oncorhynchus nerka*) decreased in accordance with expectations if the swimbladder were a free spherical balloon. Similarly, Zhao et al. 2008 showed that the *in situ* TS of another Clupeid, the Pacific anchovy (*Engraulis japonicus*), exhibited a depth-dependence according to Boyle's Law. The results reported in this Chapter support assumptions and observations of previously published investigations into the depth-dependent TS of herring (Blaxter et al. 1979; Edwards and Armstrong 1981; Edwards et al. 1984; Ona 1990; Ona 2003; Gorska and Ona 2003a; Fässler et al. 2008; Pedersen et al. 2009). Ona (1990) measured swimbladder volumes of euthanised herring *in situ* by scuba diving at depths between 3 and 25 m using the underwater dissection methods described in Section 3.2.1.1. He observed a swimbladder volume reduction with depth according to Boyle's Law. Furthermore, Ona (2003) quantified mean dorsal-aspect TS of Norwegian spring-spawning herring *in situ* at various water depths ranging from 5 to 500 m and estimated a depth-dependent relationship. The observed mean contraction-rate of the backscattering cross-section (γ = -0.23) was much lower than expected assuming isometric dorsal swimbladder area compression (γ = -2/3), and more similar to the value found in this chapter (γ = -0.36). Moreover, some of Ona's (2003) measurements, specifically his 'vertical-excursion' and 'deep herring' experiments, suggested values for γ of -0.45 and -0.35, respectively. These were both much closer to the mean value of -0.36 obtained from the models of the length standardised herring reported here. Based on modelling using a simple geometric shape (spheroid) to approximate swimbladder and fish body, Gorska and Ona (2003a) concluded that the herring swimbladder most likely compressed in a fashion where the length remained fixed but where the diameter was more sensitive to increased pressure. However, apart from providing an initial crude insight into how herring swimbladder

compression works, it is now evident that the specific modelling methods used by Gorska and Ona (2003a) were unsuitable to describe the phenomenon. Based on the findings presented in this Chapter, it is evident that the herring swimbladder cannot adequately be described by a spheroid, which is symmetric along its longitudinal axis, since the height becomes much shorter than the width at increased water depths. Pedersen et al. (2009) further support this assertion by showing that the lateral-aspect TS of herring decreases with depth to a greater extent than dorsal-aspect TS does.

It is difficult to estimate swimbladder compression indirectly from *in situ* TS measurements. This is in fact generally true for other features that dictate backscattering levels of fish, such as tilt angle distribution, fat content or gonad size, which are notoriously difficult or cumbersome to measure *in situ* (Blaxter and Batty 1990; Simmonds and MacLennan 2005). Modelling approaches have been identified as useful tools to quantify and identify processes controlling variability in TS (Horne and Clay 1998; Horne 2000; Simmonds and MacLennan 2005). The direct *in vitro* method described in this study provides an important first step in obtaining high-resolution representations of the swimbladder (Figure 4.9) to be used in more complete three-dimensional backscatter models for physostomous fish. The KRM method used in this Chapter approximates the swimbladder by inferring its surface by a series of short elliptical cylinders. Previous studies that used KRM models found generally good agreement between model and empirical measurements (Clay and Horne 1994; Jech et al. 1995; Horne and Jech 1999; Horne et al. 2000; Gauthier and Horne 2004b; Kang et al. 2004). Nevertheless, there are issues with that model approach with regards to spatial resolution, aspect angle limitations and non-validity at the (low) swimbladder resonance frequencies (see Section 2.4; Foote 1985; Stanton 1989). Horne et al. (2009) observed live walleye pollock (*Theragra chalcogramma*) in a pressure chamber and took dorsal and lateral X-ray radiographs at various water pressures from ambient to about 5 bar. The morphological swimbladder data they gathered in these two dimensions (height and width along the main axis) were adequate to describe the swimbladder surface by elliptic cylinder pieces for use with the KRM, but not to rebuild and approximate the true surface. The meshes

representing the true 3-D swimbladder surface described here may, however, be used together with more elaborate models such as the boundary element (BEM; Foote and Francis 2002; Francis and Foote 2003) or finite element method (FEM; ICES 2009a), which can be applied to any arbitrary surface at any tilt angle. These models can then be used to investigate not only how the change in true swimbladder dimensions with depth affects TS but also take into account finer morphological features on the swimbladder surface.

Estimates of intercepts of the standard depth-independent TS-L relationship (TS = 20 $\log_{10}$ (L) + b_{20}) fitted to the modelled herring TS (Table 4.2) were higher than the ones currently used to estimate biomass of Atlantic herring from acoustic data (i.e. for example -71.2 for North Sea (ICES 1982) and -71.9 for Norwegian spring-spawning herring (ICES 1988)). The mean b_{20} estimate of the relationship fitted to the length standardised TS model data differed by 3.8 dB from the values applied for North Sea herring. Some other early TS measurements on herring *in situ* and herring confined in cages revealed values of -72.1 (Foote 1987) and -71.3 (Edwards et al. 1984), which were similar to the currently used b_{20} values. However, Ona (2003) fitted the depth-independent TS relationship to his entire data set over the whole depth range and obtained a b_{20} of -67.3, which is very similar to the values obtained from model data in Chapter 3 (-67.1; see Section 3.3.2.1.) and in this Chapter from the length standardised model data (-67.4). Nevertheless, there may be a discrepancy between Norwegian spring-spawning and North Sea herring since earlier b_{20} values were based on measurements of herring from the North Sea, while the latter values reported here and by Ona (2003) are from Norwegian spring-spawners. Although these stocks are the same species and live in broadly similar environments, in contrast, for example, to herring living in the Baltic Sea, which have an entirely different salinity regime (see Chapter 3), the two herring stocks may have a different morphology (Sinclair and Solemdal 1988). Additionally, North Sea herring are on average smaller than their northern conspecifics, and TS relationships may vary depending on the size range of fish they are fitted to (Simmonds and MacLennan 2005). Mean parameters of the depth-dependent relationship (a = -3.9, b = -65.5), of

the form TS = 20 $\log_{10}$ (L) + a $\log_{10}$ (1 + z/10) + b, fitted to the model values in this chapter were similar to the one fitted to Ona's (2003) entire data set (a = -2.3, b = -65.4) and to model values presented in Chapter 3 (a = -1.9, b = -65.2; see Section 3.3.2.1.). The contraction-rate factor (a) obtained here, however, was higher than previously reported values, indicating discrepancies to the simple model used in Chapter 3 and possibly differences in tilt angles and swimbladder volumes of Ona's (2003) *in situ* herring data.

A potential shortcoming of the present investigation is the fact that only a small number of herring were scanned. Unfortunately, the presently high cost MRI precluded a more extensive investigation. However, initial X-ray examination in one case and careful rearing under controlled aquaculture conditions in all other cases assured the intactness and suitability of the chosen specimens, and the results therefore represent a valid first insight into changes of herring swimbladder surface shape with depth. Still, one might argue that a computer tomography (CT) scanner may have offered a cheaper alternative to the costly MRI scanner used in this investigation. Nonetheless, insonification of the water-filled pressure chamber with X-rays would have resulted in considerable amounts of scatter. In order to reduce artefacts, a solution would be to acquire a dual-energy CT scan, however, such CT scanner units are only available in a limited number of centres. More importantly, there are no big differences in costs for using various scanning equipment (CT: €300-420/hour; dual-energy CT: €360-420/hour; MRI: €430/hour; S.I.K. Semple, Wellcome Trust Clinical Research Facility, Edinburgh, UK, pers. comm.), with MRI being able to provide higher resolution and more information regarding various soft tissues surrounding the swimbladder.

Gas loss appeared not to be an issue in this experiment. However, possible diffusion of gas from the swimbladder over time may cause variability in observed bladder volumes of wild herring (Blaxter et al. 1979). This important aspect should be addressed in future investigations. Also, herring in the wild may release gas during vertical migration (Thorne and Thomas 1990; Nøttestad 1998) or when avoiding predators (Jones 1952; Blaxter 1985) or attempting to confuse them (Nøttestad 1998).

Depth-dependent swimbladder volumes apart, such behaviour will make any comparison between model and empirical observations immensely difficult, as swimbladders could probably exhibit any volume within certain limits. Another issue is the initial gas content of physostomes swimbladders at the sea surface. Based on indirect swimbladder volume measurements using low acoustic frequencies (1.5 - 5 kHz) around swimbladder resonance, Nero et al. (2004) estimated that the Atlantic herring they observed were neutrally buoyant at depths of 40 - 50 m. These findings were also supported by Thorne and Thomas (1990) who estimated a lower limit of herring neutral buoyancy near 60 m, based on observations of gas release at depth. Previous investigators argued that herring should be neutrally buoyant at the sea surface (Jones and Marshall 1953; Blaxter et al. 1979; Blaxter and Batty 1984; Ona 1990). However, Nero et al. (2004) found some of the herring they sampled to have up to at least three times greater swimbladder volumes than neutrally buoyant fish at the sea surface. Herring in the wild may be motivated to inflate their swimbladders to a greater or lesser extent depending on what depths they envisage diving to. The initial volume of gas in the swimbladder may vary by day and season, and is generally dependent on migratory behaviour, feeding and reproductive conditions (Ona 1990). In the experiment reported here, most of the herring samples were reared under controlled laboratory conditions and never experienced any greater depths beyond the height of their tank. It is therefore likely that their swimbladders contained enough gas to give them neutral buoyancy at surface water pressures. The question of initial swimbladder fullness of herring in the wild may also be different for different fish sizes, given for instance the size-dependent depth distribution in the North Sea with larger fish generally found in deeper waters (Rivoirard et al. 2000). Once the herring are at depth, they may also exhibit tilt angle distributions with a different mean and standard deviation from the ones at shallower depths in order to offset the deteriorating state of negative buoyancy caused by the diminishing swimbladder volume (Huse and Ona 1996; Strand et al. 2005). Differences in tilt angle distributions with depth, in addition to pressure induced swimbladder compression further complicates any attempt to model TS.

A depth-dependent TS will have significant effects on acoustic abundance estimates. According to the results presented in this Chapter (see Section 4.3.2.), the TS of a herring would be 5 dB higher when the fish migrates from a depth of 200 m during the day to surface waters at night. This would result in abundance estimates that are more than three fold different between potential night time (apparent high abundance) and day time (apparent low abundance) surveys if the same TS-L relationship was used. Additionally, potential behaviour differences between day and night may also play an additional role (Huse and Korneliussen 2000). On the other hand, the need for a depth-dependent TS relationship is less of an issue if the fish being surveyed are found more or less at similar depths throughout the survey period and between surveys. Løland et al. (2008) looked at various factors that influence abundance estimates of Norwegian spring-spawning herring such as vessel avoidance, acoustic shadowing and depth-dependence of TS. Using the findings of Ona (2003) they showed that the depth-dependent TS component may contribute from 1.5 to 12.5% to total uncertainty of the herring abundance estimate, with lower values when the herring were predominantly in surface waters (Løland et al. 2008). It is evident from the results presented here (Figure 4.12b) that, compared to the currently used depth-independent TS relationship, a 32 cm herring in the North Sea may have a higher TS at depths down to 250 m. If that depth-dependent relationship was used, it would severely reduce the abundance estimate. Nonetheless, valid statements about potential effects of a depth-dependent TS can only be made after whole survey datasets have been analysed, since analyses will be sensitive to length, depth, and spatial distributions of the herring stocks in question. If depth-dependent relationships were to be used for abundance and biomass estimation from acoustic data of herring, acoustic survey data will have to be analysed in vertically stratified depth bins, in addition to distance echo integral units. Additionally, potential vessel avoidance of herring will counteract any enhanced effects of depth-dependence of herring TS in surface waters (Ona 2003; Ona et al. 2007; Løland et al. 2008).

Future work could valuably incorporate comparison of modelled TS from swimbladder reconstruction at various pressures with *in situ* TS measurements. Given

the difficulties with regards to uncertainty of initial herring swimbladder fullness at the sea surface, such measurements will have to be accompanied with adequate estimates of swimbladder volumes at depth. New promising broadband acoustic techniques enable measurements of backscatter over a wide range of frequencies to cover the whole spectrum of Rayleigh, resonant and geometric scattering for herring (ICES 2009a; Stanton 2009). Such measurements would enable swimbladder volumes to be deduced indirectly from low frequency *in situ* acoustic data, which by definition are more dependent on the volume of the swimbladder and in addition less affected by directivity (Love 1978; Løvik and Hovem 1979; Nero and Huster 1996; Nero et al. 1998; Nero et al. 2004; Nero et al. 2007). Developing quantitative multi-beam sonars will inevitably be dependent on estimates of lateral-aspect TS (Boswell et al. 2009; Nishimori et al. 2009; Pedersen et al. 2009; Tang et al. 2009). Their swath beams of up to 180º will cover a wider range of incidence angles and therefore cause a higher degree of variability in angle-dependent TS (Henderson et al. 2008; Trenkel et al. 2008). In the case of physostomes, this will however bring obvious additional difficulties, and modelling approaches using reconstructed swimbladder shapes from fish under pressure may have some merit. For now, assumptions about tilt angle distributions and initial swimbladder volumes at the surface remain major difficulties when attempting to model depth-dependent herring TS using the true swimbladder shapes at depth, and for incorporating the findings into abundance estimates. Chapter 5 describes a statistical approach to propagate the error associated with these TS model parameters through to final results from acoustic surveys.

Chapter 5

A Bayesian approach to target strength estimation: combining target strength modelling with empirical measurements

Part of the work described here has been published as:
Fässler, S.M.M., Brierley, A.S., Fernandes P.G. (2009). A Bayesian approach to estimating target strength. ICES Journal of Marine Science 66: 1197-1204.

5.1. Introduction

Despite providing absolute estimates of abundance, estimates from acoustic surveys are usually treated just as relative indices to 'tune' population models (Simmonds 2003). This is because the total error (i.e. random and systematic components of measurements and sampling error) in acoustic surveys is generally not quantified, though work by Tesler (1989), Demer (1994, 2004), Aglen (1994), and Simmonds and MacLennan (2005) provide some examples where various components of the error are considered. Often, where errors are reported, they are usually estimates of random sampling errors alone (Rose et al. 2000) and do not account for various sources of systematic measurement error that are specific to acoustic surveys (Simmonds et al. 1992). Systematic errors can result from such sources as the

equipment (Toresen et al. 1998), acoustic shadowing (Zhao and Ona 2003), poor weather (causing ping drop outs, Aglen 1994), vessel avoidance (Vabø et al. 2002) and, most notably, the uncertainty in the fish target strength (TS; Simmonds et al. 1992). Despite the wide variety of sources that may cause variability in fish TS (see various model parameters in Chapters 2 - 4), a simple relationship to length of the form $TS = 20 \log_{10} (L) - b_{20}$ is conveniently and commonly used to convert fish length (L) into mean TS by applying a species specific value for b_{20} (Simmonds and MacLennan 2005).

The TS-L relationship currently applied to estimate the abundance of various herring and other clupeid stocks around the world was determined empirically about 25 - 30 years ago. Nakken and Olsen (1977) insonified 41 stunned and tethered herring at 38 kHz - the frequency used commonly for surveys - to determine the maximum dorsal aspect TS for fish of various lengths. Based on observations of tilt angle distributions of small herring (mean length = 13 cm), they then decided that the maximum observed TS values should be reduced by 6 dB to account for orientation effects of live, free-swimming herring. The resulting equation was: $TS = 13.6 \log_{10} (L) - 62.8$. Edwards and Armstrong (1981) measured TS at 38 kHz of a total of 565 live herring (L between 21 and 25 cm) in a cage at 17.5 m depth over a period of 340 h. They obtained a mean TS of -33.8 dB kg^{-1}. The Planning Group on ICES-Coordinated Herring and Sprat Acoustic Surveys (ICES 1982) subsequently converted Nakken and Olsen's (1977) TS-L relationship into TS per kg for a 23 cm herring (-34.6 dB kg^{-1}) to facilitate comparison with Edward and Armstrong's (1981) results. It was decided that the mean of the two TS estimates (-34.2 dB per kg) should be used together with length-weight data from northwest North Sea herring, such that the Planning Group's final recommendation was a TS-L relationship of $TS = 20 \log_{10} (L) - 71.2$.

In addition to the major factors recognised commonly as affecting TS, such as fish size, acoustic frequency and tilt angle of the fish, there is strong evidence that other parameters do affect the TS of herring. Increasing depth and the concomitant increase in water pressure forces the herring swimbladder to compress and, therefore,

decreases its TS (Ona 1990; Ona 2003; Gorska and Ona 2003a; Fässler et al. 2009a, Chapter 4). This will bias survey results if not taken into account (Ona 2003; Løland et al. 2007; Fässler et al. 2009b). Maturity stage or stomach fullness may also have an important temporal effect on swimbladder size, shape and, ultimately, TS (Ona 1990). Additionally, it has been shown that the physical environment can influence the physiology and morphology of herring leading to geographic variation in swimbladder sizes and mean TS. For instance, herring living in the Baltic Sea have larger swimbladders as compared to their conspecifics in the northeast Atlantic (see Chapter 3; Didrikas and Hansson 2004; Peltonen and Balk 2005; Fässler et al. 2008). This is linked to their low fat content and the low salinity of the Baltic Sea, increasing the importance of the swimbladder as a buoyancy regulating organ. The best estimate of *in situ* TS will need to take due consideration of the combined influences of all of these factors, and the variability in each.

This chapter describes a novel approach to estimating the expected TS of a fish species that takes into account this variability. In order to deal with TS variability, the expected herring TS was estimated by a model using distributions of parameter values that are most likely (in a probabilistic sense) when fitting the model to *in situ* data. The Kirchhoff-ray mode model (KRM; Clay and Horne 1994; see Section 2.3.5.6.) was applied together with Bayesian methods, using data from Atlantic herring TS at depth (17.5 - 45 m), to estimate the distribution of model parameters (relative swimbladder volume at the surface, tilt angle distribution, and standard deviation of the estimated mean TS). Bayesian methods were used because these enable parameter uncertainty to be incorporated, in this case into estimates of mean TS. Posterior distributions of model parameters were then used with the error propagation properties of the Bayesian framework to simulate backscattering by herring, while quantifying the precision of the TS estimate. The resulting length- and depth-dependent TS model was applied to estimate random and systematic error in TS estimation and ultimately in the estimates of North Sea herring abundance and biomass. This investigation could be an important step towards incorporating the error associated with TS in estimates of total error in acoustically derived abundance

estimates of fish. If it works, the methods could also be advantageous for ecosystem studies and stock assessment where estimates of fish abundance/biomass with estimates of total error are required.

5.2. Methods

5.2.1. Bayesian methods

Under the Bayesian approach, posterior density functions of model parameters (θ) are derived based on the goodness of fit of a model to data, and on prior information not contained in those data (McAllister and Kirkwood 1998). The posterior probability distributions $p(\theta_i \mid \text{data})$ of a set of continuous model parameter (θ_i) given the data are determined using Bayes' theorem (Bayes 1763) according to:

$$p(\theta_i \mid \text{data}) = \frac{p(\theta_i, \text{data})}{p(\text{data})} = \frac{p(\theta_i) \times L(\text{data} \mid \theta_i)}{\int p(\theta) \times L(\text{data} \mid \theta) d\theta} \quad (5.1)$$

where $p(\theta_i,\text{data})$ denotes the joint probability for a set of parameters θ_i and of obtaining the data. The data used here were derived from *in situ* TS measurements of caged Atlantic herring at water depths from 17.5 to 45 m (published in Edwards et al. 1984). Data were mean TS values for fish mean lengths ranging between 7.5 and 27.5 cm, each determined from several tens of thousands of detected single targets. Suppose that the data represent j samples of a continuous probability distribution (PDF) that is dependent on the unknown parameters θ, in a known way that can be described by a model (Lee 2004). $p(\theta)$ describes the prior PDF (i.e. the 'prior' probability) for θ. $L(\text{data}|\theta_i)$ is the probability of obtaining the data values if θ_i were the true values. $L(\text{data}|\theta)$ is commonly referred to as the likelihood function describing the dependence of the data on θ. The likelihood function of the entire TS data set is given by the product of the normal density function over all data points:

$$L(\text{data} \mid \theta) = \prod_{j=1}^{n} \frac{1}{\sigma_e \sqrt{2\pi}} \exp\left[-\frac{(Y_j - U_j)^2}{2\sigma_e{}^2} \right] \tag{5.2}$$

where σ_e is the standard deviation of the observation error. Likelihood functions can result in small numbers and, therefore, the $\log_{10}$ (likelihood) was used in the computer programming script to improve calculation time and avoid rounding issues (e.g. McAllister and Kirkwood 1998). Here, Y_j is the j^{th} observed TS value in the data set and U_j is the expected TS, estimated from a theoretical TS model described below. U_j can be described in simple terms as a function of model parameters (θ), fish length L_j and depth z_j:

$$U_j = f(\theta; L_j, z_j) \tag{5.3}$$

The prior distribution for a parameter is based on previous knowledge of the parameter, without incorporating the data used to calculate the likelihood function (Punt and Hilborn 1997). Priors are usually obtained by consulting experts or historical records. Here, prior distributions were determined for the three parameters that were deemed most important for the outcome of the model and about which there was no information available in the data. These were the standard deviation of the fish tilt angle distribution (SD_t), relative volume of the swimbladder at the sea surface (V_0) and the standard deviation of the observed mean TS (SD_{TS}; i.e. σ_e in Equation 5.2). Prior distributions of each of these parameters were constructed independently, and consequently the joint prior $p(\theta_i)$ was simply:

$$p(\theta_i) = p(SD_{t_i}) p(V_{0_i}) p(SD_{TS_i}) \tag{5.4}$$

where $p(SD_t)$, $p(V_0)$ and $p(SD_{TS})$ are the priors for the respective parameter values. These priors are assumed to be independent of each other, and of both fish length and water depth. A prior can be either informative or uninformative. An uninformative prior provides little information relative to the data (Box and Tiao 1973) and usually has the form of a uniform distribution or one with a large variance, giving all reasonable parameter values approximately equal probabilities. Informative priors provide information based on prior evidence and may have a considerable impact on the result. Priors for parameters SD_t and V_0 were based on published values (Table 5.1), whereas an uninformative prior was chosen for SD_{TS}. Due to the complexity of the model, integration of the denominator (i.e. the normalisation constant) in Equation (5.1) was not feasible. Instead, values were sampled directly from the posterior distributions of the model parameters using Markov Chain Monte Carlo (MCMC) simulation with the Random Walk Metropolis algorithm (Metropolis et al. 1953).

Table 5.1 Prior distributions and values of model parameters.

Description	Value or prior distribution (source)
Physical properties	
Density of sea water	ρ_w = 1027 kg m^{-3} (Fässler et al. 2008)
Density of fish body	ρ_w = 1049 kg m^{-3} (Fässler et al. 2008)
Density of swimbladder gas	ρ_w = 1.3 kg m^{-3} (Brawn 1969)
Sound speed in sea water	c_w = 1500 m s^{-1} (Fässler et al. 2007)
Sound speed fish body	c_{fb} = 1570 m s^{-1} (Jech et al. 1995)
Sound speed in swimbladder	c_{sb} = 340 m s^{-1} (Jech et al. 1995)
Echosounder frequency	f = 38 kHz
Fish behaviour and dimensions	
S.D. of tilt angle distribution	SD_t ~ Normal (8.6, 3.7^2) (Beltestad, 1973; Ona, 2001; Gorska and Ona, 2003)
Relative swimbladder volume at sea surface	V_0 ~ Lognormal (0.05, 0.007^2) (Harden Jones and Marshall, 1953; Ona 1990)
Precision	
S.D. of mean TS estimate	SD_{TS} ~ Normal (0,100^2) (uninformative prior)

5.2.2. Target strength and swimbladder morphology model

The theoretical expected TS component of the Bayesian model framework (U_j; Equation 5.3) was derived by applying the Kirchhoff ray-mode approximation (KRM) described as 'model III' in Chapter 2 (Clay and Horne 1994; see Section 2.3.5.6. for details of the model). The reconstructed 3-D swimbladder shapes of herring #43 obtained from MRI scans (see Section 4.3.1.) were used together with the fish body silhouette as morphological input data. The model approximated the swimbladder and fish body as series of 0.5 mm long elliptical cylinders with individual cylinder components generated from the height and width of the fish body and swimbladder along their longitudinal axes. The dimensions were scaled linearly so they could be applied to the different fish sizes in the data set. To include depth dependency into the swimbladder morphology data, height and width dimensions (d, in mm) of individual cylinder components were modelled based on:

$$d_z = \frac{1}{a_d(z/10) + b_d} \tag{5.5}$$

where d_z is the length of the respective dimension at depth (z). Parameters a_d and b_d were estimated along the longitudinal axis of the swimbladder of herring #43 over the depth range analysed (0 - 60 m; see Section 4.2.2.1.). Equation (5.5) was the relationship that gave the best fit to the observed changes in dimensions of individual cylindrical swimbladder components with water depth.

The backscattering cross-section of each scattering object was then expressed as a function of size, frequency and fish orientation relative to the transducer by summing backscattering cross-sections of all individual cylinder components. Backscatter of the fluid-filled fish body and gas-filled swimbladder representations were estimated separately. Total fish backscatter was eventually calculated as the coherent sum of swimbladder and fish body backscattering-cross section (Equation 2.4). All input parameters for the model including their sources are listed in Table 5.1. To enhance efficiency of the computation routine, a four-dimensional 'lookup matrix' was created with calculated TS values for likely ranges of values of V_0 [0.5:10 %], L [5:30 cm], z [17.5, 45 m] and fish tilt angle [0:180º]. In each iteration of the MCMC chain, expected mean TS values (U_j; Equation 5.3) were predicted for given values of V_0, L and z by averaging 10,000 samples of modelled backscatter values using tilt angle distributions with mean 0º (i.e. broadside dorsal aspect) and standard deviations based on the respective value of SD_t. All estimates were first averaged in the linear domain before being transformed logarithmically.

5.2.3. Survey analysis

Echo-integration data were taken from the Scottish component of the North Sea Herring Acoustic Survey in summer 2007 (Figure 5.1). Details of survey procedures can be found in individual survey reports (e.g. ICES 2008b). Acoustic data were collected using Simrad EK60 echosounders operating at 18, 38, 120 and 200 kHz

with split-beam transducers mounted on the drop keel typically at depths of 5 m. Transducers had nominal beam widths of 11, 7, 7 and 7º respectively and were arranged in close proximity to each other (maximal offset of 0.6 m was between the centres of the 18 and 38 kHz transducers). Data collection was from 29th June to 18th July between 0200 and 2200 GMT, with an echo integration start depth at 12 m. Post processing and analysis was conducted using Myriax EchoView software (v 4.40). A PT160 pelagic trawl was used to collect herring and other fish samples from some of the more dense fish aggregations observed throughout the survey, for identification purposes and to generate length frequency distributions for the herring in the various survey subareas. Fish lengths were recorded in groups by 0.5 cm intervals to the nearest 0.5 cm below total length. Integrated nautical area scattering coefficients (NASC) were averaged over distances surveyed each 15 minutes (~ 2.5 nautical miles). Computations were done for all length groups of herring in depth bins of 5 m ranging from 0 to 200 m. Numbers of fish in length group i in a given area were estimated by:

$$N_i = \frac{s_A}{\overline{\sigma}_{bs_i}} \cdot p_i \cdot A \tag{5.6}$$

where N_i is the number of herring in length group i, and s_A is the NASC with units m^2 nmi^{-2} (MacLennan et al. 2002). The analysed area (A) covered a total of 38,769.5 nmi^2. Biomass of herring in length group i (B_i) was calculated according to:

$$B_i = N_i \cdot a_w \cdot L_i^{\,b_w} \tag{5.7}$$

where a_w and b_w are constants determined from length and weight data of 2308 herring sampled during the 2007 North Sea herring acoustic survey (a_w = 0.002 and b_w = 3.450). L_i is the median total length of length group i. The survey area was divided into seven subareas characterised by fish with similar length frequencies. For

each area, p_i is the proportion of herring in length group i and $\boldsymbol{\sigma}_{bs_i}$ is their backscattering cross-section, so that:

$$\overline{\boldsymbol{\sigma}}_{bs_i} = \frac{\sum_i \boldsymbol{\sigma}_{bs\,i} \cdot p_i}{\sum_i p_i} \tag{5.8}$$

Distributions of expected σ_{bs} were calculated concurrently in the Bayesian framework by directly using all the model parameter values sampled from their posterior distributions in the Markov Chain. In that way, the uncertainty in the model parameters was propagated through to the 'predicted mean backscattering cross-section', and the distribution of the parameters and any correlation between them was taken into account. Samples of σ_{bs} were then drawn from a $\log_{10}$ normal distribution with estimated precision based on SD_σ. Hence, the methods applied in this paper differ from those of previous investigations (Demer 1994, 2004; Rose et al. 2000) that estimated abundances from acoustic survey data by simple Monte Carlo simulation using respective distributions of model parameters individually: the approach used here considered *interactions* between parameters. Numbers of herring were estimated using the distributions of σ_{bs} for every depth bin integration interval and length group, and consequently compared to the official ICES (2008b) acoustic survey estimate.

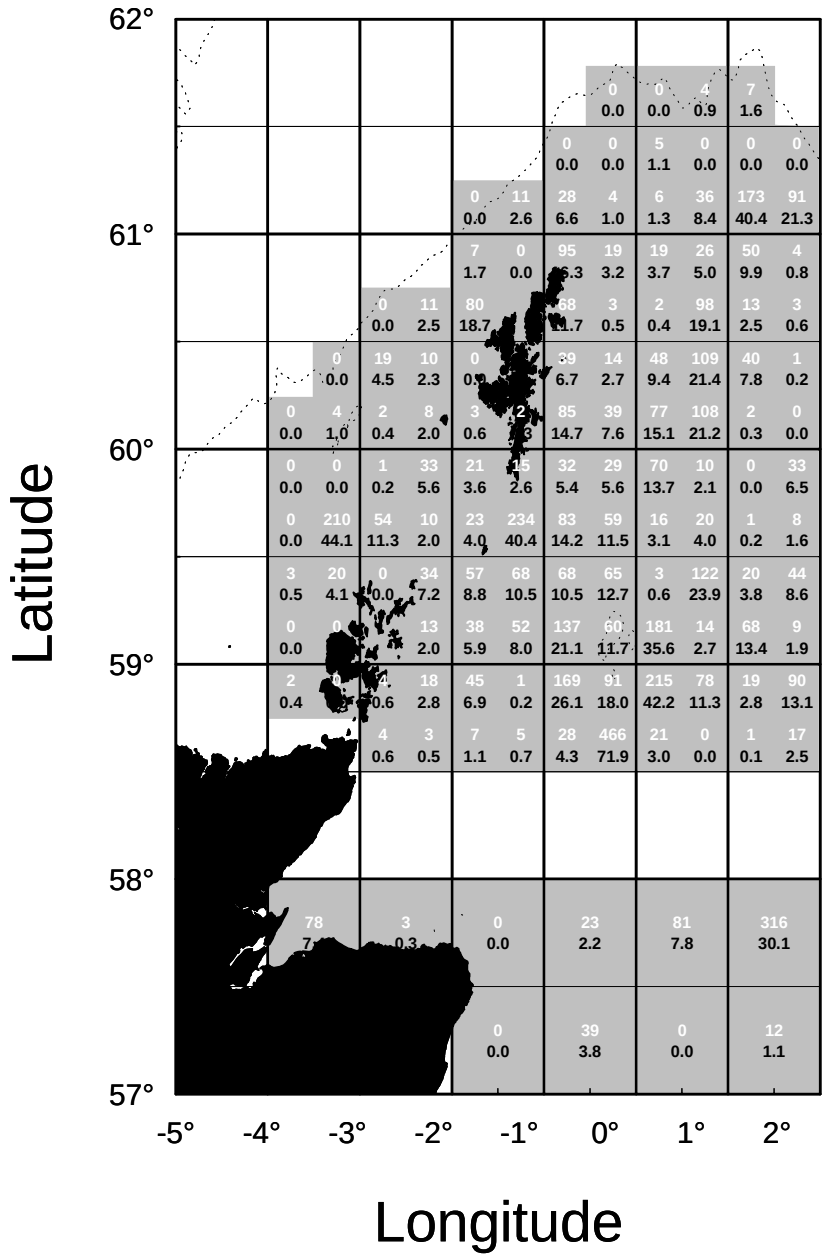

Figure 5.1 Map of the northwestern North Sea showing the survey area (grey) covered by the Scottish component of the North Sea Herring Acoustic Survey. Numbers represent the ICES acoustic-survey estimates by quarter statistical rectangle from 2007: absolute numbers (millions of fish; white, upper part of the figure) and biomass (thousand tonnes; black, lower part of the figure). The vertical axis shows degrees of latitude (North) and the horizontal axis shows degrees of longitude [East and West (-)] of the Greenwich meridian.

5.3. Results

5.3.1. Swimbladder morphology and Bayesian target strength modelling

Swimbladder morphology was modelled for water pressures equivalent to depths between 5 and 200 m. Parameter a_d described the degree of decrease of the respective swimbladder component dimension (height and width), whereas b_d was the estimated reciprocal initial size of the dimension at surface water pressures. Figure 5.2 shows the estimated values of a_d and b_d for the swimbladder cylinder components of herring #43 that were used consequently to model swimbladder dimensions in the TS model. Values of a_d increased towards the swimbladder extremities for both width and height dimensions, indicating an enhanced depth-dependent change in these sections of the swimbladder. For swimbladder width, a_d ranged from 0.004 at cylinder 25 to 0.14 for cylinders at the posterior end (Figure 5.2). For height calculations, a_d ranged from 0.02 at cylinder 23 to 0.23 at cylinder 156 (posterior end). There were no pronounced differences between estimated b_d parameters to calculate width and height dimensions. Values of b_d were highest at the anterior (1 - 10) and posterior (140 - 163) end cylinder sections, and levelled out at about 0.07 for width and at 0.05 for height for intermediate cylinders 10 to 140. There was good agreement between dimensions of cylinder approximations of the herring #43 swimbladder MRI scans and those predicted from Equation 5.5 for respective water depths (Figure 5.3).

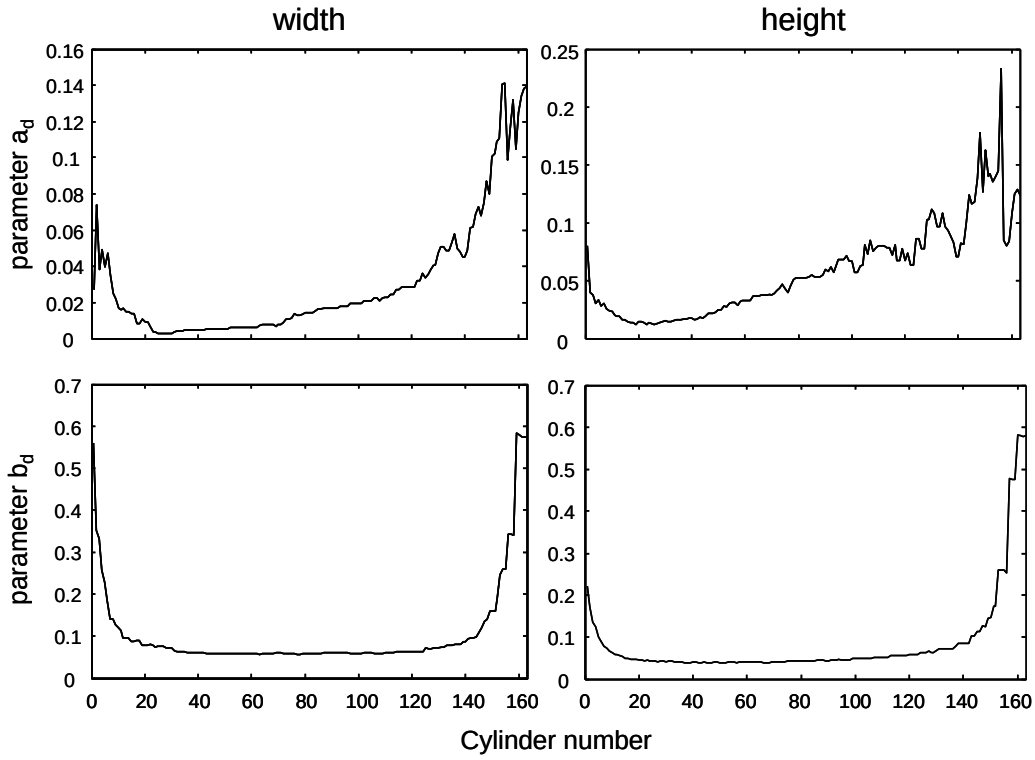

Figure 5.2 Estimated parameter values of the model (Equation 5.5) used to predict width and height of individual 0.5 mm long cylinder components (anterior end = 0) that comprise the swimbladder at a given water depth.

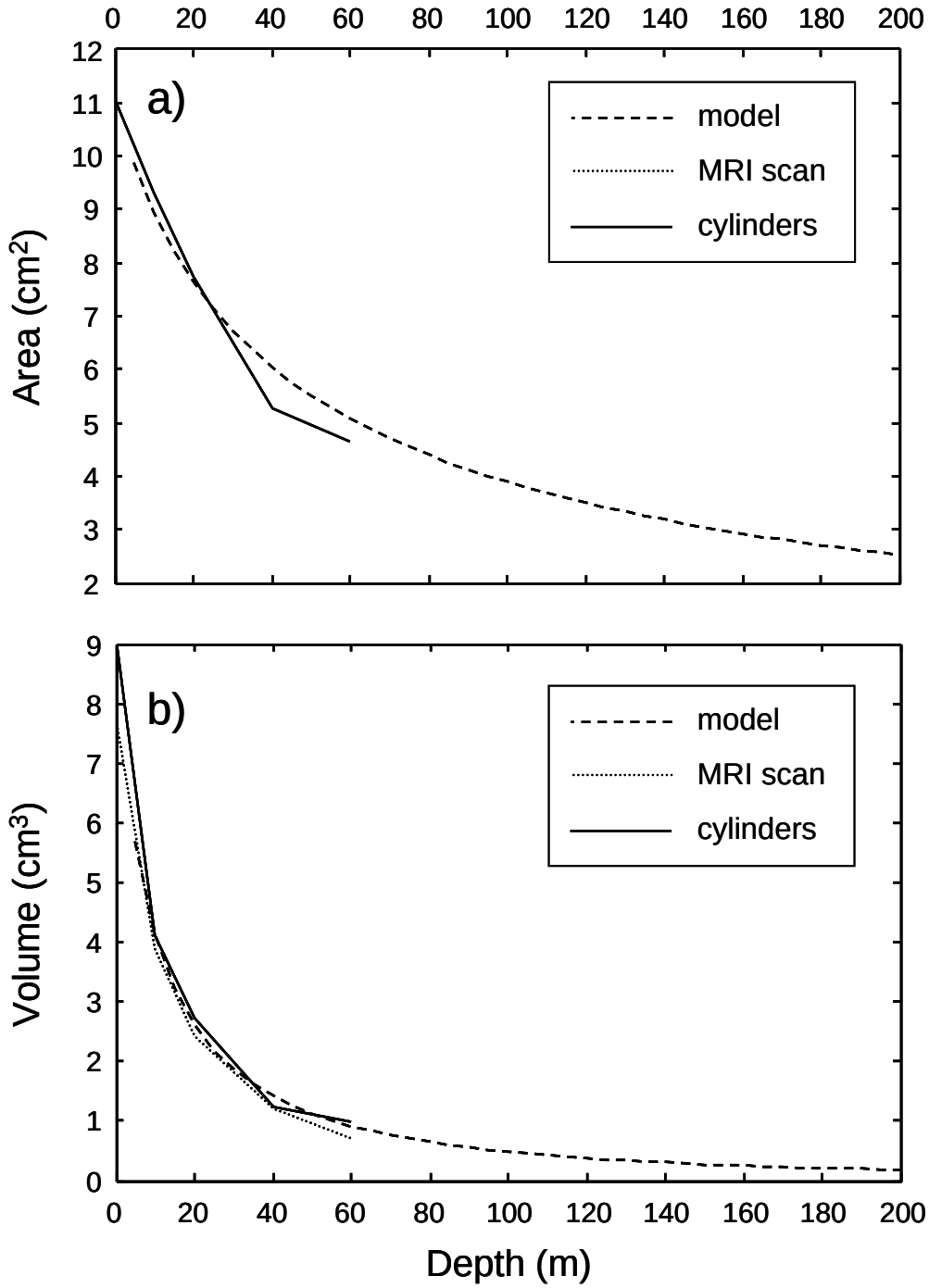

Figure 5.3 Swimbladder dorsal surface area (a) and volume (b) of herring #43 plotted against water depth. Note that the dorsal surface areas of swimbladder representations from MRI scans and from their cylinder representations are identical.

Model parameter estimation in the Bayesian framework was conducted on 200,000 samples from the posterior distributions. Posterior distributions converged after about 200 iterations, but a more conservative 'burn-in' interval (i.e. discarded values at the beginning of the MCMC chain) of 2000 iterations was chosen. The plot matrix of samples from posterior distributions of the model parameters revealed no severe autocorrelation between parameters (Figure 5.4). Possible autocorrelation could have influenced mixing and convergence of the sampled posteriors. Figure 5.5 shows the results from the Bayesian estimation of the three model parameters. The mean of the posterior distribution for the relative swimbladder volume at the surface (V_0; mean = 3.86 %) was slightly lower than that of the prior distribution (mean = 5.00 %). Conversely, there was little difference between standard deviations of the posterior (s.d. = 0.88 %) and prior (s.d. = 0.70 %) distributions. This suggests that the prior was more influential in determining the spread of the parameter estimation, whereas the mean was more affected by the data. The posterior for SD_t had a considerably greater mean and a slightly wider distribution (mean = 18.35º, s.d = 4.18º) than the prior (mean = 8.6º, s.d = 3.7º). Because of the uninformative prior assigned to SD_{TS}, all the information used to construct the posterior distribution came from the data (SD_{TS}; mean = 2.01 dB, s.d. = 0.16 dB).

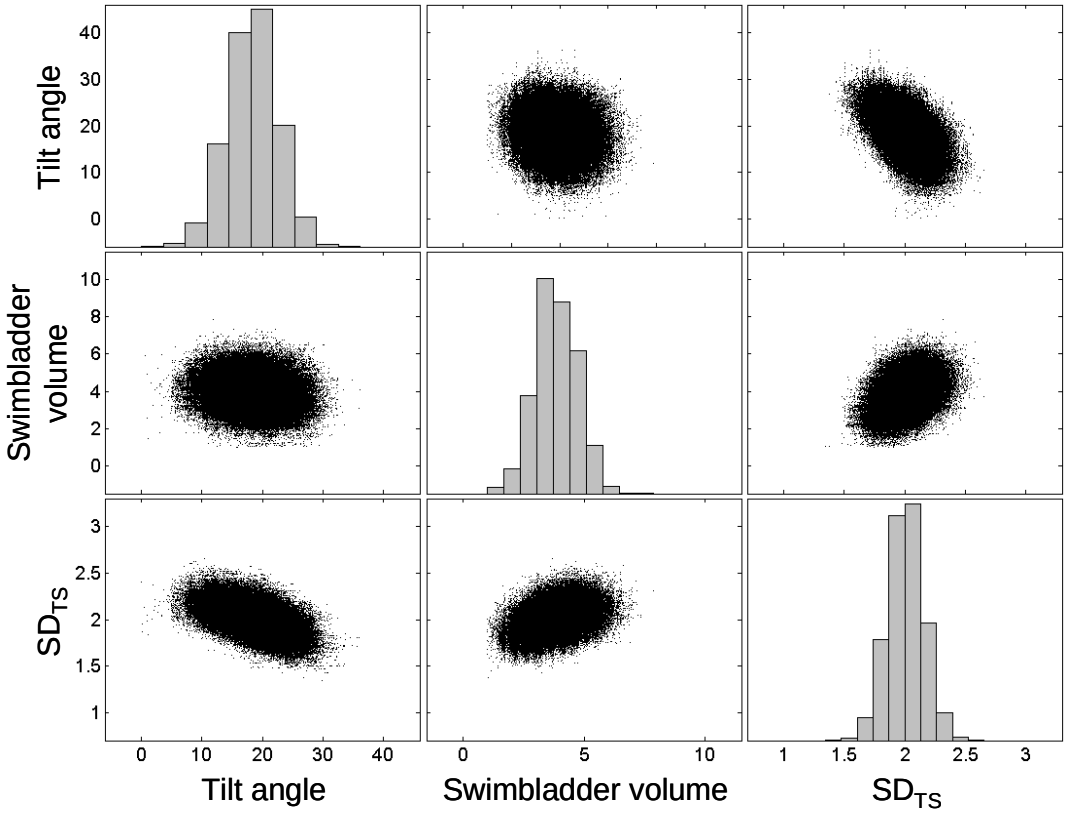

Figure 5.4 Plot matrix of 198,000 sampled posterior values of the backscattering model parameters. Histograms represent frequency distributions of parameter values given on the x-axis.

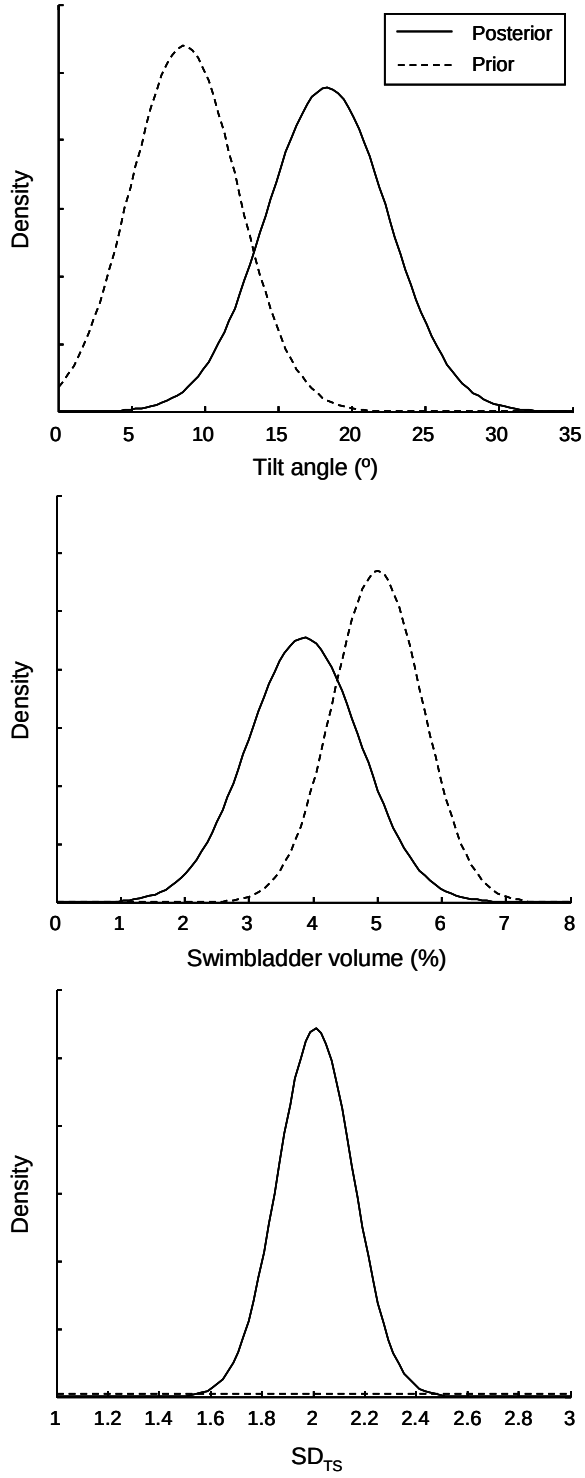

Figure 5.5 Fitted prior and posterior distributions of the backscattering model parameters. The prior for the standard deviation of the mean TS estimate (SD_{TS}) is uninformative.

Modelled mean TS values ranged from -36.2 dB for near-surface herring at the upper end of the size spectrum considered (length = 35 cm), down to -46.9 dB for herring of 19.5 cm length at a depth of 200 m (Figure 5.6a). Decrease in mean TS with depth followed an approximately linear relationship. Differences in TS between herring at surface waters and those at 200 m depth were 7.4 dB for the largest and 6.8 dB for the smallest herring analysed. Changes in TS with fish length at a given depth were not monotonically linear but followed a oscillatory pattern with smaller fish (<25 cm) having a relatively higher TS when compared to fish above 25 cm. Compared to the TS = 20 $\log_{10}$(L) - 71.2 relationship, TS values modelled here using a depth-dependent TS relationship were higher at depths ranging from surface waters to about 80 m for a 27 cm herring, and from the surface to 160 m for a 21 cm herring (Figure 5.6b). This inconsistency was due to the aforementioned non-linearity of the length-dependent TS values obtained with the model applied in this study (see KRM model output from a single fish in Figure 4.11). Generally, TS estimates of both models approximately coincide for herring of lengths between 19.5 and 23 cm at about 145 to 155 m water depth, and for 29 to 35 cm long herring at depths between 90 and 110 m. For herring of intermediate length (23 - 29 cm), the intersecting TS values of both models range over depths from about 145 to 80 m (Figure 5.6b).

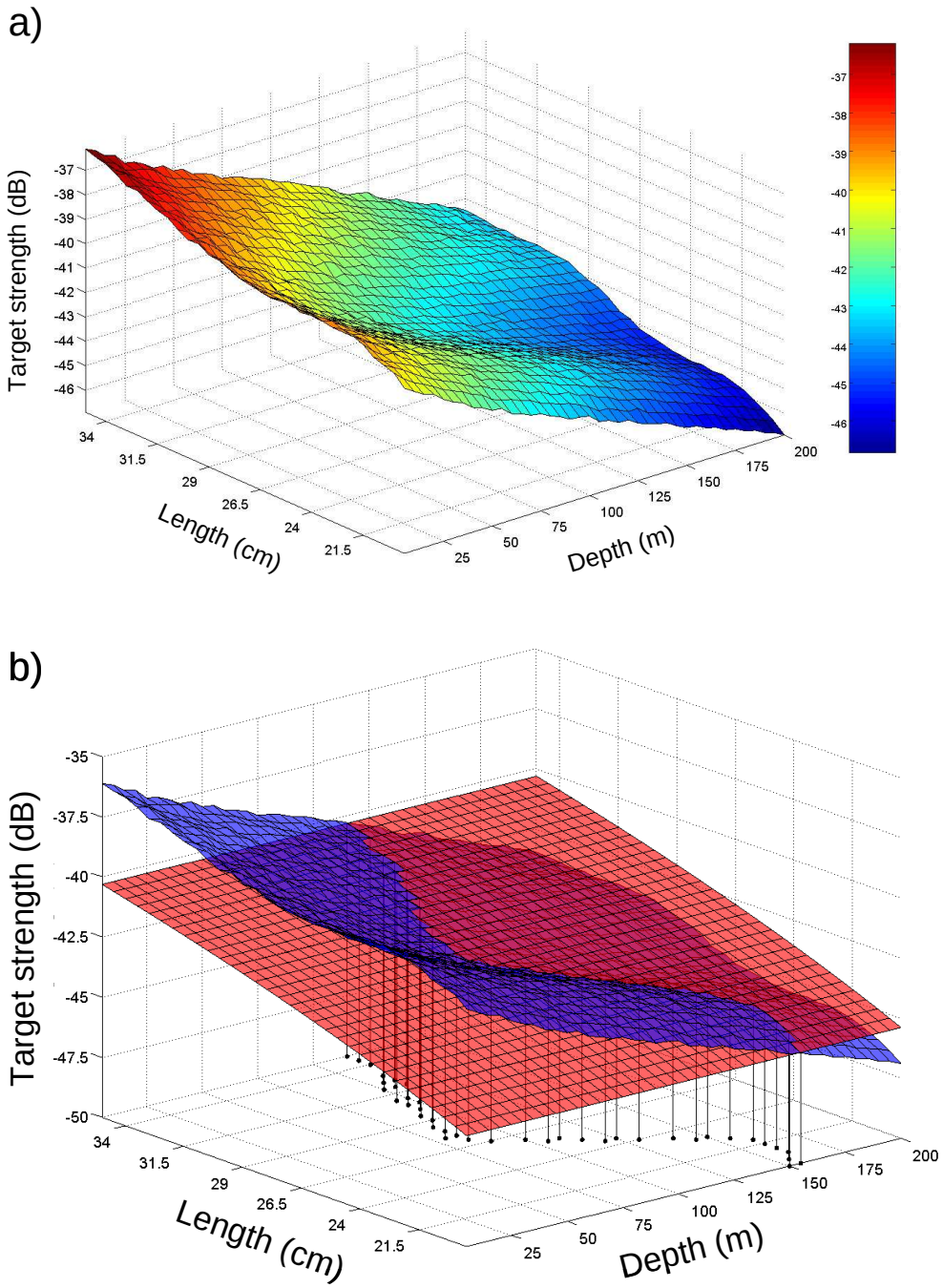

Figure 5.6 The surface of herring mean target strength (TS) values for given fish lengths and water depths predicted by the Bayesian TS model (a), also shown in blue in (b). The red surface in (b) represents TS values from the depth-independent TS-L relationship presently used to assess acoustic survey data for herring. Black circles indicate fish lengths and water depths where the two surfaces intersect.

5.3.2. Abundance and biomass estimation

Full results from the Scottish component of the North Sea Herring Acoustic Survey are given in ICES (2008b). To summarise, the estimated herring abundance for the survey area (see Figure 5.1) was 5.34×10^9 fish. This abundance estimate was derived by applying the currently accepted depth-independent TS-L relationship for herring (i.e. $TS = 20 \log_{10}(L) - 71.2$). Figure 5.7 shows a comparison between the abundance and biomass estimates of ICES (2008b) and those calculated using the TS distributions from the Bayesian methods applied in this study. The estimated normal distribution of herring abundance based on TS distributions per length group and depth bin had a mean and 95% confidence interval of 6.57×10^9 and 1.20×10^8 fish. The mean abundance calculated here is therefore 23 % higher than the ICES (2008b) estimate. Similarly, the biomass estimate determined from the Bayesian TS model had a mean and 95% confidence interval of 1.47×10^5 and 3.25×10^3 tonnes, and was just over 55 % higher than the ICES (2008b) estimate (0.94×10^5 tonnes).

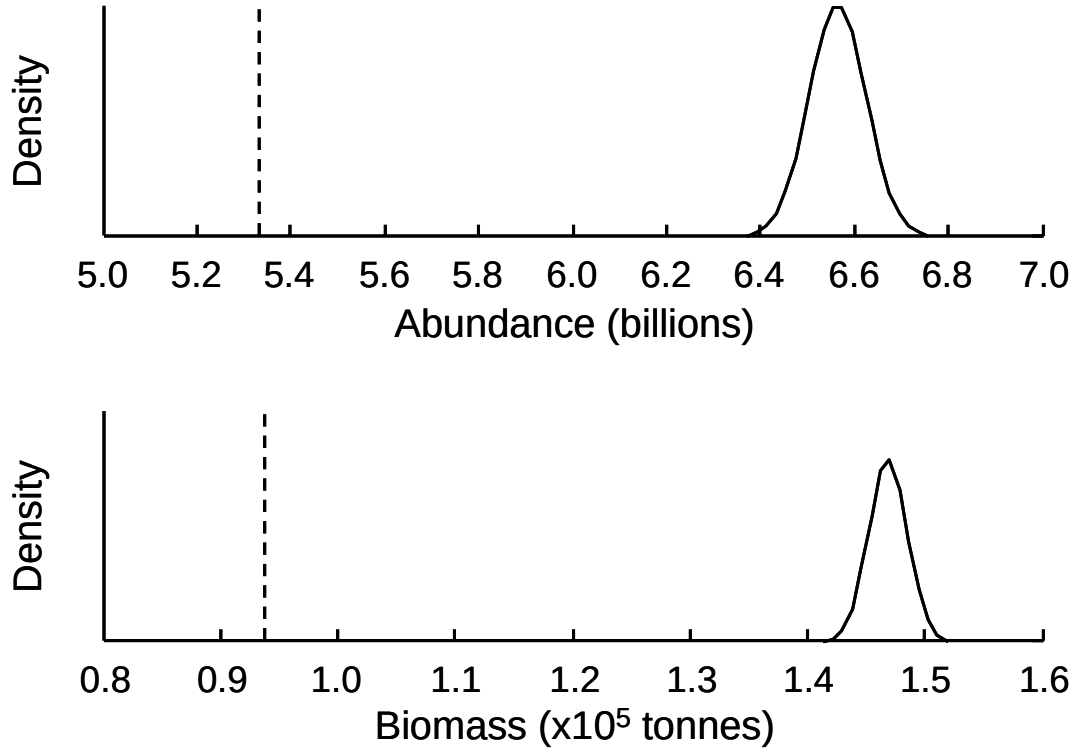

Figure 5.7 Estimated herring abundance and biomass from the Scottish component of the 2007 North Sea Herring Acoustic Survey. The dotted line represents the ICES (2008b) estimates based on the presently used target strength (TS) to fish length (L) relationship: 20 $\log_{10}$(L) - 71.2. The solid-line histograms were derived from distributions of estimated mean TS for every fish length and 5-m depth bin using a TS model and parameter estimates in a Bayesian framework.

5.4. Discussion

When interpreting results from an acoustic survey of fish it is important to recognise the stochastic nature of the target strength of the species in question and its possible dependency on a wide number of factors. It has long been known that TS is influenced significantly by fish length (Love 1977; Foote 1979), fish orientation (Nakken and Olsen 1977; Foote 1980b, 1980c) and acoustic frequency (Haslett 1965; Love 1977). Due to a lack of suitable alternatives, acoustic surveys still rely on empirically determined frequency-specific TS-L relationships, which may be biased,

particularly in the case of physostomous fish (see Chapter 4). Many of the experiments from which TS-L relationships were derived for herring were performed in only one season and neglected important biological effects such as feeding state, gonad development (Ona 1990; Ona et al. 2001) or the fact that dead/stunned fish may have different TS from live fish (McClatchie et al. 1996). On the other hand, because for the same size and species of fish, the observed TS can cover a wide range of values, acoustic surveys have relied on values of the expected mean TS (Simmonds and MacLennan 2005; Foote 1987). It is difficult to quantify the effect of a single factor on TS by means of empirical observations so, recently, theoretical TS models have been used to approximate fish backscatter and investigate its dependence on various input parameters (Clay and Horne 1994; Foote and Francis 2002; Gorska and Ona 2003a). This theoretical modelling approach offers the most promise for uncertainty due to TS variability to be estimated and incorporated into acoustic stock assessments (Demer 2004). In the current work, a theoretical approach was combined with empirical data in a Bayesian framework, to gain advantages from both approaches.

The total error in an acoustic survey is rarely quantified (Rivoirard et al. 2000; Rose et al. 2000; Tjelmeland 2002) despite the widespread use in (single-species) fish stock assessment: however, the failure to incorporate major bias is not important when one considers that the results are used almost exclusively as relative indices, not as absolute estimates. The current shift towards ecosystem-based management, however, brings with it an increased need for absolute abundance estimates of exploited species, their pray and predators, to be fed into ecosystem models as alternatives to catch-based stock assessment (Koslow 2009). The move to Bayesian methods have been identified as a valuable tool to estimate the total uncertainty in trawl surveys (Punt and Hilborn 1997; McAllister and Kirkwood 1998; Meyer and Millar 1999), and could be of use in acoustic surveys to quantify and incorporate uncertainty into abundance and biomass estimates. Results of these methods provide estimates of the random and systematic components of measurement and sampling error that are valuable for managing fisheries. Uncertainty in the advice provided by

fisheries scientists can be based on a combination of data from the stock in question and prior information of population model parameters based on data from similar fish populations (McAllister and Kirkwood, 1998). Another advantage of Bayesian methods is that uncertainty associated with model parameters can be propagated through the framework to estimate distributions of model outcomes. Based on these properties I have proposed here a Bayesian system that enables unknown parameters, or those that are difficult to estimate, to be incorporated into a conventional fish backscattering model to estimate distributions of expected TS. This can then provide a basis for estimating uncertainty associated with the TS estimate in an acoustic survey and contribute to the overall estimate of uncertainty.

The herring abundance estimates obtained in this study indicate that the uncertainty associated with this particular model is largely systematic. Assuming the ICES (2008b) estimate of herring abundance is correct, the associated accuracy of the acoustic estimate based on the Bayesian TS model was 23.0 %. This magnitude of error is in accordance with previous estimates of systematic error of the TS component in acoustic estimates of absolute abundance, where values of ±26 - ±41 % (Tesler 1989), 0 - ±50 % (Simmonds and MacLennan 2005) or 0 - ±40 % (Simmonds et al. 1992) have been reported. Factors that may have affected the accuracy of the abundance estimate in this study were the data set used to derive the model parameters and the TS model itself. The Edwards et al. (1984) data set was based on Atlantic herring captured on the Scottish west coast. These fish occupied the same geographic area and may even have consisted of fish from similar populations surveyed in the 2007 North Sea Herring Acoustic Survey. Nonetheless, the TS data set was limited in two aspects. Firstly, the herring were confined in cages and might therefore have exhibited a different behaviour to wild fish, which could have affected the TS (Simmonds and MacLennan 2005). Secondly, the water depths of the herring analysed by Edwards et al. (1984) (17.5 - 45 m) did not represent the whole depth range occupied by herring in the area covered by the Scottish component of the North Sea Herring Acoustic Survey, which may be as deep as 200 m (ICES 2008b). Similarly the morphological swimbladder data obtained from MRI scans of a North

Sea herring were based only on measurements at pressures equivalent to depths from the surface down to 60 m (see Section 4.2.2.). Hence, distributions of model parameters obtained from the Bayesian framework, based essentially on the MRI swimbladder morphology and the Edwards et al. (1984) TS data, were therefore representative of a shorter depth range than exhibited by herring in the North Sea. Even though most of the pressure induced changes in swimbladder dimensions happens within the top 60 m of the water column (Section 4.3.1.), TS values were effectively extrapolated for depth bins down to 200 m using the KRM model with the estimated model parameter distributions.

Fässler et al. (2009b) applied similar methods as described in this Chapter but used an *in situ* herring TS data set published by Ona (2003) to estimate distributions of the TS model parameters. Those data were based on Norwegian spring spawning herring as opposed to the North Sea herring data (published in Edwards et al. 1984) used in this Chapter. The TS-L relationship fitted to the whole of Ona's (2003) data set ($TS = 20 \log_{10}(L) - 67.3$) is higher by 3.9 dB than the one currently applied to estimate abundance of North Sea herring ($TS = 20 \log_{10}(L) - 71.2$). The *in situ* TS data presented by Edwards et al. 1984 was partly used to determine that North Sea herring TS-L relationship. Given these different input data, it is therefore not surprising that the Bayesian TS model described in this Chapter estimated a TS that was on average lower than the one published in Fässler et al. (2009b). This difference is reflected in the estimated posterior distributions of the model parameters. While prior parameter distributions were identical, the posterior means of SD_t and V_0 estimated in this Chapter were 2.6 times larger and 1.3 times smaller, respectively, compared to the ones presented in Fässler et al. (2009b). In terms of fish numbers, the use of Ona's (2003) TS-L relationship determined from Norwegian spring spawning herring would cause a 59.3 % reduction in estimated abundance of North Sea herring from the 2007 Scottish North Sea Herring Acoustic Survey data. Hence, because the accuracy of the Bayesian TS model is strongly dependent on the input data, acoustic survey analyses should, if at all possible, be based on reliable TS data that reflect the fish stock and species being surveyed. Since the analysis of the North Sea herring

survey data used in this Chapter was based on *in situ* TS values determined from North Sea herring, the results can be considered more accurate than those presented in Fässler et al. (2009b). Further work will have to involve collection of appropriate *in situ* TS data, ideally from wild herring (see Foote 1987), to tune the TS model and make results in this case more applicable to the herring stock surveyed. Since depth affects herring TS (see Chapter 4), it is particularly important to collect *in situ* data throughout the depth range. To improve data quality, an autonomously deployed transducer system like the one used by Ona (2003) or Pedersen et al. (2009) may be used to increase resolution and avoid detection of multiple targets (see Sawada et al. 1993) at depth. These data should ideally also be collected throughout the survey period, in the area surveyed and at various times of the day in order to take into account behavioural induced changes in TS (e.g. see Huse and Ona 1996).

Additionally, the TS model used may have been unsuitable for the species in question. The model is essentially based on a coherent addition of backscatter from interpolated elliptical cylinder approximations of the herring swimbladder and fish body shape. This improves computational efficiency and takes into account effective lateral and dorsal dimensions at a high resolution, but neglects structural details of the respective scattering body surfaces. Besides, the model does not take account of the boundary conditions at the swimbladder: it ignores the fish body component when calculating the swimbladder backscatter. Nonetheless, coherent addition is applicable in the present case, since the swimbladder is the dominant scatterer (Ding and Ye 1997; Gorska and Ona 2003a). The low accuracy of the herring abundance and biomass estimates is in sharp contrast to their high precision (CVs of 1.0 and 1.1 %, respectively), which reveals the random error associated with the TS component to be negligible. This high precision however can be attributed to the central limit theorem; since the ultimate absolute fish abundance and biomass were derived by averaging a relatively large number of estimates (Demer 2004).

Another advantage of the Bayesian model is the ability to apply a specific TS distribution to all herring schools encountered in the survey. This is of particular importance when dealing with the depth effect on herring TS. In the survey area

(Figure 5.1), NASCs were highest at depths between 100 and 150 m (Figure 5.8). At these depths, swimbladder volumes are only about 6-9 % of the size of swimbladders at the surface, resulting in significantly reduced TS values (Figure 5.6; Section 4.3.1.; Fässler et al. 2009a). Due to swimbladder compression, more fish have to contribute to the same integrated backscatter values at depth. Consequently, estimated abundance and biomass were higher when the depth-dependent TS was applied as opposed to one solely based on measurements of herring in surface waters (i.e. $TS = 20 \log_{10}(L) - 71.2$; ICES 1982). Based on the modelling results reported here, however, the relationship with depth and fish size is not trivial. From Figure 5.6 it is evident that the relationship of TS with fish length may not follow a linear pattern but be enhanced for some size ranges and vice versa. A trend of a similar nature was observed in the Edwards et al. (1984) data set (see Figure 5.9), where the TS-L relationship (Equation 3.8) of herring in shallow water (17.5 m) had a similar slope and intercept ($m = 20.7$; $b = -72.1$) to the ones of the currently used relationship (ICES 2008b; $m = 20.0$; $b = -71.2$). Conversely, the slope and intercept of the TS-L relationship fitted to the herring TS data at 45 m depth were very different ($a = 28.3$; $b = -85.9$) and deviate significantly from the $TS \propto L^2$ assumption (Foote 1979; McClatchie et al. 1996). In the case of herring, such peculiarities may be explained by the interaction between fish body and swimbladder backscatter that are both affected by either depth-dependency or an oscillating backscatter pattern (c.f. Section 3.3.2.1.). As a result, the herring at the low end of the size spectrum analysed here (~19.5 - 25 cm) had a higher TS than expected from a linear relationship. This trend was consistent with depth and gave herring within that particular size range at depths between 125 - 160 m the same TS as would be expected from the currently used TS-L relationship (Figure 5.6b). Since the majority of herring backscatter from the analysed survey area (Figure 5.1) was within this depth range (see Figure 5.8), abundance estimates obtained from the method presented here may not differ significantly from the ICES (2008b) estimate for 19.5 - 25 cm herring. Estimated TS values of larger herring (27 - 35 cm) on the other hand were similar to the ones obtained using the ICES (1982) TS-L relationship ($20 \log_{10}(L) - 71.2$) at much shallower depths (80 -

115 m). Hence, compared to the TS values presented here, their TS was overestimated by ICES (2008b) at depths where herring were typically observed (Figure 5.8). Compared to the ICES (2008b) results, the methods described in this Chapter gave higher abundance estimates of herring in the survey area. This difference was accompanied by an even higher biomass estimate due to the higher TS given to larger fish when using the ICES (1982) TS-L relationship, making them less abundant in the estimate. There is evidence for this apparent underrepresentation of large fish in the acoustic survey for herring in the North Sea: since about 2004, a block of negative residuals for estimates of older (6 - 9 year) herring from the acoustic survey index has been identified (see Figure 2.6.1.17 in ICES 2009b).

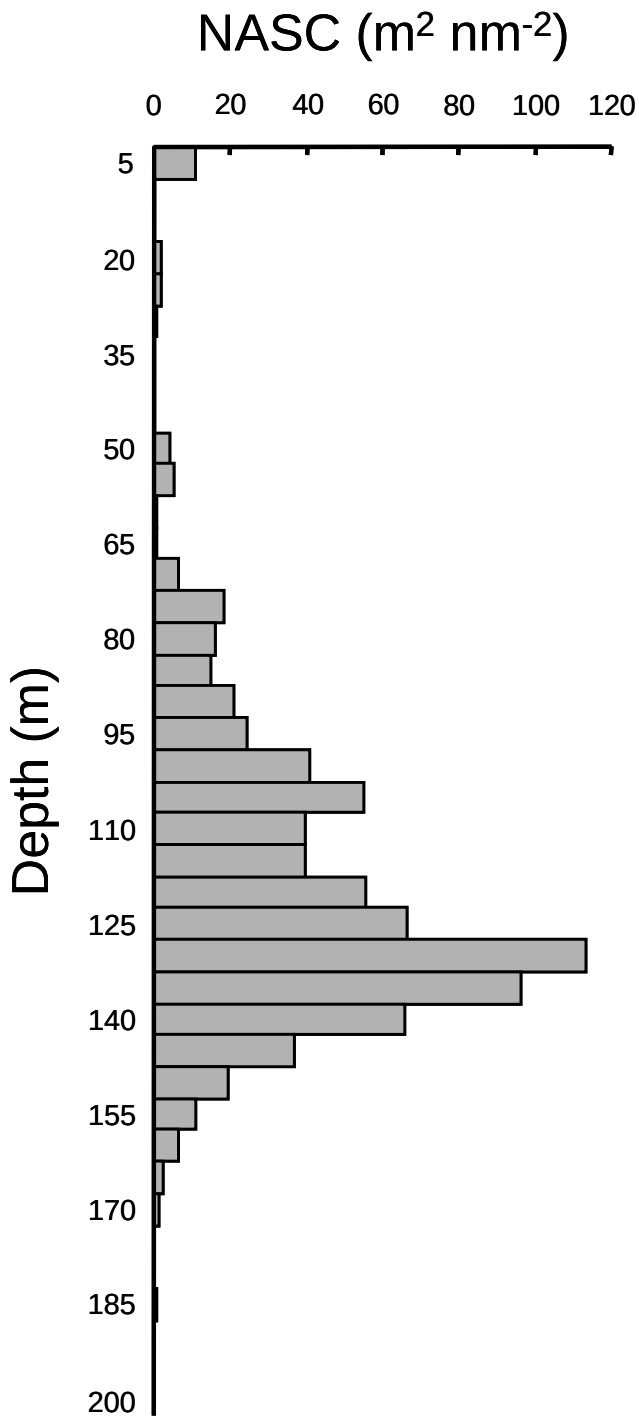

Figure 5.8 Distribution of integrated acoustic energy (Nautical Area Scattering Coefficient, NASC) allocated to herring at various 5-m depth bins in the Scottish component of the 2007 North Sea Herring Acoustic Survey.

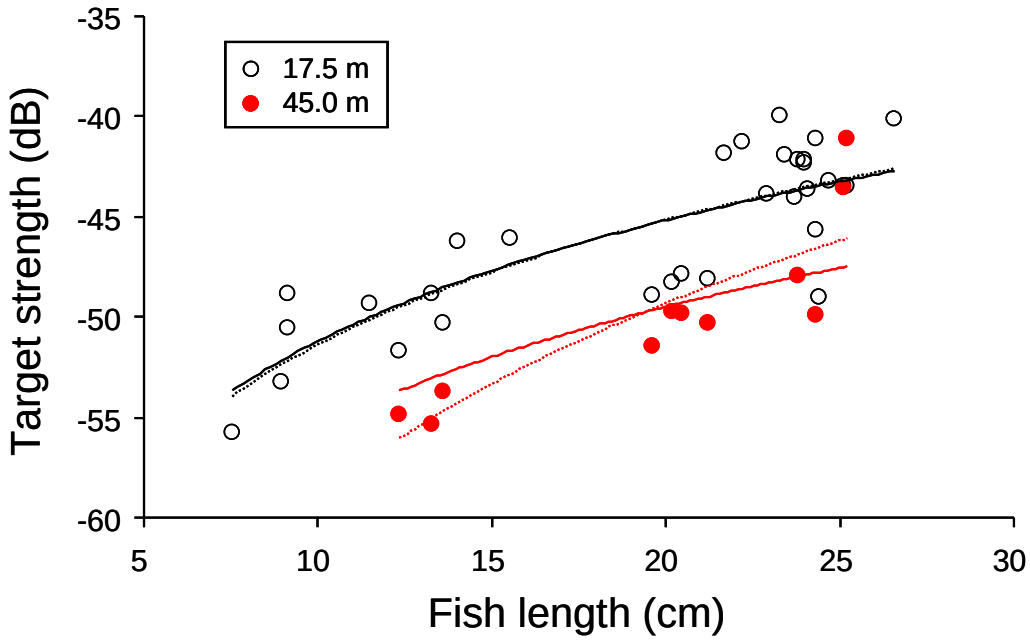

Figure 5.9 The Edwards et al. (1984) herring target strength (TS) data set used to determine distributions of parameter values in the Bayesian TS model. Values are mean TS of caged herring measured at water depths of 17.5 (white circles) and 45 m (red circles). Fitted regression lines of the form $TS = a \log_{10}(L) - b$ (dotted lines) and $TS = 20 \log_{10}(L) - b_{20}$ (solid lines), where L is the fish length in cm, are given.

There are some disadvantages of the Bayesian approach to do with selection of prior probabilities. If they are not chosen carefully they may cause bias and their construction can be tedious and require considerable effort (McAllister and Kirkwood 1998). Estimates of the prior distributions for two of the model parameters in this study were based on reliable measurements on herring and can essentially be assumed to be valid. However, in light of TS model evaluation, there is a particular need for data on tilt angle distributions. Fish behaviour, reflected in the distribution of tilt angles within an aggregation of fish, is the most important factor influencing TS and hence the accuracy of subsequent abundance estimates (Foote 1980b; Blaxter and Batty 1990; Horne and Jech 1999; Hazen and Horne 2003). Other potential drawbacks of the more complex Bayesian model are the demand on computing

resources and posterior distributions may sometimes be too complex to estimate. Nonetheless, given appropriate input data, these methods can provide an important step towards combining TS modelling approaches with *in situ* measurements and opportunistically incorporate variability associated with factors affecting TS to give an estimate of distributions of expected TS. The resulting probabilistic abundance, density and biomass estimates could become vital components in ecosystem studies and resource management.

Chapter 6

General Discussion

Fisheries management strategies have historically generally focused on maximising the catch of a single species and have usually ignored their prey, predators, bycatch species, associated habitat and other ecosystem components and interactions (Pikitch et al. 2004). As a consequence, fisheries have caused habitat destruction, and exploitation of fished species has had a far reaching impact on many other species that are part of the wider ecosystem (Pauly et al. 2005). In order to achieve a more holistic management approach, many advisory committees worldwide have suggested considering the whole ecosystem in the process of deciding on sustainable exploitation levels of the target species and rebuilding overexploited fish stocks (Marasco et al. 2007; Worm et al. 2009). Such ecosystem-based fishery management (EBFM) approaches will rely in part on accurate estimates of absolute fish stock size and its associated uncertainty to be fed into more complex food web and whole ecosystem models (Marasco et al. 2007). Underwater acoustic methods have been identified as being amongst the most promising to meet these requirements (Koslow 2009). Sound can travel through water at high speed, and high-resolution data on organism density covering vast areas of the sea can therefore be produced in a relatively short period of time (Medwin and Clay 1998). Although acoustic surveys have many advantages over the selectivity issues of net sampling surveys, they are by

definition ‘remote’ observations, and therefore there are other potential shortfalls. The major problems that contribute to the total error of estimates from acoustic surveys are concerned with identification of detected organisms and the echo produced by them - the target strength (TS) (see Table 1.1). This thesis aimed to investigate whether a range of currently applied TS models could be used to describe the TS of a herring and its variability at multiple acoustic frequencies (Chapter 2). Data from acoustic surveys for herring in the North Sea were examined and compared to model results, to attempt species identification and discrimination based on backscattering levels at different frequencies. Furthermore, morphological data from stocks of Baltic and Atlantic herring and sprat from the Baltic Sea were used to model their respective TS and explain differences previously observed in empirical data (Chapter 3). The issue of the depth-dependent TS of herring was studied by reproducing true shapes of swimbladders from MRI scans of herring under pressure (Chapter 4). Swimbladder morphology representations in 3-D were subsequently used to model the acoustic backscatter at a range of frequencies. Eventually, the TS of herring in the North Sea was modelled in a Bayesian framework (Chapter 5). Most likely distributions of model parameters were determined by fitting the model to *in situ* data. The resulting probabilistic TS was used to produce distributions of absolute abundance and biomass estimates, which were compared to official results from ICES North Sea herring stock assessment.

Acoustic backscatter models have contributed towards the understanding of how fish TS depends on a range of factors such as fish orientation, fish size and acoustic frequency (e.g. Foote 1985; Clay and Horne 1994; Hazen and Horne 2003). TS relationships currently used in fish abundance estimates from acoustic surveys, however, are exclusively based on empirical measurements. Although, the Commission for the Conservation of Antarctic Marine Living Resources (CCAMLR 2005) has adopted a TS for Antarctic krill (*Euphausia superba*) that is based on a backscattering model using the stochastic distorted-wave Born approximation (SDWBA, Demer and Conti 2005; Conti and Demer 2006). Until now, a range of data on herring TS have been collected using different methods including

insonification of dead or immobile fish, life fish constrained within cages and *in situ* measurements on fish in the wild. Available empirical data was used to define the most likely TS of herring at a given fish length at the time when acoustic surveys for herring in the North Sea were being developed. These data were not from *in situ* measurements of live herring at sea but effectively based on dead fish (Nakken and Olsen 1977) or fish confined within a small cage (diameter: 2 m, Edwards and Armstrong 1981). The issue that dead and encaged fish may produce a biased TS is well known (McClatchie et al. 1996), but in the absence of alternative solutions the results are still being used today to derive TS. Research conducted on the TS of herring has shown that significant discrepancies can occur if the size and shape of the swimbladder is affected by gonad size (Ona et al. 2001), water salinity (Fässler et al. 2008) or depth of the fish (Ona 2003; Fässler et al. 2009a). In this thesis it was shown that modelled backscatter levels of herring from the Baltic Sea were on average 2.3 dB higher than those from herring living in northeast Atlantic waters (Chapter 3). This can be attributed to differences in swimbladder sizes between the two herring stocks due to the Baltic Sea having a low salinity compared to waters of the Atlantic Ocean. Consequently, the swimbladder of herring from the Baltic Sea needs to be bigger to achieve a certain degree of buoyancy, compared to herring from, for instance, the Norwegian or North Sea. Interestingly, b_{20} values (Equation 1.11) of Norwegian spring spawning herring estimated in this Thesis (Chapter 3: b_{20} = -67.1; Chapter 4: b_{20} = -67.4) are remarkably similar to the results of Ona (2003) (b_{20} = -67.3). Given the discrepancy between these values and the one currently applied to evaluate acoustic survey data for Norwegian spring spawning herring (b_{20} = -72.1), a re-evaluation of the appropriateness of the latter may indeed be necessary. In a further investigation, morphological swimbladder dimensions of Baltic herring and sprat were found to be different (Chapter 3). Herring had a significantly larger swimbladder height at a given length compared to sprat, resulting in a modelled TS that was on average 1.2 dB stronger. Since the same TS-L relationship is currently used to estimate abundances of herring and sprat in the Baltic Sea from acoustic survey data, this approach may need to be reconsidered. Water depth, and therefore

the increase in ambient pressure, was found to have a considerable effect on the size and shape of the herring swimbladder (Chapter 4). Modelled TS values were found to be around 3 dB weaker at a depth of 50 m compared to surface waters. At 200 m, this difference was estimated to be about 5 dB. Use of the elaborate KRM model to estimate TS of realistic swimbladder shapes under pressure (see Figure 4.12b) gave results that were in good agreement with those derived from the MSB-DCM (Figure 3.6). The latter results were based on spheroid shaped swimbladder approximations, applying minimum and maximum limits of bladder compression.

Incorporating such findings into enhanced TS models will ultimately improve overall accuracy of the TS value and the derived abundance and biomass estimates. Nonetheless, the sole reliance on empirical data observed in a specific location at a specific time, to construct a TS relationship will make consideration of factors TS is dependent on immensely difficult - and will result in a model that is not universally applicable. The approach described for the first time in this thesis, combines empirical data and theoretical modelling in a Bayesian framework to produce the most likely TS under a certain situation (Chapter 5). The model, which computes the TS of herring based on its morphology, orientation, physical properties and ambient water pressure, was essentially fitted to *in situ* TS data to estimate most likely distributions of input parameters given the data. The strengths of the Bayesian framework are: its capabilities to (1) incorporate new knowledge about input parameters, should such information become available, to develop and improve prior parameter distributions. This could lead to considerably reduced uncertainty in estimated TS. (2) The data set used to fit the model can be chosen to specifically represent the survey area in question. For example, *in situ* TS data of Baltic Sea herring could be used to determine appropriate posterior distributions of model parameters for use in TS predictions for Baltic herring. These will then have particular PDFs for swimbladder volumes at the sea surface, tilt angle distributions or any other parameter that is chosen to be estimated. With use of such information, TS values could be determined dynamically for specific cases of observed fish lengths and water depths, hence increasing accuracy in subsequent abundance and biomass

estimates. (3) The Bayesian framework enables the uncertainty associated with the respective parameters to be propagated through to the final model output. This allows for the production of a probabilistic TS that can in turn be used to estimate fish abundance and biomass distributions. Ultimately, PDFs of stock sizes determined from acoustic surveys will, however, be dependent on other sources of systematic error, such as the equipment calibration, hydrographic conditions or vessel avoidance (see Chapter 1; Section 5.1). Nonetheless, the error component associated with the TS is by far the most dominant (Table 1.1; Simmonds et al. 1992). Once an acceptable stock size PDF, based on reliable determination of TS distributions, is determined, it will provide vital information about stock levels and associated uncertainties for use in stock assessment. Additionally, it could also be a key input to decision analyses for alternative management measures. For instance, McAllister and Ianelli (1997) used a Bayesian approach to estimate posterior distributions of population parameters for yellowfin sole (*Limanda aspera*) that were eventually used to evaluate trade-offs between various trawl survey designs (McAllister and Pikitch 1997). Similarly, Mäntyniemi et al. (2009) demonstrated how a Bayesian decision analysis framework could be used to determine the value of information (VoI) in having various degrees of knowledge of the functional form of the stock-recruit relationship for North Sea herring - and therefore could suggest an optimal allocation of survey resources. Such approaches could also be applied to the methods described in this thesis by estimating the level of knowledge of a particular TS model parameter value that is needed to achieve a desired (optimal) level of uncertainty in abundance and biomass estimates.

The accuracy of the Bayesian TS model outcome will be affected by the input data set. Ideally, the data set used to derive the model parameters should consist of mean *in situ* TS measurements from the same herring stock, measured in the geographic area that is being covered by the relevant acoustic survey (see Section 5.4.). This will assure applicability of the values to the wild fish observed at sea (Foote 1987). The results presented in this thesis also suggest that it is important to have TS data that cover the depth range occupied by the herring stock surveyed to minimise variability due to the effect of water pressure on swimbladder size and

shape (Chapter 4). The other factor that has a major impact on the Bayesian model parameter estimation is the TS model component. Together with the data set, it has an effect on the likelihood function of the Bayesian framework and therefore directly affects parameter estimation. Acoustic TS models have improved dramatically over the past two decades. There is a distinct move towards applying approximation solutions that can make use of the true three-dimensional shapes of various fish scattering bodies (e.g. BEM or FEM; Foote and Francis 2002; Francis and Foote 2003; ICES 2009a). Compared to models that are based on simple geometric shapes to represent scattering bodies, more sophisticated models have the potential to become more refined and are in theory able to incorporate a time domain to cover behaviour aspects such as swimming movement. With continuously improving computer processing power readily available, the choice of TS model will not be limited by time constraints either. Applicability of a particular TS model will be further enhanced by assessment of the sensitivity of its parameters by comparison to empirical measurements. Once the sensitivity of model outputs can be evaluated, their prediction power assessed statistically and values of fixed parameters determined empirically, a potential ranking system may be developed to determine the optimal choice of TS model. Incorporation of the most favourable TS model into the Bayesian model framework described here will improve overall accuracy of the TS estimate.

In order to use the depth-based Bayesian TS model to analyse acoustic data, for example from the North Sea herring acoustic survey, it is important to collect s_A stratified by depth at a resolution of maximally 5 m. Because the required processing power and software are now readily available, it would just be a matter of storing depth and species based s_A data. The required information would be the proportion of herring s_A within each sampling interval (e.g. 5 nm), for each 5 m depth interval throughout the water column. Depth-dependency of TS could be implemented into the abundance and biomass estimation by using a smoothed surface fitted to the model estimates given in Figure 5.6, to ease the applicability of the complex Bayesian TS model. To include estimates in the assessment of herring abundance for the whole North Sea stock, abundances at length would have to be calculated for the

combined survey area, instead of just parts thereof (see Chapter 5). A potential switch over to the new method applying the depth-dependent Bayesian TS model into the North Sea herring assessment would require a parallel data collection for over one generation of fish ages (approx. 5 years). At the same time other sources of error (e.g. acoustic extinction, dead zone, or multiple scatter) could also be considered. Such recommendations have now been put forward to the respective ICES working group that is responsible for planning, executing and analysing acoustic surveys for herring in the North Sea (ICES 2010).

Once more reliable absolute estimates of stock size can be determined from acoustic surveys, most importantly by reducing the systematic error associated with the TS value, they could provide important input parameters into ecosystem models, which in turn aid implementation of an EBFM. An example where acoustic methods have been an important tool in implementing ecosystem-based management is the international fishery for krill in Antarctic waters, currently managed by CCAMLR (Koslow 2009). The fishery was the first to be managed explicitly under ecosystem-based principles (Constable et al. 2000; Hewitt and Linen Low 2000). Acoustic surveys are the favourite means to assess biomass of Antarctic krill, and they have been used since the early 1980s to cover the large area over which the krill occur (Brierley et al. 1999). Several improvements have been made to the acoustic krill survey methods since they have started (Everson et al. 1990; Greene et al. 1991; Hewitt and Demer 1991). These surveys provide data for studies on krill recruitment and population dynamics (Hill et al. 2006) and form the basis of the precautionary limit on krill harvest established by CCAMLR (Hewitt and Linen Low 2000).

A number of different ecosystem model concepts have been developed over the past three decades. Generally, the ever increasing computer power has enabled construction of increasingly complex models that cover multiple trophic levels and various abiotic components. These can be seen as more holistic approaches compared to ‘fisheries models’ that focus on one or several species at the top end of the food web (e.g. MSVPA, Sparre 1991). Attempts to produce marine ‘whole ecosystem’ models include the ECOPATH with ECOSIM and ECOSPACE models (Christensen

et al. 2000; Pauly et al. 2000), the European regional seas ecosystem model (ERSEM, Baretta et al. 1995), the integrated generic bay ecosystem model (IGBEM) and Bay Model 2 (Fulton 2001), or the North Pacific Ecosystem Model for Understanding Regional Oceanography (NEMURO) and NEMURO.FISH (Werner et al. 2007). Compared to the widely applied fisheries models, the use of ecosystem models has been limited due to their higher complexity, increased data needs and uncertainty associated with predictions (Fulton et al. 2003). Nonetheless, since holistic models attempting to describe the processes of the entire ecosystem are the only models that have the potential to answer questions asked by an ecosystem based fisheries management (Hollowed et al. 2000; Mace 2001), their advantages inadvertently have to outweigh their drawbacks for now. The majority of ecosystem models focusing on mid- and high-trophic level systems apply a mass-balance model approach (e.g. ECOPATH). This essentially considers the flow of energy and biomass between various trophic levels and species are usually combined into functional groups, resulting in behaviour, age- and size-structures not being taken into account. Such model approaches have a particular advantage in that they can be assembled relatively quickly to give answers to questions regarding likely outcomes of alternative fishing policies or environmental changes that would cause shifts in the balance of trophic interactions (Pauly et al. 2000). ECOPATH models have for instance been used to predict the effect of fisheries on ecosystem maturation (Trites et al. 1999) or have shown the importance of predation by fish and marine mammals in addition to fishing mortality on a global level (Christensen 1996). Pauly and Christensen (1995) combined calculated transfer efficiencies and estimates of trophic levels of major species in world fish catches using the ECOPATH model to compute the primary production to sustain global fisheries. The “Fishing down marine food webs” concept was also identified by means of the mass-balance ecosystem model approach, showing that the weighted mean trophic level of landed fish has been declining in most areas of the world (Pauly et al. 1998 Science). Acoustic survey methods and multifrequency species identification techniques could provide vital input data for mass-balance ecosystem models in the form of biomass estimates by

trophic level. In an ideal case, mass-balance models of shelf sea ecosystems could in that way be developed in a relatively short time period by covering the area with a standard acoustic survey. Nonetheless, these models lack the spatial and temporal dimensions that are fundamental to real ecosystems and inherently contained in acoustic data. In addition, they generally lack a more fundamental description of the lowest trophic levels and therefore fail to be useful to assess effects of climatic variability on recruitment (Koslow 2009). The more sophisticated dynamic ecosystem models (e.g. ECOSPACE or NEMURO) describe spatial and temporal distribution of trophic groups that characterise an underlining food web corresponding to different habitat types. Such sophisticated, more realistic models may combine hydrodynamic, biogeochemical and fish models, and have the potential to address issues related to climate change. The ECOSPACE model has been used to look at effects of marine protected areas (MPAs) on fish production and distribution (Walters et al. 2000). Megrey et al. (2007) used the NEMURO to look at how the different life histories of Pacific saury (*Cololabis saira*) and herring (*Clupea harengus pallasi*) might influence growth responses to different climate characteristics. Unfortunately, more dynamic models of ecosystems still need much work due to their greater complexity and many more parameters. A major limitation still is the incomplete understanding of how fish interact with the environment (Koslow 2009) - a problem that will undermine any accurate biomass estimate on a high-resolution temporal and spatial scale derived from acoustic survey data.

Further investigations into TS variability will have to take into account ongoing technological developments. New multi-beam sonars (e.g. Simrad ME70) with angular swaths of up to 180º will insonify fish at a far greater range of incidence angles compared to single beam echosounders traditionally used on surveys (Burwen et al. 2007; Henderson et al. 2008; Berger et al. 2009; Doray et al. 2009; Weber et al. 2009). Coupled with depth-dependent changes in swimbladder morphology, TS variability will be enhanced and the development of 3-D TS models will become vital in order to produce a reasonably accurate abundance estimate. Nishimori et al. (2009) described a three-dimensional echo-integration method (i.e. ‘3DEI’) to analyse data

obtained from a quantitative scanning sonar (Furuno FSV-30). They used a prolate spheroid model assuming distributions of fish orientations relative to the sonar beam to estimate the average backscattering cross-section of individual fish within a school. Analyses of data from a herring school revealed that the estimation of total school backscattering cross-section and the number of fish contained within the school was primarily dependent on the assumed orientation distribution. Using a similar principle, Cutter et al. (2009) reported on a method to derive orientation distributions of Antarctic krill (*Euphausia superba*) from multi-beam echosounder data, assuming backscattering intensities at various tilt angles predicted from a DWBA model. The development of accurate TS models to achieve robust backscattering estimates at the full range of potential insonification angles will especially be challenging for physostomes, where depth effects play an additional important role (Chapter 4; Fässler et al. 2009a; Pedersen et al. 2009). Once the pressure-related changes in swimbladders dimensions of physostomes can be satisfactorily described, additional data on swimbladder volume will be essential to make any model-based TS predictions. One would have to assume that 3-D swimbladder dimensions can be linked to a given swimbladder volume, which in turn is affected by water pressure and/or amount of gas contained within. In that way, the TS could be modelled based on *in situ* swimbladder volume measurements and morphological reconstructions from, for instance, MRI scans of swimbladders under pressure. A promising approach that can provide *in situ* estimates of swimbladder volume is the use of low frequency acoustics to exploit the resonance features of the swimbladder (Nero et al. 2004, 2007). If the low frequency backscatter signals are explored with broadband technology, the distinct shape and position of the swimbladder resonance peak reveals information about swimbladder size and thus also fish size with little ambiguity (Stanton 2009; Stanton and Chu 2009; Stanton et al. 2009). Furthermore, at the low frequencies where swimbladders of herring typically exhibit a resonance peak (1 - 10 kHz), echoes are not strongly affected by the orientation of the fish. Therefore, reliance on dubious assumptions about tilt angle distributions required for interpretation of backscatter at high frequencies typically used in fish surveys can be

avoided. Research by Stanton and Chu (2009) and Stanton et al. (2009) demonstrated the potential of an ‘off the shelf’ low frequency broadband (1.7 - 100 kHz) system to investigate scattering characteristics of herring schools over Georges Bank. Resonance of observed herring swimbladders was at approximately 3.7 kHz. Interestingly, encountered herring schools over a 1.5 km transect exhibited the same resonance frequency but different volume backscattering strengths. From the combined information it was evident that the herring had similar swimbladder volumes (and presumably similar lengths), however, they appeared in patches of different numerical densities. Furthermore, using backscattering models, together with the length information obtained from the low frequency data, the volume backscattering strength could be converted directly into numerical densities. Reliable TS estimates at multiple incidence angles will make multi-beam sonars useful tools to provide quantitative acoustic data at higher spatial resolution. Additionally, surveys based on localised transects could greatly benefit if accompanied by techniques such as the Ocean Acoustic Waveguide Remote Sensing (OAWRS, Makris et al. 2006; Makris et al. 2009) system. OAWRS allows an instantaneous imaging of the ocean over thousands of square kilometres, thus providing valuable data on spatial species distributions.

A combination of the aforementioned methods may reduce uncertainty in interpreting backscatter data and provide accurate absolute estimates of herring stock sizes by using: (1) high-resolution representations of swimbladders under pressure as input data for fully 3-D TS models, (2) multi-beam echosounders to increase sampling volume and complement data from traditional single-beam echosounders, and (3) low-frequency broadband systems to provide unambiguous *in situ* information on swimbladder and fish size and fish packing densities.

References

Aglen, A. (1994). Sources of error in acoustic estimation of fish abundance, pp 107-133. In: A. Fernö, and S. Olsen [ed.], Marine Fish Behaviour in Capture and Abundance Estimation. Fishing News Books, Oxford.

Agnew, D., Pearce, J., Pramod, G., Peatman, T., Watson, R., Beddington, J.R., Pitcher, T.J. (2009). Estimating the worldwide extent of illegal fishing. PLoS One 4: e4570.

Aidos, I., van der Padt, A., Luten, J.B., Boom, R.M. (2002). Seasonal changes in crude and lipid composition of herring fillets, byproducts, and respective produced oils. Journal of Agriculture and Food Chemistry 50: 4589-4599.

Andreeva, I.B. (1964). Scattering of sound by air bladders of fish in deep sound-scattering ocean layers. Soviet Physics Acoustics 10: 17-20.

Axenrot, T., Ogonowski, M., Sandström, A., Didrikas, T. (2009) Multifrequency discrimination of fish and mysids. ICES Journal of Marine Science 66: 1106-1110.

Bailey, M.C., Maravelias, C.D., and Simmonds, E.J. (1998). Changes in the distribution of autumn spawning herring (*Clupea harengus* L.) derived from annual acoustic surveys during the period 1984-1996. ICES Journal of Marine Science 55: 545-555.

Bailey, R.S., Simmonds, E.J. (1990). The use of acoustic surveys in the assessment of the North Sea herring stock and a comparison with other methods. Rapports et Procès-Verbaux des Réunions du Conseil International pour l'Exploration de la Mer 189 : 9-17.

Bakun, A. (2006). Wasp-waist populations and marine ecosystem dynamics: Navigating the "predator pit" topographies. Progress in Oceanography 68: 271-288.

Barange, M. (1994). Acoustic identification, classification and structure of biological patchiness on the edge of the Agulhas Bank and its relationship to frontal features. South African Journal of Marine Science 14: 333-347.

Baretta, J.W., Ebenhoh, W., Ruardij, P. (1995). The European Regional Seas Ecosystem Model: a complex marine ecosystem model. Netherlands Journal of Sea Research 33: 233-246.

Bayes, T. (1763). Essay towards solving a problem in the doctrine of chances. (Reprinted in) Biometrika (1958) 45: 293-315.

Beare, D.J., Reid, D.G., Petitgas, P. (2002). Spatio-temporal patterns in herring (Clupea harengus L.) school abundance and size in the northwest North Sea: modelling space–time dependencies to allow examination of the impact of local school abundance on school size. ICES Journal of Marine Science 59: 469-479.

Beaugrand, G. (2004). The North Sea regime shift: Evidence, causes, mechanisms and consequences. Progress in Oceanography 60: 245-262.

Beltestad, A.K. (1974). Beiteatferd, vertikalvandring of stimdannelse hos-gruppe sild (*Clupea harengus* L.) i relasjon til lysintensiteten. PhD thesis. University of Trømso.

Berger, L., Poncelet, C., Trenkel, V. (2009). A method for reducing uncertainty in estimates of fish-school frequency response using data from multifrequency and multibeam echosounders. ICES Journal of Marine Science 66: 1155-1161.

Bethke, E., Arrhenius, F., Cardinale, M., Håkansson, N. (1999). Comparison of the selectivity of three pelagic sampling trawls in a hydroacoustic survey. Fisheries Research 44: 15-23.

Beverton, R.J.H. (1990). Small marine pelagic fish and the threat of fishing; are they endangered? Journal of Fish Biology 37: 5-16.

Bignert, A., Nyberg, E., Asplund, L., Eriksson, U., Wilander, A., Haglund, P. (2007). Metaller och organiska miljögifter i marin biota, trend- och områdesövervakning. Sakrapport, Swedish Museum of Natural History, Stockholm.

Blaxter JHS (1985). The herring: a successful species? Canadian Journal of Fisheries and Aquatic Sciences 42: 21-30.

Blaxter, J.H.S., Batty, R.S. (1984). The herring swimbladder: loss and gain of gas. Journal of the Marine Biological Association of the United Kingdom 64: 441-459.

Blaxter, J.H.S., Batty, R.S. (1990). Swimbladder "behaviour" and target strength. Rapports et Procès-Verbaux des Réunions du Conseil International pour l'Exploration de la Mer 189: 233-244.

Blaxter, J.H.S., Denton, E.J., Gray, J.A.B. (1979). The herring swimbladder as a gas reservoir for the acoustico-lateralis system. Journal of the Marine Biological Association of the United Kingdom 59: 1-10.

Blaxter, J.H.S., Hunter, J.R. (1982). The biology of the clupeoid fishes. Advances in Marine Biology 20: 1-223.

Bodholt, H., Ness, H., Solli, H. (1989). A new echo-sounder system. Proceedings of the Institute of Acoustics 11: 123-130.

Bone, Q., Marshall, N.B., Blaxter, J.H.S. (1995). Biology of fishes, 2nd edition. Blackie, N.Y.

Boswell, K.M., Roth, B.M., Cowan, Jr J.H. (2009). Simulating the effects of side-aspect fish orientation on acoustic biomass estimates. ICES Journal of Marine Science 66: 1398-1403.

Box, G.E.P., Tiao, G.C. (1973). Bayesian inference in statistical analysis. Wilez, New York.

Brawn, V.M. (1962). Physical properties and hydroacoustic function of the swimbladder of herring (*Clupea harengus* L.). Journal of the Fisheries Research Board of Canada 19: 635-656.

Brawn, V.M. (1969). Buoyancy of Atlantic and Pacific herring. Journal of the Fisheries Research Board of Canada 26: 2077-2091.

Brierley, A.S., Watkins, J.L., Goss, C., Wilkinson, M.T., and Everson, I. (1999). Acoustic estimates of krill density at South Georgia, 1981 to 1998. CCAMLR Science 6: 47-57.

Burwen, D.L., Nealson, P.A., Fleischman, S.J., Mulligan, T.J., Horne, J.K. (2007). The complexity of narrowband echo envelopes as a function of fish side-aspect angle. ICES Journal of Marine Science 64: 1066-1074.

CCAMLR. 2005. Report of the first meeting of the subgroup on acoustic survey and analysis methods. SC-CCAMLR-XXIV/BG/3.

Cardinale, M., Arrhenius, F. (2000). Decreasing weight-at-age of Atlantic herring (*Clupea harengus*) from the Baltic Sea between 1986 and 1996: a statistical analysis. ICES Journal of Marine Science 57: 882-893.

Christensen, V. (1996). Managing fisheries involving predator and prey species. Review in Fish Biology and Fisheries 6: 1-26.

Christensen, V., Walters, C.J., Pauly, D. (2000). Ecopath with Ecosim: A User's Guide. Fisheries Centre, University of British Columbia. Vancouver, Canada.

Chu, D., Stanton, T.K., Wiebe, P.H. (1992). Frequency dependence of sound backscattering from live individual zooplankton. ICES Journal of Marine Science 49: 97-106.

Clay, C.S. (1983). Deconvolution of the fish scattering PDF from the echo PDF for a single transducer sonar. Journal of the Acoustical Society of America 73: 1989-1994.

Clay, C.S. (1991). Low-resolution acoustic scattering models: Fluid-filled cylinders and fish with swim bladders. Journal of the Acoustical Society of America 89: 2168-2179.

Clay, C.S. (1992). Composite ray-mode approximations for backscattered sound from gas-filled cylinders and swimbladders. Journal of the Acoustical Society of America 92: 2173-2180.

Clay, C.S., Horne, J.K. (1994). Acoustic models of fish: the Atlantic cod (*Gadus morhua*). Journal of the Acoustical Society of America 96: 1661-1668.

Constable, A.J., de la Mare, W.K., Agnew, D.J., Everson, I., Miller, D. (2000). Managing fisheries to conserve the Antarctic marine ecosystem: practical implementation of the Convention on the Conservation of Antarctic Marine Living Resources (CCAMLR). ICES Journal of Marine Science 57: 778-791.

Conti, S.G., Demer, D.A. (2006). Improved parameterization of the SDWBA for estimating krill target strength. ICES Journal of Marine Science 63: 928-935.

Corten, A. (2000). A possible adaptation of herring feeding migrations to a change in timing of the *Calanus finmarchicus* season in the eastern North Sea. ICES Journal of Marine Science 57: 1261-1270.

Craig, R.E., Forbes, S.T. (1969). Design of a sonar for fish counting. Fiskeridirektoratets skrifter serie havundersokelser 15: 210-219.

Crawford, R.J.M., Shannon, L.V., and Pollock, D.E. (1987). The Benguela Ecosystem. 4. The major fish and invertebrate resources, pp. 353-505. In: M. Barnes [ed.], Oceanography and Marine Biology: An Annual Review 25. Aberdeen University Press.

Cury, P., Bakun, A., Crawford, R.J.M., Jarre, A., Quinones, R.A., Shannon, L.J., Verheye, H.M. (2000). Small pelagics in upwelling systems: patterns of interaction and structural changes in "wasp-waist" ecosystems. ICES Journal of Marine Science 57: 603-618.

Cury, P.M., Christensen, V. (2005). Quantitative ecosystem indicators for fisheries management. ICES Journal of Marine Science 62: 307-310.

Cushing, D.H. (1996). Towards a science of recruitment in fish populations. Ecology Institute, Oldendorf/Luhe, Germany.

Cutter, G.R., Renfree, J.S., Cox, M.J., Brierley, A.S., Demer, D.A. (2009). Modelling three-dimensional directivity of sound scattering by Antarctic krill: progress towards biomass estimation using multibeam sonar. ICES Journal of Marine Science 66: 1245-1251.

Degnbol, P., Lassen, H., Stæhr, K.J. (1985). *In situ* estimates of target strength of herring and sprat at 38 and 120 kHz. Dana 5: 45-54.

Demer, D.A. (1994). Accuracy and precision of acoustic surveys of Antarctic krill. Ph.D. thesis, University of California, San Diego.

Demer, D.A. (2004). An estimate of error for the CCAMLR 2000 survey estimate of krill biomass. Deep-Sea Research Part II 51: 1237-1251.

Demer, A.D., Conti, S.G. (2005). New target-strength model indicates more krill in the Southern Ocean. ICES Journal of Marine Science 62: 25-32.

Demer, D.A., Martin, L. (1995). Zooplankton target strength: Volumetric or areal dependence? Journal of the Acoustical Society of America 98: 1111-1118.

Didrikas, T. (2005). Estimation of *in situ* target strength of the Baltic Sea herring and sprat. Dept. Systems Ecology, Stockholm University, Sweden.

Didrikas, T., Hansson, S. (2004). *In situ* target strength of the Baltic Sea herring and sprat. ICES Journal of Marine Science 61: 378-382.

Diner, N. (2001). Correction on school geometry and density: approach based on acoustic image simulation. Aquatic Living Resources 14: 211-222.

Ding, L., Ye, Z. (1997). A method for acoustic scattering by slender bodies. Comparison with laboratory measurements. Journal of the Acoustical Society of America 102: 1977-1981.

Do, M.A., Surti, A.M. (1990). Estimation of dorsal aspect target strength of deep-water fish using a simple model of swimbladder backscattering. Journal of the Acoustical Society of America 87: 1588-1596.

Doray, M., Berger, L., Trenkel, V. (2009) Influence of beam-angle incidence on fish acoustic backscatter recorded with ME70 multibeam echosounders. ICES CM /I:08.

Edwards, J.I., Armstrong, F. (1981). Measurement of the target strength of live herring and mackerel. ICES CM /B:26.

Edwards, J.I., Armstrong, F. (1983). Measurement of the target strength of live herring and mackerel. FAO Fisheries Report 300: 69-77.

Edwards, J.I., Armstrong, F. (1984). Target strength experiments on caged fish. Scottish Fisheries Bulletin 48: 12-20.

Edwards, J.I., Armstrong, F., Magurran, A.E., Pitcher, T.J. (1984). Herring, mackerel and sprat target strength experiments with behavioural observations. ICES CM /B:34.

Edwards, M., Richardson, A.J. (2004). Impact of climate change on marine pelagic phenology and trophic mismatch. Nature 430: 881-884.

Edwards, M., Beaugrand, G., Reid, P.C., Rowden, A.A., Jones, M.B. (2002). Ocean climate anomalies and the ecology of the North Sea. Marine Ecology Progress Series 239: 1-10.

Ehrenberg, J.E. (1973). Estimation of the intensity of a filtered Poisson process and its application to the acoustic assessment of marine organisms. University of Washington Sea Grant Publications WSG 73-2.

Ehrenberg, J.E. (1974). Two applications for a dual beam transducer in hydroacoustic fish assessment systems. Engineering in the Ocean Environment. IEEE, New York, Halifax, Nova Scotia, pp 152-155.

Ehrenberg, J.E., Torkelson, T.C. (1996). Application of dual-beam and split-beam target tracking in fisheries acoustics. ICES Journal of Marine Science 53: 329-334.

Everson, I. (1982). Diurnal variations in mean volume backscattering strength of an Antarctic krill (*Euphausia superba*) patch. Journal of Plankton Research 4: 155-162.

Everson, I., Watkins, J.L., Bone, D.G., Foote, K.G. (1990). Implications of a new acoustic target strength for abundance estimates of Antarctic krill. Nature 345: 338-340.

Everson, I., Tarling, G.A., Bergström, B. (2007). Improving acoustic estimates of krill: experience from repeat sampling of northern krill (*Meganyctiphanes norvegica*) in Gullmarsfjord, Sweden. ICES Journal of Marine Research 64: 39-48.

FAO (2008a). The state of world fisheries and aquaculture. FAO, Rome.

FAO (2008b). FishStat PLUS. FAO, Rome.

Farquhar, G.B. (1977). Biological sound scattering in the oceans: a review, pp. 493-527. In: N.R. Andersen, B.J. Zahuranec [ed.], Oceanic Sound scattering Prediction. Plenum, N.Y.

Fässler, S.M.M., Fernandes, P.G., Semple, S.I.K. and Brierley, A.S. (2009a). Depth-dependent swimbladder compression in herring *Clupea harengus* observed using magnetic resonance imaging. Journal of Fish Biology 74: 296-303.

Fässler, S.M.M., Brierley, A.S., Fernandes, P.G. (2009b). A Bayesian approach to estimating target strength. ICES Journal of Marine Science 66: 1197-1204.

Fässler, S.M.M., Gorska, N. (2009). On the target strength of Baltic clupeids. ICES Journal of Marine Science 66: 1184-1190.

Fässler, S.M.M., Gorska, N., Ona E., Fernandes, P.G. (2008). Differences in swimbladder volume between Baltic and Norwegian spring spawning herring: consequences for mean target strength. Fisheries Research 92: 314-321.

Fässler, S.M.M., Santos, R., García-Núñez, N., Fernandes, P.G. (2007). Multifrequency backscattering properties of Atlantic herring (*Clupea harengus*) and Norway pout (*Trisopterus esmarkii*). Canadian Journal of Fisheries and Aquatic Sciences 64: 362-374.

Fernandes, P.G. (2009). Classification trees for species identification of fish-school echotraces. ICES Journal of Marine Science 66: 1073-1080.

Fernandes, P.G., Simmonds, E.J. (1996). Practical approaches to account for receiver delay and the TVG start time in the calibration of the Simrad EK500. ICES CM /B:17.

Fernandes, P.G., Korneliussen, R.J., Lebourges-Dhaussy, A., Massé, J., Iglesias, M., Diner, N., Ona, E., et al. (2006). The SIMFAMI project: species identification methods from acoustic multifrequency information. Final Report to the EC No. Q5RS-2001-02054. FRS Marine Laboratory Aberdeen, Aberdeen, Scotland, UK.

Feuillade, C., Nero, R.W. (1998). A viscous-elastic swimbladder model for describing enhanced-frequency resonance scattering from fish. Journal of the Acoustical Society of America 103: 3245-3255.

Flath, L.E., Diana, J.S. (1985). Seasonal energy dynamics of the alewife in southeastern Lake Michigan. Transactions of the American Fisheries Society 114: 328-337.

Fofonoff, N.P., Millard, R.C. (1983). Algorithms for computation of fundamental properties of seawater. UNESCO Technical Papers in Marine Science, 44. UNESCO Division of Marine Science, Paris.

Foote, K.G. (1979). On representations of length dependence of acoustic target strengths of fish. Journal of the Fisheries Research Board of Canada 36: 1490-1496.

Foote, K.G. (1980a). Importance of the swimbladder in acoustic scattering by fish: A comparison of gadoid and mackerel target strengths. Journal of the Acoustical Society of America 67: 2084-2089.

Foote, K.G. (1980b). Effect of fish behaviour on echo energy: the need for measurements of orientation distributions. ICES Journal of Marine Science 39: 193-201.

Foote, F.G. (1980c). Averaging of fish target strength functions. Journal of the Acoustical Society of America 67: 504-515.

Foote, K.G. (1985). Rather-high-frequency sound scattering by swimbladdered fish. Journal of the Acoustical Society of America 78: 688-700.

Foote, K.G. (1987). Fish target strengths for use in echo integrator surveys. Journal of the Acoustical Society of America 82: 981-987.

Foote, K.G., Aglen, A., Nakken, O. (1986). Measurement of fish target strength with a split beam echo sounder. Journal of the Acoustical Society of America 80: 612-621.

Foote, K.G., Francis, D.I.T. (2002). Comparing Kirchhoff-approximation and boundary-element models for computing gadoid target strength. Journal of the Acoustical Society of America 111: 1644-1654.

Foote, K.G., Hansen, K.A., Ona, E. (1993). More on the frequency dependence of target strength of mature herring. ICES CM /B:30.

Foote, K.G., Kristensen, F.H., Solli, H. (1984). Trial of a new, split-beam echo sounder. ICES CM /B:21.

Foote, K.G., Traynor, J.J. (1988). Comparison of walleye pollock target strength estimates determined from *in situ* measurements and calculations based on swimbladder form. Journal of the Acoustical Society of America 83: 9-17.

Francis, D.T.I. (1993). A gradient formulation of the Helmholtz integral equation for acoustic radiation and scattering. Journal of the Acoustical Society of America 93: 1700-1709.

Francis, D.T.I., Foote, K.G. (2003). Depth-dependent target strength of gadoids by the boundary element method. Journal of the Acoustic Society of America 114: 3136-3146.

Frederiksen, M., Edwards, M., Richardson, A.J., Halliday, N.C., Wanless, S. (2006). From predation to top predators: bottom-up control of a marine food web across four trophic levels. Journal of Animal Ecology 75: 1259-1268.

Frid, C.L.J., Paramor, O.A.L., Scott, C.L. (2006). Ecosystem-based management of fisheries: is science limiting? ICES Journal of Marine Science 63: 1567-1572.

Fulton, E.A. (2001). The effects of model structure and complexity on the behaviour and performance of marine ecosystem models. PhD thesis, School of Zoology. University of Tasmania, Hobart, Australia.

Fulton, E.A., Smith, A.D.M., Johnson, C.R. (2003). Effects of complexity on marine ecosystem models. Marine Ecology Progress Series: 253 1-16.

Garcia, S.M., Cochrane, K.L. (2005). Ecosystem approach to fisheries: a review of implementation guidelines. ICES Journal of Marine Science 62: 311-318.

Gauthier, S., Horne, J.K. (2004a). Potential acoustic discrimination within boreal fish assemblages. ICES Journal of Marine Science 61: 836-845.

Gauthier, S., Horne, J.K. (2004b). Acoustic characteristics of forage fish species in the Gulf of Alaska and Bering Sea based on Kirchhoff-approximation models. Canadian Journal of Fisheries and Aquatic Sciences 61: 836-845.

Gislason, H., Sinclair, M., Sainsbury, K., O'Boyle, R. (2000). Symposium overview: incorporating ecosystem objectives within fisheries management. ICES Journal of Marine Science 57: 468-475.

Gjøsæter, H. (1995). Pelagic fish and the ecological impact of the modern fishing industry in the Barents Sea. Arctic 48: 267-278.

Gorska, N., Ona, E. (2003a). Modelling the acoustic effect of swimbladder compression in herring. ICES Journal of Marine Science 60: 548-554.

Gorska, N., Ona, E. (2003b). Modelling the effect of swimbladder compression on the acoustic backscattering from herring at normal or near-normal dorsal incidence. ICES Journal of Marine Science 60: 1381-1391.

Gorska, N., Ona, E., Korneliussen, R. (2005). Acoustic backscattering by Atlantic mackerel as being representative of fish that lack a swimbladder. Backscattering by individual fish. ICES Journal of Marine Science 62: 984-995.

Gorska, N., Korneliussen, R., Ona, E. (2007). Acoustic backscatter by schools of adult Atlantic mackerel. ICES Journal of Marine Science 64: 1145-1151.

Greene, C.H., Wiebe, P.H., McClatchie, S., Stanton, T.K. (1991). Acoustic estimates of Antarctic krill. Nature 349: 110.

Greenstreet, S.P.R., Armstrong, E., Mosegaard, H., Jensen, H., Gibb, I.M., Fraser, H.M., Scott, B.E., Holland, G.J., Sharples, J. (2006). Variation in the abundance of sandeels *Ammodytes marinus* off southeast Scotland: an evaluation of area-closure fisheries management and stock abundance assessment methods. ICES Journal of Marine Science 63: 1530-1550.

Greenstreet, S.P.R., McMillan, J.A., Armstrong, E. (1998). Seasonal variation in the importance of pelagic fish in the diet of piscivorous fish in the Moray Firth, NE Scotland: a response to variation in prey abundance? ICES Journal of Marine Science 55: 121-133.

Greenstreet, S.P.R., Rogers, S.I. (2006). Indicators of the health of the North Sea fish community: identifying reference levels for an ecosystem approach to management. ICES Journal of Marine Science 63: 573-593.

Griffiths, M.H. (2002). Life history of South African snoek, *Thyrsites atun* (Pisces: Gempylidae): a pelagic predator of the Benguela ecosystem. Fisheries Bulletin 100: 690-710.

Hall, S.J., Mainprize, B. (2004). Towards ecosystem-based fisheries management. Fish and Fisheries 5: 1-20.

Halldorsson, O., Reynisson, P. (1983). Target strength measurement of herring and capelin *in situ* at Iceland. FAO Fisheries Report 300: 78-84.

Hamre, J., Dommasnes, A. (1994). Test experiments of target strength of herring by comparing density indices obtained by acoustic method and purse seine catches. ICES CM /B:17.

Haslett, R.W.G. (1965). Acoustic backscattering cross sections of fish at three frequencies and their representation on a universal graph. British Journal of Applied Physics 16: 1143-1150.

Hazen, E.L., Horne, J.K. (2003). A method for evaluating the effects of biological factors on fish target strength. ICES Journal of Marine Science 60: 555-562.

Hazen, E.L., Horne, J.K. (2004). Comparing the modelled and measured target-strength variability of walleye pollock, *Theragra chalcogramma*. ICES Journal of Marine Science 61: 363-377.

Hempel, G. (1978). North Sea fisheries and fish stocks - A review of recent changes. Rapports et Procès-Verbaux des Réunions du Conseil International pour l'Exploration de la Mer 173: 145-167.

Henderson, M.J., Horne, J.K., Towler, R.H. (2008). The influence of beam position and swimming direction on fish target strength. ICES Journal of Marine Science 65: 226-237.

Hewitt, R.P., Demer, D.A. (1991). Krill abundance. Nature 353: 310.

Hewitt, R.P., Linen Low, E.H. (2000). The fishery on Antarctic krill: defining an ecosystem approach to management. Reviews in Fisheries Science 8: 235-298.

Hill, S.L., Murphy, E.J., Reid, K., Trathan, P.N., Constable, A.J. (2006). Modelling Southern Ocean ecosystems: krill, the food-web, and the impacts of harvesting. Biological Reviews 81: 581-608.

Holliday, D.V. (1972). Resonance structure in echoes from schooled pelagic fish. Journal of the Acoustical Society of America 51: 1322-1332.

Hollowed A.B., Bax, N., Beamish, R., Collie, J., Fogarty, M., Livingston, P., Pope, J., Rice, J.C. (2000). Are multispecies models an improvement on single-species models for measuring fishing impacts on marine ecosystems? ICES Journal of Marine Science 57: 707-719.

Horne, J.K. (2000). Acoustic approaches to remote species identification: a review. Fisheries Oceanography 9: 356-371.

Horne, J.K. (2003). The influence of ontogeny, physiology, and behaviour on the target strength of walleye pollock (*Theragra chalcogramma*). ICES Journal of Marine Science 60: 1063-1074.

Horne, J.K., Clay, C.S. (1998). Sonar systems and aquatic organisms: matching equipment and model parameters. Canadian Journal of Fisheries and Aquatic Sciences 55: 1296-1306.

Horne, J.K., Jech, J.M. (1999). Multi-frequency estimates of fish abundance: constraints of rather high frequencies. ICES Journal of Marine Science 56: 184-199.

Horne, J.K., Sawada, K., Abe, K., Kreisberg, R.B., Barbee, D.H., Sadayasu, K. (2009). Swimbladders under pressure: anatomical and acoustic responses by walleye pollock. ICES Journal of Marine Science 66: 1162-1168.

Horne, J.K., Walline, P.D., Jech, J.M. (2000). Comparing acoustic model predictions to *in situ* backscatter measurements of fish with dual-chambered swimbladders. Journal of Fish Biology 57: 1105-1121.

Hunt, G.L., McKinnell, S. (2006). Interplay between top-down, bottom-up, and wasp-waist control in marine ecosystems. Progress in Oceanography 68: 115-124.

Huse, I., Korneliussen, R. (2000). Diel variation in acoustic density measurements of overwintering herring (*Clupea harengus* L.). ICES Journal of Marine Science 57: 903-910.

Huse, I., Ona, E. (1996). Tilt angle distribution and swimming speed of overwintering Norwegian spring spawning herring. ICES Journal of Marine Science 53: 863-873.

Hutchings, J.A. (2000). Collapse and recovery of marine fishes. Nature 406: 882-885.

ICES (1980). Reports of the Herring Assessment Working Group for the Area South of 62ºN. ICES Cooperative Research Report 96: 98-100

ICES (1982). Report of the 1982 planning group on ICES-coordinated herring and sprat acoustic surveys. ICES Document CM /H:04.

ICES (1983). Report of the 1983 planning group on ICES-coordinated herring and sprat acoustic surveys. ICES CM /H:12.

ICES (1988). Report of the working group on Atlanto-Scandian herring and capelin. ICES CM /Assess:04.

ICES (1997). Report of the study group on Baltic acoustic data. ICES CM /J:03.

ICES (2002). Report of the Advisory Committee on Fisheries Management. ICES Cooperative Research Report 255.

ICES (2006). Report of the study group on target strength estimation in the Baltic Sea (SGTSEB) ICES CM 2006/FTC:08.

ICES (2007). Report of the Working Group on Northern Pelagic and Blue Whiting Fisheries (WGNPBW). ICES CM /ACFM:29.

ICES (2008a). Report of the Herring Assessment Working Group for the Area South of 62º N (HAWG). ICES CM /ACOM:02.

ICES (2008b). Report of the Planning Group for Herring Surveys (PGHERS). ICES CM /LRC:01.

ICES (2009a). Report of the Working Group on Fisheries Acoustic Science and Technology (WGFAST). ICES CM / FTC:01.

ICES (2009b). Report of the Herring Assessment Working Group for the Area South of 62 N (HAWG). ICES CM / ACOM:03.

ICES (2010). Report of the Working Group for International Pelagic Surveys (WGIPS). ICES CM / SSGESST:03.

Jech JM, Schael DM, Clay CS (1995). Application of three sound scattering models to threadfin shad (*Dorosoma petenense*). Journal of the Acoustical Society of America 98: 2262-2269.

Jech, J.M., Reeder, D.B., Stanton, T.K., Chu, D. (2000). Three-dimensional visualisation of acoustic backscattering and models by alewife. Journal of the Acoustical Society of America 108: 2457-2458.

Jones, J.R.E. (1952). The reaction of fish to water of low oxygen concentration. Journal of Experimental Biology 29: 403-415.

Jones, F.R.H., Marshall, N.B. (1953). The structure and function of the teleostean swimbladder. Biological Reviews 28: 16-83.

Jones, F.R.H., Pearce, G. (1958). Acoustic reflexion experiments with Perch (*Perca Fluviatilis* Linn.) to determine the proportion of the echo returned by the swimbladder. Journal of Experimental Biology 35: 437-450.

Kaartvedt, S. (2000). Life history of *Calanus finmarchicus* in the Norwegian Sea in relation to planktivorous fish. ICES Journal of Marine Science 57: 1819-1824.

Kang, M., Furusawa, M., Miyashita, K. (2002). Effective and accurate use of difference in mean volume backscattering strength to identify fish and plankton. ICES Journal of Marine Science 59: 794-804.

Kang, D.H., Sadayasu, K., Mukai, T., Iida, K., Hwang, D.J., Sawada, K., Miyashita, K. (2004). Target strength estimation of black porgy *Acanthopagrus schlegeli* using acoustic measurements and a scattering model. Fisheries Science 70, 819-828.

Kasatkina, S. (2007). Target strength of Baltic herring and sprat in relation to changes of their biological characteristics: effects on acoustic abundance indices estimates. ICES CM /H:06.

Kasatkina, S. (2009). The influence of uncertainty in target strength on abundance indices based on acoustic surveys: examples of the Baltic Sea herring and sprat. ICES Journal of Marine Science 66: 1404-1409.

Kiviranta, H., Vartiainen, T., Parmanne, R., Hallikainen, A., Koistinen, J. (2003). PCFF/Fs and PCBs in Baltic herring during the 1990s. Chemosphere 50: 1201-1216.

Kloser, R., Ryan, T., Sakov, P., Williams, A., Koslow, J.A. (2002). Species identification in deep water using multiple acoustic frequencies. Canadian Journal of Fisheries and Aquatic Sciences 59: 1065-1077.

Knorr, G. (1974). Clupea harengus: Linnaeus, 1758. Atlas zur Anatomie und Morphologie der Nutzfische für den praktischen Gebrauch in Wissenschaft und Wirtschaft. No. 6.

Kondo, K. (1980). The recovery of the Japanese sardine - the biological basis of stock size fluctuations. Rapports et Procès-Verbaux des Réunions du Conseil International pour l'Exploration de la Mer 177: 332-345.

Korneliussen, R.J., Diner, N., Ona, E., Berger, L., and Fernandes, P.G. (2008). Proposals for the collection of multifrequency acoustic data. ICES Journal of Marine Science 65: 982-994.

Korneliussen, R.J., Heggelund, Y., Eliassen, I.K., Johansen, G.O. (2009a). Acoustic species identification of schooling fish. ICES Journal of Marine Science 66: 1111-1118.

Korneliussen, R.J., Heggelund, Y, Eliassen, I.K., Øye, O.K., Knutsen, T., Dalen, J. (2009b). Combining multibeam-sonar and multifrequency-echosounder data: examples of the analysis and imaging of large euphausiid schools. ICES Journal of Marine Science 66: 991-997.

Korneliussen, R.J., Ona, E. (2002). An operational system for extraction of plankton and fish from mixed recordings. ICES Journal of Marine Science 59: 293–313.

Korneliussen, R.J., Ona, E. (2003). Synthetic echograms generated from the relative frequency response. ICES Journal of Marine Science 60: 636–640.

Korneliussen, R.J., Ona, E. (2004). Verified acoustic identification of Atlantic mackerel. ICES CM /R:20.

Koslow, J.A. (2009). The role of acoustics in ecosystem-based fishery management. ICES Journal of Marine Science 66: 966-973.

Lasker, R. (1985). What limits clupeoid production? Canadian Journal of Fisheries and Aquatic Sciences 42: 31-38.

Lassen, H., Stæhr, K.J. (1985). Target strength of Baltic herring and sprat measured in situ. ICES CM /B:41.

Lavery, A.C., Stanton, T.K., McGehee, D.E., Chu, D. (2002). Three-dimensional modeling of acoustic backscattering from fluid-like zooplankton. Journal of the Acoustical Society of America 111: 1197-1210.

Lluch-Belda, D., Crawford, R.E., Kawasaki, T., McCall, A.D., Parrish, R.H., Schwartzlose, R.A., Smith, P.A. (1989). World-wide fluctuations of sardine and

anchovy stocks: the regime problem. South African Journal of Marine Science 8: 195-205.

Løland, A., Aldrin, M., Ona, E., Hjellvik, V., Holst, J.C. (2007). Estimating and decomposing total uncertainty for survey-based abundance estimates of Norwegian spring-spawning herring. ICES Journal of Marine Science 64: 1302-1312.

Love, R.H. (1971a). Measurements of fish target strength: A review. Fishery Bulletin 69: 703-715.

Love, R.H. (1971b). Dorsal-aspect target strength of an individual fish. Journal of the Acoustical Society of America 49: 816-823.

Love, R.H. (1977). Target strength of an individual fish at any aspect. Journal of the Acoustical Society of America 62: 1397-1403.

Love, R.H. (1978). Resonant acoustic scattering by swimbladder-bearing fish. Journal of the acoustical society of America 64: 571-580.

Love, R.H. (1993). A comparison of volume scattering strength data with model calculations based on quasisynoptically collected fishery data. Journal of the Acoustical Society of America 94: 2255-2268.

Løvik, A., Hovem, J.M. (1979). An experimental investigation of swimbladder resonance in fishes. Journal of the Acoustical Society of America 66: 850-854.

Macaulay, G.J. (2002). Anatomically detailed acoustic scattering models of fish. Bioacoustics 12: 275-277.

Mace, P.M. (2001). A new role for MSY in single-species and ecosystem approaches to fisheries stock assessment and management. Fish and Fisheries 2: 2-32.

Machias, A., Tsimenides, N. (1995). Biological factors affecting the swimbladder volume of sardine (*Sardina pilchardus*). Marine Biology 123: 859-867.

Mackinson, S., Freeman, S., Flatt, R., Meadows, B. (2004). Improved acoustic surveys that save time and money: integrating fisheries and ground-discrimination acoustic technologies. Journal of Experimental Marine Biology and Ecology 305: 129-140.

MacLennan, D.N. (1990). Acoustical measurement of fish abundance. Journal of the Acoustical Society of America 87: 1-15.

MacLennan, D.N., Fernandes, P.G., Dalen, J. (2002). A consistent approach to definitions and symbols in fisheries acoustics. ICES Journal of Marine Science 59: 365-369.

Madureira, L.S.P., Everson, I., Murphy, E.J. (1993). Interpretation of acoustic data at two frequencies to discriminate between Antarctic krill (*Euphausia superba* Dana) and other scatterers. Journal of Plankton Research 15: 787-802.

Makris, N.C., Ratilal, P., Symonds, D.T., Jagannathan, S., Lee, S., Nero, R.W. (2006). Fish population and behavior revealed by instantaneous continental shelf-scale imaging. Science 311: 660-663.

Makris, N.C., Ratilal, P., Jagannathan, S., Gong, Z., Andrews, M., Bertsatos, I., Godø, O.R., Nero, R.W., Jech, J.M. (2009). Critical Population Density Triggers Rapid Formation of Vast Oceanic Fish Shoals. Science 323: 1734-1737.

Mäntyniemi, S., Kuikka, S., Rahikainen, M., Kell, L.T., Kaitala, V. (2009) The value of information in fisheries management: North Sea herring as an example. ICES Journal of Marine Science (in press).

Marasco, R.J., Goodman, D., Grimes, C.B., Lawson, P.W., Punt, A.E., Quinn II, T.J. (2007). Ecosystem-based fisheries management: some practical suggestions. Canadian Journal of Fisheries and Aquatic Sciences 64: 928-939.

McAllister, M.K., Ianelli, J.N. (1997) Bayesian stock assessment using catch-age data and the sampling-importance resampling algorithm. Canadian Journal of Fisheries and Aquatic Sciences 54: 284-300.

McAllister, M.K., Pikitch, E.K. (1997) A Bayesian approach to choosing a design for surveying fishery resources: application to the eastern Bering Sea trawl survey. Canadian Journal of Fisheries and Aquatic Sciences 54: 301-311.

McAllister, M.K., Kirkwood, G.P. (1998). Bayesian stock assessment: a review and example application using the logistic model. ICES Journal of Marine Science 55: 1031-1060.

McClatchie, S., Alsop, J., Coombs, R.F. (1996). A re-evaluation of relationships between fish size, acoustic frequency, and target strength. ICES Journal of Marine Science 53: 780-791.

McClatchie, S., Macaulay, G.J., Coombs, R.F. (2003). A requiem for the use of 20 $\log_{10}$ Length for acoustic target strength with special reference to deep-sea fishes. ICES Journal of Marine Science 60: 419-428.

McClatchie, S., Thorne, R.E., Grimes, P., Hanchet, S. (2000). Ground truth and target identification for fisheries acoustics. Fisheries Research 47: 173-191.

McGehee, D.E., O'Driscoll, R.L., Traykovski, L.V.M. (1998). Effects of orientation on acoustic scattering from Antarctic krill at 120 kHz. Deep-Sea Research Part 2 45: 1273-1294.

McQuinn, I.H. (1997). Metapopulations and the Atlantic herring. Reviews in Fish Biology and Fisheries 7: 297-329.

McQuinn, I.H., Winger, P.D. (2003). Tilt angle and target strength: target tracking of Atlantic cod (*Gadus morhua*) during trawling. ICES Journal of Marine Science 60: 575-583.

Medwin, H., Clay, C.S. (1998). Fundamentals of acoustical oceanography. Academic Press, San Diego.

Megrey, B.A., Rose, K.A., Ito, S., Hay, D.E., Werner, F.E., Yamanaka, Y., Aita, M.N. (2007). North Pacific basin-scale differences in lower and higher trophic level marine ecosystem responses to climate impacts using a nutrient–phytoplankton–zooplankton model coupled to a fish bioenergetics model. Ecological Modelling 202: 196-210.

Meyer, R, Millar, R.B. (1999). Bayesian stock assessment using a state-space implementation of the delay difference model. Canadian Journal of Fisheries and Aquatic Sciences 56: 37-52.

Metropolis, H., Rosenbluth, A.W., Rosenbluth, M.N., Teller, A.H., Teller, E. (1953). Equation of state calculations by fast computing machines. Journal of Chemical Physics 21: 1087-1092.

Midttun, L. (1984). Fish and other organisms as acoustic targets. Rapports et Procès-Verbaux des Réunions du Conseil International pour l'Exploration de la Mer 184: 25-33.

Misund, O.A., Beltestad, A.K. (1996). Target-strength estimates of schooling herring and mackerel using the comparison method. ICES Journal of Marine Science 53: 281-284.

Morse, P.M., and Ingard, K.U. (1968). Theoretical Acoustics. Princeton University Press, Princeton, NJ.

Mukai, T., Iida, K. (1996). Depth dependence of target strength of live kokanee salmon in accordance with Boyle's law. ICES Journal of Marine Science 53: 245-248.

Nakken, O., Olsen, K. (1977). Target strength measurements of fish. Rapports et Procès-Verbaux des Réunions du Conseil International pour l'Exploration de la Mer 170: 52-69.

Nero, R.W., Huster, M.E. (1996). Low-frequency acoustic imaging of Pacific salmon on the high seas. Canadian Journal of Fisheries and Aquatic Sciences 53: 2513-2523.

Nero, R.W., Feuillade, C., Thompson, C.H. (2007). Near-resonance scattering from arrays of artificial fish swimbladders. Journal of the Acoustical Society of America 121: 132-143.

Nero, R.W., Thompson, C.H., Jech, J.M. (2004). *In situ* acoustic estimates of the swimbladder volume of Atlantic herring (*Clupea harengus*). ICES Journal of Marine Science 61: 323-337.

Nero, R.W., Thompson, C.H., Love, R.H. (1998). Lowfrequency acoustic measurements of Pacific hake, *Merluccius productus*, off the west coast of the United States. Fisheries Bulletin 96: 329-343.

Nishimori, Y., Iida, K., Furusawa, M., Tang, Y., Tokuyama, K., Nagai, S., Nishiyama, Y. (2009). The development and evaluation of a three-dimensional, echo-integration method for estimating fish-school abundance. ICES Journal of Marine Science, 66: 1037-1042.

Northridge, S.P., Tasker, M.L., Webb, A., Williams, J.M. (1995). Distribution and relative abundance of harbour porpoises (*Phocoena phocoena* L.), white-beaked dolphins (*Lagenorhynchus albirostris* Gray), and minke whales (*Balaenoptera acutorostrata* Lacepede) around the British Isles. ICES Journal of Marine Science 52: 55-66.

Nøttestad, L. (1998). Extensive gas bubble release in Norwegian spring spawning herring (*Clupea harengus*) during predator avoidance. ICES Journal of Marine Science 55: 1133-1140.

Ona, E. (1990). Physiological factors causing natural variations in acoustic target strength of fish. Journal of the Marine Biological Association of the U.K. 70: 107-127.

Ona, E. (2001). Herring tilt angles measured through target tracking, pp. 509-519. In: F. Funk, J. Blackburn, D. Hay, A.J. Paul, R. Stephenson, R. Toresen, D. Witherell [ed.], Herring: expectations for a new millenium. Lowell Wakefield Fisheries Symposia Series, Fairbanks, Alaska.

Ona, E. (2003). An expanded target-strength relationship for herring. ICES Journal of Marine Science 60: 493-499.

Ona, E., Godø, O.R., Handegard, N.O., Hjellvik, V., Patel, R., Pedersen, G. (2007). Silent research vessels are not quiet. Journal of the Acoustical Society of America 121: 145-150.

Ona, E., Zhao, X., Svellingen, I., Fosseidengen, J.E. (2001). Seasonal Variation in Herring Target Strength, pp 461-487. In: F. Funk, J. Blackburn, D. Hay, A.J. Paul, R. Stephenson, R. Toresen, D. Witherell [ed.], Herring: expectations for a new millenium. Lowell Wakefield Fisheries Symposia Series, Fairbanks, Alaska.

Parish, J. (2004). Using behavior and ecology to exploit schooling fishes. Environmental Biology of Fishes 55: 157-181.

Patterson, K.R., Melvin, G.D. (1996). Integrated catch at age analysis, version 1.2. Scottish Fisheries Research Report 58.

Pauly, D., Christensen, V. (1995). Primary production required to sustain global fisheries. Nature 374: 255-257.

Pauly, D., Christensen, V., Dalsgaard, J., Froese, R., Torres, F. Jr. (1998). Fishing down marine food webs. Science 279: 860-863.

Pauly, D., Christensen, V., Walters, C. (2000). Ecopath, Ecosim, and Ecospace as tools for evaluating ecosystem impact of fisheries. ICES Journal of Marine Science 57: 697-706.

Pauly, D., Christensen, V., Guenette, S., Pitcher, T.J., Sumaila, U.R., Walters, C.J., Watson, R., Zeller, D. (2002). Towards sustainability in world fisheries. Nature 418: 689-695.

Pauly, D., Muck, P., Mendo, J., Tsukayama, I. (1989). The Peruvian upwelling system: dynamics and interactions. ICLARM. Conference Proceedings, pp 189-206.

Pauly, D., Watson, R., Alder, J. (2005). Global trends in world fisheries: impacts on marine ecosystems and food security. Philosophical Transactions of the Royal Society B 360: 5-12.

Pedersen, G., Handegard, N.O., Ona, E. (2009). Lateral-aspect, target-strength measurements of *in situ* herring (*Clupea harengus*). ICES Journal of Marine Science 66:1191-1196.

Pedersen, G., Korneliussen, R.J. (2009). The relative frequency response derived from individually separated targets of northeast Arctic cod (*Gadus morhua*), saithe (*Pollachius virens*), and Norway pout (*Trisopterus esmarkii*). ICES Journal of Marine Science 66: 1149-1154.

Peltonen, H., Balk, H. (2005). The acoustic target strength of herring (*Clupea harengus* L.) in the northern Baltic Sea. ICES Journal of Marine Science 62: 803-808.

Peña, H., Foote, K.G. (2008). Modelling the target strength of *Trachurus symmetricus murphyi* based on high-resolution swimbladder morphometry using an MRI scanner. ICES Journal of Marine Science 65: 1751-1761.

Pikitch, E.K., Santora, C., Babcock, E.A., Bakun, A., Bonfil, R., Conover, D.O., Dayton, P., et al. (2004). Ecosystem-based fishery management. Science 305: 346-347.

Pope, J.G., Shepherd, J.G. (1982). A simple method for the consistent interpretation of catch-at-age data. ICES Journal of Marine Science 40: 176-184.

Prokopchuk, I., Sentyabov, E. (2006). Diets of herring, mackerel, and blue whiting in the Norwegian Sea in relation to *Calanus finmarchicus* distribution and temperature conditions. ICES Journal of Marine Science 63: 117-127.

Pruessmann, K.P., Weiger, M., Scheidegger, M.B. Boesiger, P. (1999). SENSE: sensitivity encoding for fast MRI. Magnetic Resonance in Medicine 42: 952-962.

Punt, A.E., and Hilborn, R. (1997). Fisheries stock assessment and decision analysis: the Bayesian approach. Reviews in Fish Biology and Fisheries 7: 35-63.

Reid, D.G., Fernandes, P.G., Bethke, E., Couperus, A., Goetze, E., Håkansson, N., Pedersen, J., Stæhr, K.J., Simmonds, E.J., Toresen, R., Tortensen, E., 1998. On visual scrutiny of echograms for acoustic stock estimation. ICES CM /J:3.

Reid, D.G., Simmonds, E.J. (1993). Image analysis techniques for the study of fish school structure from acoustic survey data. Canadian Journal of Fisheries and Aquatic Sciences 50: 886-893.

Reynisson, P. (1993). In situ target strength measurements of Icelandic summer spawning herring in the period 1985-1992. ICES CM /B:40.

Rice, J. (1995). Food web theory, marine food webs, and what climate change may do to northern marine fish populations, pp. 516-568. In: R.J. Beamish [ed.], Climate Change and Northern Fish Populations. Canadian Special Publication of Fisheries and Aquatic Sciences, No. 121.

Rivoirard, J., Simmonds, J., Foote, K.F., Fernandes, P., Bez, N. (2000). Geostatistics for estimating fish abundance. Blackwell Science Ltd., Oxford.

Reeder, D.B., Jech, J.M., Stanton, T.K. (2004). Broadband acoustic backscatter and high-resolution morphology of fish: Measurement and modeling. Journal of the Acoustical Society of America 116: 747-761.

Rivoirard, J., Simmonds, J., Foote, K. F., Fernandes, P., Bez, N. (2000). Geostatistics for Estimating Fish Abundance. Blackwell Science, Oxford.

Rose, G., Gauthier, S., Lawson, G. (2000). Acoustic surveys in the fully monte: simulating uncertainty. Aquatic Living Resources 13: 367-372.

Rudstam, L.G., Lindem, T., Hansson, S. (1988). Density and in-situ target strength of herring and sprat: a comparison between two methods of analyzing single beam sonar data. Fisheries Research 6: 305-315.

Rudstam, L.G., Hansson, S., Lindem, T., and Einhouse, D.W. (1999). Comparison of target-strength distributions and fish densities obtained with split- and single-beam echosounders. Fisheries Research 42: 207-214.

Sand, O., Hawkins, A.D. (1973). Acoustic properties of the cod swimbladder. Journal of Experimental Biology 58: 797-820.

Saville, A., Bailey, R.S. (1980). The assessment and management of the herring stocks in the North Sea and to the west of Scotland. ICES Marine Science Symposia 177: 112-142.

Sawada, K., Furusawa, M., Williamson, N.J. (1993). Conditions for the precise measurement of fish target strength in situ. Fisheries Science 20: 15-21.

Scalabrin, C., Diner, N., Weill, A., Hillion, A., and Mouchot, M-C. (1996). Narrowband acoustic identification of monospecific fish shoals. ICES Journal of Marine Science 53: 181-188.

Schwartzlose, R., Alheit, J., Bakun, A., Baumgartner, T., Cloete, R., Crawford, R., Fletcher, W., et al. (1999). Worldwide large-scale fluctuations of sardine and anchovy populations. South African Journal of Marine Science 21: 289-347.

Simmonds, E.J. (2003). Weighting of acoustic- and trawl-survey indices for the assessment of North Sea herring. ICES Journal of Marine Science 60: 463-471.

Simmonds, E.J. (2007). Comparison of two periods of North Sea herring stock management: success, failure, and monetary value. ICES Journal of Marine Science 64: 686-692.

Simmonds, E.J., MacLennan, D.N. (2005). Fisheries acoustics: theory and practice, 2nd edition. Blackwell Publishing, Oxford.

Simmonds, E.J., Williamson, N.J., Gerlotto, F. Aglen, A. (1992). Acoustic survey design and analysis procedure: a comprehensive review of current practise. ICES Cooperative Research Report 187.

Sinclair, M., Solemdal, P. (1988). The development of “population thinking” in fisheries biology between 1878 and 1930. Aquatic Living Resources 1: 189-213.

Sparre, P. (1991). Introduction to multispecies virtual population analysis. ICES Marine Science Symposia 193: 12-21.

Stanton, T.K. (1988). Sound scattering by cylinders of finite length. I. Fluid cylinders. Journal of the Acoustical Society of America 83: 55-63.

Stanton, T.K. (1989). Sound scattering by cylinders of finite length. III. Deformed cylinders. Journal of the Acoustical Society of America 86: 691-705.

Stanton, T.K. (2009). Broadband acoustic sensing of the ocean. Journal of the Marine Acoustical Society of Japan 36: 95-107.

Stanton, T.K., Chu, D. (2009). Non-Rayleigh echoes from resolved individuals and patches of resonant fish at 2-4 kHz. IEEE Journal of Ocean Engineering (in press).

Stanton, T.K., Chu, D., Jech, J.M., Irish, J.D. (2009). Resonance classification and high-resolution imagery of swimbladder-bearing fish using a broadband echosounder. ICES Journal of Marine Science (in press).

Stanton, T.K., Chu, D., Wiebe, P.H., Clay, C.S. (1993). Average echoes from randomly-oriented random-length finite cylinders: zooplankton models. Journal of the Acoustical Society of America 94: 3463-3472.

Stanton, T.K., Chu, D., Wiebe, P.H., Martin, L.V., Eastwood, R.L. (1998). Sound scattering by several zooplankton groups. II. Scattering models. Journal of the Acoustical Society of America 103: 236-253

Strand, E., Jorgensen, C., Huse, G. (2005). Modelling buoyancy regulation in fishes with swimbladders: bioenergetics and behaviour. Ecological Modelling 185: 309-327.

Suuronen, P., Lehtonen, E., Wallace, J. (1997). Avoidance and escape behaviour of herring encountering midwater trawls. Fisheries Research 29: 13-24.

Tang, Y., Nishimori, Y., Furusawa, M. (2009). The average three-dimensional target strength of fish by spheroid model for sonar surveys. ICES Journal of Marine Science 66: 1176-1183.

Tesler, W.D. (1989). Bias and precision in acoustic biomass estimation. Proceedings of the Institute of Acoustics 11: 202-211.

Thomas, G.L., Kirsch, J., Thorne, R.E. (2002). *Ex situ* target strength measurements of Pacific herring and Pacific sand lance. North America Journal of Fisheries Management 22: 1136-1145.

Thompson, P.M., Pierce, G.J., Hislop, J.R.G., Miller, D., Diack, J.S.W. (1991). Winter Foraging by Common Seals (*Phoca vitulina*) in Relation to Food Availability in the Inner Moray Firth, N.E. Scotland. Journal of Animal Ecology 60: 283-294.

Thorne, R.E., Thomas, G.L. (1990). Acoustic observations of gas bubble release by Pacific herring (*Clupea harengus pallasi*). Canadian Journal of Fisheries and Aquatic Sciences 47: 1920-1928.

Tjelmeland, S. (2002). A model for the uncertainty around the yearly trawl-acoustic estimate of biomass of Barents Sea capelin, *Mallotus villosus* (Müller). ICES Journal of Marine Science 59: 1072-1080.

Toresen, R., Gjøsæter, H., de Barros, P. (1998). The acoustic method as used in the abundance estimation of capelin (*Mallotus villosus* Müller) and herring (*Clupea harengus* Linné) in the Barents Sea. Fisheries Research 34: 27-37.

Trenkel, V.M., Mazauric, V., Berger, L. (2008). The new fisheries multibeam echosounder ME70: description and expected contribution to fisheries research. ICES Journal of Marine Science 65: 645-655.

Trites, A.W., Livingston, P.A., Vasconcellos, M.C., Mackinson, S., Springer, A., Pauly, D. (1999). Ecosystem considerations and the limitations of Ecosim models in fisheries management: insights from the Bering Sea. In: S. Keller

[ed.], Ecosystem Approaches for Fisheries Management. University of Alaska Sea Grant, Fairbanks.

Vabø, R., Olsen, K., Huse, I. (2002). The effect of vessel avoidance of wintering Norwegian spring spawning herring. Fisheries Research 58: 59-77.

Verheye, H.M., Richardson, A.J. (1998). Long-term increase in crustacean zooplankton abundance in the southern Benguela upwelling region (1951-1996): bottom-up or top-down control? ICES Journal of Marine Science 55: 803-807.

Walters, C., Pauly, D., Christensen, V. (2000). Ecospace: prediction of mesoscale spatial patterns in trophic relationships of exploited ecosystems, with emphasis on the impacts of marine protected areas. Ecosystems 2: 539-554.

Warner, D.M., Rudstam, L.G., Klumb, R.A. (2002). *In situ* target strength of alewives in freshwater. Transactions of the American Fisheries Society 131: 212-223.

Watkins, J.L., Brierley, A.S. (2002). Verification of the acoustic techniques used to identify Antartic krill. ICES Journal of Marine Science 59: 1326-1336.

Wahlberg, M., Westerberg, H. (2003). Sound produced by herring (*Clupea harengus*) bubble release. Aquatic Living Resources 16: 271-275.

Weber, T.C., Peña, H., Jech, J.M. (2009). Consecutive acoustic observations of an Atlantic herring school in the Northwest Atlantic. ICES Journal of Marine Science 66: 1270-1277.

Werner, F.E., Ito, S., Megrey, B.A., Michio, J.K. (2007). Synthesis of the NEMURO model studies and future directions of marine ecosystem modeling. Ecological Modeling 202: 211-223.

Weston, D.E. (1967). Sound propagation in the presence of bladder fish, pp. 56-88. In: V.A. Albers [ed.], Underwater acoustics. Plenum, N.Y.

Wilson, B., Batty, R.S., Dill, L.M. (2003). Pacific and Atlantic herring produce burst pulse sounds. Proceedings of the Royal Society London, Series B: Biological Sciences 271: 95-97.

Woillez, M., Rivoirard, J., Fernandes, P.G. (2009). Evaluating the uncertainty of abundance estimates from acoustic surveys using geostatistical simulations. ICES Journal of Marine Science 66: 1377-1383.

Worm, B., Hilborn, R., Baum, J.K., Branch, T.A., Collie, J.S., Costello, C., Fogarty, M.J. (2009). Rebuilding global fisheries. Science 325: 578-585.

Ye, Z. (1997). Low-frequency acoustic scattering by gas-filled prolate spheroids in liquids. Journal of the Acoustical Society of America 101: 1945-1952.

Zar, J.H. (1984). Biostatistical analysis, 2nd edition. Prentice-Hall, Inc., Englewood Cliffs, N.J.

Zhao, X., Ona, E. (2003). Estimation and compensation models for the shadowing effect in dense fish aggregations. ICES Journal of Marine Science 60: 155-163.

Appendix A

This appendix contains copies of the published papers that resulted from the research described in this thesis. The papers and corresponding statements of contribution are given in chronological order :

Fässler, S.M.M., Santos, R., García-Núñez, N., Fernandes P.G. (2007). Multifrequency backscattering properties of Atlantic herring (*Clupea harengus*) and Norway pout (*Trisopterus esmarkii*). Canadian Journal of Fisheries and Aquatic Sciences 64: 362-374.

I estimate that I contributed 65% of the total effort towards the paper. Acoustic survey data were collected on standard surveys conducted by the Marine Laboratory, Aberdeen. The paper contains the result of work that emerged from a combination of ideas by all authors. NGN and RS did an extensive initial data analysis while I conducted subsequent analyses in relation to size-based distinction and developed the backscatter model. The paper was mostly written by myself with help from RS and PGF.

* * *

Fässler, S.M.M., Gorska, N., Ona, E. Fernandes, P.G. (2008). Differences in swimbladder volume between Baltic and Norwegian spring-spawning herring: consequences for mean target strength. Fisheries Research 92: 314-321.

I estimate that I contributed 75% of the total effort towards the paper. Swimbladder volume data were collected by EO and colleagues in the late 1980s. The idea emerged from a discussion between EO, NG and myself. I did the data analysis and modelling work with guidance from NG. The paper was written by myself with assistance from PGF.

* * *

Fässler, S.M.M., Fernandes, P.G., Semple, S.I.K., Brierley, A.S. (2009). Depth-dependent swimbladder compression in herring *Clupea harengus* observed using magnetic resonance imaging. Journal of Fish Biology 74: 296-303.

I estimate that I contributed 85% of the total effort towards the paper. MRI scan data were collected by myself with assistance from SIKS. The inspiration for the work came from the initial literature review and discussions between ASB, PGF and myself. PGF and ASB provided the necessary funding. I did all the data analysis and wrote the paper with assistance in the form of reviews provided by all co-authors.

* * *

Fässler, S.M.M., Gorska, N. (2009). On the target strength of Baltic clupeids. ICES Journal of Marine Science 66: 1185-1190.

I estimate that I contributed 75% of the total effort towards the paper. The X-ray data were initially collected by colleagues from Denmark, whereas I extracted the morphological swimbladder data. The work represents a continuation of ideas developed in Fässler et al. 2008. I did the data analysis and modelling work with guidance from NG. The paper was written by myself and reviewed by NG.

* * *

Fässler, S.M.M., Brierley, A.S., Fernandes P.G. (2009). A Bayesian approach to estimating target strength. ICES Journal of Marine Science 66: 1197-1204.

I estimate that I contributed 80% of the total effort towards the paper. Data analysis and development of the model framework was done by myself with advice from colleagues at the Marine Laboratory and University of St Andrews. The inspiration for the work came from discussions between ASB, PGF and myself. The paper was written by myself but reviewed by ASB and PGF.